BAROCLINIC INSTABILITY OF A MERIDIONALLY VARYING BASIC' STATE

Stephen P. Meacham

B.A., University of Cambridge (1979)
M.A., University of Cambridge (1983)

Subnitted in Partial Fulfillment of the
Requirements for the Degree of
Doctor of Philosophy

at the

Massachusetts Institute of Technology

and the

Woods Hole Oceanographic Institution

June, 1984

Signature of Author S. Meacham
Join4Program in Oceanography, Massachusetts Institute of Technology - Woods Hole Oceanographic Institution,- June, 1984.

Certified by
~h@is SdPervisor.

Accepted by
Chairman, Joint Committee' for Physical Oceanography, Massachusetts Institute of' Technology - Woods Hole Oceanographic Institution.

BAROCLINIC INSTABILITY OF A MERIDIONALLY VARYING BASIC STATE

by

Stephen P. Meacham

Submitted to the Joint Commitee for Physical Oceanography
of the Massachusetts Institute of Technology and the
Woods Hole Oceanographic Institution, in June, 1984, in
Partial Fulfillment of the Requirements for the Degree of
Doctor of Philosophy

ABSTRACT

Several problems are addressed herein. They are loosely connected by the theme of resonant triad interactions. The main topic is the finite amplitude evolution of weakly unstable, linear eigenmodes in a meridionally varying version of Phillips' two-layer model. It is shown in chapter four that interactions between neutral modes and the unstable mode strongly influence the evolution of the latter and are capable of stabilising it before significant changes occur in the zonally averaged flow. The evolution of the unstable wave in the absence of such resonant triad effects is also considered and it is shown by example that the combined influence of changes to the mean flow and higher harmonics of the unstable wave is sufficient to equilibrate the unstable wave. (The higher harmonics are unimportant in the meridionally uniform version of this model). The enhanced importance of neutral sidebands and the details of the evolution are interpreted as being consequences of the

structure of the eigenmodes of the linear problem. It is shown in chapter three that, near minimum critical shear, meridional variation of the potential vorticity gradient of the basic flow can introduce dramatic changes in the structure of the normal modes.

Some aspects of resonant triad dynamics in a meridionally uniform, vertically sheared, two-layer model are considered in chapter two. It is shown that non-linear interactions between a resonant triplet of neutral waves can lead to baroclinic instability. It is also demonstrated that resonant interactions between a slightly supercritical unstable linear mode and two neutral waves can destabilise the weakly finite amplitude equilibration of the unstable mode that would occur in the absence of the sidebands. This demonstration is limited to the case in which the basic state is not close to minimum critical shear. Finally, the work of Loesch (1974), who examined the evolution of a weakly unstable mode and a pair of neutral waves in a basic flow that is close to minimum critical shear, is repeated with the difference that critical layer effects are included.

Thesis supervisor: Joseph Pedlosky, Senior Scientist
Department of Physical Oceanography
Woods Hole Oceanographic Institution

ACKNOWLEDGEMENTS

I would like to take this opportunity to express my gratitude to my advisor, Joseph Pedlosky, who has been a steady and patient source of advice and encouragement since I first arrived in Woods Hole. I have benefited greatly from his perceptive criticism and the example of his intellectual curiosity. The several people who have been associated with my thesis committee: Glenn Flierl, Peter Rhines, Paola Rizzoli, Mark Cane and Erik Mollo-Christensen, have also been generous with their time and advice over the past few years.

My thanks go to Dale Haidvogel and Breck Owens for initiating me in the mysteries of spectral algorithms and vectorised FORTRAN. Thanks too to Bill Young, Bill Dewar and Bruce Cornuelle for suggesting the idea of enrolling in the Joint Program and for making it as much fun as they promised it would be.

During my time as a graduate student, I have had the good fortune to be in the company of a very stimulating and diverse group of people, namely the students and staff at both the Woods Hole Oceanographic Institution and M.I.T.'s Center for Meteorology and Physical Oceanography. Their contribution over the past four years to the life and work of this particular student has been large and I would like to make some acknowledgement of it here.

Large parts of this thesis could not have been completed without the aid of computers. The computing staff of I.P.C. in Woods Hole and in the consulting office at NCAR have been extremely helpful when I have

come to them with my pitiful tales of what the big, bad computer has done to me now. In particular, Karl Lindstrom, Cathy Sweet and Warren Sass deserve words of only the higkest praise.

Just as indispensible to the preparation of this thesis has been the skillful typing of Anne-Marie Michael, who has shown an indefatigable good humour in the face of far too many equations.

The work in this thesis has been supported by the National Science Foundation under grant ATM 79-21431. In addition, part of the numerical work was performed on machines located at the National Center for Atmospheric Research at Boulder, Colorado. NCAR is funded by the National Science Foundation.

Contents

List of Figures

Figure

1.1 (After Phillips, 1954, fig. 1) Contours of growth rate as a function of zonal wavelength L and vertical shear dU/dz , where $L = 2\pi/k_0$ and $dU/dz = U_*/H$. The numbers on the contours indicate the doubling time (in days) of the gravest unstable mode in Phillips' two-layer model. The parameters of the model were chosen so that:
$H = 4.08$ km , $L_D = 930$ km , $\beta = 1.6 \times 10^{-11}$ m s^{-1}

2.1 Possible forms of F(x) in the region to the right of the largest positive root, x_1. In (a) and (b), F(x) intersects the x-axis at a finite angle. In (c) and (d), x_1 is a double or triple root.

2.2 The evolution of the total perturbation energy of an unstable neutral wave triad over the interval $0 < T < 950$. The triad is the one discussed in the text and the figure shows the results of a numerical integration of the potential vorticity equations.

2.3 A map of the areas in the (β , a^2) plane in which may be found neutral Rossby waves that are elements of an unstable triad in which the waves have meridional structures given by $n = (1,1,-2)$. The vertical structures of the three waves are assumed to be given by $m = (-1,-1,1)$. Three regions are shown shaded, two of which overlap. Region D_j corresponds

to possible values of a_j^2. Given a particular value of β, for each choice of a_j^2 in D_j one can find a pair of values (a_k^2 , a_l^2) lying in $D_k \times D_l$ ([j,k,l] = a cyclic permutation of [1,2,3]) which complete an unstable resonant triad. Note, for $\beta < 12.95$, there are no unstable triads with this meridional and vertical structure.

2.4 A similar map to that in fig. 2.3, but with n = (1,2,3) and m = (-1,-1,1).

2.5 a) Plots of M_1, M_2 and N_0 as functions of β for a resonant triad consisting of two neutral modes and a marginal mode. The marginal mode corresponds to the left (long-wave) branch of the marginal curve. The meridional and vertical structures of the triad are n = (1,-3,2) , m_1 = -1 , m_2 = 1 (case A in the text). b) K_0 as a function of β for the same triad as in fig. 2.5a.

2.6 a) As in fig. 2.5a but with neutral modes of different vertical structures (m_1 = 1 , m_2 = -1 : case B in the text). b) K_0 as a function of β for the same triad as in fig. 2.6a.

2.7 An example of the evolution of an unstable triad (case A, β = 13.0). The amplitudes of each of the three waves is shown. During the early part of the run (up to about T = 16), the scale at the left applies. After about T = 16, the three curves are rescaled to accomodate their rapid growth and one should refer to the right-hand scale.

2.8 Similar to fig. 2.7 but for case B at $\beta = 11.0$.

2.9 The evolution of a resonant triad near minimum critical shear. The triad consists of the marginal mode and two neutral waves. (a) - (d) show the evolution when the critical layer effect is excluded, (e) - (h) include this effect.

(a) and (e) : A_0
(b) and (f) : A_1
(c) and (g) : A_2
(d) and (h) : P_1

($F = 8$, $A_0(0) = .0707$, $A_1(0) = .0177$, $A_2(0) = 0.0$; case 1)

2.10 Similar to fig. 2.9 but for $F = 8$, $A_0(0) = 0.0354$, $A_1(0) = 0.0354$, $A_2(0) = 0.0354$ (case 2).

2.11 Similar to fig. 2.9 but for $F = 8$, $A_0(0) = 0.0354$, $A_1(0) = 0.0707$, $A_2(0) = 0.0707$ (case 4).

2.12 Similar to fig. 2.9 but for $F = 12$, $A_0(0) = 0.582$, $A_1(0) = 0.0146$, $A_2(0) = 0.0291$ (case 9).

3.1 The tip of the numerically determined marginal curve plotted in the (k^2, β) plane. Case 1: $F = 10.0$, $U = 1.0$, $h_2 = 5.0$ ($\beta_m = 15.0$).

3.2 The full marginal curve for the gravest unstable mode of Case 1.

3.3 The real and imaginary parts of the phase speed, c_r and c_i, plotted against the square of the wavenumber. β = 14.96, Δ = 0.04 (F = 10.0, U = 1.0, h_2 = 5.0).

3.4 The phase speed along the right-hand branch of the marginal curve, $c_0(\beta)$, plotted against the supercriticality Δ. (F = 10.0, U = 1.0, h_2 = 5.0).

3.5 a) The magnitude of the lower layer streamfunction for the unstable mode at β = 14.96, k = 2.261 (F = 10.0, U = 1.0, h_2 = 5.0).
b) The magnitude of the upper layer streamfunction.
c) Zonally averaged heat flux (multiplied by F) as a function of y.

3.6 The marginal curve for the gravest unstable mode when F = 6.6164, U = 1.0, h_2 = 9.8836 (Case 2).

3.7 a) The magnitude of the lower layer streamfunction for the unstable mode at β = 16.3, k = 2.544 (F = 6.6164, U = 1.0, h_2 = 9.8836).
b) The magnitude of the upper layer streamfunction.
c) Zonally averaged heat flux (multiplied by F) as a function of y.

3.8 Quantities associated with the unstable eigenmode of fig. 3.7: a) heat flux, b) temperature tendency, c) upper layer momentum flux, d) lower layer momentum flux, e) upper layer Reynolds' stress divergence f) lower layer Reynolds' stress

divergence g) secondary circulation: upper layer meridional velocity h) secondary circulation: vertical velocity i) upper mean zonal acceleration j) lower mean zonal acceleration.

3.9 Dispersion curves for the first three slow, neutral mode solutions of (3.26).

4.1 Kinetic energy of the $^{(0)}k$ Fourier component (wave 0) of the upper layer perturbation during run A1.

4.2 As fig. 4.1 but showing all three principal Fourier components (waves 0-2).

4.3 As fig. 4.1 but during run B1.

4.4 As fig. 4.2 but during run B1.
——— wave 0, ——— wave 1, – – – – wave 2.

4.5 Rates of baroclinic conversion of energy between an individual wave and the mean flow during B1.
——— wave 0 , ——— wave 1, – – – – wave 2.

4.6 Meridional profiles of the heat flux associated with the unstable wave, wave 0, at several times during run B1. Profiles are plotted only for $0 < y < 0.5$, they are symmetric about $y = 0.5$.
a) $t = 0.0$, b) $t = 4000.0$, c) $t = 5500.0$, d) $t = 11500.0$,

e) t = 12500.0, f) t = 14500.0, g) t = 16500.0

4.7 The kinetic energy of the upper layer perturbation associated with wave 0 during several different runs. The initial amplitude of wave 0 was the same for each run. The values of F, U, β and h_2 are the same as those used in run A1. The wavenumbers and/or the initial sideband amplitudes differ between runs.
R22/24 is the first part of run B1.
R26: As R22/24 but with initial sideband amplitudes increased by a factor of 2.
R27: As R22/24 but with initial sideband amplitudes decreased by a factor of 2.
R31: Similar initial amplitudes as R22/24 but with $^{(0)}k$ = 2.253, $^{(1)}k$ = -1.2944, $^{(2)}k$ = -0.95858. This corresponds to a triad in which wave 0 has a smaller value of k_2^2 than in R22/24.
R32: Similar initial amplitudes as R22/24 but with $^{(0)}k$ = 2.267, $^{(1)}k$ = -1.3008, $^{(2)}k$ = -0.96622. Here k_2^2 is larger than in R22/24.

4.8 As fig. 4.2 but during run A2.

4.9 As fig. 4.2 but during run B2.

4.10 As fig. 4.1 but during run A3.

4.11 As fig. 4.1 but during run B3.

4.12 As fig. 4.1 but during B4.

CHAPTER 0

0. Introduction

The work in this thesis addresses some problems in the general area known as the theory of baroclinic instability. The purpose of this introductory chapter is two-fold, to give a succinct statement of the problems dealt with in the remainder of the thesis and to provide a setting and motivation for those problems by briefly describing the phenomenon of baroclinic instability and some of the the techniques used to analyze it. We will tackle the second objective first.

The main driving force behind the recognition and subsequent exploration of baroclinic instability has been the study of meteorology. It was recognized that, for a model Earth consisting of a rotating, spherical planet surrounded by a vertically, but stably, stratified atmosphere, a possible equilibrium response to the meridionally asymmetric net input of solar radiation was a steady, axisymmetric, convective circulation. To some extent this resembles the average properties of the tropospheric circulation. The mean winds are predominantly zonal and there is usually a large-scale meridional circulation in lower latitudes, the Hadley cell. However, there are many points of difference between the theoretical equilibrium circulation and the terrestrial troposphere. The real atmosphere is unsteady. Large, planetary scale waves may be seen standing or slowly propagating zonally in the height fields of the upper air pressure surfaces. The equator-pole temperature difference on the Earth is substantially less than that predicted by the equilibrium model, suggesting a

meridional heat transport that is stronger than that associated with the meridional circulation of the equilibrium model.

It was shown by Charney (1947) that steady equilibrium flows like that of the model above tend to be unstable. Such a state contains a larger amount of potential energy than would a resting atmosphere in which the isopycnals lay parallel to the geopotential surfaces. The excess potential energy is often referred to as available potential energy (Lorenz, 1967). Charney showed that there is a class of wave-like perturbations to such an equilibrium which can convert the potential energy of the equilibrium state to kinetic and potential energy of the wave. These waves can then grow at the expense of the equilibrium flow and are therefore known as baroclinically unstable perturbations. As the potential energy of the equilibrium flow is depleted, the isopycnal surfaces must become more nearly parallel to the geopotentials, i.e., the meridional temperature gradient is reduced by the growing perturbations. As it grows, the unstable perturbation produces a meridional flux of density down the horizontal density gradient, or equivalently, a meridional heat flux.

Such an instability mechanism can go a considerable way toward explaining the existence of unsteady wave-like motions superposed on the general zonal circulation, the reduced equator-pole temperature difference, and the reduced zonal velocities of the general circulation. Sufficient evidence seems to have been accumulated for it to be undeniable that the mechanism of baroclinic instability plays an important role in maintaining the average circulation of the Earth's troposphere. A description of such a role in the context of a general circulation theory can

be found in the discussion by Charney (1959) of an idealized model atmosphere.

By dynamical analogy, there are some environments in the ocean which may support baroclinic instability by virtue of the available potential energy of the flow. These include vertically sheared boundary currents such as the Gulf Stream, open ocean currents such as the North Equatorial Current and the Antarctic Circumpolar Current, and broader areas of vertically sheared flow such as the recirculation regions adjoining the Gulf Stream and the Kuroshio. Direct evidence for the existence of baroclinic instability in the ocean is scantier than in the atmosphere and the role that baroclinic instability might play in the circulation of the ocean is less clear-cut. Since a down-gradient eddy heat flux is a symptom of a baroclinic conversion mechanism in the act of depleting the available potential energy of a larger scale flow, some investigators, notably Bryden (1979 and 1982) have looked for such fluxes as evidence of baroclinic instability. Bryden seems to have found such energy converting fluxes in the Antarctic Circumpolar Current in the neighborhood of Drake Passage and in the Gulf Stream recirculation area.

The general circulation of the ocean is neither as well observed nor as well understood as that of the atmosphere, and one cannot say with certainty whether baroclinically active eddies are responsible for significant meridional transports of heat across the main ocean basins. It is, however, known that the main ocean basins contain a substantial amount of energy at scales of the order of the internal deformation radius (e.g., Dantzler, 1977). In the interior of the subtropical gyres, this eddy

energy dominates the kinetic and available potential energy of the larger scale, slow, mean circulation. The question of what are the sources of this eddy activity is an intriguing one. One candidate for supplying part of this may be baroclinic instability of the stronger current and recirculation regions.

In recent years a considerable effort has been made to construct numerical models of the wind-driven circulation in idealized ocean basins, that are capable of resolving eddies on the 100 km scale (e.g., Holland, 1978). These models, which have had some success in reproducing features such as western boundary currents that subsequently separate and the strong recirculation regions associated with them, also show the production of an active eddy field, some of which is converting available potential energy of the larger scale flow into eddy energy.

One last possible area in which baroclinic instability may be a feature is in the dynamics of the large rotating dust clouds that are precursors of galaxies and galactic clusters.

Theoretical studies of baroclinic instability have had several goals: to elucidate the physical mechanism responsible for the instability, to discover which types of equilibrium state are unstable, to determine the distribution of the heat flux associated with the wave and to be able to describe how an initially small, unstable disturbance may evolve. Given the rather turbulent nature of the atmosphere and ocean, it is of interest to discover which horizontal scales are preferred by growing disturbances and how this energy is transferred to other scales to set up the observed energy spectra.

The usual starting point for theoretical investigations has been to take an equilibrium flow of simple form, which satisfies the equation of motion; for example, a steady, uni-directional, non-divergent flow, and to study the evolution of small disturbances to this state by linearizing the equations of motion about this equilibrium solution. The linear problem can then be treated either as an initial value problem (Farrell, 1984; Pedlosky, 1964) or as a normal mode problem. Solutions in which the energy of the perturbation increases with time are then classed as unstable. The philosophy behind such an approach is that if one starts with a very small perturbation to the equilibrium state, then the effects of the omitted non-linear terms will, at first, be small. The time scale for changes produced by the action of the non-linear terms will therefore be long. If the intrinsic properties of the linear solution are such that the energy of that solution can increase on a finite time scale, then one can claim that the linear dynamics will give a good approximation to the evolution of the unstable perturbation for as long as its energy is sufficiently small that the time scale of non-linear effects remains larger than the linear growth time scale. One expects that if the growth is sustained, then, after some initial period, the linear dynamics will become invalid and any consistent description of the subsequent evolution must also include non-linear effects. Several investigators have developed techniques to follow the solution beyond the linear first phase.

Although the linear theory cannot tell us about the stability of an equilibrium flow to arbitrary disturbances of finite amplitude it apparently provides us with very useful information. It tells us something

about which flows will be stable to a class (but not all) of small perturbations (more precisely, it tells us about the ability of flows to support instabilities which have a finite value for the initial growth rate in the limit that the initial amplitude of the perturbation tends to zero). It describes what spatial structures disturbances which belong to this class adopt. In some cases it tells us that a particular horizontal scale will grow more rapidly than others. It can even provide some idea of how a growing disturbance in this class will try to modify the equilibrium flow, if we calculate the quadratic fluxes of momentum and density that are associated with the growing disturbance by using the linear structure of that disturbance.

What linear theory fails to tell us about disturbances of weak initial amplitudes is whether there are types of small amplitude disturbance that do not possess any "linear" means of extracting energy from the equilibrium state (in the sense that they do not contain an unstable normal mode of the linear system), yet nevertheless, by virtue of the non-linear terms in the equation of motion, can extract energy from that state. One would expect that any such disturbances would exhibit initial growth rates that are slower and slower as we make the initial amplitudes smaller and smaller (the linear limit). Yet is seems that from a physical point of view, such disturbances might be important since in studying the stability of physical equilibria, one is concerned with stability to physical perturbations which will have a finite amplitude, even if this is small. A second property that one might speculate upon for instabilities in which the energy extraction process depends on the non-linear rather than the

linear terms in the perturbation equations of motion, is whether the growth rate will not increase as the disturbance grows since the relative size of the non-linear terms, and hence the extraction rate, will increase as the square of the disturbance amplitude. Such an effect might make the instability of one of these weak, non-linear instabilities, whose development would be initially rather slow, ultimately rather powerful.

For the normal mode instabilities of linear theory, we have the unphysical result that the growing wave increases its amplitude at the same exponential rate forever and that no mechanism for diminishing the lack of stability of the underlying basic state is included. From the point of view of circulation modelling, one would like to know what changes the growing wave induces in the mean flow that is supporting the instability. One can obtain some insight into this by adopting a quasi-linear approach (Phillips, 1956; Charney, 1959). In this, the structure of the unstable wave is taken from linear theory, an amplitude for this wave is assigned or determined, the quadratic eddy fluxes are calculated and the resulting changes in the mean circulation are computed. Omitted in Phillips' theory is the feedback mechanism associated with the fact that, as the growing eddy field modifies the mean flow, so the instability properties of the mean flow change and the growth characteristics of the eddy field are altered. If the modifications to the mean flow are such as to reduce its degree of instability, then the feedback loop is negative and one has a way of restraining the growth of the eddy field.

The fully non-linear problem which one would have to solve in order to follow the evolution of an unstable disturbance whose growth time scale according to linear theory was of the same order as the time scale

for the advection of the disturbance by the mean flow, would be extremely complicated. Charney (1959) simplified the problem by making the ad hoc assumption that the shape of the unstable Fourier component is unchanged by the non-linear interaction process. However, studies by Pedlosky (1970), Drazin (1970) and Pedlosky (1979) have shown that there is a class of non-linear evolution problems which are tractable. The technique that they exploit is to examine the evolution of a normal mode whose linear growth rates are slow in comparison to the advective time scale. Over much longer time scales, relatively weak non-linear interactions can compete with the linear instability. Non-linearity therefore becomes significant when the unstable wave is still small and one can develop a theory utilizing perturbation methods, centered around the linear solution, in which the problem has two intrinsic time scales, the time scale of advection by the mean flow and the longer evolutionary time scale over which the disturbance amplitude changes. It is in this small amplitude limit that Charney's shape assumption becomes justified.

By using such a "weakly finite amplitude" theory, one can explore the mechanisms by which non-linear effects curb the growth of an unstable disturbance once it reaches some sort of equilibrium amplitude (here and subsequently, the idea of an equilibrated amplitude will include the case of a state in which the disturbance amplitude fluctuates yet remains at a constant order of magnitude). This is not equivalent to a fully finite amplitude problem. If the tendency of a growing instability to push the mean flow towards stability persists into more strongly non-linear regimes, then one might expect a natural tendency for an unstable flow to linger close to a stable state, i.e., be only moderately supercritical.

In such a situation, the degree of supercriticality would depend upon the forcing for the basic state and the dissipative mechanisms operating. This preference for a small degree of supercriticality would depend crucially on the power of the wave-mean flow interaction mechanism. Stone (1978) has pointed to observations which suggested that the mean state of the troposphere is not too far removed from neutral, suggesting that weakly finite amplitude theories may be more relevant than just giving a mechanistic insight into the operation of non-linear processes.

Spectral transfers of energy must also be taken into account when deciding how a growing disturbance equilibrates. If the disturbance reaches an amplitude at which interactions between the unstable wave and neutral waves transport energy away from the unstable wavenumber at a rate comparable with that of the extraction of energy by the unstable wave, then the wave must eventually stop growing. For a statistically steady state to develop by such a means, one again requires either dissipation at some range of space scales, for example, small scales, to mop up the cascade of energy ultimately released by the agency of baroclinic instability, or the modification of either the mean flow or the structure of the unstable and neutral wave modes in such a way that baroclinic energy conversion is inhibited. An adequate model of the continuous spectrum of waves that results from wave-wave interaction processes as a result of the baroclinic instability of a range of wavenumbers does not seem to have been developed. Instead, mechanistic models of how baroclinic instability can couple to wave-wave interaction processes have been constructed, e.g., Loesch (1974).

The problem that I have attempted to address in this thesis is that of the non-linear evolution of a weakly, baroclinically unstable wave when the unstable equilibrium flow has a special type of meridional structure that makes the meridional potential vorticity gradient of the basic state exhibit a minimum within the channel. This sort of basic state has some of the features that a jet flow in a geophysical situation might exhibit and as such seems a worthwhile departure from the rather artificial meridionally uniform states studied by Phillips, Charney and Eady. A study of the linear problem, Chapter 3, shows that the presence of a potential vorticity gradient, of the form described above, imparts some distinctive features to the weakly unstable normal modes of the basic flow that are not observed in the meridionally uniform counterpart of this model. When one attempts to formulate the finite amplitude evolution of these weakly growing modes (Chapter 4), one discovers that the peculiar nature of the linear modes affects the way in which the finite amplitude evolution proceeds. In particular, the effects of wave-wave interactions between the unstable wave and neutral eigenmodes of the linear problem can exert a more powerful restraint on the growth of the unstable wave than the alteration to the mean flow that the growing wave produces. Because of the prominent role played by wave-wave interactions in this non-linear model, some aspects of the interplay between wave-wave interactions and baroclinic instability are explored in Chapter 2. In particular, we note there that disturbances consisting of non-linearly interacting triads of neutral modes of the linear problem, with small amplitudes, can release potential energy from the equilibrium flow. These furnish an example of

a non-modal form of baroclinic instability. In Chapter 1, we present a synopsis of some works whose content will be relevant to the research subsequently discussed.

CHAPTER 1

1. Background Theory

In this chapter we will review some of the theoretical results presented in four papers which deal with material germane to the work of Chapters 2, 3 and 4. These papers both serve as introductions to the ideas exploited in the later chapters and furnish results with which the material of this thesis can be compared. The aim is not to present a comprehensive summary but to select some of the most pertinent details. At the same time we will introduce some of the notation that will be used later. The four papers in question are those of Phillips (1954), which looks at the linear theory of baroclinic instability in a meridionally uniform two-layer model; Pedlosky (1970), which looks at the finite amplitude development of the slowly growing modes of Phillips' model; Longuet-Higgins and Gill (1967), which discusses resonantly interacting triads of neutral waves in a barotropic model and of Loesch (1974) who examines the interaction of a growing baroclinic instability in Phillips' model with two neutral Rossby waves.

Phillips (1954) presents, as part of a theoretical study of the general circulation of the atmosphere, the properties of linearized perturbations to a quasigeostrophic model of a zonal baroclinic jet. This idealized model allows only two degrees of freedom in the vertical by adopting a very coarse, finite-difference representation of the vertical structure. Such a model can be re-interpreted in terms of a system comprising two homogeneous layers of fluid, the second slightly more

dense than the first and lying beneath it. The two-layer and two-level models can be shown to be equivalent (Flierl, 1978), and in an earlier work Phillips (1951) chose a two-layer approach. Since the layer model can be realized physically and since the investigations of Pedlosky (1970) and Loesch (1974) were couched in terms of the two-layer model, we will adopted the layer formalism. Before continuing with Phillips' paper, we will pause to describe the model in the notation that will be used subsequently in this thesis.

The two layers of fluid are confined in a channel between rigid boundaries at latitude circles $y = 0$ and $y = L$, and heights $z = 0$ and $z = 2H$. This channel is assumed to be of infinite zonal extent and to be in a frame of reference which rotates with an angular velocity $1/2\ f$ about a vertical axis. We desire to model geophysical flows whose width L is of the order of, but smaller than, the radius of the Earth. Following Rossby (1939), we choose to include the dynamical influence of the Earth's sphericity by using the β-plane approximation with $f = f_0 + \beta y$. We are therefore constrained to working in mid-latitudes, where f_0 is significantly non-zero, and in a channel of limited meridional extent, such that $L\beta/f_0 << 1$.

We consider motions which have intrinsic and advective time scales that are long in comparison to the inertial period. Such motions include the traveling cyclone disturbances observed in the atmosphere and the synoptic scale eddying motions of the ocean. We adopt, as a filtering approximation, the quasigeostrophic approximation of Charney (1948). A detailed discussion of this and of the ancillary approximations that are used is given in Pedlosky (1979b).

The quasigeostrophic potential vorticity equations for the two-layer model of Phillips are

$$\partial_t[\nabla^2 \phi_j + (-1)^j \lambda^2 (\phi_1 - \phi_2)] + J[\phi_j, \nabla^2 \phi_j + (-1)^j \lambda^2 (\phi_1 - \phi_2) + \beta y] = 0$$

$$j = 1, 2 \tag{1.1}$$

where our notation is closer to that of Loesch and Pedlosky than Phillips. $\rho_j f_0 \phi_j$ is the pressure in the j^{th} layer, where 1 is assumed to refer to the upper layer, hence ϕ_j is a streamfunction for the geostrophic flow in layer j. J is a Jacobian operator $J(a,b) \equiv a_x b_y - a_y b_x$. λ^2 is given by

$$\lambda^2 = f_0^2 \; / \; (gH \frac{\Delta\rho}{\rho_1}) \tag{1.2}$$

where $\Delta\rho$ is the density difference between the two layers. We have used the Boussinesq approximation. In accordance with Phillips treatment, no bottom relief has been included and the interface between the two layers has been taken to lie at z = H when the fluid is quiescent, i.e., the layers are of equal nominal depth, H. $L_D = \lambda^{-1}$ is a dynamical length scale inherent to the system, often known as the internal deformation radius.

Following the several treatments of Pedlosky and others, we shall non-dimensionalize (1.1) at the outset. We do this by scaling: x and y with L_R, z with 2H, t with L_R/U_R and ϕ with $U_R L_R$, where L_R and U_R are characteristic length and velocity scales of the motions of interest. Equation (1.1) then becomes

$$\partial_t q_j + J(\phi_j, q_i) = 0 \tag{1.3}$$

$$q_j \equiv \nabla^2 \phi_j + (-1)^j F (\phi_1 - \phi_2) + \hat{\beta} y \tag{1.4}$$

In (1.3) and (1.4) ϕ_j are scaled and dimensionless. q_j is the potential vorticity of fluid columns in the j^{th} layer after the large but constant term $f_0 L_R/U_R$ has been subtracted. F and $\hat{\beta}$ are two dimensionless constants. The first is an internal Froude number and $F^{1/2}$ is the ratio of the intrinsic scale of the motions L_R, to the dynamical scale λ^{-1}. $\hat{\beta}$ is given by $\beta L_R^2/U_R$ and is a ratio of the planetary vorticity gradient to the relative vorticity gradient of the fluid motions. We will make the assumption that, relative to the Rossby number, $R = U_R/(L_R f_0)$, both F and $\hat{\beta}$ are O(1). We will also drop the caret from $\hat{\beta}$. It is convenient to use a channel whose width is comparable to the horizontal scale of the motions of interest so we will set $L_R = L$. The horizontal boundaries are therefore located at y = 0 and y = 1 in this non-dimensional system. The physical condition applied at the lateral boundaries is one of no normal flow which can be shown (Phillips, 1954) to imply that

$$\phi_{jx} = 0 \qquad \text{at} \qquad y = 0, 1 \tag{1.5a}$$

and

$$\partial_y \partial_t \int dx\, \phi_j = 0 \quad \text{at } y = 0, 1 \tag{1.5b}$$

where $\int dx$ is to be interpreted as $\lim_{L \to \infty} (1/2L) \int_{-L}^{L} dx$ and we have assumed that ϕ_j is uniformly bounded. Boundary conditions at z = 0 and z = 1 are not explicitly required, but they are implicit in the derivation of (1.1). We have used the condition of no normal flow through the horizontal boundaries. Dissipative and direct forcing mechanisms have been excluded. In particular, no Ekman layers have been included at the horizontal boundaries.

Phillips (1954, Section 5) has described the properties of linear disturbances to a basic flow which consists of a uniform zonal velocity U_j in each layer. In our notation, the linearized vorticity equations for the perturbation are

$$(\partial_t + U_j \partial_x) \; q_j' + [\beta - (-1)^j F (U_1 - U_2)] \phi_{jx}' = 0 \qquad (1.6)$$

Here the total streamfunction for each layer is decomposed into a basic flow plus a perturbation

$$\phi_j = - U_j y + \phi_j'$$

and q_j' is the potential vorticity of the perturbation. Phillips looks for normal mode solutions of the form

$$(\phi_1', \phi_2') = (1, \gamma_j) \sin n \pi y \exp [ik(x-ct)]$$

and finds that the phase speed, c, of these modes is given by

$$c = \overline{U} + \frac{1}{2a^2(a^2+2f)} \left[- (a^2+F) \beta \pm [4 \beta^2 F^2 - U_s^2 a^4 (4F^2 - a^4)]^{1/2} \right] \qquad (1.7)$$

In this expression, $a^2 = k^2 + n^2 \pi^2$ is the total wavenumber of the the perturbation, $\overline{U} = 1/2 (U_1 + U_2)$ is the mean velocity of the basic state and $U_s = (U_1 - U_2)$ is the vertical shear of the basic state in terms of the limited vertical resolution of the two-layer model. In general, there are two values of c for each wavenumber, a, corresponding to the two vertical modes possible in this system. The vertical structure of these modes is represented by the coefficient γ_j which is given by

$$\gamma_j = \frac{a^2 + F}{F} - \frac{\beta + F\, U_s}{U_1 - c} \tag{1.8}$$

The system is insensitive to a uniform zonal translation of the reference frame so we may choose $U_2 = 0$, $U_1 = U$ without any loss of generality, whence $\bar{U} = 1/2\ U$ and $U_s = U$.

The disturbance mode grows exponentially in time when c is complex with $c_i \equiv I_m(c)$ positive [for the conventional choice of positive k. Note that only k^2 occurs in (1.7) and (1.8)]. These unstable modes will have a complex γ_j and it can be shown that for each unstable mode

$$0 > \arg(\gamma_j) > \pi/2$$

This phase lag between the upper and lower layer means that the heat flux associated with the perturbation, when averaged over a wavelength and integrated across the channel, i.e.,

$$\int_0^1 dy\ \frac{k}{2\pi} \int_0^{2\pi/k} dx\ \frac{1}{2} F\, U\, (v_1 + v_2)\, (\phi_1 - \phi_2)$$

is positive. It is this meridional transport of heat that is the mechanism by which potential energy is released from the mean flow and converted into energy of the perturbation.

Phillips found that the contours of constant growth rate for the disturbance take the form shown in Figure 1.1. In Figure 1.1, the contours of constant growth rate are mapped on a plane with axes corresponding to the basic shear and the disturbance wavelength. There are several fea-

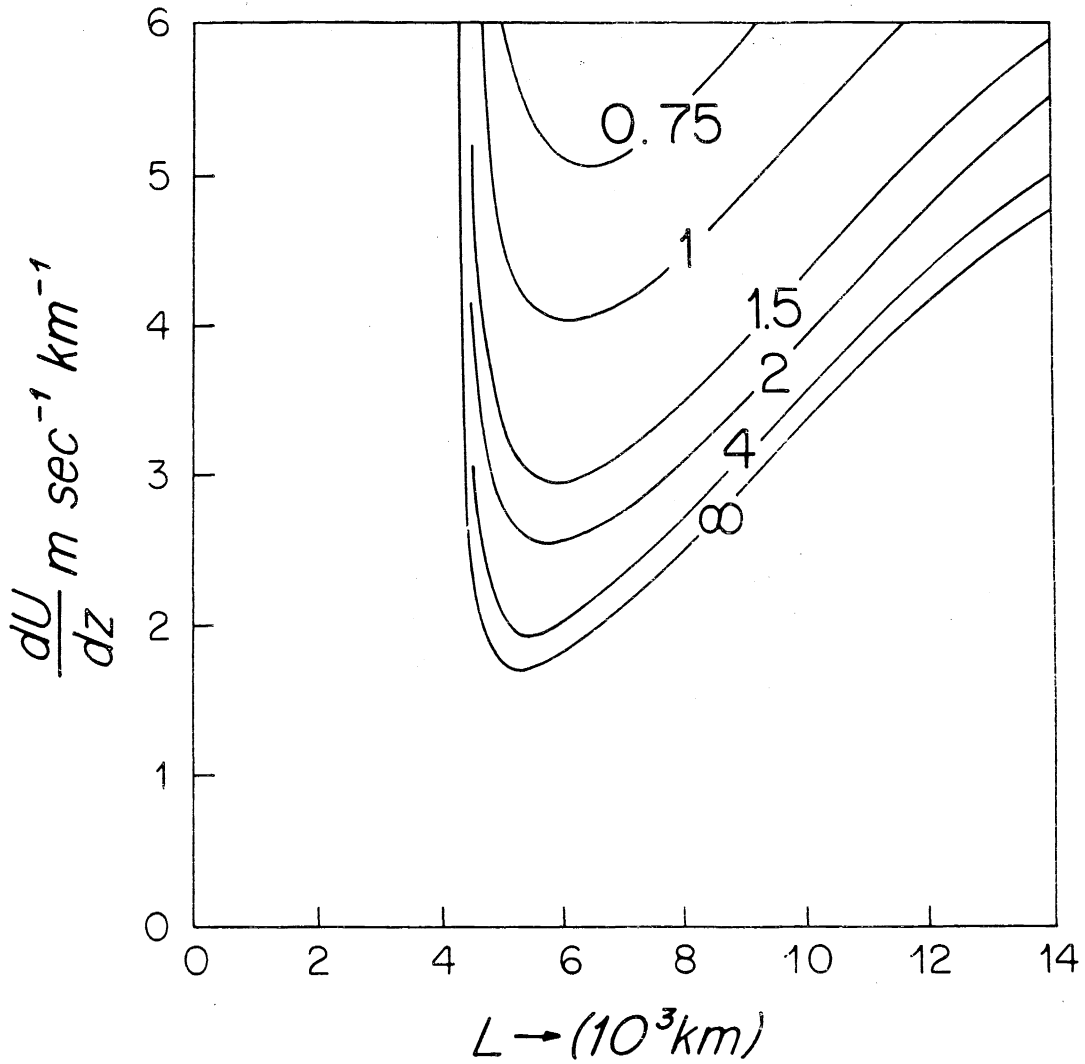

Figure 1.1: (After Phillips, 1954, Fig. 1) Contours of growth rate as a function of zonal wavelength L and vertical shear dU/dz , where $L = 2\pi/k_D$ and $dU/dz = U_*/H$. The numbers on the contours indicate the doubling time (in days) of the gravest unstable mode in Phillips' two-layer model. The parameters of the model were chosen so that:
$H = 4.08$ km , $L_D = 930$ km , $\beta = 1.6 \times 10^{-11}$ m s^{-1}

tures of this graph which we wish to note for future reference. There is a minimum critical shear below which baroclinic instability is not possible. This is also the value of the shear parameter above which the two-layer model version of the sufficient criterion for stability derived by Charney and Stern (1962) is no longer satisfied. If one rearranges the dispersion relation, one can show that the boundary between neutral and unstable perturbations is determined by only two parameters β/FU and a^2/F. Thus for fixed F, increasing U is equivalent, as far as stability properties are concerned, to decreasing β. Thus, if we view F and U as fixed, the stability threshold noted above corresponds to a minimum critical β above which instability is not possible. In subsequent chapters, this is the view which we will adopt. This should not be allowed to obscure the fact that what we are really doing is varying the dynamically significant parameter β/FU which, in the dimensional variables, is

$$\frac{\beta_*}{U_{s*}} L_D^2$$

The asterisks are to denote true dimensional quantities and L_D is the internal deformation radius defined earlier. The stability threshold amounts to requiring that the vertical shear U_{s*} exceed a value determined by the strength of the restoring force for vorticity oscillations, represented by β_* and the inertia of the system to internal oscillations represented by L_D^2.

For values of the shear above the critical threshold only a limited range of wavenumbers is unstable; both a long and a short wave cutoff are

present. Near the critical value of U, the marginal curve (i.e., the stability boundary in Figure 1.1) is parabolic. The growth rate tends to zero as one approaches the stability boundary, i.e., the modes close to the marginal curve grow only slowly with time.

Using the analytically determined forms of the linear eigenmodes, Phillips went on to compute the eddy heat flux associated with the unstable mode and thence the secondary meridional circulation and the changes to the mean zonal flow that these fluxes would have produced after a certain time had elapsed. Phillips' aim in using this quasilinear theory was to estimate the redistribution of heat and momentum that the baroclinic eddies might produce when they had grown to amplitudes that might be typical of the Earth's atmosphere. Because such a theory does not include any feedback between the changes induced in the mean flow by the growing waves and the instability properties of the waves, the choice of wave amplitude used in such a calculation is, in a sense, arbitrary. Phillips chose the wave amplitude by requiring that the rate at which the heat transported by the eddies warmed the northern half of the "northern hemisphere", that his model represented, match the estimated diabatic cooling rate for the same region. Phillips provided a rather successful theoretical model of some of the qualitative effects of eddies on the mean circulation that had been postulated by Jeffreys (1926, 1933). But this model still leaves unclear the answer to the question of how the growth of the unstable eddies is curtailed. However, the seeds of a possible mechanism are contained within this model. The alteration to the mean flow calculated by Phillips as a consequence of the growing waves

was such as to reduce the average vertical shear of the mean flow. The linear results indicated that the mean flow was less unstable (the growth rates at a given wavenumber were less) at smaller shears, so that this second order effect should be stabilizing. The non-linear analysis required to incorporate this feedback mechanism in the general case of initial parameters that corresponded to an unstable wave whose growth rate was O(1) seems rather intractable. Charney later refined Phillips' model (Charney, 1959) and included this stabilizing mechanism in a heuristic way by balancing the rate at which energy was released from the modified mean flow against the rate at which perturbation energy is dissipated. Pedlosky (1970) recognized that under some circumstances, the non-linear analysis could be simplified and this feedback mechanism successfully included in a more rigorous fashion.

The essence of Pedlosky's method is to look at a single unstable wave whose growth rate is small because one has chosen values of β/FU and a^2/F that lie close to the position of the marginal curve. We shall describe the case for which β/FU does not correspond to the position of minimum critical shear but rather a^2/F and β/FU are such that the point they define on a stability diagram such as Figure 1.1 lies near to one side of the marginal curve. The original basic flow is then only slightly unstable for a disturbance at the wavenumber described. As the initially linear unstable eigenmode grows, it produces a correction to the mean flow that is proportional to the square of the eigenmode amplitude. This reduces the mean vertical shear. However, since the original mean flow was only slightly unstable, only a relatively small modification is required

to stabilize the mean flow. Thus while the unstable wave is still fairly weak, it has succeeded in choking the mechanism that was allowing it to grow. The fact that throughout this process the unstable wave has never reached a large amplitude enables one to develop the non-linear solution as a perturbation series in the amplitude of the unstable wave or, more conveniently, in the distance below the marginal curve that the initial value of β/FU lies, since it is this that controls the amplitude that the unstable wave can reach.

The above is a rather sketchy summary of the basic mechanism operating in the non-linear model considered by Pedlosky. The detailed picture is somewhat more involved and one should refer to the paper in question for the precise nature of the evolution. Pedlosky's analysis shows that the growth of the unstable wave is halted by the mean flow modifications and that, in the absence of friction, the amplitude of the unstable wave vacillates in a regular, periodic way. Because the parameters are such that the unstable wave lies close to the marginal wave, the e-folding time scale of the linear unstable eigenmode is long in comparison to the periods of most of the neutral waves. This fact is used in the method of analysis, which considers separating the dynamics that occur on the two time scales. The amplitude vacillations of the unstable wave are characterized by the longer, e-folding time scale.

In choosing to site this weakly finite amplitude analysis close to the side of the marginal curve rather than in the vicinity of minimum critical shear, one is including an element of inconsistency in that, for the same value of β/FU, there are wavenumbers further into the interior of the unstable region which have larger, $O(1)$, growth rates that would

overpower the unstable wave on which the analysis has been concentrated, and to which the weakly finite amplitude analysis would be inapplicable. One situation in which this might be avoided would the case of a periodic zonal domain such as an annular channel in which the quantization was such that the only unstable wave which fit the domain was one close to the marginal curve.

One would prefer to look at an unstable mode in the vicinity of minimum critical shear. For the meridionally uniform model, the finite amplitude problem in the neighborhood of minimum critical shear is a little degenerate and one finds a critical layer effect which alters the behavior of the problem (Pedlosky, 1982). Alterations to the mean flow can cause the unstable wave to equilibrate but the finite amplitude evolution is more complicated than a periodic amplitude vacillation and many zonal scales are stimulated (Pedlosky, 1982; Boville, 1981). The inclusion of meridional variation in the potential vorticity gradient or velocity field of the lower layer should remove this effect.

It may at first seem something of a limitation to confine attention only to the weakly growing waves near the marginal curve, however, this is not so strong a constraint as it might appear. The weakly supercritical waves are those which one first encounters as one gradually increases the mean shear to pass from the stable regime to the unstable regime. If the tendency of a growing baroclinic disturbance to stabilize the vertical shear is robust, as the work of Phillips would suggest, then one has a dynamical reason for the mean flow to lie not too far from critically stable conditions.

Pedlosky's model of non-linear equilibration has demonstrated a mechanism for curbing the growth of a baroclinic instability that linear theory alone would not have predicted and shown how this pivots on the way in which the growing wave modifies the mean flow. One of the reasons for being interested in the dynamics of finite amplitude eddies was their ability to transport heat. In the equilibrated inviscid model of Pedlosky (1970), the mean meridional eddy heat flux, when averaged over a vacillation period, is zero! However, the introduction of dissipation (e.g., Pedlosky, 1971) enables one to recover a non-zero average heat flux in a model which retains the wave-mean flow interaction process as a method of containing the growth of an unstable perturbation.

The model described above does not include any interaction between the unstable wave and neutral waves of the system. The inclusion of non-linear processes allows the possibility of such interactions. Pedlosky's model is consistent in that, given initial conditions in which neutral Rossby waves are absent, they will not, in general, be forced by the dynamics of the unstable wave at amplitudes that would be significant. However, if such waves are included in the initial conditions, alongside the unstable wave, it is possible under some circumstances that they will interact with the unstable wave on the time scale of the weakly finite amplitude evolution theory.

Such wave-wave interactions (as distinct from the wave-mean flow interactions present in Pedlosky's model) may be of interest for several reasons. They may, for example, allow the energy extracted from the mean flow by the primary baroclinic instability to be transported to other

length scales that are not directly unstable. There may be significant transport of energy to shorter, more dissipative length scales. Such an effect might alter the size of the heat flux associated with the unstable wave in an "equilibrated" state. The forcing of neutral waves having amplitudes comparable to the unstable wave and fluctuating on the same timescale as the unstable wave would produce additional modifications to the mean flow of similar size to that produced by the unstable wave and so modify the equilibration process described by Pedlosky (1970).

A general attempt to model interactions between a range of unstable waves and a spectrum of neutral waves would be extremely complicated. However, models which included only one unstable zonal Fourier component and a small number of neutral Rossby modes would be more manageable and should give some insight into the interplay between wave-wave and wave-mean flow interactions. An attempt to construct such a model has been made by Loesch (1974). Amongst waves of weak amplitude it can be shown that the strongest wave-wave interactions occur between waves which form certain resonant multiplets. For the particular dispersive properties of the eigenmodes of the two-layer model, the appropriate multiplets are triplets. Before discussing Loesch's paper, it will be useful to briefly consider the dynamics of resonant triads. These are discussed, albeit for a different physical system, by Longuet-Higgins and Gill (1967).

Longuet-Higgins and Gill considered interactions between Rossby waves in an equivalent barotropic model on an infinite β-plane in which there was no mean flow. Such waves interact most readily when three of the waves satisfy resonance conditions similar to

$$\sum_{j=1}^{3} [\underset{\sim}{k}_j , \sigma_j (\underset{\sim}{k}_j)] = (\underset{\sim}{0}, 0)$$

where $\underset{\sim}{k}_j$ are the horizontal wavenumbers of the three waves and $\sigma_j (\underset{\sim}{k}_j)$ are the frequencies. In the above paper, equations governing the slow evolution of the amplitudes of three waves, satisfying these resonance conditions, are obtained for the case in which each of the waves is of small amplitude. If ε, $<< 1$, is a small number characterizing the amplitudes of the three waves, then the non-linear interactions between the elements of the resonant triad modify the amplitudes on a time scale, ε^{-1}. The evolution, in general, takes the form of a phase locked vacillation in the amplitudes of the three waves, where the relative phases are such that the energy of the triad as a whole remains constant. When the three waves satisfy a further constraint on their relative phases, Longuet-Higgins and Gill show that the amplitudes of the three waves may be described by Jacobian elliptic functions. It can be shown that this is also true for general relative phases of the waves. The authors also showed that in the case of the single layer model without any mean flow, the triad must conserve its total wave energy. They also calculated the amplitude of one of the waves non-resonantly forced by the non-linear interaction and showed that the small amplitude dynamics are consistent when the ratio of particle velocity to phase speed is small for each of the three principal waves.

The importance of this triad interaction phenomenon is that it indicates a preferred mechanism for the transfer of energy between wavenumbers in a weak wave-field. Each element of the triad would, in a more

realistic system, be involved simultaneously in triad interaction with other neutral modes. In a situation in which energy is being injected slowly and over a limited range of wavenumbers, one might expect that resonant triad interactions, at least initially, will be important in redistributing this energy over the wavenumber spectrum. If there is sufficient dissipation to allow an equilibrium spectrum of weak energy to be established, then triad interaction will continue to be important. Such a slow injection of energy at a narrow band of spatial scales could be the result of baroclinic instability under weakly supercritical conditions.

Loesch (1974) considered a model in which a single baroclinically unstable wave, in a flow similar to that considered by Phillips (1954), was allowed to interact resonantly with a pair of neutral Rossby waves. The unstable wave was presumed to lie a small distance Δ below the marginal curve so that in the absence of the neutral waves it would evolve according to the weakly finite amplitude theory of Pedlosky (1970, 1982). The two neutral waves were chosen to form a resonant triad with the marginal wave adjacent to the unstable wave. Loesch showed that when the unstable wave was near one of the sides of the marginal curve, i.e., away from minimum critical shear, the dynamics of both the wave-mean flow interaction process and the resonant triad interaction would be significant (i.e., the time scales of changes in the amplitude of the unstable wave to wave-mean flow interaction and in the amplitudes of all three waves due to wave-wave interactions between the triad elements, are similar and are comparable to the e-folding time scale of the linear instabil-

ity) when the amplitude of the unstable wave is $O(|\Delta|^{1/2})$, where Δ is the supercriticality, and the amplitudes of the sidebands are $O(|\Delta|^{3/4})$. Loesch did not consider this case any further and moved on to the case in which the slightly supercritical mode lies just below minimum critical shear, showing that again the processes of wave-mean flow interaction and triad interaction could be equally significant. In this instance, the natural scales for the wave amplitudes are each $O(|\Delta|^{1/2})$.

The two features of such a system are firstly that the energy of the "unstable" mode is shared with waves whose length scales are stable according to linear theory and secondly that the finite amplitude evolution of the unstable wave is modified by the presence of the sidebands. However, we emphasize that the wave-mean flow interaction mechanism nevertheless remains an integral part of this evolution. This should be contrasted with the results that will be presented in Chapter 4. The numerical computations of Loesch did not allow for the critical layer effect noted by Pedlosky (1982) so we will not discuss their results here, but the discussion of amplitude scaling and hence the relative importance of the two non-linear interaction mechanisms remains valid.

CHAPTER 2

2. Triad Interactions in Vertical Shear Flows

Abstract

Three related problems concerning the evolution of disturbances in Phillips' model are considered. Firstly, it is shown that non-linear interactions between a resonant triplet of neutral waves in a vertically sheared flow can lead to baroclinic instability. Secondly, we demonstrate that resonant interactions between a slightly supercritical unstable linear mode and two neutral waves can destabilize the weakly finite amplitude equilibration of the unstable mode that would occur in the absence of the sidebands. This demonstration is limited to the case in which the basic state is not close to minimum critical shear. Thirdly, we repeat the work of Loesch (1974) in examining the evolution of a weakly unstable mode and a pair of neutral waves in a basic flow that is close to minimum critical shear with the difference that critical layer effects are included.

A feature of the finite amplitude analysis to be presented in Chapter 4 will be the inclusion of wave-wave interactions between members of a resonant triad. It became clear while studying this material that there were some interesting differences between resonant triad interactions in a shear flow and their counterparts in a fluid at rest. For that reason, we have included the brief studies that make up this chapter.

A simple environment in which to observe the dynamics of resonant triads, when embedded in a vertically sheared flow, is the meridionally uniform, two-layer model of Phillips (1954). Loesch's study of 1974 considers triad interactions in such a model in the case that one of the triad members is a slowly growing wave near minimum critical shear. In this chapter we shall consider this case further and also look at triads composed entirely of neutral linear modes. There will thus be three sections. In the first we consider the dynamics of three neutral Rossby wave modes of Phillips' model, each of small amplitude, when they form a resonant triad. It will be shown that such a triad can exhibit a non-modal form of baroclinic instability, a finite amplitude instability that depends crucially on the weak non-linear interactions between the three waves. In the second section, we consider a resonant triad composed of two neutral Rossby waves and a weakly growing, baroclinically unstable mode which lies close to the marginal curve of Phillips' problem, but away from minimum critical shear. This was a problem mentioned by Loesch, but not considered by him in detail. We shall see that under some circumstances, the presence of the two neutral sidebands can lead to a finite amplitude instability that the wave-mean flow interaction, which is also included in the model, is powerless to overcome. At first sight, this seems significant in that it had been generally thought that the single wave dynamics of Pedlosky (1970), in which a weakly growing mode was equilibrated by wave-mean flow interaction, would be fairly robust, in the sense that allowing parallel triad interactions would not remove this equilibration process. However, we are still in the unsatisfactory posi-

tion of developing our analysis around a point on the marginal curve that is well away from minimum critical shear. In such a case there is, in addition to the weakly growing unstable modes, a range of wavenumbers at which there exist unstable modes with O(1) growth rates. The evolution of these latter modes would overshadow our weakly finite amplitude problem. For this reason we would like to consider the case of a triad containing two neutral waves and a slightly unstable mode that lies close to minimum critical shear. With the restriction that the neutral waves be dispersive modes, this is the situation that Loesch examined. Although Loesch did not include the complicated disturbance forced by critical layer effects, his model equations contained the direct interactions between unstable wave and the neutral sidebands which we would expect to be the cause of any finite amplitude instability, should one exist. Since Loesch did not find any finite amplitude instability, it seems unlikely that one would occur in a more complete model that included critical layer effects. In the third section of this chapter, we present the equations governing such a triad interaction near minimum critical shear, when critical layer effects have been included. It is not possible to confirm that all solution trajectories of which these equations admit are bounded, but, in view of the sign restrictions placed on some of the more important coefficients in these equations, we conjecture that this is likely. To buttress this conjecture, we show examples of numerical integrations of this system for parameter values similar to those used by Loesch.

2.1: Non-Modal Baroclinic Instability

In this section a class of non-linear instabilities of a vertically sheared zonal flow is discussed. This is a type of baroclinic instability that lies outside the purview of a linear eigenmode analysis of baroclinic instability problems. The form taken by the instability is that of an ensemble of three neutral Rossby waves whose amplitudes are slowly modified by their mutual non-linear interactions. For a triad of small amplitude, these interactions introduce a weak, vertical variation of phase to the structure of the individual waves. This allows the generation of rectified heat fluxes and an exchange of energy with the mean flow.

This instability exhibits explosive growth and spans a range of horizontal wavenumbers that exceeds the range that is unstable in the corresponding linear model. It is shown that the type of instability discussed can only occur when the model used is linearly unstable.

The mechanism for the non-linear instability here discussed is believed to be fairly general and should exist also in the context of a horizontally sheared flow where it would take the form of a barotropic instability.

Since the discussion that follows is fairly detailed, we will break it up into numbered subsections. Equations in this part of the thesis will only be numbered (n.m), where n is the subsection and m is the position of the equation within that subsection.

2.1.1: Introduction

Investigations of baroclinic instability generally fall into one of two classes. The first comprises linear models of baroclinic instability.

The majority of these, e.g., the studies of Charney (1947), Eady (1969) and Phillips (1954), take advantage of the linearity of the problem and the stationarity of the basic state being examined to pose the question of stability in terms of the time dependence of the normal modes of the stability problem. In such a case, instability is manifested as a normal mode which exhibits a vertical phase shift and hence intrinsically possesses a mechanism for extracting potential energy from the mean flow, namely its ability to produce a non-zero, zonally averaged, meridional heat flux.

A second type of investigation of baroclinic instability consists of studies of the weakly finite amplitude evolution of slowly growing modes, e.g., Pedlosky (1979a), Drazin (1970) and Pedlosky (1970). These are non-linear but concentrate on the evolution of a particular unstable linear eigenmode as it is circumscribed by weak non-linear effects.

Here, we wish to demonstrate another type of weakly non-linear model in which there appears a different version of the baroclinic instability mechanism. The model examines the evolution of a resonant triad of neutral Rossby waves, i.e., neutral eigenmodes of the appropriate linearized model, of weak amplitude, in a vertically sheared flow. Although each wave is neutral in the linear sense, and hence, as a linear mode, contains no vertical phase shift, we will discover that non-linear interactions between the waves will produce slight phase shifts that enable the modified waves to generate non-zero heat fluxes, and so exchange energy with the mean flow. Note that a prerequisite for energy exchange between the waves and the mean flow is the presence of vertical shear in the mean

flow. We will show further that there exist some triads for which the net effect of the heat fluxes is an extraction of energy from the mean flow by the triad. As a consequence, the triad grows. In general, this growth is faster than exponential.

This phenomenon seems significant for two reasons. On the one hand there is the fact that, while the underlying mechanism for the instability is precisely that of linear baroclinic instability, namely, the extraction of available potential energy from the mean flow by the production of a down-gradient transport of heat; the way in which this heat transport is brought about is inherently different. The instability is non-modal rather than modal, relying as it does on the non-linear interactions between linearly neutral modes to generate the necessary phase shifts. The second reason for interest derives from the fact that, for the type of model that we will consider, the range of wavenumbers that are directly unstable in the linear, modal problem is finite. Non-modal instability will be shown to extend the range of wavenumbers that may increase in energy as a direct result of baroclinic instability. (The implied contrast here is to wavenumbers that increase in energy because that energy is transferred to them from wavenumbers at which active baroclinic conversion is proceeding.)

It may be shown that for this particular type of non-linear baroclinic instability, the appropriate version of the Charney-Stern criterion applies. Thus the type of instability to be described here can occur only when the linear problem is unstable. This, in itself, is of some interest since the theorem deduced by Charney and Stern was originally a linear result. In part, the evidence for the applicability of the aforemen-

tioned stability condition relies on the fact that the instability does not require that the initial amplitudes of the three neutral waves exceed any finite threshold. There may still be other types of non-linear instability which do involve such thresholds that can exist when the Charney-Stern condition would predict stability.

We will begin by considering, in Section 2.1.2, the evolution of three weak neutral waves governed by amplitude equations that are common to several wave problems. We establish a general property of the triads which determines whether or not they are unstable. We also indicate the general solution of the amplitude equations. In Section 2.1.3, we show that the Charney-Stern theorem can be applied to such disturbances to yield stability criteria for the basic state being considered. Here and in the remainder of the chapter we specialize to a two-layer model of baroclinic instability. Section 2.1.4 discusses the energy transformations involved in a growing triad instability. In Section 2.1.5, we show that there do indeed exist some triads which, according to the asymptotic theory of Section 2.1.2, will be unstable. Using the results of Section 2.1.2, we predict the evolution of this triad and then compare this to some non-asymptotic results obtained by integrating the full potential vorticity equations, after restricting the zonal spectrum to the three resonant neutral waves. Lastly, Section 2.2.6 illustrates the range of wavenumbers that can be unstable to this mechanism.

2.1.2: The Evolution of a Triad of Neutral Waves

We first of all note that much of this section is taken from the existng theory of resonant triads which may be seen, for example, in the

work of McGoldrick (1965). Very little background material will be included here so that any reader unfamiliar with the idea of resonant triads is referred to McGoldrick's paper.

There are a number of quadratically non-linear dynamical systems, whose linearized versions support wave modes, that permit certain groups of the linear waves to interact in a way that can be simply described by the equations to be presented below. An example of such a system will be given in Section 2.1.4. The linear modes of a stationary, three-dimensional system will generally take the form

$$\phi = \psi_\lambda (\underset{\sim}{x})\, e^{i\omega_\lambda t} + \text{c.c.}$$

where ϕ is the disturbance quantity, $\psi_\lambda(\underset{\sim}{x})$ the spatial structure of the eigenmode in question, and ω_λ its frequency. c.c. denotes the complex conjugate of the preceding term while λ is an index denoting the particular mode chosen. For several systems of interest, a small amplitude disturbance consisting of a superposition of linear modes will behave almost as if these linear modes were interacting non-linearly in trios. This particular form of non-linear interaction, which affords a way of transporting energy from one scale of motion to another, can be studied in detail be restricting the initial conditions so that only three of the linear modes were present. Subsequently, the disturbance field ϕ is composed predominantly of these three waves plus some small corrections, i.e.,

$$\phi = \varepsilon \left[\sum_{j=0}^{2} A_j \psi_{\lambda_j} (\underset{\sim}{x})\, e^{i\omega_{\lambda_j} t} + \text{c.c.} \right] + O(\varepsilon^2) \quad ,$$

where ε is some small number characteristic of the smallness of the amplitude of the disturbance field and εA_j is the amplitude of the j^{th} wave. Because of the weakness of the disturbance field, the non-linear interactions between the three waves are very weak and only significantly affect the amplitudes of the waves on some long time scale, of $O(\mu^{-1})$ say, where $\mu << 1$. If the frequencies and spatial structures of the three waves satisfy certain conditions, which amount to requiring that the non-linear interaction between each pair of waves produces a resultant which contains a component that resonantly forces the third wave, then μ can be taken to be ε. Such a wave triad is usually referred to as being resonant. If these conditions are not satisfied, then the interaction time scale is longer. In a general weak wave field, these resonance conditions act to select triads of waves which can readily communicate their energy. It is possible for a system to be such that the linear dispersion relations do not permit any triad to satisfy the resonance conditions, e.g., Phillips (1960), in which cases higher order interactions become important.

Defining a slow time variable by $T = \varepsilon t$ one can show that, to a good approximation, the amplitudes of the three waves of a resonant triad can be treated as functions only of T and evolve according to equations of the form

$$\left.\begin{aligned} A_{0T} &= i\, M_0\, A_1^*\, A_2^* \\ A_{1T} &= i\, M_1\, A_2^*\, A_0^* \\ A_{2T} &= i\, M_2\, A_0^*\, A_1^* \end{aligned}\right\} \qquad (2.1)$$

The superscripted asterisks denote complex conjugation. The quantities M_j are constants which depend on the parameters of the system supporting the waves and on the particular waves chosen. We confine our attention to systems for which the M_j are real. The physical example in Section 2.1.4 is such a system. We will note the solution of (2.1) for general initial conditions and then consider some properties of the solution.

From (2.1) one can deduce that

$$\left|A_j\ (T)\right|^2 = \left|A_j(0)\right|^2 + M_j/M_0\ \left[\left|A_0\ (T)\right|^2 - \left|A_0(0)\right|^2\right] \qquad j = 1,2$$

and that

$$A_{0TT} - \sigma^2 A_0 - N A_0 \left(\left|A_0\right|^2 - \left|A_0(0)\right|^2\right) = 0 \tag{2.2}$$

where

$$\left.\begin{aligned} \sigma^2 &= M_0 M_2 \left|A_1(0)\right|^2 + M_0 M_1 \left|A_2(0)\right|^2 \\ N &= 2 M_1 M_2 \end{aligned}\right\} \tag{2.3}$$

We note that if M_0, M_1 and M_2 have the same signs, then σ^2 and N are both positive for all initial conditions other than $A_1(0) = 0 = A_2(0)$.

Equation (2.2) is similar to that governing the weakly finite amplitude evolution of a slowly growing, baroclinically unstable mode found in the study by Pedlosky (1970). It may be solved by setting

$$A_0 = R\ (T)\ e^{i\theta(T)}$$

where R and θ are real. From (2.1),

$$R_{TT} - \theta_T^2 R - \sigma^2 R - NR\,[R^2 - R^2(0)] = 0$$

and,

$$\partial_T (R^2 \theta_T) = 0$$

whence

$$R^2 \theta_T = h \ ,$$

a constant determined by the initial conditions, and

$$R_T = \pm \left(\frac{1}{2} N R^4 + [\sigma^2 - NR^2(0)] R^2 - \frac{h^2}{R^2} + \zeta\right)^{1/2}$$

ζ is another constant determined by the initial conditions. Initially, the leading sign should be chosen to correspond to the initial sense of R_T. Thereafter, the sign should be reversed whenever the argument of the radical becomes zero. R_T is always real. We will suppress this sign hereafter.

Setting $x = R^2$, we find

$$\frac{1}{2} x_T = \left(\frac{1}{2} N x^3 + [\sigma^2 - Nx(0)] x^2 + \zeta x - h^2\right)^{1/2} \qquad (2.4)$$

Thus

$$2T = \int_{x(0)}^{x} dx \left[\frac{1}{2} N x^3 + [\sigma^2 - Nx(0)] x^2 + \zeta x - h^2\right]^{-1/2} \qquad (2.5)$$

(2.5) is an implicit statement of the fact that x(T) is a Jacobian elliptic function (Jeffries and Jeffries, 1956, Ch. 25). Such functions are tabulated. To complete the solution, it is only necessary to determine

the (constant) parameters of the elliptic function. These depend on ζ, h^2, σ^2 and N, and hence on the initial conditions, and require the solution of a cubic polynomial which is tedious but straightforward to obtain, should one need to use the explicit solution. Here we will be content with (2.5).

The amplitude equations (2.1) can be reduced to one of two canonical forms. The first of these can be obtained when M_0, M_1, and M_2 each have the same sign. Applying the transformation

$$A_j = \text{sgn}\,(M_j)\ \frac{|M_j|^{1/2}}{(|M_0M_1M_2|)^{1/2}}\ B_j$$

reduces (2.1) to the form

$$\begin{aligned} B_{0T} &= i\,B_1^*\,B_2^* \\ B_{1T} &= i\,B_2^*\,B_0^* \\ B_{2T} &= i\,B_0^*\,B_1^* \quad . \end{aligned}$$

The second canonical form may be obtained when one of M_0, M_1, and M_2 has a sign different to the other two. Without loss of generality, we assume that M_1 and M_2 have the same sign while that of M_0 opposes this. Then the same transformation yields

$$\begin{aligned} B_{0T} &= i\,B_1^*\,B_2^* \\ B_{1T} &= -i\,B_2^*\,B_0^* \\ B_{2T} &= -i\,B_0^*\,B_1^* \quad . \end{aligned}$$

Within each system the variety of trajectories possible for the solution vector (B_0, B_1, B_2) can be seen to be a consequence only of the variety of possible initial conditions.

It is possible to obtain some general information about the solutions without having recourse to an explicit solution. In particular, we have the following results:

(A) If M_0, M_1 and M_2 are not all of the same sign then the solution always remains bounded.

(B) If M_0, M_1 and M_2 all have the same sign (positive or negative), then most initial conditions will lead to solutions which become infinite in a finite time.

Statement (A) is simple to prove. Suppose M_0 is of opposite sign to M_1 and M_2. From (2.1)

$$\partial_T\left[\frac{|A_0|^2}{M_0} - \frac{|A_j|^2}{M_j}\right] = 0 , \qquad \text{for } j = 1 \text{ and } 2$$

hence $$\frac{|A_0|^2}{|M_0|} + \frac{|A_j|^2}{|M_j|} = \frac{|A_0(0)|^2}{|M_0|} + \frac{|A_j(0)|^2}{|M_j|}$$

Thus $$|A_j(T)|^2 \leq |M_j|\left[\frac{|A_0(0)|^2}{|M_0|} + \frac{|A_j(0)|^2}{|M_j|}\right]$$

and $$|A_0(T)|^2 \leq |A_0(0)|^2 + \min\left[\frac{|M_0|}{|M_1|}|A_1(0)|^2, \frac{|M_0|}{|M_2|}|A_2(0)|^2\right]$$

To prove (B) we use a geometrical argument which we give here. The end of this is denoted by a block, thus ■ . Equation (2.4) is equivalent to

$$\frac{1}{2} x_T = \left[\frac{N}{2} F(x)\right]^{1/2} \tag{2.6}$$

$$F(x) = x^3 + 2\left[\frac{\sigma^2}{N} - x(0)\right] x^2 + 2\frac{C}{N} x - \frac{2h^2}{N} \tag{2.7}$$

We except as a special case initial conditions in which only one wave amplitude is initially non-zero. Equation (2.1) shows that this situation is invariant, albeit unstable, a result which we might expect in the case of Rossby wave propagation on a β-plane since a single linear Rossby wave is a solution of the fully non-linear potential vorticity equation. Thus we assume that at least two of the wave amplitudes were initially non-zero and that A_0 is one of them. Then, when M_0, M_1, and M_2 all have the same sign, σ^2 and N are positive. Thus $F(0) = -2h^2/N \leq 0$ and $F \to +\infty$ as $x \to +\infty$. This means that either one or three roots of $F(x) = 0$ must be greater than or equal to zero and that for all x greater than the most positive real root, F(x) is positive. Let us label the three roots of $F(x) = 0$ as x_1, x_2, x_3. If all of these are real, then let us order them so that

$$x_1 \geq x_2 \geq x_3 \quad .$$

If there is only one real root, let this be x_1.

We seek to prove first that the initial condition, $x_0 \equiv x(0)$, must satisfy

$$x_0 \geq x_1 \quad . \tag{2.8}$$

We know that x_0 must be such that $F(x_0) \geq 0$. We also know that $x \geq 0$. When x_2 and x_3 are complex, $F(x) \geq 0$ for all $x \geq x_1$ and $F(x) < 0$ for all $x < x_1$. Thus $x_0 \geq x_1$.

When x_2 and x_3 are real

$$F(x) \leq 0 \qquad \text{for} \qquad x \leq x_3$$

$$F(x) \geq 0 \qquad \text{for} \qquad x_3 \leq x \leq x_2$$

$$F(x) \leq 0 \qquad \text{for} \qquad x_2 \leq x \leq x_1$$

$$F(x) \geq 0 \qquad \text{for} \qquad x_1 \leq x$$

Since $F(0) \leq 0$, we must have either

$$\text{(a)} \quad x_3 \leq x_2 \leq 0 \leq x_1$$

$$\text{(b)} \quad 0 \leq x_3 \leq x_2 \leq x_1$$

In case (a) $F(x_0) \geq 0$ and $x_0 > 0$ implies that $x_0 \geq x_1$. In case (b) we must be a little more subtle. We note from the form of $F(x)$ that

$$x_1 + x_2 + x_3 = 2 \quad (x_0 - \sigma^2/N) \quad .$$

But $\sigma^2/N > 0$, hence

$$2\, x_0 > x_1 + x_2 + x_3 \geq 2\, x_2 \quad .$$

Thus $x_0 > x_2$. But $F(x) \leq 0$ when $x_2 \leq x \leq x_1$ and the inequality is strict, if $x_2 \neq x_1$ and $x_2 < x < x_1$. Hence $x_0 \geq x_1$.

What we have shown in proving (2.8) is that the initial conditions, x_0, lie on a portion of $F(x)$ that intersects the axis, $F(x) = 0$, at a point $x_1 \geq 0$ to the left of x_0 and tends to infinity to the right of x_0 without recrossing the $F(x) = 0$ axis. Figure 2.1 shows possible forms that the curve $F(x)$ may take to the left of x_1.

Consider now what happens as the solution evolves from the initial conditions. For all of the cases in Figure 2.1, if $x_T(0) > 0$, then x will march rightward along the curve $F(x)$. After some finite distances along the x axis, $F(x)$ increases monotonically with x and is asymptotically proportional to x^3. If we integrate (2.6), we find that the solution is given implicitly by

$$(2N)^{1/2} (T - T_0) = \int_{x_0}^{x} [F(x)]^{-1/2} \, dx$$

where T_0 is the initial time. Since $F(x) \sim x^3$ as $x \to \infty$, we know that $\int_{x_0}^{\infty} [F(x)]^{-1/2} \, dx$ is finite, equal to $\mathcal{J}$, say. This means that $x \to \infty$ as $T \to T_0 + \mathcal{J}(2N)^{-1/2}$.

The other possibility is that $x_T(0) < 0$. Then we must discriminate between Figure 2.1 (a) and (b), on the one hand, and Figure 2.1 (c) and (d) on the other. In the case of (a) and (b), the solution commences to march leftward from x_0 until it reaches x_1. Since $F(x)$ crosses the x-axis at a finite angle at $x = x_1$, the solution will reach x_1 in a finite time, T_1, say. At $x = x_1$, $x_T = 0$, but $x_{TT} > 0$ and so the solution turns around to proceed rightward in the direction from which it has come. It now behaves in the same fashion as the solution when $x_T(0) > 0$ and

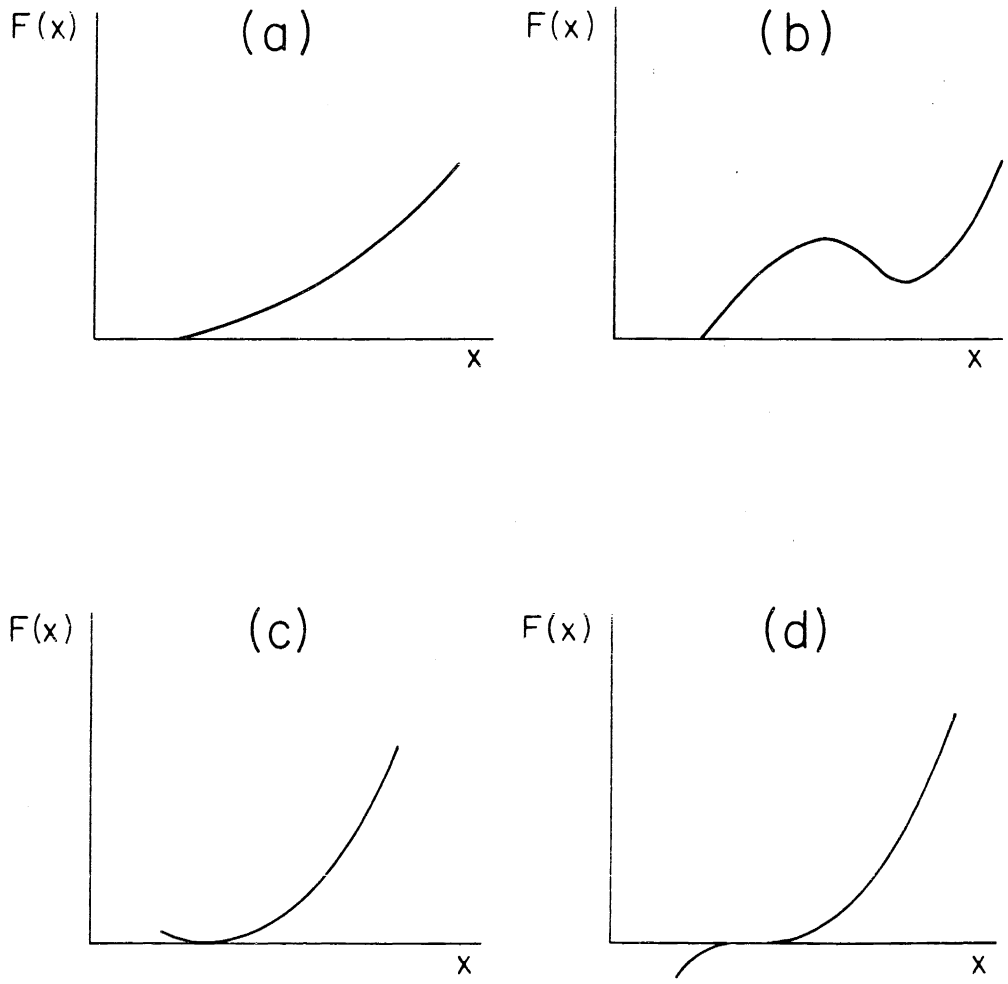

Figure 2.1: Possible forms of F(x) in the region to the right of the largest positive root, x_1. In (a) and (b), F(x) intersects the x-axis at a finite angle. In (c) and (d), x_1 is a double or triple root.

becomes infinite at some finite $T = T_0$. The solution is given implicitly by

$$(2N)^{1/2} (T - T_0) = \int_{x}^{x_0} [F(x)]^{-1/2} \, dx , \qquad T_0 < T < T_1$$

$$(2N)^{1/2} (T - T_1) = \int_{x_1}^{x} [F(x)]^{-1/2} \, dx , \qquad T_1 < T < T_2$$

$$T_1 = T_0 + (2N)^{-1/2} \int_{x_1}^{x_0} [F(x)]^{-1/2} \, dx$$

$$T_2 = T_1 + (2N)^{-1/2} \int_{x_1}^{\infty} [F(x)]^{-1/2} \, dx$$

The instance of a curve shaped like Figure 2.1 (c) or (d), in which x_1 is a double or triple root of $F(x) = 0$, and an initial condition, $X_T(0) < 0$, is a little different. The solution starts to move leftward approaching x_1, but because of the multiple root at x_1, $\int_x^{x_0} [F(x)]^{-1/2} \, dx$ $\to \infty$ as $x \to x_1 +$, taking infinitely long to actually reach x_1. The solution in this case is

$$(2N)^{1/2} (T - T_0) = \int_{x}^{x_0} [F(x)]^{-1/2} \, dx, \quad T_0 < T < \infty .$$

Starting with an initial condition $X_T(0) = 0$ corresponds to a case in which x_0 coincides with x_1. When F(x) has a shape as in 2.1 (a) or 2.1 (b), the solution leaves x_1 and proceeds to infinity. If F(x) has the shape 2.1 (c) or 2.1 (d), the solution will sit at x_1 forever. However, this latter case corresponds only to the initial conditions $A_1(0) = 0 = A_2(0)$ which we have excluded.

The shape of F(x) is determined by the full set of initial conditions for the three waves, i.e., the complex initial values of A_0, A_1 and A_2, which determines σ^2, h, R(0) and $R_T(0)$. It is only for a rather special subset of the initial conditions that the positive most root of $F(x) = 0$ will correspond to a double or triple root. We, therefore, conclude that, for most initial conditions, the solution will become singular in a finite time. ■

A particular example of a class of solutions which will be useful later, is the one in which the initial conditions are such that

$$\theta_0(0) + \theta_1(0) + \theta_2(0) = (2n+1)\pi/2$$

where $\theta_j(0)$ is the initial phase of A_j. Then θ_0, θ_1 and θ_2 remain constant and the amplitude equations reduce to the simpler form

$$R_{0T} = (-1)^n M_0 R_1 R_2$$

$$R_{1T} = (-1)^n M_1 R_2 R_0$$

$$R_{2T} = (-1)^n M_2 R_0 R_1$$

Equation (2.4) simplifies to

$$R_{0T} = \left(\frac{1}{2} N R_0^4 + [\sigma^2 - NX(0)] R_0^2 + C\right)^{1/2} \tag{2.9}$$

Choosing n so that $(-1)^n M_0$ is positive, we can integrate (2.9) to obtain

$$T-T_0 = (M_1M_2)^{-1/2} \tag{2.10}$$

$$\int_{R_0(0)}^{R_0} dR \left[[R^2 - \left(R_0^2(0) - \frac{M_0}{M_1} R_1^2(0)\right)][R^2 - \left(R_0^2(0) - \frac{M_0}{M_2} R_2^2(0)\right)] \right]^{-1/2}$$

and the solution becomes singular at $T = T_s$ where

$$T_s-T_0 = (M_1M_2)^{-1/2} \tag{2.11}$$

$$\int_{R_0(0)}^{\infty} dR \left[[R^2 - \left(R_0^2(0) - \frac{M_0}{M_1} R_1^2(0)\right)][R^2 - \left(R_0^2(0) - \frac{M_0}{M_2} R_2^2(0)\right)] \right]^{-1/2}$$

If we restrict our initial conditions further, to the case where

$$\frac{R_1^2(0)}{M_1} = \frac{R_2^2(0)}{M_2}$$

then we can evaluate the integral in (2.11) to obtain

$$T_S-T_0 = \frac{1}{2(M_1M_2)} 1/2 \left[R_0^2(0) - \frac{M_0}{M_1} R_1^2(0)\right]^{-1/2} \tag{2.12}$$

$$\ln \left\{ \frac{R_0(0) + \left[R_0^2(0) + \frac{M_0}{M_1} R_1^2(0)\right]^{1/2}}{R_0(0) - \left[R_0^2(0) - \frac{M_0}{M_1} R_1^2(0)\right]^{1/2}} \right\}$$

if $R_0^2(0) > \frac{M_0}{M_1} R_1^2(0)$, or

$$T_S - T_0 = \frac{1}{(M_1 M_2)} 1/2 \left[\frac{M_0}{M_1} R_1^2(0) - R_0^2(0) \right]^{-1/2} \left(\frac{\pi}{2} - \tan^{-1} \left\{ \frac{R_0(0)}{\left[\frac{M_0}{M_1} R_1^2(0) \quad R_0^2(0) \right]^{1/2}} \right\} \right) \tag{2.13}$$

if $R_0^2(0) < \frac{M_0}{M_1} R_1^2(0)$.

2.1.3: A Global Stability Constraint

We can make an extremely plausible argument that a result derived by Charney and Stern (1962) for linear stability problems should extend to this particular non-linear problem of an unstable resonant triad, also. We will demonstrate this here in the particular context of a two-layer model although a more general result can readily be obtained. The theorem of Charney and Stern is really a constraint that the conservation of potential vorticity places on the possible classes of quasi-geostrophic disturbances to a quasi-geostrophic flow. It should be borne in mind that it does not explicitly consider the energy balance of the system as some other stability constraints do.

We wish to consider the fate of perturbations to an equilibrium state in which the upper and lower layers move with zonal velocities $U_1(y)$

and $U_2(y)$ when the depth is assumed to be independent of x. Decomposing the flow into a basic part plus a disturbance

$$\phi_j = -\int^y dy\, U_j(y) + \phi_j' ,$$

the vorticity equations become, after dropping primes,

$$\left.\begin{aligned} (\partial_t + U_1\,\partial_x)\, q_1 + \pi_{1y}\,\phi_{1x} + J(\phi_1, q_1) = 0 \\ (\partial_t + U_2\,\partial_x)\, q_2 + \pi_{2y}\,\phi_{2x} + J(\phi_2, q_2) = 0 \end{aligned}\right\} \qquad (3.1)$$

Now q_j is the potential vorticity associated with the perturbation and π_{jy}, the meridional gradient of potential vorticity associated with the equilibrium flow:

$$\pi_{1y} = \beta + F\,U_s - U_{1yy}$$

$$\pi_{2y} = \beta - F\,U_s - U_{2yy} + h_y$$

where $U_s = U_1 - U_2$. The potential vorticity of the equilibrium flow is just $\pi_j(y)$ in layer j.

Provided that our initial perturbation is made in a way consistent with the conservation of potential vorticity, this conservation law implies that, for the subsequent motion

$$q_j = \pi_j\,(y - \eta_j) - \pi_j(y) \quad .$$

We will consider only disturbances whose streamfunctions and their first two derivatives are uniformly bounded on the interval $-\infty < x < \infty$. Defining a zonal averaging operation ($\overline{}$) by

$$\bar{z} = \lim_{L \to \infty} \frac{1}{2L} \int_{-L}^{L} dx\, z \ ,$$

this latter assumption guarantees that

$$\overline{\partial_x \text{ (any term involving multiples of } \eta, \phi, u, v \text{ or } q)} = 0$$

$$\int_0^1 dy\, \overline{v_j q_j} = \int_0^1 dy\, \overline{\frac{d\eta_j}{dt}\, \pi_j\, (y-\eta_j)} - \int_0^1 dy\, \overline{\phi_{jx}}\, \pi_j(y)$$

$$= \int_0^1 dy\, \overline{\frac{d\eta_j}{dt}\, \pi_j\, (y-\eta_j)}$$

$$= \int_0^1 dy\, \overline{\frac{d}{dt}\, [\eta_j\, \pi_j\, (y-\eta_j)]}$$

$$= \partial_t \int_0^1 dy\, \overline{\eta_j\, \pi_j\, (y-\eta_j)} \qquad (3.2)$$

But $$\int_0^1 dy\, \overline{v_1 q_1} = \int_0^1 dy\, \overline{\phi_{1x}\, [\,^2\, \phi_1 + F\, (\phi_2 - \phi_1)]} = \int_0^1 dy\, \overline{\phi_{1x}\, F\phi_2}$$

Similarly $$\int_0^1 dy\, \overline{v_2 q_2} = \int_0^1 dy\, \overline{\phi_{2x}\, F\phi_1}$$

Hence $$\int_0^1 dy\, (\overline{v_1 q_1} + \overline{v_2 q_2}) = 0 \ , \qquad (3.3)$$

which means that

$$\frac{d}{dt}\int_0^1 \overline{[\eta_1\,\pi_1\,(y-\eta_1) + \eta_2\,\pi_2\,(y-\eta_2)]} = 0 \quad , \tag{3.4}$$

i.e., $\int_0^1 dy \sum_{j=1}^{2} \overline{\eta_j \pi_j\,(y-\eta_j)}$ is conserved by non-linear, quasi-geostrophic motions. This result seems rather elegant, although it is not clear whether any very general global stability criterion may be deduced from it.

However, for the particular triad instability with which we are concerned, we can make an educated guess at a global stability criterion. In doing so we need to make use of a peculiar feature of the triad instability namely, that given an unstable set of initial conditions, the same initial conditions reduced by any factor λ lead to a similar, though slower, instability. To see this we note that (2.1) is invariant under the transformation

$$(A_0,\ A_1,\ A_2,\ T) \quad \longrightarrow \quad (\lambda A_0,\ \lambda A_1,\ \lambda A_2,\ \lambda^{-1} T) \quad .$$

Such a transformation, since it affects each wave amplitude in the same way, leaves the spatial structure of the leading order part of the disturbance field unchanged. We can find perturbations that are as small as we please and yet vary smoothly in y, which are unstable and will grow.

Since

$$\frac{d}{dt}\int_0^1 dy\ \overline{\eta_j \pi_j (y-\eta_j)} = \frac{d}{dt}\left[\int_0^1 dy\ \overline{\eta_j}\ \pi_j(y) - \int_0^1 \overline{\eta_j^2}\ \pi_{jy}(y) + \ldots.\right]$$

and

$$\overline{\partial_t \eta_j} = -\partial_y\,(\overline{v_j \eta_j}) = -\partial_y\,[\partial_t \tfrac{1}{2}\overline{\eta_j^2} + \partial_y\,(\overline{v_j \eta_j^2})]$$

$$= -\partial_y\left(\partial_t \tfrac{1}{2}\overline{\eta_j^2} + \partial_y\,[\partial_t \tfrac{1}{6}\overline{\eta_j^3} + \partial_y\,(\overline{v_j \eta_j^3})]\right)$$

we have that

$$\partial_t \int_0^1 dy\ \overline{\eta_j \pi_j(y-\eta_j)} = \partial_t[-\tfrac{1}{2}\int_0^1 \overline{\eta_j^2}\pi_{jy}(y) + \int_0^1 \overline{\eta_j \int_y^{y-\eta_j} dy' \int_y^{y'} dy'' \int_y^{y''} dy'''\ \pi_{jyyy}(y)}]$$

$$+ \int_0^1 \overline{v_j \eta_j^3}\ \pi_{jyyy}(y)$$

$$\therefore \left|\partial_t \tfrac{1}{2}\sum_{j=1}^{2}\int_0^1 \eta_j^2 \pi_{jy}\right| \leq \sum_{j=1}^{2}(2\ \sup|\eta_{jt}| + \sup|v_j|)(\sup|\eta_j|)^3\ \sup(|\pi_{jyyy}(y)|)$$

If it could be proven that the perturbation solution that we have developed is a truly asymptotic solution with the amplitude as a small parameter, ε, say, then we could argue as follows. From the transformation noted above, for a particular choice of spatial structure for the leading part of the perturbation (i.e., a particular choice of wavenumbers and initial amplitude ratios, A_1/A_0 and A_2/A_0) the right-hand side of the above inequality can be put in the form

$$\varepsilon^4 R$$

where R is a finite positive constant independent of the amplitude ε. The left-hand side may be written

$$\varepsilon^3 \partial_T \frac{1}{2} \sum_{j=1}^{2} \int_0^1 \overline{\eta_j^2} \pi_{jy} + \varepsilon^4 Q$$

where

$$\eta_j = \varepsilon \eta_j + O(\varepsilon^2), \; t = \varepsilon T,$$

and

$$|Q| < \text{a finite positive constant } S, \text{ independent of } \varepsilon$$

Note that it is the assumed asymptotic property of the pertrubation solution that allows us to assert that S and R are independent of ε.

We see at once that under such circumstances that the equilibrium flow cannot be unstable to small finite amplitude triads of the sort discussed above if π_{jy} does not change sign within layer j and both π_{1y} and π_{2y} have the same sign.

Unfortunately, I am unable to prove that the perturbation solution is also an asymptotic solution so that the applicability of the Charney-Stern result to this form of instability must remain a conjecture only. In more heuristic terms, we have said that, in view of the ability of the instability to persist for arbitrarily small initial conditions, we expect the stability theorems of linear theory to extend also to this class of disturbances. Consequently, we can only expect to find unstable resonant triads of neutral waves in a case where the basic state also exhibits linear normal mode instabilities. Note that we have not established a stability criterion for any types of finite amplitude instability which involve exceeding an amplitude threshold as a necessary condition for their growth.

2.1.4: Dynamics of a Resonant Triad in a Two-Layer Model

In this section, we will first of all demonstrate that the amplitudes of a resonant triad of weak Rossby waves in a vertically-sheared, two-layer model do evolve according to equations of the form (2.1) and derive expressions for the interaction coefficients M_j which are given as (4.12) below. Since the principles involved are by now well established (see, for example, Longuet-Higgins and Gill, 1967) the presentation will be brief. After this, the discussion will turn to the energy balance in the two-layer system.

We will consider a two-layer model similar to that discussed in Section 3 but without any meridional variation. Thus we will take $h_y = 0$ and look at the stability of an equilibrium flow in which the zonal velocity is uniform in each layer. For convenience we take,

$$U_2 = 0 \ , \quad U_1 = U$$

The perturbation potential vorticity equations become (c.f., Chapter 1)

$$\begin{aligned} (\partial_t + U\partial_x)\,[\nabla^2\phi_1 + F\,(\phi_2 - \phi_1)] + (\beta + FU)\,\phi_{1x} + J\,(\phi_1, q_1) = 0 \\ \partial_t\,[\nabla^2\phi_2 + F\,(\phi_1 - \phi_2)] + (\beta + FU)\,\phi_{2x} + J\,(\phi_2, q_2) = 0 \end{aligned} \tag{4.1}$$

with q_j being the perturbation potential vorticity, as before. The eigenmodes of the linear problem are just (Phillips, 1954)

$$(\phi_1, \phi_2) = (1, \gamma)\,\sin n\pi y\, e^{ik(x-ct)} + c.c. \tag{4.2}$$

where

$$c - \frac{1}{2}U = [a^2(a^2+2F)]^{-1}\left(-\beta\,(a^2+F) + m_j[\beta^2F^2 - \frac{1}{4}U^2a^4\,(4F^2-a^4)]^{1/2}\right) \qquad (4.3)$$

$$a^2 = k^2 + n^2\pi^2$$

$$m_j = \pm 1$$

$$\gamma = (a^2 + F)/F - (\beta + FU)/(U - c) \qquad (4.4)$$

When $\beta < FU$, the potential vorticity gradient of the lower layer becomes negative, the conditions of the Charney-Stern criterion no longer hold and the flow need not be stable. The dispersion relation (4.3) shows that unstable modes do exist when $\beta < FU$ provided that $F > \pi^2/2^{1/2}$, i.e., provided the channel is not too narrow.

We wish to follow the evolution of a triad of neutral waves of small amplitude ε and we expect the amplitudes of these waves to vary on a time-scale ε^{-1}. Accordingly, we shall look at a disturbance of the form

$$\underset{\sim}{\phi} \equiv (\phi_1, \phi_2) = \varepsilon\,(\phi_1^{(0)}, \phi_2^{(0)}) + \varepsilon^2\,(\phi_1^{(1)}, \phi_2^{(1)}) + \ldots \qquad (4.5)$$

$$\underset{\sim}{\phi}^{(0)} \equiv [\phi_1^{(0)}, \phi_2^{(0)}] = \sum_{j=0}^{2} A_j(T)\,(1, \gamma_j)\,e^{ik_j\,(x-c_jt)}\sin n_j\pi y + \text{c.c.} \qquad (4.6)$$

where each of the three waves $(1, \gamma_j)\,e^{ik_j\,(x-c_jt)}\sin n_j\pi y$ is a neutral mode of the linear problem. We have introduced a slow time variable $T = \varepsilon t$ and assumed that the amplitudes of the waves $A_j(T)$ vary on the ε^{-1} time scale. If we insert (4.5) into the non-linear equations (4.1), we

obtain, since $\underset{\sim}{\phi}^{(0)}$ is just a superposition of linear solutions,

$$\begin{aligned}
&\varepsilon\left[(\partial_t+U\partial_x)(\nabla^2\phi_1^{(1)} + F\,[\phi_2^{(1)}-\phi_1^{(1)}]) + (\beta + FU)\,\phi_{2x}^{(1)}\right] \\
&\qquad = \varepsilon\left[-\partial_T\, q_1^{(0)} - J\,[\phi_1^{(0)}, q_1^{(0)}]\right] + O(\varepsilon^2) \\
&\varepsilon\left[\partial_t\,(\nabla^2\phi_1^{(1)} + F\,[\phi_1^{(1)}-\phi_2^{(1)}]) + (\beta + FU)\,\phi_{2x}^{(1)}\right] \\
&\qquad = \varepsilon\left[-\partial_T\, q_2^{(0)} - J\,[\phi_2^{(0)}, q_2^{(0)}]\right] + O(\varepsilon^2)
\end{aligned} \tag{4.7}$$

where $q_j^{(0)} = \nabla^2\,\phi_j^{(0)} + F\,(-1)^j\,[\phi_1^{(0)}-\phi_2^{(0)}]$.

The linear operator on the left of (4.7) is singular, since we know it possesses non-trivial eigenmodes. In order that (4.7) be well-posed, the terms in $O(\varepsilon)$ on the right-hand side must be orthogonal to the adjoint solutions of the linear problem. This amounts to a secularity condition

$$\begin{aligned}
\int_0^1 dy \int dx \int dt\; e^{ik_p(x-c_pt)} \sin n_p\,\pi y \Bigg[&\frac{1}{u-c_p}\,[\partial_T\, q_1^{(0)} + J\,(\phi_1^{(0)}, q_1^{(0)})] \\
&- \frac{\gamma_p}{c_p}\,[\partial_T\, q_T^{(0)} + J\,(\phi_2^{(0)}, q_2^{(0)})]\Bigg] = 0
\end{aligned} \tag{4.8}$$

for each normal mode $e^{ik_p(x-c_p)} \sin n_p\,\pi y\;(1,\gamma_p)$ of the linear system. Here $\int dx$ is to be interpreted as $\underset{L\to\infty}{\mathrm{Lim}}\,\frac{1}{2L}\int_{-L}^{L} dx$ and $\int dt$ as $\underset{\varepsilon\to 0}{\mathrm{Lim}}\,\frac{1}{2}\,\varepsilon^{\alpha}\int_{\varepsilon^{-\alpha}}^{\varepsilon^{\alpha}} dt$ for some α, $0 < \alpha < 1$.

The x and t dependence of the Jacobian terms will be carried by terms proportional to $\exp[\pm\, i\,(kx-\omega t)]$. Where the advection of one wave's

potential vorticity by the velocity field of a second wave, produces a component whose total horizontal wavenumber and frequency match that of the third wave, that component will be resonant with the third wave and will be able to interact with it relatively strongly. It is this sort of dynamics that we wish to describe so we will assume that the three waves satisfy a trio of relations of the form

$$\left.\begin{aligned} k_0 \pm k_1 \pm k_2 &= 0 \\ n_0 \pm n_1 \pm n_2 &= 0 \\ k_0 c_0 \pm k_1 c_1 \pm k_2 c_2 &= 0 \end{aligned}\right\} \qquad (4.9)$$

For simplicity, we assume that the trio satisfied correspond to the choice of positive signs everywhere

$$\left.\begin{aligned} \sum_{j=0}^{2} k_j &= 0 \\ \sum_{j=0}^{2} n_j &= 0 \\ \sum_{j=0}^{2} k_j c_j &= 0 \end{aligned}\right\} \qquad (4.10)$$

In general, not more than one of the possible trios of relations (4.9) will be satisfied and we will assume that the particular wave triad that we examine conforms to this generality. For a fuller description of the nature of resonant interactions between waves in quadratic systems, the reader is referred to McGoldrick (1965).

For a triad satisfying (4.10) there are only three non-trivial, independent conditions of the form (4.8) which are obtained when $k_p = -k_j$, etc., j = 0, 1 and 2. If we substitute for $q_1^{(0)}$ $q_2^{(0)}$, $\phi_1^{(0)}$ and $\phi_2^{(0)}$, in (4.8) and perform the integration with respect to t, these conditions may be written

$$\int_0^1 dy \int dx \left(e^{-ik_j x} \sin n_j \pi y \; x \left\{ \frac{1}{U-c_j} \left[A_{jT} \frac{\beta+FU}{U-c_j} \sin n_j \pi y \, e^{ik_j x} \right.\right.\right.$$

$$+ A_l^* A_m^* \left(J\left(e^{-ik_l x} \sin n_l \pi y, \frac{\beta+FU}{U-c_m} e^{-ik_m x} \sin n_m \pi y \right) \right.$$

$$\left.\left.\left. + J\left(e^{-ik_m x} \sin n_m \pi y , \frac{\beta+FU}{U-c_l} e^{-ik_l x} \sin n_l \pi y \right) \right) \right]$$

$$+ \frac{\gamma_j}{c_j} \left[\gamma_j A_{jT} \frac{\beta-FU}{c_j} \sin n_j \pi y \, e^{ik_j x} \right.$$

$$+ A_l^* A_m^* \gamma_l \gamma_m (\beta-FU) \left(J\left(e^{-ik_l x} \sin n_l \pi y, \frac{1}{c_m} e^{-ik_m x} \sin n_m \pi y \right) \right.$$

$$\left.\left.\left. + J\left(e^{-ik_m x} \sin n_m \pi y, \frac{1}{c_l} e^{-ik_l x} \sin n_l \pi y \right) \right) \right] \right\} \Bigg)$$

for each j = 0, 1,2, with l and m defined such that (j, l, m) is a cyclic permutation of (0, 1,2). From this it is apparent that the secularity conditions will reduce to a form

$$A_{jT} = iM_j A_l^* A_m^* \quad ; \quad j = 0, 1, 2 \tag{4.11}$$

The M_j's are real constants which can be calculated and take the form

$$M_j = -\frac{\pi}{2}(k_m n_l - k_l n_m)\left[\frac{\beta + FU}{(U-c_0)(U-c_1)(U-c_2)} - \frac{\beta - FU}{c_0 c_1 c_2}\gamma_0\gamma_1\gamma_2\right] \tag{4.12}$$

$$\times\left[\frac{\beta + FU}{(U-c_j)^2} + \frac{\gamma_j^2}{c_j^2}(\beta - FU)\right]^{-1}(c_m - c_l)$$

Note that $(k_2 n_1 - k_1 n_2) = (k_0 n_2 - k_2 n_0) = (k_1 n_0 - k_0 n_1)$. Thus M_j may be written

$$M_j = Q\, R_j^{-1}(c_m - c_l)$$

where $Q = \frac{\pi}{2}(k_0 n_1 - k_1 n_0)\left[\frac{\beta + FU}{(U-c_0)(U-c_1)(U-c_2)} - \frac{\beta - FU}{c_0 c_1 c_2}\gamma_0\gamma_1\gamma_2\right]$ and is independent of j, while

$$R_j = \frac{\beta + FU}{(U-c_j)^2} + \frac{\gamma_j^2}{c_j^2}(\beta - FU) \quad .$$

In this case we can verify the application of our stability criterion directly. Recall that the results of Section 3 showed that the resonant triad instability, corresponding to a triad with M_0, M_1, M_2 all of the same sign, could not occur when the potential vorticity gradient was everywhere of the same sign, i.e., when $(\beta + FU)$ and $(\beta - FU)$ have the same sign. Under these circumstances, R_j may take only one sign, irrespective of which wave $_j$ is chosen. Since

$$(c_2 - c_1) + (c_0 - c_2) + (c_1 - c_0) = 0,$$

it immediately follows that the M_j's cannot all have the same sign.

Energy Balance

We can obtain an energy equation for the perturbation field by multiplying the potential vorticity equation for the j^{th} layer by ϕ_j, summing the two, zonally averaging, and then integrating between $y = 0$ and $y = 1$. The result is,

$$\partial_T \frac{1}{2} \int_0^1 dy \; \overline{[|\nabla\phi_1|^2 + |\nabla\phi_2|^2 + F(\phi_1 - \phi_2)^2]} = UF \int_0^1 \overline{dy\, \phi_1\phi_{2x}}$$

The term on the right represents the exchange of energy between the perturbation flow and the mean flow via the baroclinic conversion of energy due to heat fluxes associated with the perturbation. To leading order, the perturbation energy is just the sum of the energies of the three neutral waves. Note that the net non-linear exchange of energy between these waves is zero, i.e., direct wave-wave interactions conserve the sum of the energies of the three waves. However, each wave in the triad can exchange energy with the mean flow through the baroclinic conversion mechanism. At first sight, this seems odd since each of the waves is a neutral solution of the linear problem, to leading order in ε. A heuristic explanation of what is happening goes something as follows. If we calculate $\underset{\sim}{\phi}^{(1)}$, the solution of (4.7), we find that the non-linear interaction between each pair of waves forces a small correction, $\underset{\sim}{\phi}^{(1)}$, to the Fourier component of the streamfunction with the wavenumber of the

third wave. This correction has neither the same phase nor the same vertical structure as the neutral mode of that wavenumber so that the sum of the neutral wave plus the correction term exhibits a small, $O(\varepsilon)$, phase shift between the upper and lower layer streamfunctions. This is precisely the condition that the wave must satisfy if it is to have a non-zero heat flux associated with it, the latter being proportional to $\phi_1\phi_{2x}$. In the absence of any meridional temperature gradient (or equivalently, vertical shear) in the basic state, this heat flux does no work and so the triad as a whole neither gains nor loses energy. However, when we have a meridional temperature gradient, the triad members can exchange energy with the mean state. Such exchanges can be either oscillatory, as when M_0, M_1 and M_2 have differing signs, or can lead to a net extraction of energy from the mean state, when M_0, M_1, and M_2 have the same sign.

By projecting the potential vorticity equations onto the three wavenumbers of the triad elements and then multiplying by that Fourier component of the streamfunction, we can obtain equations for the energy balance of each Fourier component of the form

$$\partial_t E_j = v_j + T_j \tag{4.13}$$

Here $E_j = \frac{1}{2}\int_0^1 dy\ \overline{|\nabla^{(j)}\phi_1|^2 + |\nabla^{(j)}\phi_2|^2 + F\,(^{(j)}\phi_1 - {}^{(j)}\phi_2)^2}$ is the energy of the Fourier component, $^{(j)}\underset{\sim}{\phi}$.

$v_j = FU\int_0^1 dy\ \overline{{}^{(j)}\phi_1\,{}^{(j)}\phi_{2x}}$ is the rate at which the j^{th} component exchanges energy with the mean flow and

$$T_j = \int_0^1 dy \ \overline{{}^{(j)}\phi_1 \, J_{(j)}(\phi_1, q_1)} + \int_0^1 dy \ \overline{{}^{(j)}\phi_2 \, J_{(j)}(\phi_2, q_2)}$$

is the rate at which the j^{th} Fourier component exchange energy directly with the other wave components. $J_{(j)}(a,b)$ is the projection of $J(a,b)$ onto $e^{ik_j x}$.

E_j is of $O(\varepsilon^2)$ while v_j and T_j are of $O(\varepsilon^3)$. E_j is changing on the long time scale $O(\varepsilon^{-1})$. If we rescale, E_j, v_j and T_j to be $O(1)$ (4.13) becomes

$$\partial_T E_j = v_j + T_j \ .$$

To leading order the scaled $E_j = 1/2\,[n_j^2 \pi^2 + k^2 + F(1-\gamma_j)^2]|A_j|^2$ and its rate of change may be calculated explicitly, using the amplitude equations, to be

$$\partial_T E_j = M_j \,[n_j^2 \pi^2 + k^2 + F(1-\gamma_j)^2] \ I_m (A_0 A_1 A_2) \tag{4.14}$$

One can also calculate v_j and T_j to leading order. These are

$$T_j = \frac{\pi}{2} I_m (A_0 A_1 A_2)(k_m n_1 - k_1 n_m)$$

$$\times \left[(\beta - FU)\left(\frac{1}{c_1} - \frac{1}{c_m}\right) \gamma_j \gamma_1 \gamma_m - (\beta + FU)\left(\frac{1}{U-c_1} - \frac{1}{U-c_m}\right) \right] \tag{4.15}$$

$$v_j = \frac{\pi}{2} I_m (A_0 A_1 A_2)(k_m n_1 - k_1 n_m) \frac{(\beta^2 - F^2U^2)}{c_j^2 (U-c_j)^2} \gamma_j \, U \left[\frac{\beta + FU}{(U-c_j)^2} + \frac{\gamma_j^2}{c_j^2}(\beta - FU) \right]^{-1}$$

$$\times \left[\gamma_1 \gamma_m \left(\frac{c_j}{c_m} - \frac{c_j}{c_1}\right) - \gamma_j \left(\frac{U-c_j}{U-c_m} - \frac{U-c_j}{U-c_1}\right) \right] \tag{4.16}$$

One can verify directly that $T_j+v_j = \partial_T E_j$. Note that although Im $(A_0A_1A_2)$ occurs as a common factor, a three-wave state in which the sum of the phases of A_0, A_1, and A_2 is an integer multiple of π cannot be a steady amplitude solution when M_0, M_1, and M_2 are all of the same sign. (When M_0, M_1, and M_2 have differing signs, one can find such constant amplitude solutions in which the phases of A_0, A_1, and A_2 are steadily rotating.)

Thus far we have noted a possible mechanism for triad growth and explained that this cannot occur unless the triad is such that M_0, M_1, and M_2 each have the same sign. We have not yet shown that it is possible to find triads which satisfy this condition.

2.1.5: An Example of an Unstable Triad

To establish the existence of an unstable resonant triad, we must first locate a resonant triad using the dispersion relation of the linear problem in conjunction with the resonance conditions (4.10), and then calculate the values of M_j using the formula (4.12). This is a little tedious, but if we do so, we can readily find examples of unstable triads. We will give one example here.

For the choice F = 20.0, U = 1.0, β = 14.14, one can verify, from the dispersion relations that the following wavenumbers correspond to a resonant triad:

Wave 0:	k = -1.90624,	n = 1,	m = -1
Wave 1:	k = 5.27,	n = 1,	m = -1
Wave 2:	k = -3.36376,	n = -2,	m = +1

To distinguish between the two possible vertical modes corresponding to the choice of sign for the root in the dispersion relation (4.3), we have specified a "vertical wavenumber", m, equal to ± 1 where the sign matches that chosen in the dispersion relation. Using (4.2) one can calculate the interaction coefficients, these take the values,

$$M_0 = 10.381, \qquad M_1 = 4.740, \qquad M_2 = 1.745$$

Each of these is positive, so this triad is an unstable triad.

In view of the algebra involved it would be reassuring to have an independent test of the results. Such a check was made as follows. Using a simple spectral scheme, the non-linear, quasigeostrophic potential vorticity equations were integrated directly after limiting the zonal Fourier spectrum to just three wavenumbers, the three listed above. The initial conditions used specified amplitudes for the three waves of the form

$$\begin{aligned} A_0 &= 2^{1/2}\, N\, e^{i\pi/2} \\ A_1 &= (M_1/M_0)^{1/2}\, N \\ A_2 &= (M_2/M_0)^{1/2}\, N \end{aligned} \tag{5.1}$$

where N was chosen to be

$$N = [\ln (2^{1/2} + 1)/(M_1 M_2)^{1/2}] \times 10^{-3} \tag{5.2}$$

The small amplitude theory of Section 2.1.2 predicts that, for initial amplitudes of the form (5.1), the trajectories controlled by (2.1) will become singular at a time T_s given by (2.12). Substituting (5.1) in

(2.12) and setting the initial time equal to zero, yields

$$T_s = (M_1 M_2)^{-1/2} \; N^{-1} \; \ln (2^{1/2} + 1)$$

In view of (5.2) this means that $T_s = 1000$. Since T_s is significantly larger than the periods of the neutral waves, which for the chosen triad are $T_0 = 10.073$, $T_1 = 6.660$ and $T_2 = 4.009$, we can expect that the numerical results will start by following the asymptotic theory. Differences between the full integration and the small amplitude theory should only become apparent when the wave amplitudes, which are initially $O(10^{-3})$, become $O(1)$.

Figure 2.2 shows the results of the numerical integration over the interval $0 \leq T \leq 950$. The quantity plotted is the total energy of the perturbation. The results seem to bear out the prediction of the small amplitude theory rather well, the difference between the numerical and the asymptotic results being less than one percent at $T = 950$.

An interesting feature of this triad is that the total square wavenumber of wave 2, namely $(3.36376)^2 + 4\pi^2 = 50.793$ is larger than $2F$ ($2F = 40$) and so this wave lies outside the range of waves that are unstable according to linear theory, even when $\beta = 0$. The triad instability allows not only stronger growth than the linear theory but also a larger range of wavenumbers that can extract energy directly from the mean flow.

2.1.6: The Range of Unstable Wavenumbers

Because of the algebraic complexity, both of the resonance conditions and of the formulae for the interaction coefficients, it is difficult to

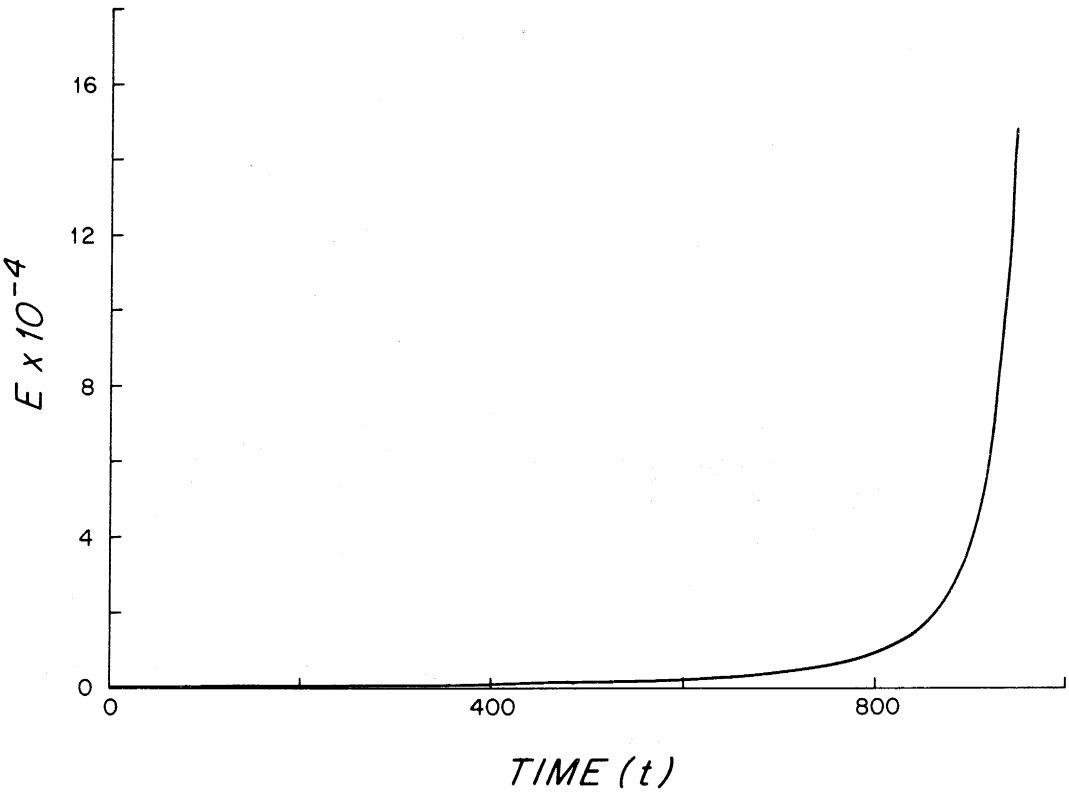

Figure 2.2: The evolution of the total perturbation energy of an unstable neutral wave triad over the interval $0 < T < 950$. The triad is the one discussed in the text and the figure shows the results of a numerical integration of the potential vorticity equations.

calculate the extent of the range of wavenumbers that can be involved in unstable triads. Instead, we have chosen to map the extent of the unstable domain in the case of two particular triads as an example of what one might expect. This was done by fixing F = 20.0 and U = 1.0, choosing a value of β between zero and the maximum value at which the triad instability can occur, $\beta_m = FU = 20$, choosing a particular trio of meridional wavenumbers and vertical structures, and then computing the locus of resonant triads formed by these waves as one varies the zonal wavenumbers. At the same time, the interaction coefficients were also calculated. The regions in which one can find unstable resonant triads of linearly neutral modes were then mapped on a plane whose coordinate axes correspond to total, squared, horizontal wavenumber, and β. These maps are shown in Figures 2.3 and 2.4. The marginal curve of linear theory is also shown.

In Figure 2.3, the waves making up the triad have the following vertical and meridional structures:

Wave 0	n = 1	m = -1
Wave 1	n = 1	m = -1
Wave 2	n = -2	m = +1

In Figure 2.4, the vertical and meridional structures used were

Wave 0	n = 1	m = -1
Wave 1	n = 2	m = +1
Wave 2	n = -3	m = -1

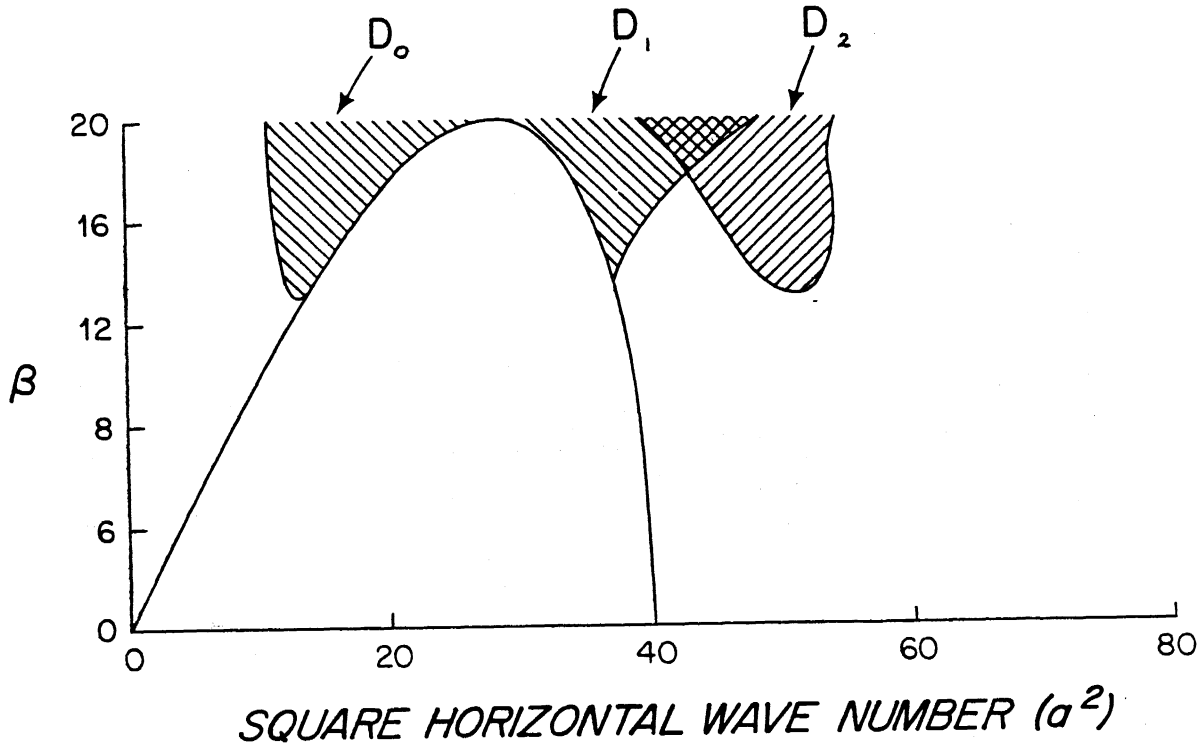

Figure 2.3: A map of the areas in the (β , a^2) plane in which may be found neutral Rossby waves that are elements of an unstable triad in which the waves have meridional structures given by n = (1,1,-2). The vertical structures of the three waves are assumed to be given by m = (-1,-1,1). Three regions are shown shaded, two of which overlap. Region D_j corresponds to possible values of a_j^2. Given a particular value of β, for each choice of a_j^2 in D_j one can find a pair of values (a_k^2 , a_l^2) lying in D_k X D_l ([j,k,l] = a cyclic permutation of [0,1,2]) which complete an unstable resonant triad. Note, for $\beta < 12.95$, there are no unstable triads with this meridional and vertical structure.

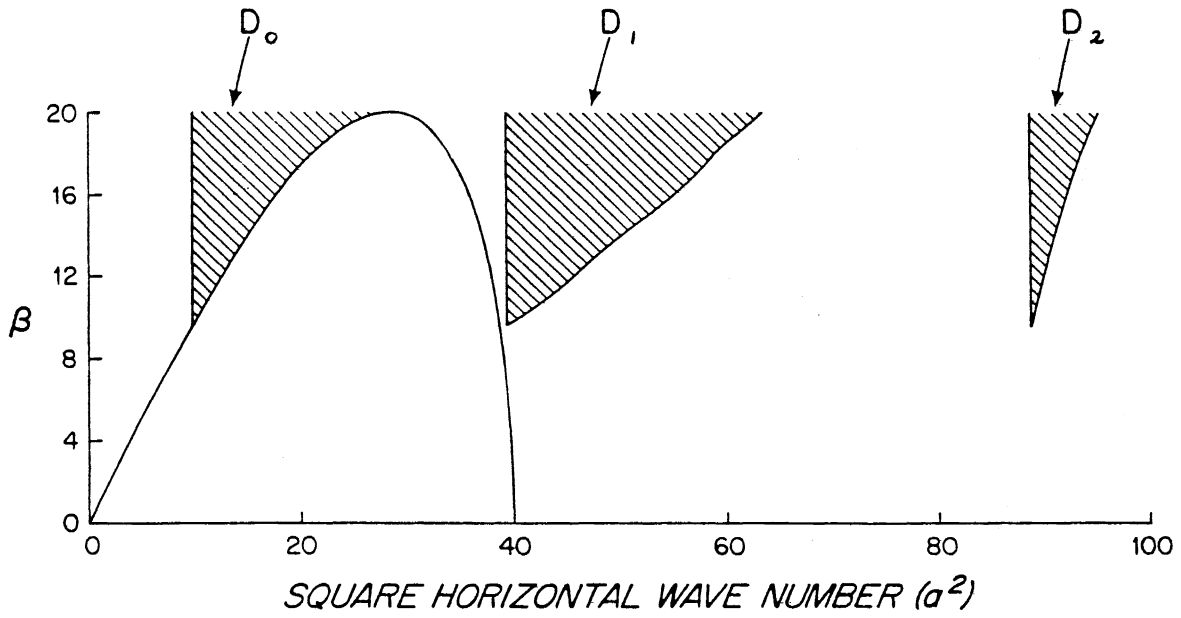

Figure 2.4: A similar map to that in Fig. 2.3, but with n = (1,2,3) and m = (-1,-1,1).

For each wave, a range of total wavenumbers that can be involved in an unstable triad is marked on the appropriate figure. For each choice of wavenumber in the unstable domain marked for a particular wave, one can find an unstable triad for which the horizontal wavenumber of that wave has the value chosen. The horizontal wavenumbers of the remaining waves will then lie somewhere within the unstable domains marked for those waves.

The distinctive feature of these plots is that the range of unstable wavenumbers for the triad instability extends beyond the short wave cutoff of the linear f-plane theory. Since the cases considered are merely arbitrarily chosen examples, it is likely that there are unstable triads, with different vertical and meridional structures, for which the range of unstable wavenumbers extends even further into the short wave region.

2.1.7: Concluding Remarks

Linear theories of baroclinic instability overlook a class of nonmodal instabilities which depend on weak non-linear interactions between "neutral modes" of the linear theory for their ability to extract potential energy from the basic flows. These take the form of a growing triad of waves whose rate of increase is "faster than exponential", until the triad amplitudes reach O(1) levels at which the small amplitude theory becomes invalid. These instabilities can be triggered by initial conditions of arbitrarily small amplitude although, unlike linear instabilities, the growth rates are proportional to the disturbance amplitudes and so are at first very small, if the initial conditions are weak.

Although they are non-linear in nature, it seems likely that this class of instability is obedient to the Charney-Stern criterion for

stability. Thus, for the two-layer model considered, the triad instability can only exist when linear instability also exists. It remains an open question whether there exist other forms of non-linear instability which are not constrained by the Charney-Stern result. For any such instabilities, there will probably be an amplitude threshold that must be exceeded before growth can occur.

Of the two types of instability, the growth of linearly unstable modes with O(1) e-folding time scales can be expected to overshadow the triad form of instability. Crudely speaking, if one starts with initial amplitudes of $O(\varepsilon)$, then the linear mode will reach an O(1) amplitude in a time of $O[\ln(1/\varepsilon)]$, while the non-linear instability will take a time of $O(\varepsilon^{-1})$ to achieve the same result. Triad instability, at least in the particular model discussed here, is of only secondary physical importance. However, it remains an interesting phenomenon by virtue of the novel mechanism responsible for the instability and of the more extensive range of wavenumbers that may be excited.

Because of the quantization of zonal wavenumbers present in annular models of baroclinic instability, it is only in very special cases that one would expect to see such triad instabilities. However, for a basic flow in which the zonal scale is much larger than the internal deformation radius, one might expect such instabilities to occur. This has some consequences for attempts to numerically follow the finite amplitude evolution of an initial disturbance to such a flow when the flow is only weakly supercritical. In a spectral model of such evolution, the practical requirement that one truncate the zonal wavenumber spectrum effec-

tively imposes an artificial quantization condition which may go some way towards suppressing such instabilities.

Although non-modal instability has been discussed here in the context of a baroclinic model, there seems to be no reason why growing triads cannot occur in cases of barotropic shear flow.

For a particular triad, the domain of instability is bounded. In effect, there is a boundary analogous to the marginal curve of the linear instability problem. For triads only slightly inside this boundary, the flow is, in a sense, only slightly supercritical and the growth of the triad should be less intense. We may, therefore, be able to construct a finite amplitude theory of weakly growing triads, analogous to theories describing the weakly finite amplitude evolution of linear instabilities, such as that of Pedlosky (1970). It will be interesting to discover whether alterations to the mean flow become significant for slightly supercritical triads and whether it is possible to find equilibrated solutions. For triads that are a O(1) distance from a stability boundary, the corrections to the mean flow that are induced by the growing waves are unimportant until the triad amplitudes become of O(1).

2.2: Interactions Between Two Neutral Modes and a Weakly Unstable Mode Away From Minimum Critical Shear

Loesch (1974) demonstrated that a slowly growing unstable mode that lay close to the marginal curve but at a point some distance from minimum critical shear, could interact with a pair of neutral waves, via a resonant triad interaction, on the same time scale as that of the former's interaction with the mean flow. This situation was not, however, consid-

ered in detail. We take up this topic again here because we are curious about the "stability" of the equilibration mechanism studied by Pedlosky (1970). As we noted in Chapter 1, in that work Pedlosky demonstrated that a slowly growing mode could be equilibrated as a result of the changes in the mean flow wrought by the evolution of the unstable wave. This is a rather important demonstration: The question we wish to pose here is, how this equilibration is affected by the presence of neutral Rossby waves. We will show in this section that, away from minimum critical shear, the presence of Rossby waves can destabilize this equilibration process. However, in the more physical case in which the unstable wave lies close to minimum critical shear, which we shall consider in Section 2.3, we shall see that this sort of destabilization seems unlikely.

2.2.1: Evolution Equations

The two-layer model we will use is exactly the same version of Phillips' model as that used in Section 2.1, the potential vorticity equations for which were given by (4.1) in Section 2.1.4. We will consider a disturbance dominated by three zonal Fourier components. The leading order part of each of these will correspond to a normal mode of the linear system and the amplitudes will be taken to be small so that non-linear interactions between the components are weak (although non-negligible). We choose a value of β that is less than the maximum critical β (β_m say) for instability, and decompose this as

$$\beta = \beta_c - \Delta \qquad (1.1)$$

Here β_c is O(1), $0 < \Delta << 1$ and $\beta_c < \beta_m$. We take one of the principal zonal wavenumbers, k_0, to correspond to a mode which is marginal when $\beta = \beta_c$ so that for the value of β given in (1.1) this mode is slightly supercritical with a growth rate of $O(\Delta^{1/2})$. The remaining two principal zonal wavenumbers, k_1 and k_2, we take to correspond to neutral waves lying a O(1) distance from the marginal curve.

The evolution time scale of the slowly growing wave is $O(\Delta^{-1/2})$ so we define a slow time variable, $T = \Delta^{1/2} t$, and treat the perturbation quantities as functions of both t and T. We therefore replace ∂_t by $\partial_t + \Delta^{1/2} \partial_T$. Loesch showed that the natural scales for the three waves were as follows: the amplitude of the unstable wave should scale as $\Delta^{1/2}$, while the amplitudes of the sidebands scale as $\Delta^{3/4}$.

With our definitions of β and the time variables, the potential vorticity equations become

$$\begin{aligned} (\partial_t + U\partial_x)\, q_1 + (\beta_c + FU)\, \phi_{1x} &= -\Delta^{1/2}\, \partial_T\, q_1 - J(\phi_1, q_1) + \Delta\, \phi_{1x} \\ \partial_t\, q_2 + (\beta_c - FU)\, \phi_{2x} &= -\Delta^{1/2}\, \partial_T\, q_2 - J(\phi_2, q_2) + \Delta\, \phi_{2x} \end{aligned} \tag{1.2}$$

We expand the streamfunctions in the forms

$$\underset{\sim}{\phi} = \Delta^{1/2}\, {}^{(0)}\underset{\sim}{\phi} + \Delta^{3/4} \sum_{j=1}^{2} {}^{(j)}\underset{\sim}{\phi} + \Delta\, \underset{\sim}{\Phi} + \ldots \tag{1.3}$$

$${}^{(j)}\underset{\sim}{\phi} = \left[A_j(T)\, [{}^{(j)}\psi_1(y), {}^{(j)}\psi_2(y)] + \Delta^{1/2}\, [{}^{(j)}\phi_1^{(1)}(y,T), {}^{(j)}\phi_2^{(1)}(y,T)] \right] e^{ik_j(x - c_j t)} + * \quad \text{for } j = 0, 1, 2$$

In what follows, we obtain equations for the evolution of the A_j's. These may be found as Equations (1.15) below. We assume that the three principal waves are resonant and that their wavenumbers and phase speeds satisfy the following relations

$$\sum_{j=0}^{2} (k_j, k_j c_j) = (0, 0) \tag{1.4}$$

A third constraint, which deals with the meridional structures of the waves, must also be satisfied for the resonance to occur. This will be discussed later. We make the assumption that combinations of the wavenumbers and frequencies other than those appearing on the left side of (1.4) do not simultaneously sum to zero and satisfy the meridional constraint, an assumption that will generally be true. The non-linear terms in the vorticity equations will give rise to both resonant and non-resonant forcing. We have neglected the non-resonantly forced components in writing the streamfunction expansions (1.3) as these do not affect the evolution of the A_j's on the $O(\Delta^{-1/2})$ time scale.

We substitute (1.3) into the vorticity equations (1.2) and obtain a series of differential problems at different orders in Δ. At $O(\Delta^{1/2})$ we have a linear problem for the meridional structure of the unstable wave

$$\begin{aligned}
&(U - c_0)\,[(\partial_y^2 - k_0^2 - F)\,{}^{(0)}\psi_1 + F\,{}^{(0)}\psi_2] + (\beta_c + FU)\,{}^{(0)}\psi_1 = 0 \\
&-c_0\,[(\partial_y^2 - k_0^2 - F)\,{}^{(0)}\psi_2 + F\,{}^{(0)}\psi_1] + (\beta_c - FU)\,{}^{(0)}\psi_2 = 0
\end{aligned} \tag{1.5}$$

whose solution is

$${}^{(0)}\underset{\sim}{\psi} = (1, \gamma_0)\ \sin n_0 \pi y$$

$$\frac{c_0}{U} = \frac{1}{2} - \frac{\beta_c}{FU} \frac{(a_0^2/F + 1)}{a_0^2/F\,(a_0^2/F + 2)}$$

$$\gamma_0 = \frac{a_0^2}{F} + 1 - \frac{\beta_c/FU + 1}{1 - c_0/U}$$

where $a_0^2 = k_0^2 + n_0^2 \pi^2$. We will restrict our attention to the case where the marginal mode has the gravest possible meridional structure, $n_0 = 1$.

At this order, the perturbation potential vorticity associated with this Fourier component is given by

$$({}^{(0)}q_1, {}^{(0)}q_2) = \left(- \frac{\beta_c + FU}{U - c_0} \, {}^{(0)}\phi_1, \frac{\beta_c - FU}{c_0} \, {}^{(0)}\phi_2 \right)$$

$$= \left(- \frac{\beta_c + FU}{U - c_0}, \frac{\beta_c - FU}{c_0} \, \gamma_0 \right) A_0 \sin n_0 \pi y \; e^{ik_0(x - c_0 t)} + *$$

At $O(\Delta^{3/4})$ we find a linear problem for the meridional structure of the two neutral waves. Their modal structure is given by

$${}^{(j)}\underset{\sim}{\psi} = (1, \gamma_j) \sin n_j \pi y$$

$$\frac{c_j}{U} = \frac{1}{2} - \frac{1}{a_j^2/F\,(a_j^2/F + 2)} \left[\frac{\beta_c}{FU} \left(\frac{a_j^2}{F} + 1 \right) + m_j \left[\frac{\beta_c^2}{F^2 U^2} - \frac{a_j^4}{F} \left(1 - \frac{1}{4} \frac{a_j^4}{F} \right) \right]^{1/2} \right]$$

$$\gamma_j = a_j^2/F + 1 - \frac{\beta_c/FU + 1}{1 - c_j/U}$$

Note that m_j is a quantity analogous to a vertical wavenumber in this low vertical resolution system. It may take either of the values ± 1 and one is free to choose which. Having arranged the zonal wavenumbers so that the resonance conditions are satisfied for a particular choice m_j, one will not in general be able to satisfy the resonance conditions with the alternative m_j.

The meridional structures of the principal waves are trigonometric, a consequence of the meridional uniformity of the basic state. In order that the non-linear interaction product of two waves should have a non-zero projection onto the third wave, an additional resonance condition must be satisfied. There are several equivalent forms for this. We will take it to be

$$\sum_{j=0}^{2} n_j = 0 \quad .$$

We will jump ahead of ourselves a little and consider the vorticity equations at $O(\Delta^{5/4})$. After projecting onto the Fourier component $e^{ik_j x}$ $(j = 1,2)$ we obtain

$$L_j \underset{\sim}{{}^{(j)}\phi^{(1)}} = \frac{1}{ik_j}$$

$$\left\{ \begin{array}{l} \frac{1}{U-c_j}\left[- \partial_T {}^{(j)}q_1^{(0)} - J_{(j)}({}^{(0)}\phi_1^{(0)}, {}^{(j')}q_1^{(0)}) - J_{(j)}({}^{(j')}\phi_1^{(0)}, {}^{(0)}q_1^{(0)}) \right] \\ \frac{1}{-c_j}\left[- \partial_T {}^{(j)}q_2^{(0)} - J_{(j)}({}^{(0)}\phi_2^{(0)}, {}^{(j')}q_2^{(0)}) - J_{(j)}({}^{(j')}\phi_2^{(0)}, {}^{(0)}q_2^{(0)}) \right] \end{array} \right\}$$

where $j' = 3 - j,$

$J_{(j)}(a,b)$ is the projection of $J(a,b)$ onto $e^{ik_j x}$

and

$$L_j(\psi_1, \psi_2) \equiv \begin{Bmatrix} [\partial_y^2 - k_j^2 - F)\psi_1 + F\psi_2] + \frac{\beta c + FU}{U - c_j}\psi_1 \\ [\partial_y^2 - k_j^2 - F)\psi_2 + F\psi_1] - \frac{\beta c - FU}{c_j}\psi_2 \end{Bmatrix}$$

After evaluating the Jacobians, the equation for $^{(j)}\phi^{(1)}$ becomes

$$L_j \underset{\sim}{{}^{(j)}\phi^{(1)}} = \frac{1}{ik_j} \underset{\sim}{{}^{(j)}R} \tag{1.6}$$

where

$$\underset{\sim}{{}^{(j)}R} = \begin{Bmatrix} \frac{\beta c + FU}{(U-c_j)^2} A_{jT} + \frac{\beta c + FU}{U-c_j} \frac{i\pi}{2} A_0^* A_{j'}^* (k_0 n_{j'} - k_{j'} n_0)(\frac{1}{U-c_{j'}} - \frac{1}{U-c_0}) \\ \frac{\beta c - FU}{c_j^2} A_{jT} + \frac{\beta c - FU}{c_j} \frac{i\pi}{2} A_0^* A_{j'}^* \gamma_0 \gamma_{j'} (k_0 n_{j'} - k_{j'} n_0)(\frac{1}{c_{j'}} - \frac{1}{c_0}) \end{Bmatrix}$$

Since L_j is a singular operator (1.8) is soluble only if the forcing satisfies the secularity condition

$$\int_0^1 dy \ (^{(j)}\psi_1 \ {}^{(j)}R_1 + {}^{(j)}\psi_2 \ {}^{(j)}R_2) = 0$$

from which we obtain an equation governing the evolution of A_j, viz.

$$A_{jT} = iM_j A_0^* A_j^* , \tag{1.7}$$

where

$$M_j = \left[\frac{\beta_c + FU}{(U-c_j)^2} + \frac{\beta_c - FU}{c_j^2}\gamma_j^2\right]^{-1} \frac{\pi}{2}(c_0-c_{j'})(k_0 n_{j'} - k_{j'} n_0) \times$$

$$\times\left[\frac{\beta_c + FU}{(U-c_0)(U-c_1)(U-c_2)} - \gamma_0\gamma_1\gamma_2 \frac{\beta_c - FU}{c_0 c_1 c_2}\right] \tag{1.8}$$

The potential vorticity equations at $O(\Delta)$, when projected onto e^{ik_0x} give an equation similar to (1.7) for $\underset{\sim}{\phi}^{(0)}(1)$, namely

$$L_0 \underset{\sim}{\phi}^{(0)}(1) = \frac{1}{ik_0}\left(\frac{-1}{U-c_0}\partial_T q_1^{(0)}, \frac{1}{c_0}\partial_T q_2^{(0)}\right) \tag{1.9}$$

The secularity condition for this is empty, since c_0 corresponds to a marginal wave, and we can proceed to solve for $\underset{\sim}{\phi}^{(0)}(1)$. We normalize this solution by choosing $\phi_2^{(0)}(1) = 0$. Then

$$\phi_1^{(0)}(1) = \frac{1}{ik_0} \frac{\beta_c - FU}{F c_0^2} \gamma_0 A_{0T} \sin n_0 \pi y \ .$$

The linear operator in the full potential vorticity equations involves x and t derivatives at each term and so admits of a homogeneous solution

$$\underset{\sim}{\phi} = \underset{\sim}{\Phi}(y, T)$$

for a $\underset{\sim}{\Phi}$ of arbitrary dependence on y and T. We must include an homogeneous solution of this form at $O(\Delta)$ even though there is no direct forcing for it. We will see that it is indirectly forced by the secularity conditions of the $O(\Delta^{3/2})$ problem.

It is at $O(\Delta^{3/2})$ that the evolution of A_0 is determined. If we consider the $O(\Delta^{3/2})$ part of the potential vorticity equations, we find that the non-linear terms and the slow time derivatives contribute two types of forcing that are resonant to the linear operator. The first of these consists of terms that are independent of x and t while the second type is composed of terms that are proportional to e^{ik_0x}.

Collecting together the terms in the $O(\Delta^{3/2})$ part of the potential vorticity equation that are independent of x we find that

$$0 = - \partial_T Q_1 - n_0\pi \frac{\beta_c + FU}{(U-c_0)^2} \left(|A_0|^2\right)_T \sin 2 n_0 \pi y$$

$$0 = - \partial_T Q_2 - n_0\pi \frac{\beta_c - FU}{c_0^2} \gamma_0^2 \left(|A_0|^2\right)_T \sin 2 n_0 \pi y$$

where $Q_j, \equiv \partial_y^2 \Phi_j + (-1)^j F (\Phi_1 - \Phi_2)$, is the potential vorticity associated with the correction to the mean flow. If we use initial conditions that consist only of the basic state and the three principal waves, then

$$Q_1 = - Q_2 = - n_0\pi \frac{\beta_c + FU}{(U-c_0)^2} \left[|A_0(T)|^2 - |A_0(0)|^2\right] \sin 2 n_0 \pi y$$

Thus

$$\partial_y^2 (\Phi_1 + \Phi_2) = 0$$

We have initial conditions $\Phi_j = 0$ at $T = 0$ and boundary conditions $\partial_y \partial_T \Phi_j = 0$ at $y = 0$ and 1, hence

$$\underset{\sim}{\Phi}_1 = -\underset{\sim}{\Phi}_2$$

$$= \frac{n_0\pi}{2F + n_0^2\pi^2} \frac{\beta_c + FU}{(U - c_0)^2} \left[|A_0|^2 - |A_0(0)|^2\right] \left[\sin 2n_0\pi y - \frac{2n_0\pi}{\sqrt{2F}} \frac{\text{sh}\sqrt{2F}\,(y-1/2)}{\text{ch}\,\sqrt{F}/2}\right]$$

We now go to that part of the $O(\Delta^{3/2})$ potential vorticity equation that is proportional to e^{ik_0x}. This forms a forced linear problem for the $O(\Delta^{3/2})$ correction to $^{(0)}\underset{\sim}{\phi}$ which, abstractly, is

$$L_0\, {}^{(0)}\underset{\sim}{\phi}^{(2)} = \frac{i}{ik_0}$$

$$\left(\begin{array}{l}
\frac{1}{U-c_0}\left[-\partial_T\, {}^{(0)}q_1^{(1)} + \left[\frac{\beta_c + FU}{U - c_2} J_{(0)}({}^{(1)}\phi_1, {}^{(2)}\phi_1) + \frac{\beta_c + FU}{U - c_1} J_{(0)}({}^{(2)}\phi_1, {}^{(1)}\phi_1)\right]\right. \\
\quad \left. - \left[J_{(0)}({}^{(0)}\phi_1^{(0)}, {}^{(0)}q_1^{(1)}) + J_{(0)}({}^{(0)}\phi_1^{(1)}, {}^{(0)}q_1^{(0)})\right] + ik_0\, {}^{(0)}\phi_1^{(0)}\right] \\
\frac{1}{-c_0}\left[-\partial_T\, {}^{(0)}q_2^{(1)} - \left[\frac{\beta_c - FU}{c_2} J_{(0)}({}^{(1)}\phi_2, {}^{(2)}\phi_2) + \frac{\beta_c - FU}{c_1} J_{(0)}({}^{(2)}\phi_2, {}^{(1)}\phi_2)\right]\right. \\
\quad \left. - \left[J_{(0)}({}^{(0)}\phi_2^{(0)}, {}^{(0)}q_2^{(1)}) + J_{(0)}({}^{(0)}\phi_2^{(1)}, {}^{(0)}q_2^{(0)})\right] + ik_0\, {}^{(0)}\phi_2^{(0)}\right]
\end{array}\right)$$

Writing this as $$L_0\, {}^{(0)}\underset{\sim}{\phi}^{(2)} = \frac{1}{ik_0}\, \underset{\sim}{R} \qquad (1.10)$$

and evaluating the several forcing terms we find that

$$R_1 = \frac{1}{U-c_0}\left[-\frac{1}{ik_0}\left(-\frac{(\beta_c^2 - F^2U^2)\gamma_0}{F\,c_0^2\,(U-c_0)} + \frac{\beta_c + FU}{(U-c_0)^2}\right)A_{0TT} \sin n_0\pi y + ik_0A_0 \sin n_0\pi y\right.$$

$$+ \frac{i\pi}{2} (\beta_c + FU) (k_1 n_2 - k_2 n_1) \frac{c_1 - c_2}{(U-c_1)(U-c_2)} A_1^* A_2^* \sin n_0 \pi y$$

$$- ik_0 \left(Q_{1y} + \frac{\beta_c + FU}{U - c_0} \Phi_{1y} \right) A_0 \sin n_0 \pi y \Bigg]$$

$$R_2 = \frac{1}{-c_0} \Bigg[- \frac{1}{ik_0} \frac{\beta_c - FU}{c_0^2} \gamma_0 A_{0TT} \sin n_0 \pi y + ik_0 \gamma_0 A_0 \sin n_0 \pi y$$

$$+ \frac{i\pi}{2} (\beta_c - FU) \gamma_1 \gamma_2 (k_1 n_2 - k_2 n_1) \frac{c_2 - c_1}{c_1 c_2} A_1^* A_2^* \sin n_0 \pi y$$

$$- ik_0 \gamma_0 \left(Q_{2y} - \frac{\beta_c - FU}{c_0} \Phi_{2y} \right) A_0 \sin n_0 \pi y \Bigg]$$

Unlike the $O(\Delta)$ problem, the secularity condition for (1.10) yields a non-trivial relation and provides us with an equation governing the evolution of A_0, namely

$$A_{0TT} = k_0^2 c_i^2 A_0 - K_0 A_1^* A_2^* - N_0 A_0 \left(|A_0|^2 - |A_0(0)|^2 \right) \tag{1.11}$$

where

$$c_i^2 = \left[\frac{\gamma_0^2}{c_0} - \frac{1}{U-c_0} \right] \frac{(U-c_0)^2}{\beta_c + FU} \Bigg/ \left[\frac{1}{U-c_0} + \frac{(a^2 + F) \gamma_0}{F c_0} \right] \tag{1.12}$$

$$K_0 = \frac{\pi}{2} k_0 (k_1 n_2 - k_2 n_1)(c_1 - c_2) \left[\frac{\beta_c - FU}{c_0 c_1 c_2} \gamma_0 \gamma_1 \gamma_2 - \frac{\beta_c + FU}{(U-c_0)(U-c_1)(U-c_2)} \right]$$

$$\times \frac{(U-c_0)^2}{\beta_c + FU} \Bigg/ \left[\frac{1}{u-c_0} + \frac{(a^2 + F)\gamma_0}{F c_0} \right] \tag{1.13}$$

$$N_0 = \frac{1}{2} k_0^2 n_0^2 \pi^2 \frac{1}{F + 2 n_0^2 \pi^2} \frac{U}{\beta_c + a^2 U} \times \tag{1.14}$$

$$\times \left[2 (a^2 - F)(F + 2 n_0^2 \pi^2) + (2F^2 - a^4) \left(1 + 2 \frac{2 n_0^2 \pi^2 / F}{1 + 2 n_0^2 \pi^2 / F} \frac{\tanh (F/2)^{1/2}}{(F/2)^{1/2}} \right) \right]$$

Equations (1.7) and (1.11) form a closed set and determine the evolution of A_0, A_1, and A_2. For ease of reference, we collect them here.

$$\left.\begin{aligned} A_{0TT} &= k_0^2 c_i^2 A_0 - K_0 A_1^* A_2^* - N_0 A_0 (|A_0|^2 - |A_0(0)|^2) \\ A_{1T} &= i M_1 A_0^* A_2^* \\ A_{2T} &= i M_2 A_0^* A_1^* \end{aligned}\right\} \tag{1.15}$$

In the latter two equations of this set we recognize relations that are typical of the usual form of triad interactions between neutral waves. The first equation is similar to the equation governing the amplitude of a weakly growing wave in the single-wave theory, modified only by the inclusion of a forcing term arising from the non-linear interaction between the two sidebands, $- K_0 A_1^* A_2^*$. The constants N_0 and $k_0^2 c_i^2$ are independent of the choice of sidebands. They are the same constants that occur in the

evolution equation of single-wave theory for a slowly growing mode at wavenumber k_0.

2.2.2: Asymptotically Unstable Trajectories

From the single-wave theory of Pedlosky (1970), we know that the term $-N_0 A_0 (|A_0|^2 - |A_0(0)|^2)$ in (1.15a) represents the stabilizing effect of the alteration to the mean flow produced by the growth of the unstable wave. In the single wave theory, this effect is sufficient to ensure that A_0 remains bounded and causes A_0 to vacillate in a regular, periodic fashion. One might wonder whether the inclusion of the interaction with the sidebands, i.e., $-K_0 A_1^* A_2^*$, can destabilize this equilibration process and lead to an unbounded increase of A_0 (within the current ordering scheme). We will show that for this system, such a finite amplitude instability is indeed possible.

Although the system of equations (1.15) looks fairly simple it is difficult to obtain a general analytical solution. What we shall do in this section is show that there are solution trajectories which approach infinity and find the large-amplitude asymptotic form of these. In Section 2.2.3, we shall give an example of a numerical integration of (1.15) which exhibits a finite-amplitude instability and tends asymptotically to such a trajectory. This establishes that the unstable trajectories have some non-zero domain of attraction and hence represent a non-trivial finite amplitude instability.

We will look for trajectories along which A_0, A_1 and A_2 approach infinity as T approaches some finite value T_0 from below. We further assume

that, asymptotically, the A_j's behave like inverse algebraic powers of (T_0-T). For simplicity, we will suppress unnecessary constants and minus signs by shifting the temporal origin to T_0 and reversing the sense of time. Under this transformation we seek instability as T --> 0 from above. The backwards equations are

$$\begin{aligned} A_{0TT} &= \sigma^2 A_0 - K_0 A_1^* A_2^* - N_0 A_0 (|A_0|^2 - |A_0(0)|^2) \\ A_{1T} &= - i M_1 A_0^* A_2^* \\ A_{2T} &= - i M_2 A_0^* A_1^* \end{aligned} \tag{2.1}$$

where $\sigma^2 = k_0^2 c_i^2$.

By inspection, the leading order form of unstable trajectories T --> 0+ will be given by

$$\begin{aligned} A_0 &\sim \alpha_0 T^{-1 + i\theta_0} \\ A_1 &\sim \alpha_1 T^{-3/2 + i\theta_1} \\ A_2 &\sim \alpha_2 T^{-3/2 + i\theta_2} \end{aligned} \tag{2.2}$$

where α_0, α_1, α_2 are complex constants and θ_0, θ_1 and θ_2 are real constants. Substitution of (2.2) into (2.1) will provide us with details of the α_j and θ_j appropriate to such trajectories and will furnish constraints which the constant coefficients in (2.1) must satisfy, if unstable trajectories of this type are to be possible. These constraints may be found as inequalities (2.21) and (2.22) below.

Putting (2.2) into (2.1) and retaining only the higher order terms yields

$$\alpha_0 (1-i\theta_0)(2-i\theta_0) T^{-3+i\theta_0} = - K_0 \alpha_1^* \alpha_2^* T^{-3-i(\theta_1+\theta_2)} - N_0 \alpha_0|\alpha_0|^2 T^{-3+i\theta_0}$$

$$\alpha_1 (-\tfrac{3}{2} + i\theta_1) T^{-5/2+i\theta_1} = - iM_1 \alpha_0^* \alpha_2^* T^{-5/2-i(\theta_0+\theta_2)}$$

$$\alpha_2 (-\tfrac{3}{2} + i\theta_2) T^{-5/2+i\theta_2} = - iM_2 \alpha_0^* \alpha_1^* T^{-5/2-i(\theta_0+\theta_1)}$$

Hence

$$\theta_0 + \theta_1 + \theta_2 = 0 \tag{2.3}$$

and setting $\alpha_j = r_j e^{is_j}$, $S = s_0 + s_1 + s_2$, we have

$$(1 - i\theta_0)(2-i\theta_0) + K_0 \frac{r_1 r_2}{r_0} e^{-iS} + N_0 r_0^2 = 0 \tag{2.4}$$

$$(-\tfrac{3}{2} + i\theta_1) = M_1 \frac{r_0 r_2}{r_1} e^{-i(S + \pi/2)} \tag{2.5}$$

$$(-\tfrac{3}{2} + i\theta_2) = M_2 \frac{r_0 r_1}{r_2} e^{-i(S + \pi/2)} \tag{2.6}$$

From (2.5) and (2.6) we have that $\theta_2 = \theta_1$, and we see that one of the restrictions on coefficients is that M_1 and M_2 must have the same sign. Define sign variables v_0 and v_1 by

$$K_0 = v_0 |K_0|$$

$$M_1 = v_1 |M_1|$$

and set $\Gamma e^{i\gamma} = (-3/2 + i\theta_1)$, then (2.5) and (2.6) become

$$\Gamma e^{i\gamma} = |M_1| \frac{r_0 r_2}{r_1} e^{-i(S+v_1\pi/2)}$$

$$\Gamma e^{i\gamma} = |M_2| \frac{r_0 r_1}{r_2} e^{-i(S+v_1\pi/2)}$$

whence

$$\gamma + S + v_1 \pi/2 = 2n\pi \tag{2.7}$$

$$r_0^2 = \Gamma^2/M_1 M_2 \tag{2.8}$$

$$r_2 = \frac{r_1}{|M_1|} \frac{\Gamma}{r_0} \tag{2.9}$$

Returning to (2.4), it follows that

$$(2 - 4\theta_1^2 + N_0 r_0^2) + 6 i\theta_1 = - K_0 \frac{r_1 r_2}{r_0} e^{-iS}$$

and hence

$$\mathcal{F} e^{if} \equiv \left(2 - 4\theta_1^2 + \frac{N_0^2}{M_1 M_2}\right) + 6 i\theta_1 = r_1^2 \frac{|M_2||K_0|}{\Gamma} e^{-i(S+\pi/2+v_0\pi/2)}$$

or

$$f + S + \frac{\pi}{2} + v_0 \frac{\pi}{2} = 2n'\pi \tag{2.10}$$

and

$$r_1^2 = \frac{\mathcal{F}\Gamma}{|M_2|\,|K_0|} \tag{2.11}$$

From (2.7) and (2.10) we see that

$$f = \gamma - \frac{\pi}{2} + (v_1 - v_0)\frac{\pi}{2} + 2n''\pi \tag{2.12}$$

whether K_0 has the same sign as, or the opposite sign to that of M_1, (2.12) is of the form

$$f = \gamma - \frac{\pi}{2} + m\pi$$

for some integer m and hence

$$\tan f = -\cot \gamma \tag{2.13}$$

Using the definitions of f and γ, (2.13) affords us an equation determining θ_1, namely

$$(8 - \frac{N_0}{M_1 M_2})\,\theta_1^2 = 2 + \frac{N_0}{M_1 M_2}\frac{9}{4} \tag{2.14}$$

We have already noted that a necessary requirement for a solution of this form is that $M_1 M_2 > 0$. Equation (2.14) furnishes a second restriction, that

$$-\frac{8}{9} < \frac{N_0}{M_1 M_2} < 8 \tag{2.15}$$

Provided that this holds, we obtain

$$\theta_1 = \pm\left[(2 + \frac{N_0}{M_1 M_2}\ 9/4) \Big/ (8 - \frac{N_0}{M_1 M_2})\right]^{1/2} \tag{2.16}$$

This determines $\mathcal{F}$ and Γ and so by using (2.11), (2.8) and (2.9) we find that

$$r_0 = \left(\frac{20}{M_1 M_2}\right)^{1/2}\left(8 - \frac{N_0}{M_1 M_2}\right)^{-1/2} \tag{2.17}$$

$$r_1 = 2\left(\frac{20}{|M_2|\,|K_0|}\right)^{1/2}\left(8 - \frac{N_0}{M_1M_2}\right)^{-1}\left[\left(2 + \frac{N_0}{M_1M_2}\,\frac{9}{4}\right)\left(8 - \frac{N_0}{M_1M_2}\right)\right]^{1/4} \tag{2.18}$$

$$r_2 = \left(\frac{M_2}{M_1}\right)^{1/2} r_1 = 2\left(\frac{20}{|M_1|\,|K_0|}\right)^{1/2}\left(8 - \frac{N_0}{M_1M_2}\right)^{-1}\left[\left(2 + \frac{N_0}{M_1M_2}\,\frac{9}{4}\right)\left(8 - \frac{N_0}{M_1M_2}\right)\right]^{1/4} \tag{2.19}$$

The three phases θ_0, θ_1 and θ_2 are given by (2.16) and $\theta_2 = \theta_1$, $\theta_0 = -2\theta_1$. The phases s_0, s_1 and s_2 are not uniquely determined by this asymptotic analysis, however, their sum must satisfy

$$\sum_{j=0}^{2} s_j = \tan^{-1}\frac{2\theta_1}{3} - v_1\,\frac{\pi}{2} + 2n\pi \tag{2.20}$$

We have found that trajectories approaching infinity after a finite time can exist when the constants in (2.1) satisfy

$$M_1M_2 > 0 \tag{2.21}$$

and

$$-\frac{8}{9} < \frac{N_0}{M_1M_2} < 8 \tag{2.22}$$

This suggests that the system (2.1) may exhibit a non-linear instability. To confirm this, we must first of all verify that there exist triads which yield values of N_0, M_1 and M_2 that satisfy (2.21) and (2.22). It will then be necessary to show that the unstable trajectories can attract a set of solutions generated by some non-trivial set of initial conditions. The first step is simply a question of solving the linear dispersion relations to find resonant triads and then computing N_0, M_1

and M_2 from the appropriate algebraic formulae. We will take a numerical approach to the second step. If we find initial conditions for which a numerical integration of (2.1), with appropriate values of N_0, M_1, and M_2, yields a solution which approaches a trajectory of the sort discussed above, then we will have established that the unstable trajectories have a non-trivial attractive domain. These steps are taken in Section 2.2.3.

It may at first seem odd that the coefficient K_0 which, in a sense, measures the extent to which the non-linear interaction between the two neutral waves forces the evolution of A_0, does not appear explicitly in the stability conditions (2.21) and (2.22). The term $-K_0 A_1^* A_2^*$ on the right of Equation (2.1a) is clearly necessary, if A_0 is to grow without bound, rather than follow the equilibration of the single-wave theory. We note that, were $K_0 = 0$, we could not deduce (2.10). We also observe that the ratios r_0/r_1 and r_0/r_2 are proportional to $|K_0|$. As we reduce K_0, we reduce the magnitude of A_0 relative to A_1 and A_2, in the neighborhood of the singularity. In addition, because we have used an asymptotic analysis, we have not obtained any expression for the time at which the singularity occurs for a given set of initial conditions. It seems likely that this will depend on K_0 (as well as the other constants) and will increase as $|K_0|$ is decreased.

2.2.3: Examples of Triads Exhibiting Non-linear Instability

We will look at two examples of this triad destabilization of the single wave equilibration process. For ease of reference, we will dis-

tinguish them as examples A and B. In each case, we will follow the same procedure. After choosing the meridional and vertical structures of the two sidebands, we fix β at a subcritical value and determine a pair of zonal wavenumbers for the two neutral modes for which the triad is resonant. We then compute the coefficients σ^2, K_0, M_1, M_2, N_0 and check to see whether (2.21) and (2.22) are satisfied. This was repeated for a number of different values of β, retaining the same choice of meridional and vertical structure for the sidebands. Finally, a particular value of β, for which (2.21) and (2.22) were satisfied, was chosen and the amplitude equations (2.1) were integrated using values of σ^2, K_0, M_1, M_2 and N_0 appropriate to this β. The difference between example A and example B lies in the choices of vertical structure for the sidebands.

The above calculations were performed numerically. In Figures 2.5 and 2.6, we have plotted the values of K_0, M_1, M_2, and N_0 as β is varied, for the two cases. Figures 2.7 and 2.8 then show the evolution of the wave amplitudes under the assumptions of weakly non-linear theory for the particular unstable examples selected.

The meridional and vertical structures for the two cases are:

A: Wave 0 : $n_0 = 1$

Wave 1 : $n_1 = -3$ $\quad m_1 = -1$

Wave 2 : $n_2 = 2$ $\quad m_2 = 1$

B: Wave 0 : $n_0 = 1$

Wave 1 : $n_1 = -3$ $\quad m_1 = 1$

Wave 2 : $n_2 = 2$ $\quad m_2 = -1$

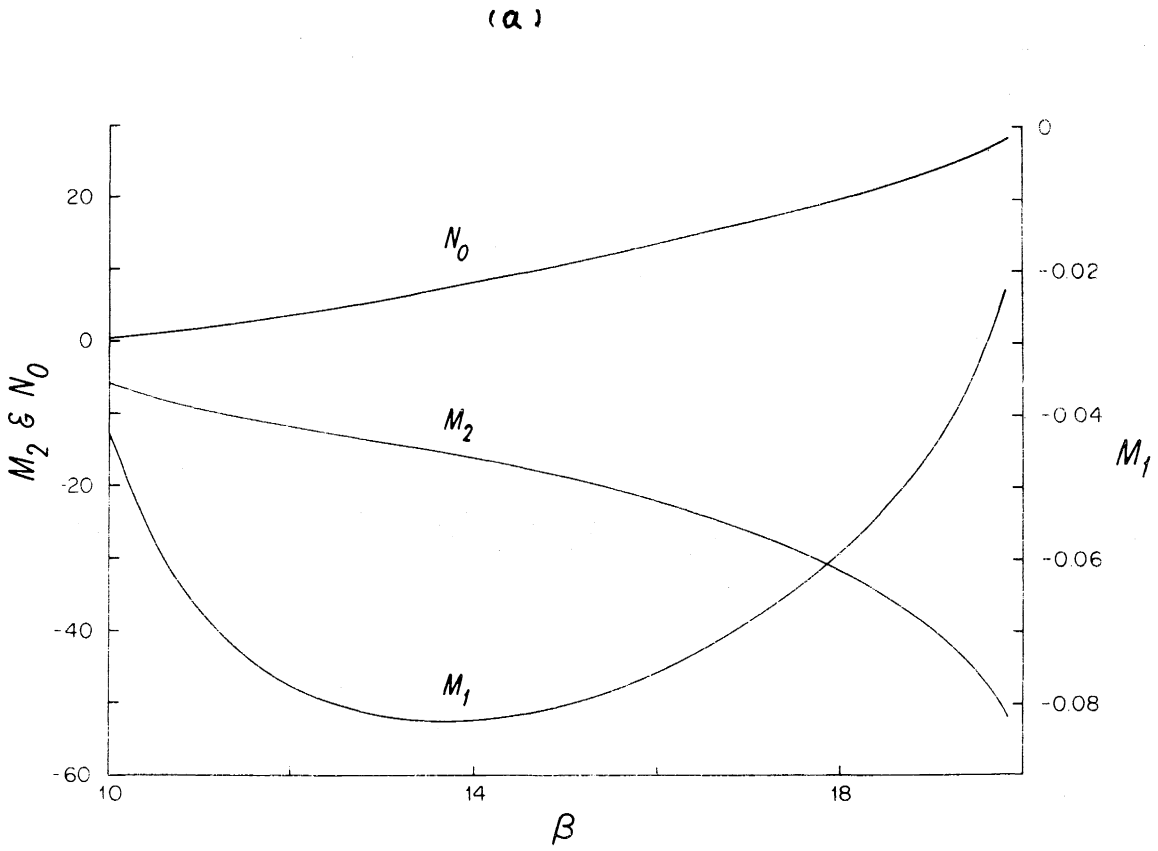

Figure 2.5: a) Plots of M_1, M_2 and N_0 as functions of β for a resonant triad consisting of two neutral modes and a marginal mode. The marginal mode corresponds to the left (long-wave) branch of the marginal curve. The meridional and vertical structures of the triad are n = (1,-3,2) , $m_1 = -1$, $m_2 = 1$ (case A in the text).
b) K_0 as a function of β for the same triad as in Fig. 2.5a.

(b)

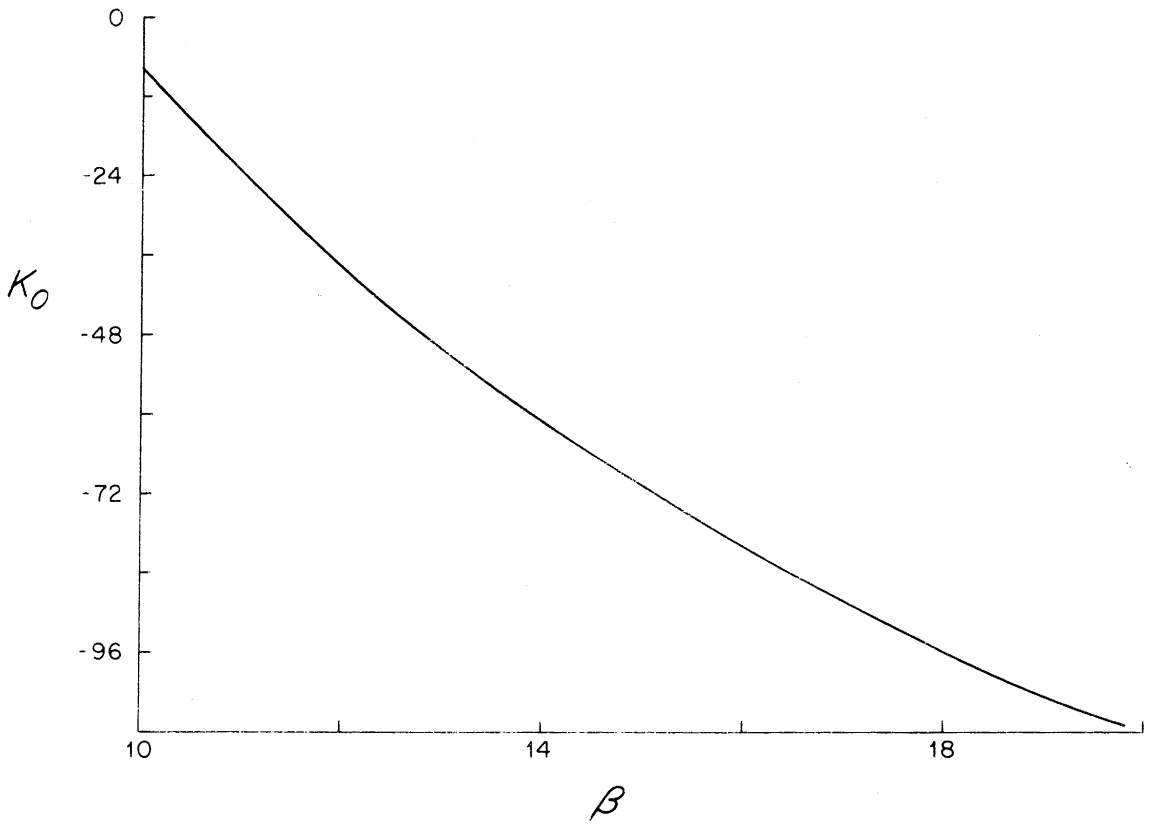

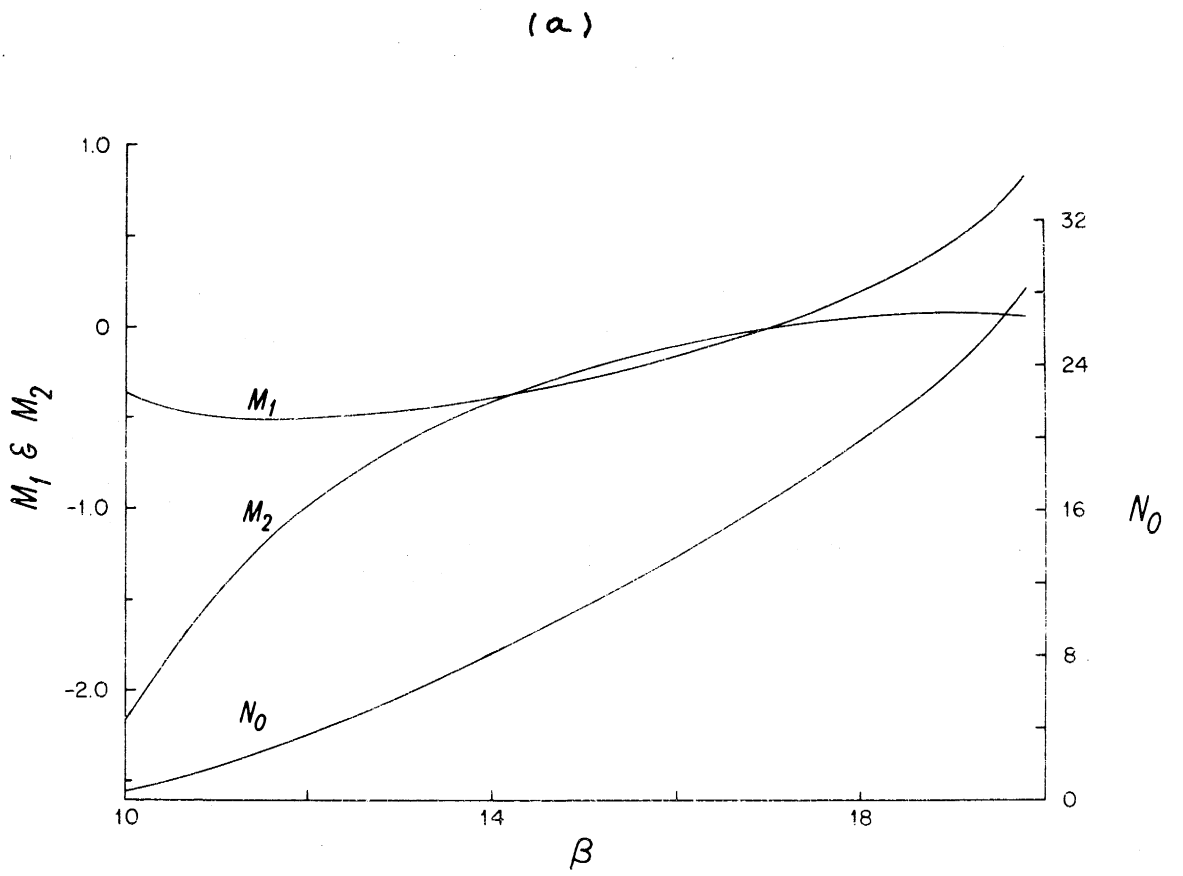

Figure 2.6: a) As in Fig. 2.5a but with neutral modes of different vertical structures ($m_1 = 1$, $m_2 = -1$: case B in the text).
b) K_0 as a function of β for the same triad as in Fig. 2.6a.

(b)

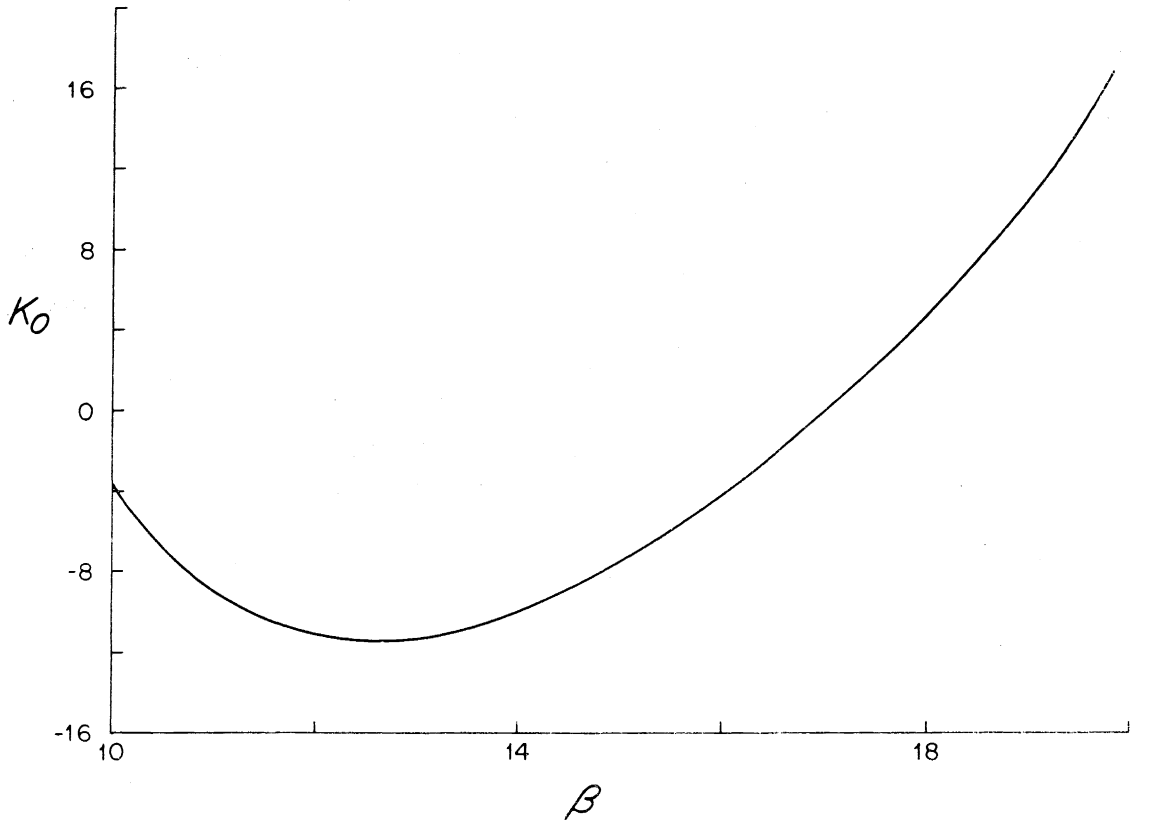

In each case the marginal mode was chosen to lie on the left side of the marginal curve. Given the particular choice of meridional structure this is a necessity, since for this particular triad only wave 0 has an unstable domain that is contiguous to the marginal curve and then only to the left branch of that curve (refer to Figure 2.4). To examine the case in which the marginal mode lies on the right side of the marginal curve, one would have to consider another triad. Figure 2.5 shows how the interaction coefficients vary with β for example A. M_1 and M_2 have the same sign over the entire range plotted, but N_0/M_1M_2 is less than 8 only for values of β less than a threshold value, β_0, of about 15.9. Figure 2.6 is a similar plot for example B.

In example A, when $\beta = 13.0$, the interaction coefficients are:

$$K_0 = -49.49366$$

$$M_1 = -8.193586 \times 10^{-2}$$

$$M_2 = -13.91703$$

$$N_0 = 5.719176$$

while $$\sigma^2 = 7.446278 \times 10^{-2}$$

Using these values, the amplitude equations (2.1), derived with weakly non-linear theory, were integrated numerically. The initial conditions were taken to be

$$A_0(0) = i \times 10^{-2}$$

$$A_1(0) = 1 \times 10^{-2}$$

$$A_2(0) = 1 \times 10^{-2} \qquad (3.1)$$

$$A_{0T}(0) = \sigma A_0(0)$$

The subsequent evolution is shown in Figure 2.7. The solution approaches a singularity after about T = 17.49. The behavior of the solution near this trajectory is similar to that predicted for the asymptotic trajectories of Section 2.2.2. If we set $T_1 = 17.2$, $T_2 = 17.3$, and define $R_j = A_j(T_2)/A_j(T_1)$, then we find that

$$R_0 = 1.54291$$

$$R_1 = 1.91666$$

$$R_2 = 1.91668$$

$$R_1/R_0^{3/2} = 1.00008$$

$$R_1/R_0^{3/2} = 1.00009$$

These latter two ratios are close to unity. For the asymptotic trajectories of 2.2.2 we expect these ratios to approach one as the singularity is approached.

Figure 2.8 represents the evolution of a similar triad corresponding to Case B. We chose $\beta = 11.0$, for which

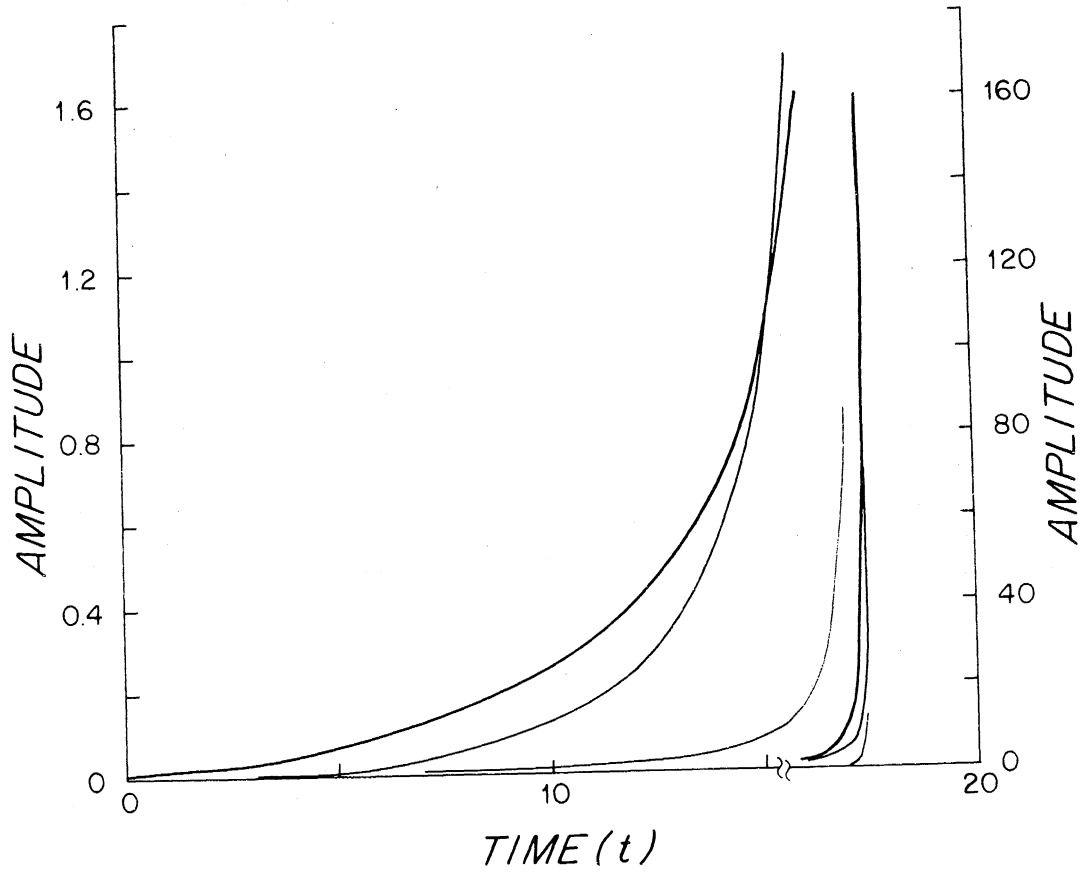

Figure 2.7: An example of the evolution of an unstable triad (case A, $\beta = 13.0$). The amplitudes of each of the three waves is shown. During the early part of the run (up to about T = 16), the scale at the left applies. After about T = 16, the three curves are rescaled to accomodate their rapid growth and one should refer to the right-hand scale.

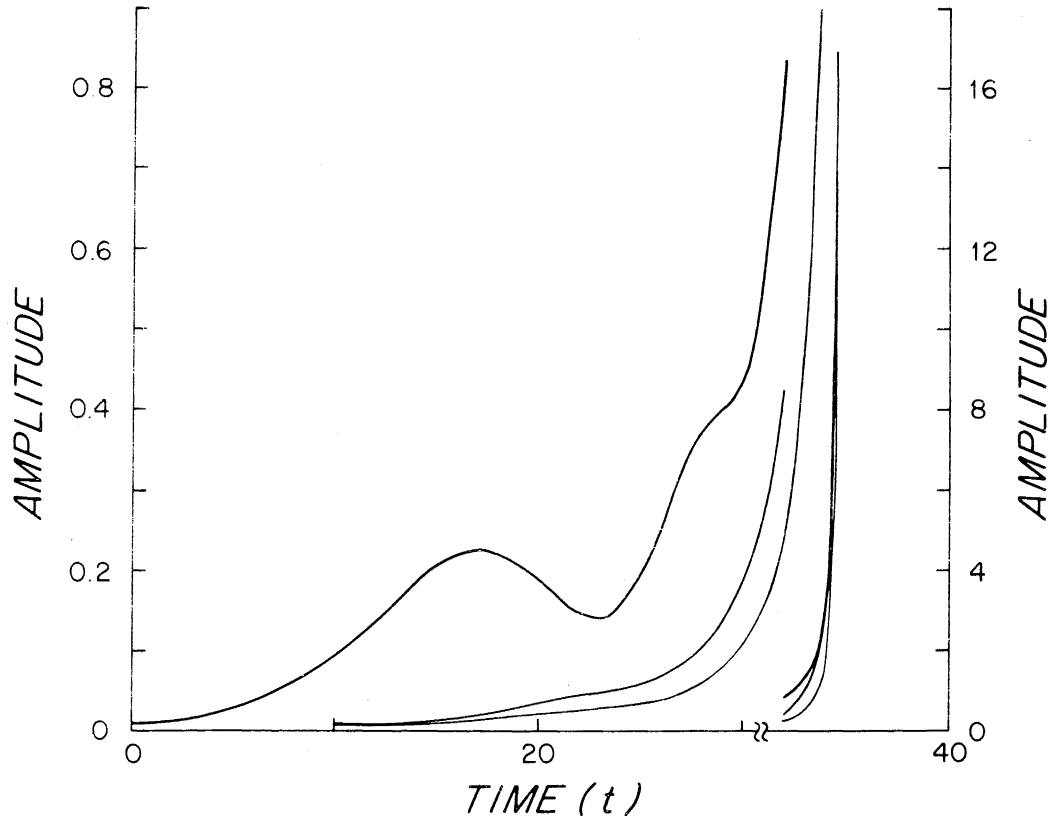

Figure 2.8: Similar to Fig. 2.7 but for case B at $\beta = 11.0$.

$$K_0 = -8.917685$$

$$M_1 = -0.4922978$$

$$M_2 = -1.472019$$

$$N_0 = 1.786117$$

$$\sigma^2 = 4.0630695 \times 10^{-2}$$

The initial conditions used were again those in (3.1). The non-linear growth of all three waves is again apparent.

We have found that the single wave equilibration of a slightly supercritical unstable mode, located well away from minimum critical shear in parameter space, that is produced by the distortion of the mean flow, can be unstable to a multi-wave interaction involving an additional pair of neutral waves. We have also observed that this growth can be rather powerful in that it can force the amplitudes of the three waves involved to become O(1) within the $O(\Delta^{-1/2})$ time scale. At such a stage the weakly finite amplitude analysis becomes invalid.

In view of these results, it would be interesting to discover whether the equilibration process suggested for weakly supercritical instabilities near minimum critical shear, is also unstable. We turn to this question in Section 2.3 below.

2.3 Three-Wave Interactions Near Minimum Critical Shear

We have seen that the equilibration of a weakly growing unstable wave as described by single-wave theory may be unstable to interactions with

sidebands when the basic state does not lie close to minimum critical shear. In addition to weakly growing instabilities, a strongly supercritical flow possesses unstable modes with O(1) growth rates which, unless absent for such reasons as zonal quantization conditions, will tend to dominate the evolution of the flow. A more significant question is whether interactions between a slowly growing mode and neutral waves can produce a non-linear instability that surpasses the ability of the wave-mean flow interaction mechanism to contain it, when the basic flow is only slightly supercritical. For such a flow, all of the unstable modes are weakly growing.

While it is the discovery of the non-linear instability of Section 2.2 which suggests looking at the interaction between a slowly growing wave and a pair of neutral waves in a slightly supercritical flow, we already know that the dynamics of this three-wave problem must differ somewhat from that of the one in Section 2.2. As Loesch (1976) pointed out, the appropriate scaling for the amplitudes of dispersive sidebands in a three-wave interaction near minimum critical shear are $O(\Delta^{1/2})$ rather than $O(\Delta^{3/4})$. This is in part due to the critical layer effect that is manifest at minimum critical shear. Instead of producing a secular forcing term at $O(\Delta)$, the interaction between the two sidebands produces a variable , $O(\Delta^{1/2})$ phase shift between the upper and lower layer streamfunction of the zonal Fourier component with the wavenumber of the unstable wave. This augments the phase shift due to the slow rate of change of the potential vorticity of the leading order part of this Fourier component.

The problem described above is just the one attempted by Loesch (1974), although in our development of it we will endeavor to include the critical layer dynamics described by Pedlosky (1982). Although Loesch omits these, the amplitude equations that he obtains form the core of the extended set of amplitude equations that govern the full system. In view of the consistently stable solutions found by Loesch, one might suspect that the extended system will also be stable.

Amplitude Equations

We will work with the same two-layer model used in earlier sections. We will take the basic flow to be only slightly supercritical and set

$$\beta = FU - \Delta \equiv \beta_m - \Delta \tag{2.3.1}$$

For such a choice of β, only a small, $O(\Delta^{1/2})$, range of wavenumbers is unstable. We will assume $F < 2\sqrt{2}\pi^2$ so that only the gravest meridional mode is unstable, then the unstable range of zonal wavenumbers is centered on k_0 where

$$k_0^2 = \sqrt{2}\,F - \pi^2 \tag{2.3.2}$$

Our aim is to follow the evolution of a trio of waves, each of small amplitude, as they slowly interact. One of these waves will be the slightly unstable mode at $k = k_0$, with a meridional wavenumber $n_0 = 1$. The remaining pair of waves will be neutral Rossby waves whose wavenumbers are such that the triad as a whole is resonant in the sense of Section 2.2. We noted earlier the amplitudes for which the wave-wave interactions, the

wave-mean flow interaction associated with the unstable wave and the growth due to linear instability, all develop on the same time scale. Accordingly expand the streamfunction for the system in the form

$$\underset{\sim}{\phi} = \Delta^{1/2} \underset{\sim}{\phi}^{(0)} + \Delta \underset{\sim}{\phi}^{(1)} + \ldots. \tag{2.3.3}$$

$$\underset{\sim}{\phi}^{(0)} = \sum_{j=0}^{2} {}^{(j)}\underset{\sim}{\phi}^{(0)} = \sum_{j=0}^{2} A_j(T)\,[{}^{(j)}\psi_1(y), {}^{(j)}\psi_2(y)]\, e^{ik_j(x-c_jt)} + *$$

where ${}^{(j)}\psi_1(y)\ e^{ik_j(x-c_jt)}$ are the three linear modes which form our main triad. As before, we expect the amplitudes to vary on a slow time scale, $O(\Delta^{-1/2})$ and have set $T = \Delta^{1/2}t$. As in 2.2, the meridional modal structure is trigonometric with

$${}^{(j)}\underset{\sim}{\psi}(y) = (1, \gamma_j) \sin n_j \pi y$$

The conditions that the triad be resonant are then

$$\sum_{j=0}^{2} (k_j,\ k_j c_j,\ n_j) = (0,\ 0,\ 0) \tag{2.3.4}$$

As is the case at other values of β, there are generally two distinct vertical modes at wavenumbers other than that of the marginal mode. However, at minimum critical shear, one of these modes exhibits a peculiar feature, namely a loss of any dispersive characteristics. At minimum critical shear the dispersion relation may be written

$$c/U = \left[\left(\frac{a^2}{F} + 2\right)\frac{a^2}{F}\right]^{-1}\left[\left(\frac{a^4}{2F^2} - 1\right) \pm \left(\frac{a^4}{2F^2} - 1\right)\right] \qquad (2.3.5)$$

where the choice of sign corresponds to the choice of vertical mode. Choosing the negative sign yields $c = 0$, whatever the value of the horizontal wavenumber a, i.e., a non-dispersive mode. The marginal wave also has this phase speed. This phase speed is the same as the flow speed in the lower layer, which in this treatment has been taken to be zero. Thus, the non-linear interaction between any pair of non-dispersive Rossby waves will produce a resultant that is resonant with a third non-dispersive Rossby wave. For the present, we shall follow Loesch and consider only sidebands that are dispersive neutral modes, i.e., we will take the positive sign in (2.3.5). Loesch shows that when $\pi^2/\sqrt{2} < F < 4\pi^2/\sqrt{2}$ there is just one such pair of dispersive modes that satisfy the resonance conditions.

Having chosen the triad we can substitute the expansion of the streamfunctions into the potential vorticity equations and use a perturbation technique to determine the evolution of the amplitudes of the three main waves. Since the analysis is really just a superposition of that of Loesch (1974) and that of Pedlosky (1982), we will not present it here. We shall just provide the evolution equations that result.

One effect of the non-linear interaction between the marginal wave and each sideband is to produce a forcing term resonant with the other sideband. Much as before, this gives rise to an amplitude equation of the form

$$A_{jT} = iM_j A_0^* A_{j'}^*$$

for each sideband where $j' = 3-j$.

The non-linear interaction of the two sidebands produces a non-resonant forcing of the same wavenumber and frequency as the marginal wave. This, together with the slow rate of change of the potential vorticity of the marginal wave in the upper layer, produces an $O(\Delta^{1/2})$ phase shift between the upper and lower streamfunctions of the Fourier component having the marginal wavenumber. This is an extension of the phase shift observed in linear theory. This phase shift appears as an $O(\Delta)$ correction to the streamfunctions of the marginal wave. Three other corrections to the streamfunction field as a whole are generated at $O(\Delta)$. The first is the familiar zonally independent correction to the mean flow. Unlike the case considered in Section 2.2, this correction is forced by both the weak phase shift associated with the near-marginal wave and the phase shifts associated with the sidebands as a result of their slow changes in amplitude. The difference between the current problem and that of Section 2.2 is that now the sidebands are $O(\Delta^{1/2})$ so that the heat fluxes associated with the sidebands are of the same order as those associated with the slightly unstable wave.

The second correction consists of a collection of non-resonantly forced Rossby waves generated by the non-linear interactions between the three principal waves. Although these are not free modes of the system, their own interaction with the principal waves can produce weak $O(\Delta^{3/2})$ forcing that is resonant. Part of the latter is a component that is

independent of x and t. It is at the $O(\Delta^{3/2})$ level that the structure of the mean flow correction is determined. This component of the forcing contributes to the structure of the mean flow correction. However, forcing of this type only occurs in the potential vorticity equation for the upper layer. The potential vorticity in the lower layer associated with the mean flow correction is independent of the type of forcing discussed here. In so far as determining the evolution of the amplitudes of the three main waves is concerned, we need not explicitly calculate this second type of $O(\Delta)$ correction to the streamfunction fields.

The third correction arises as part of the critical layer dynamics discussed by Pedlosky (1982). At minimum critical shear, any disturbances that propagates with a phase speed equal to the flow speed of the lower layer will be a homogeneous solution of the linear part of the potential vorticity equation for the lower layer, regardless of its horizontal or vertical structure. Since the flow speed of the lower layer is zero in this instance, such disturbances are those with no dependence on the fast time variable t. The linear part of the upper layer potential vorticity equation provides a constraint on the vertical structure of these perturbations. Thus we have that any disturbance of the form

$$\underset{\sim}{\phi} = [X_1(x,y,T),\ X_2(x,y,T)] \tag{2.3.6}$$

where

$$X_2 = -\frac{1}{F}\ (\nabla^2 + F)\ X_1 \tag{2.3.7}$$

will be a solution of the linear part of the potential vorticity equations. This is a class of solution that does not exist when the basic

flow does not correspond to minimum critical shear. In the current problem, it represents another set of linear solutions which can be resonantly forced by the non-linear terms. Forcing of this type does indeed occur at $O(\Delta^{3/2})$, being produced by the interaction between the mean flow correction and the unstable wave. To maintain a non-secular solution, we must include a correction of the form given in (2.3.6) and (2.3.7). The slow rate of change of the potential vorticity associated with this correction then balances the forcing at $O(\Delta^{3/2})$. We have not specified the horizontal structure of X_1 and X_2. The interaction between the unstable wave and the mean flow correction, mentioned above will directly force components of $\underset{\sim}{X}$ proportional to $e^{\pm ik_0x}$. However, the resultant of non-linear interaction between these Fourier components of strength $O(\Delta)$ and the unstable wave includes terms of $O(\Delta^{3/2})$ proportional to $e^{\pm 2ik_0x}$. Since these have no fast time dependence, this forcing is resonant and its effect is to generate additional Fourier components as part of X_1 and X_2. We are forced to include an infinite set of Fourier components, both in x and in y, in the structure of $\underset{\sim}{X}$.

In the preceding few paragraphs, we have given a heuristic account of the structure of the term $\underset{\sim}{\phi}^{(1)}$ in (2.3.3) that a more complete analysis would reveal. This may be summarized as

$$\underset{\sim}{\phi}^{(1)} = (0, \phi_{2p}^{(1)}) + (\phi_{1j}^{(1)}, \phi_{2j}^{(1)}) + (X_1, X_2) + (\Phi_1, \Phi_2)$$

where

$$\phi_{2p}^{(1)} = \frac{2}{ik_0U}\left[A_{0T} + i\frac{\pi}{2}U\,(k_1n_2 - k_2n_1)\,\frac{c_2 - c_1}{(U-c_2)(U-c_1)}\,A_1^*A_2^*\right]\sin \pi y\, e^{ik_0x} + *$$

represents a phase shift in the Fourier component with the same horizontal structure as the marginal wave.

$\phi_j^{(1)}$ contains the non-resonantly forced Rossby waves. $\underset{\sim}{X} = [X_1(x,y,T), X_2(x,y,T)]$ is the correction arising from the critical layer effect. We Fourier expand $\underset{\sim}{X}$ so that

$$X_1 = \sum_{\substack{m=1 \\ n=1}}^{\infty} e^{imk_0 x} \sin n\pi y \; \chi_{m,n}(T) + *$$

and X_2 is given by (2.3.7). We will adopt the normalization condition that $\chi_{1,1} \equiv 0$.

$\underset{\sim}{\Phi} = \underset{\sim}{\Phi}(y,T)$ is the correction to the mean flow. We will not determine $\underset{\sim}{\Phi}$ fully. Instead, we will define

$$Q_j = (\partial_y^2 - F)\underset{\sim}{\Phi}_j + F(-1)^j (\underset{\sim}{\Phi}_1 - \underset{\sim}{\Phi}_2) \qquad j = 1,2$$

as the potential vorticity of the mean flow correction. Only Q_2 is required in determining the evolution of A_0. We will expand

$$Q_2 = \frac{1}{F} \sum_{n=1}^{\infty} P_n(T) \sin 2 n\pi y \quad .$$

Before continuing we note that the lower layer potential vorticity due to $\underset{\sim}{X}$ is given by

$$-\frac{1}{F}(\nabla^4 - 2F^2) X_1 = \frac{1}{F} \sum_{\substack{n=1 \\ m=1}}^{\infty} e^{imk_0 x} \sin n\pi y \, [(m^2k_0^2 + n^2\pi^2)^2 + 2F^2] \chi_{m,n} + *$$

To simplify subsequent equations it is convenient to define

$$B_{m,n} = [(m^2k_0^2 + n^2\pi^2) + 2F^2]\xi_{m,n}$$

Because of certain symmetries in the system, it will further simplify matters if we define

$$C_{m,n} = B_{2m-1,\,2n-1} \quad \text{and} \quad D_{m,n} = B_{2m,\,2n}\,.$$

Note that half of the possible $B_{m,n}$'s are not included in these definitions; those of the form $B_{2m,\,2n-1}$ and $B_{2m-1,\,2n}$. It turns out that these are not forced by the dynamics and so need not be included provided that they do not form part of the initial conditions. (Note that this is similar to the idea used in the development of the single-wave theory of the finite amplitude evolution to discard the neutral modes. One could, if one wished, examine the stability of the evolution to be described below to disturbances with $B_{2m,\,2n-1}$ and $B_{2m-1,\,2n}$ non-zero!)

The $O(\Delta^{3/2})$ terms in the perturbation expansion of the potential vorticity equations pose a forced linear problem for $O(\Delta^{3/2})$ modifications to the streamfunction field. The linear operator is singular and the secularity conditions for this problem furnish evolution equations for A_0, $\underset{\sim}{\Phi}$ and $\underset{\sim}{X}$. These, together with the equations already derived for A_{1T} and A_{2T} form the closed system given below.

$$A_{0TT} = A_0\,(M_0M_2|A_1|^2 + M_0M_1\,|A_2|^2 + \sigma^2 + \frac{\sigma^2\pi}{F}P_1) \qquad (2.3.8a)$$

$$P_{1T} = -H\,\partial_T\,(|A_0|^2 - \frac{M_0}{M_1}\,|A_1|^2) - 2iD\,(A_0^*\,C_{1,2} - A_0\,C_{1,2}^*) \qquad (2.3.8b)$$

$$\partial_T C_{1,n} = 2iD\left[A_0[nP_n-(n-1)\,P_{n-1}] + A_0^*[nD_{1,n-1}-(n-1)\,D_{1,n}]\right] \quad n\geq 2 \qquad (2.3.8c)$$

$$\partial_T P_n = 2iDn[(A_0^*C_{1,n}-A_0C_{1,n}^*) - (A_0^*C_{1,n+1}-A_0C_{1,n+1}^*)] \quad n\geq 2 \qquad (2.3.8d)$$

$$\partial_T C_{m,n} = 2iD[(n+m-1)(A_0^*D_{m,n-1}+A_0D_{m-1,n}) - (n-m)(A_0^*D_{m,n}+A_0D_{m-1,n-1})]$$

$$m\geq 2,\ n\geq 1 \qquad (2.3.8e)$$

$$\partial_T D_{m,n} = 2iD[(n+m)(A_0^*C_{m+1,n}+A_0C_{m,n+1}) - (n-m)(A_0^*C_{m+1,n+1}+A_0C_{m,n})]$$

$$m\geq 1,\ n\geq 1 \qquad (2.3.8f)$$

$$\partial_T A_1 = iM_1\, A_0^*A_2^* \qquad (2.3.8g)$$

$$\partial_T A_2 = iM_2\, A_0^*A_1^* \qquad (2.3.8h)$$

By definition, $D_{0,n} = D_{m,0} = C_{0,n} = C_{m,0} = C_{1,1} = 0$

The constants appearing in the above equations are as follows:

$$\sigma^2 = k_0\gamma_0^2\, U/2F \qquad H = 2\pi F^2/U \qquad D = \tfrac{\pi}{2} k_0\gamma_0 \qquad (2.3.9)$$

$$M_j = \tfrac{\pi}{2}(U-c_j)^2\,(k_1n_2-k_2n_1)\,\frac{c_l - c_m}{(U-c_0)(U-c_1)(U-c_2)}$$

where (j,l,m) is a cyclic permutation of (0,1,2). Because we are working at minimum critical shear

$$k_0^2 = \sqrt{2F} - \pi^2 \quad \text{and} \quad \gamma_0 = 2^{1/2} - 1$$

when the gravest unstable mode is chosen.

For comparison, a set of equations equivalent to those integrated by Loesch may be obtained by formally setting D equal to zero. For the moment, let us do this. Assuming that $C_{m,n} = 0 = D_{m,n} = P_n$ initially, the amplitude equations reduce to

$$A_{0TT} = A_0 \left[(M_0 M_1 + \frac{\sigma^2 \pi}{F} H \frac{M_0}{M_1}) |A_1|^2 + M_0 M_1 |A_2|^2 - H \frac{\sigma^2 \pi}{F} |A_0|^2 \right] \tag{2.3.10}$$

$$+ \left[\sigma^2 + \frac{\sigma^2 \pi}{F} H \left(|A_0(0)|^2 - \frac{M_0}{M_1} |A_1(0)|^2 \right) \right] A_0$$

$$A_{1T} = iM_1 A_0^* A_2^* \tag{2.3.11}$$

$$A_{2T} = iM_2 A_0^* A_1^* \tag{2.3.12}$$

The constants σ^2 and H are both positive. One can see from the formula for M_j [Equation (2.3.9)] that M_0, M_1 and M_2 cannot all have the same sign. If M_1 and M_2 have opposing signs, then it follows from (2.3.11) and (2.3.12) that $|A_1|$ and $|A_2|$ are bounded. In (2.3.10), the effect of the term in $A_0|A_0|^2$ is stabilizing because of its negative coefficient. If $|A_0|$ were to grow, the $A_0|A_0|^2$ term in (2.3.10) must eventually overshadow the remaining terms on the right-hand side of (2.3.10) and we would not

therefore expect to see any unbounded growth of A_0. If M_1 and M_2 have the same sign, then M_0M_2, M_0M_1 and M_0/M_1 must all be negative and so (2.3.10) will have the form

$$A_{0TT} = -A_0 (\lambda_1 |A_1|^2 + \lambda_2 |A_2|^2 + \lambda_0 |A_0|^2) + \lambda_3 A_0$$

where all of the λ's are positive constants. Any growth of $|A_1|$ or $|A_2|$ is going to inhibit the growth of A_0. Furthermore, the $-\lambda_0 A_0 |A_0|^2$ term alone will be sufficient to prevent A_0 growing without bound.

The above discussion makes plausible the conjecture that $|A_0|$ will be bounded whenever M_0, M_1 and M_2 do not all possess the same sign. Conversely, it is easy to see that $|A_0|$, $|A_1|$ and $|A_2|$ can grow without bound for some initial conditions when M_0, M_1 and M_2 all have the same sign. Since we know that M_0, M_1 and M_2 have differing signs, we would not expect any finite amplitude instability to occur. Loesch's numerical integrations of (2.3.10)-(2.3.12) bear this out. It remains for us to see whether, when the critical layer dynamics are restored by taking a non-zero value of D, the system remains bounded.

Numerical Solutions

We have attempted to answer the question of the finite amplitude stability of the system (2.3.8) by numerically integrating these equations for two values of F and a variety of initial conditions. None of these integrations exhibited any unbounded growth in energy of the three main waves. While this does not guarantee the absence of any instability, it strongly suggests that the evolution of the triad is stable.

For F in the range of $\pi^2/\sqrt{2} < F < 2\sqrt{2}\pi^2$, only one meridional mode can be unstable near minimum critical shear, namely, $n_0 = 1$. The work of Loesch (1974) has shown that for such values of F, there is only one pair of neutral waves capable of forming a resonant triad with the unstable wave. The meridional structures of these waves are given by $n_1 = -2$, $n_2 = 1$. Loesch showed numerically that for $F < 10.5$, $M_1 < 0$ while for $F > 10.5$, $M_1 > 0$. The coefficients M_0 and M_2 are negative and positive respectively for all values of F. The remaining coefficients in (2.3.8) are all positive. There is, therefore, a structural change in the system (2.3.8) as F passes through the value 10.5. (One consequence of this can be readily predicted. When F is less than 10.5, a solution that starts with most of the initial energy in wave (0) and only small amplitudes for both sidebands will continue to have only small sideband energies. When $F > 10.5$, we would expect that a solution starting with very weak sidebands would exhibit growth of the sideband energies.)

Our numerical analysis follows Loesch (1974). We choose two values of F. One, 8, less than 10.5, the other, 12, greater than this threshold. Fixing F fixes the zonal and meridional wavenumbers of the one possible resonant triad. For $F = 8$, the zonal wavenumbers are

$$(k_0, k_1, k_2) = (1.2017, 2.6821, -3.8838)$$

while for $F = 12$, these become

$$(k_0, k_1, k_2) = (2.6648, -0.7999, -1.8648)$$

At a fixed F, the only freedom in generating solutions is the choice of initial conditions. Loesch, after making a number of numerical integra-

tions of (2.3.10)-(2.3.12) for different initial conditions, discovered that the solutions could be distinguished as being one of nine distinct types, four occurring for F = 8 and five occurring for F = 12. In the work already cited, Loesch exhibits a solution of each type and specifies the initial conditions necessary to generate each of these.

Using Loesch's values of F and U, we have integrated the fuller system (2.3.8) for some of the same sets of initial conditions as those used by Loesch and compared these with Loesch's solutions. These will be displayed below. In our integrations, the infinite set of equations (2.3.8) was truncated at either $n = m = 8$ or $n = m = 16$ as appropriate. Loesch refers to his canonical solutions as cases 1-9 of which cases 1-4 are for F = 8 and the remainder, for F = 12. The initial phases of A_0, A_1 and A_2 are chosen so that $ph(A_0) + ph(A_1) + ph(A_2) = \pi/2$, under which condition the three separate phases remain constant throughout the integration. We list the initial moduli of A_0, A_1, and A_2 below for the four cases that we will consider, together with the size of the truncation. The subsequent figures show how the moduli evolve with time. It is necessary to specify an initial value for A_{0T}. In each case we use

$$A_{0T}(0) = \sigma A_0(0)$$

where σ is the linear growth rate of the unstable mode.

Case	$\lvert A_0(0)\rvert$	$\lvert A_1(0)\rvert$	$\lvert A_2(0)\rvert$	Truncation
1	.0707	.0177	0.0	16
2	.03535	.03535	.03535	16
4	.03535	.0707	.0707	8
9	.0577	.0144	..0289	16

Figures 2.9 - 2.12 show the results of our integrations. In each case the evolution of $|A_0|$, $|A_1|$ and $|A_2|$ are shown for both the system with critical layer effects excluded (the left side of the figure) and the full version of (2.3.8). The results on the left side of the figures are thus equivalent to those of Loesch although the graphical format is different. A perusal of the figures reveals that the proper inclusion of the harmonics associated with the critical layer effect does not produce any recognizable tendency towards non-linear instability. The solutions remain bounded and are not terribly different from the solutions of Loesch. Those solutions of Loesch which contain relatively frequent zero crossings of $|A_0|$ (e.g., Case 4) are hardly affected by the inclusion of higher harmonics. Those solutions with longer intervals between zero crossings are more noticeably affected.

There is scope for a larger survey of the solutions of (2.3.8), but, in view of the form of (2.3.8), and the already noted fact that M_0, M_1 and M_2 cannot all take the same sign, it seems unlikely that unstable trajectories exist.

Figure 2.9: The evolution of a resonant triad near minimum critical shear. The triad consists of the marginal mode and two neutral waves. (a) - (d) show the evolution when the critical layer effect is excluded, (e) - (h) include this effect.

(a) and (e) : A_0
(b) and (f) : A_1
(c) and (g) : A_2
(d) and (h) : P_1

($F = 8$, $A_0(0) = .0707$, $A_1(0) = .0177$, $A_2(0) = 0.0$; case 1)

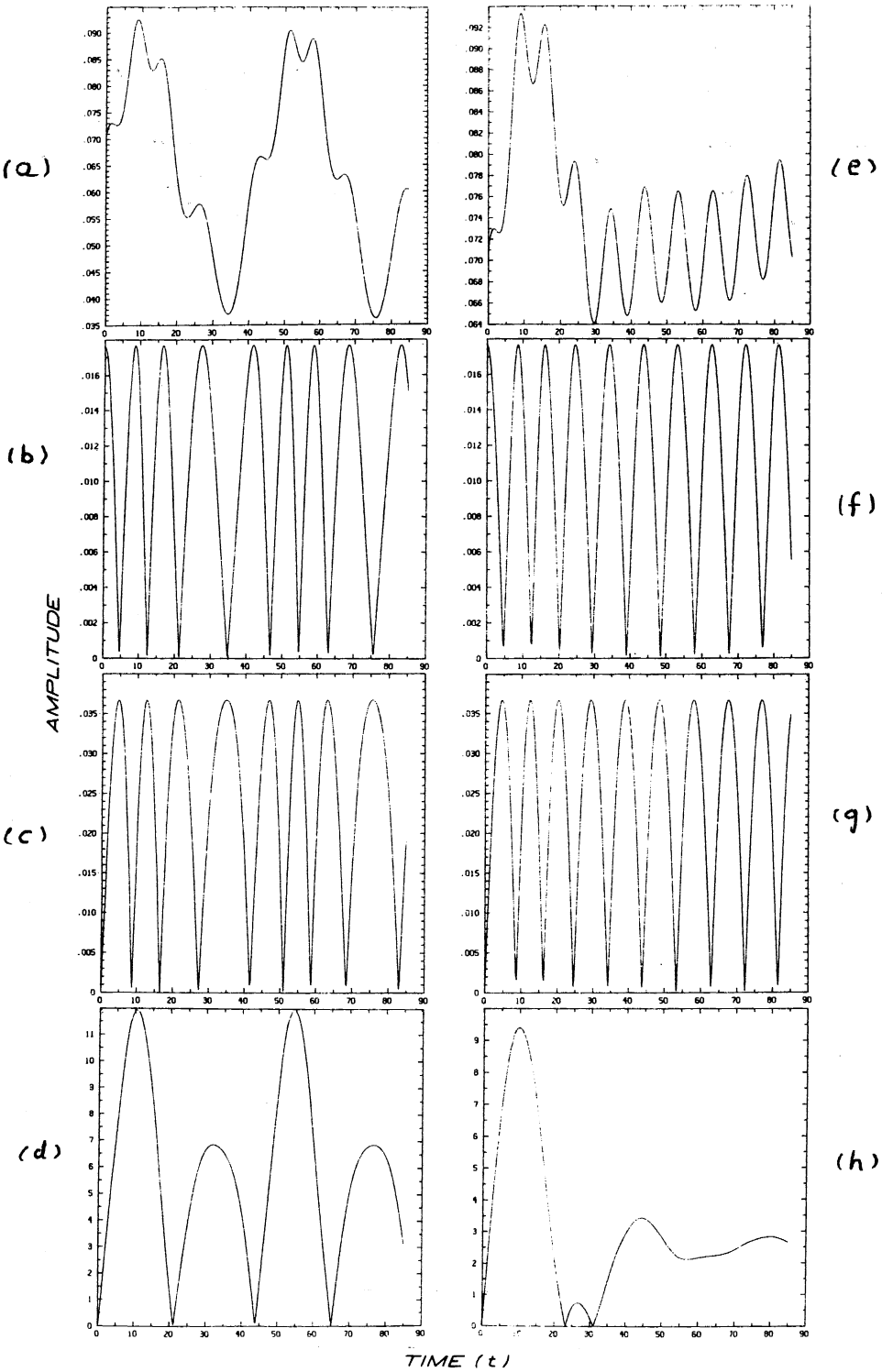
(a)
(b)
(c)
(d)
(e)
(f)
(g)
(h)
AMPLITUDE
TIME (t)

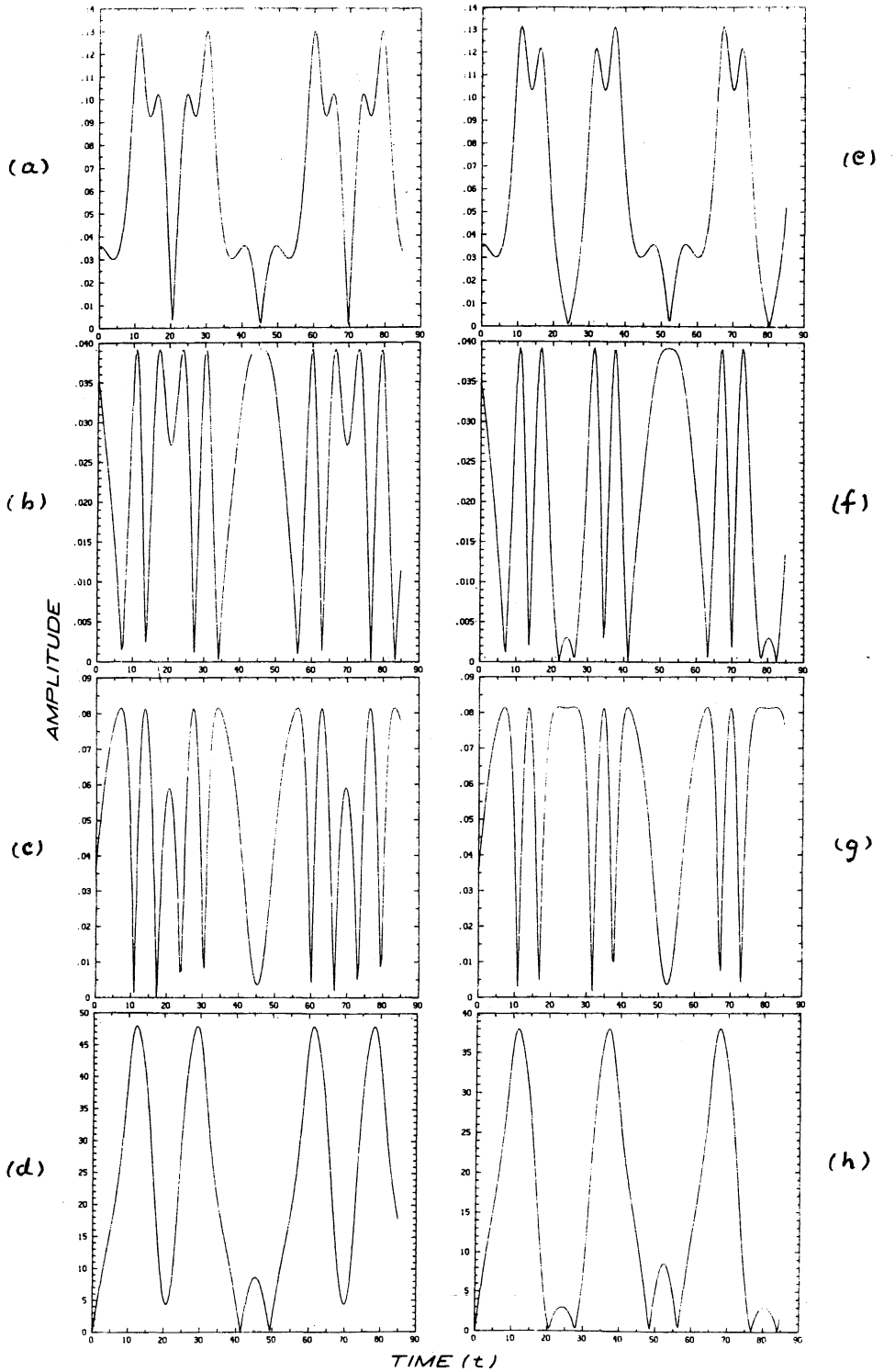

Figure 2.10: Similar to Fig. 2.9 but for F = 8, $A_0(0)$ = 0.0354, $A_1(0)$ = 0.0354, $A_2(0)$ = 0.0354 (case 2).

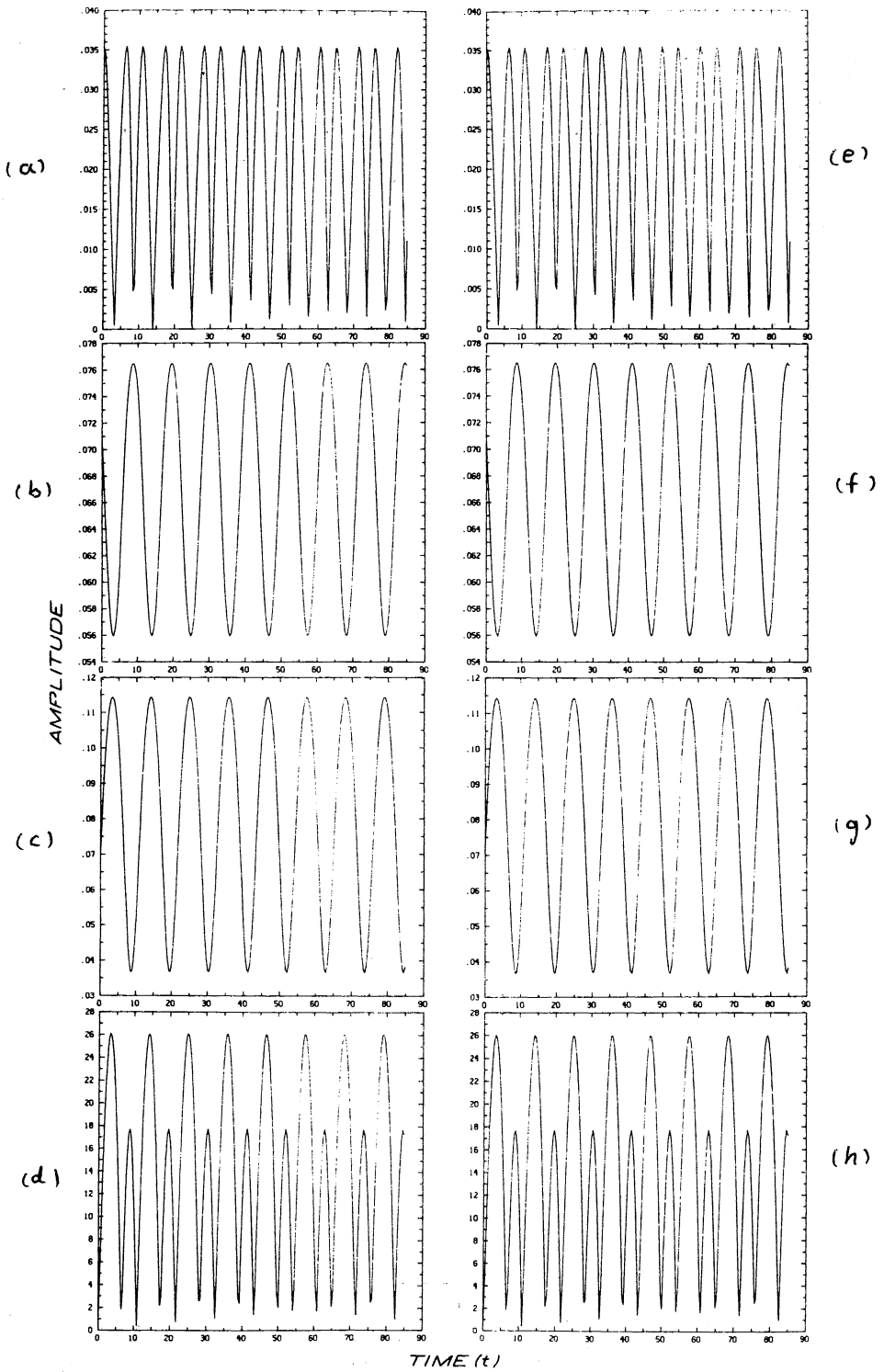

Figure 2.11: Similar to Fig. 2.9 but for F = 8, $A_0(0)$ = 0.0354, $A_1(0)$ = 0.0707, $A_2(0)$ = 0.0707 (case 4).

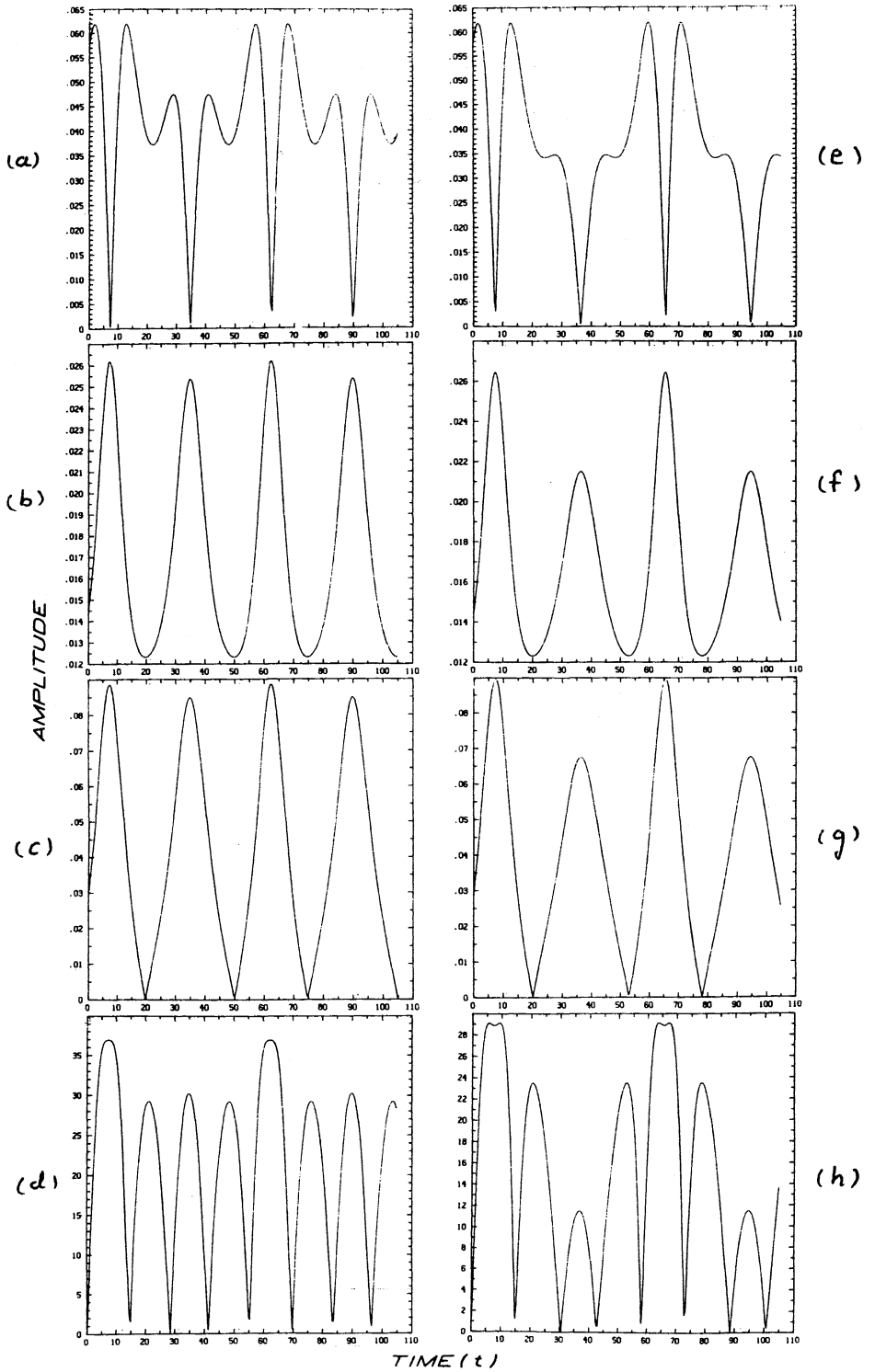

Figure 2.12: Similar to Fig. 2.9 but for F = 12, $A_0(0)$ = 0.582, $A_1(0)$ = 0.0146, $A_2(0)$ = 0.0291 (case 9).

CHAPTER 3

3. Baroclinic Instability in a Meridionally Varying, Two-Layer Model: Linear Theory

We begin here the main investigation of this thesis, an examination of the nature of baroclinic instability in a system in which, to the fundamental property permitting baroclinic instability, namely, a reserve of available potential energy, we have added a single complicating feature, the presence of meridional variation in the potential vorticity gradient of the equilibrium flow. Some reasons for wishing to do so will be given momentarily. Let us note here that this study will concentrate on the properties of slowly growing unstable modes and on the evolution of such modes. The presentation will be divided into two parts. The first will comprise this chapter and will look at a linearized model of instability. Chapter 4 will then deal with the subsequent evolution of weakly growing modes once they enter the finite amplitude domain.

This chapter is composed as follows. An introductory section is followed first by a short formal description of the theoretical model under consideration and then a presentation of the behavior of the eigenvalues as determined by a numerical model. Next we discuss the spatial structure of the unstable eigenfunction and its attendant eddy fluxes as they are revealed by the numerical study. A critical layer effect near the center of the channel is noted. In particular, ϕ_2 is confined to a narrow region about the center of the channel. It is shown that the eigenfunction structure may be related to the horizontal structure of the basic potential vorticity gradient of the lower layer. An analytical

model, asymptotic in the supercriticality, is developed for the case in which the basic state is close to minimum critical shear. Some comparison is made between the analytical and the numerical results. In a consideration of the energy balance for an unstable mode, some properties of the heat flux are emphasized, notably its confinement to the middle of the channel and the occurrence of both northward and southward fluxes within this region which almost cancel. Finally, we draw attention to a class of slow neutral modes and point out their relevance to a weakly non-linear theory for the slightly supercritical model.

The most frequently cited linear models of baroclinic instability, Eady (1969), Charney (1947) and Phillips (1954), examine situations in which the mechanism of baroclinic instability is isolated in a fairly pure form. The basic flows possess only vertical shear and have meridional temperature gradients that are independent of y. In each example, the potential vorticity gradients of the basic flow are functions only of the vertical coordinate. The normal modes supported by each of these models can be obtained analytically. Thus one can determine the growth rates and eigenfunction structure of those modes that are unstable and find the boundaries between stable and unstable domains in the parameter space of the model (typical parameters being the Froude number, the vertical shear, the relative importance of β, etc.).

In a geophysical system such as the atmosphere or ocean, we are often interested in the stability properties of relatively long, sustained, jet-like flows. Rather than being a flow that is uniform in the cross-stream direction, these geophysical jets vary significantly across their path,

from an interior maximum to a small velocity at the edges of the jet. The interior of the jet may include more than one maximum as is perhaps the case at times in the Gulf Stream. Typically one is interested in the stability of a feature that is both confined in the cross-stream direction and varying in that direction. A channel model will simulate the confinement of the feature of interest -- probably too well, since by preventing radiation perpendicular to the jet, rigid channel walls probably enhance the instability of a jet. However, confinement alone is not sufficient to reproduce a dynamically significant feature of a free jet, namely, the cross-stream variation of the cross-stream gradient of potential vorticity that will typically be present. Since the work already carried out on the nature of baroclinic instability, e.g., Charney and Stern (1962), has demonstrated the importance of the potential vorticity gradient of the equilibrium state to the dynamics of unstable perturbations to that state, it seems worthwhile to study the effects of including a more realistic, varying gradient.

A second consequence of the cross-flow variations that will generally be present in baroclinic instability problems taken from the physical world, is that the cross-stream structure of the linear wave modes supported by the equilibrium flow will not be trigonometric. This has important consequences for the non-linear interactions between these modes. The dynamical equations are quadratically non-linear. If we Fourier decompose a disturbance into linear eigenmodes, then the evolution of these modes is coupled through the non-linear terms. In general, one can think of the modes as interacting in threesomes; see, for exam-

ple, Pedlosky (1979b, Section 3.26). In the case of a flow whose linear perturbation problem is separable in its spatial dependence, in order that three waves interact significantly, the product of the non-linear interaction between two of the waves must have a non-zero projection onto both the temporal and the three-dimensional spatial structure of the third wave (this interpretation of wave interactions is really appropriate only for a weak perturbation field). In particular, the cross-stream structure of the interaction product must not be orthogonal to the cross-stream structure of the third wave. When a flow is such that the cross-stream structures of the linear eigenmodes are trigonometric, the quadratic interaction between two modes will give rise to a product that is orthogonal to all but two of the possible cross-stream eigenstructures. For example, if wave w_1 has a streamfunction proportional to sin $n\pi y$ and wave w_2, a streamfunction proportional to sin $m\pi y$, an interaction like $w_1 \times \partial_y w_2$ will produce terms proportional to sin $(n\pm m)\ \pi y$ only. If the eigenmodes do not have trigonometric cross-stream dependence, then it will usually be the case that the cross-flow structure of an interaction product will be non-orthogonal to all or a large set of the possible modal cross-flow structures. In the non-trigonometric case many more interacting triads will be possible (e.g., Domaracki and Loesch, 1977).

Thirdly, the meridional variations of the basic state will promote the influence of harmonics of the unstable wave. In Phillips' meridionally uniform model, the self-interaction of the slowly changing unstable wave generates a correction to the mean flow but not a second or higher zonal harmonic of that wave at any significant amplitude. This is a con-

sequence of the very simple meridional structure of that model. In general, the introduction of a meridionally varying basic state will lead to the generation of higher zonal harmonics of the unstable wave in addition to the mean flow correction. When, in the latter part of Chapter Four, we examine the evolution of a weakly unstable wave against a meridionally varying background in the absence of triad interactions, we will find that these higher harmonics are as significant as the mean flow correction in their effect on the amplitude of the fundamental wave. It is not clear in advance, whether the effects of higher harmonics will be stabilizing or destabilizing.

In the non-linear dynamics that is to follow in Chapter 4, we wish to examine not only the interaction of an unstable wave with the mean flow, but also its interaction with other linear eigenmodes. The enhanced variety of inter-modal energy exchanges that is made possible by the inclusion of meridional variation will be a factor in this. In the model that we intend to study, the streamwise direction will be the zonal direction and the cross-stream direction, the meridional direction. Although the description above suggested meridional shear of the zonal velocity field as a source of cross-stream variation it is both algebraically simpler and computationally simpler to introduce meridional variation via the bottom boundary condition, as a meridionally varying topographic slope. As well as reflecting a genuine physical source of meridional variation, this produces effects dynamically equivalent to those features of interest that were indicated above, namely the introduction of meridional variation into the potential vorticity gradient and non-trigonometric meridional dependence in the linear eigenfunctions.

A few more general remarks are appropriate here. Usually problems which, while retaining the vertical variation of the potential vorticity gradient necessary to support baroclinic instability, also include meridional variations of that gradient, are difficult to solve analytically. They involve partial differential equations with coefficients that vary in y and z. Several investigators have examined the linear stability properties of such flows and have usually used numerical techniques (e.g., Pedlosky, 1964; Simmons, 1974; Brown, 1969). They have usually looked at such problems from a rather global point of view and have not explored in detail the nature of the slowly growing unstable modes lying close to the stability boundary. The main objective of the next chapter is to look at the finite amplitude evolution of weakly baroclinically unstable modes of one such flow when the flow is close to critical. As a prerequisite for this, we need to have a fairly detailed understanding of the linear problem in a part of parameter space that corresponds to slowly growing unstable modes. In what follows, we will present a numerical survey of one such region and then, by taking advantage of the fact that we are interested in only a small region of parameter space, develop an analytic description of the properties of the unstable modes in that region.

Model Description

We wish to examine a model that (a) has a vertical structure that is as simple as possible yet capable of supporting baroclinic instability and (b) contains meridional variations of the meridional gradient of potential vorticity yet cannot support barotropic instability. Conse-

quently, we choose to use a two-layer model confined to a zonal channel (c.f. the two-level model of Phillips, 1954). The basic flow consists of a zonal velocity U in the upper layer and a resting lower layer. U is independent of y (the meridional direction) thus the model contains vertical shear but not horizontal shear. The height of the lower boundary is allowed to vary meridionally so that the topographic slope is a function of y, $h_y(y)$. The contribution of the topographic β-effect introduces meridional variation into the basic potential vorticity gradient of the lower layer, Π_{2y}.

Making the usual quasigeostrophic scaling assumptions (Pedlosky, 1979b), the linear problem can be described in the following, non-dimensional form:

$$(U\partial_x + \partial_t)\,[(\nabla^2 - F)\,\phi_1 + F\,\phi_2] + (\beta + FU)\,\phi_{1x} = 0 \qquad (3.1)$$

$$\partial_t\,[(\nabla^2 - F)\,\phi_2 + F\,\phi_1] + [\beta - FU + h_y(y)]\,\phi_{2x} = 0 \qquad (3.2)$$

The layer depths have been taken to be the same, β and U are positive and the channel walls lie at y=0 and y=1. Subscript 1 identifies the upper layer. We will take h_y to have the form:

$$h_y = h_2 \cos 2\pi y \quad , \qquad h_2 > 0 \qquad (3.3)$$

Define

$\Pi_{1y} = \beta + FU$, the potential vorticity gradient in the upper layer.

$\Pi_{2y} = \beta - FU + h_y(y)$, the potential vorticity gradient in the lower layer.

Π_{1y} is uniform and positive. Π_{2y}, which contains contributions from the planetary vorticity gradient, the equilibrium slope of the interface, and the topographic slope, has a minimum $\Pi_{2ymin} = \beta - FU - h_2$, on the center line of the channel. Define $\beta_m \equiv FU + h_2$. When $\beta > \beta_m$, Π_{2y} is positive throughout the lower layer. The Charney-Stern (1962) sufficient condition for stability is satisfied; the flow must be stable. When $\beta < \beta_m$, Π_{2y} becomes negative near the middle of the channel. It may now be possible for unstable modes to exist. When $\beta = \beta_m - \Delta$ where Δ is small and positive, π_{2y} takes the form shown in the accompanying sketch.

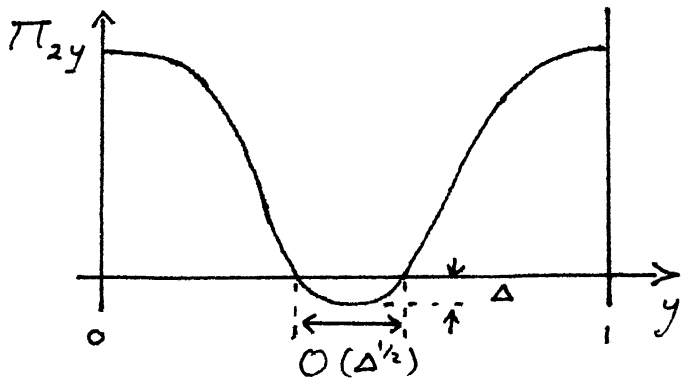

Before discussing the numerical results we note, for reasons that will become apparent later, the existence of a neutral mode that is completely trapped to the upper layer. The system possesses normal modes of the form

$$\phi = [\phi_1(y), \phi_2(y)] \exp [ik(x - ct)] \tag{3.4}$$

A particular eigensolution is the one:

$$c = 0, \qquad \phi_1 = \sin \pi y , \qquad \phi_2 = 0 \tag{3.5}$$

which occurs at a wavenumber k given by

$$k^2 = (\beta/U - \pi^2)$$

Provided only that $\beta > \pi^2 U$, this mode exists for both $\beta < \beta_m$ and $\beta > \beta_m$ and is distinguished by the fact that it is stationary in a frame moving with the velocity of the lower layer (which, in this exposition, has been chosen to be zero).

Numerical Results

After substituting the normal mode form (3.4) for ϕ, the differential equations (3.1) and (3.2) can be transformed to normal form by writing them in terms of

$$\phi_T = (\phi_1 + \phi_2)/2, \qquad \phi_C = (\phi_1 - \phi_2)/2$$

By representing ϕ_T and ϕ_C by a spectral expansion in sines and truncating, the differential problem may be expressed approximately as a matrix eigenvalue problem. The latter may be solved numerically using standard routines.

The search procedure adopted was to fix $F = 10.0$, $U = 1.0$, $h_2 = 5.0$ and then to vary β and k^2. The results will be represented in a two-dimensional parameter domain with axes corresponding to β and k^2. For the parameters chosen, $\beta_m = 15.0$. Since $\beta > \beta_m$ corresponds to a stable flow, we concentrate on $\beta < 15.0$. Numerically, we find that $\beta = \beta_m$ is indeed a stability threshold. Given our predilection for weakly growing instabilities, our attention will focus on the region close to this threshold.

Our first result is that, for values of β close to but less than β_m, only values of k^2 in the vicinity of $k_0^2 = 5.13$ are unstable. The domain of instability is shown in Figure 3.1 and Figure 3.2. The unstable domain

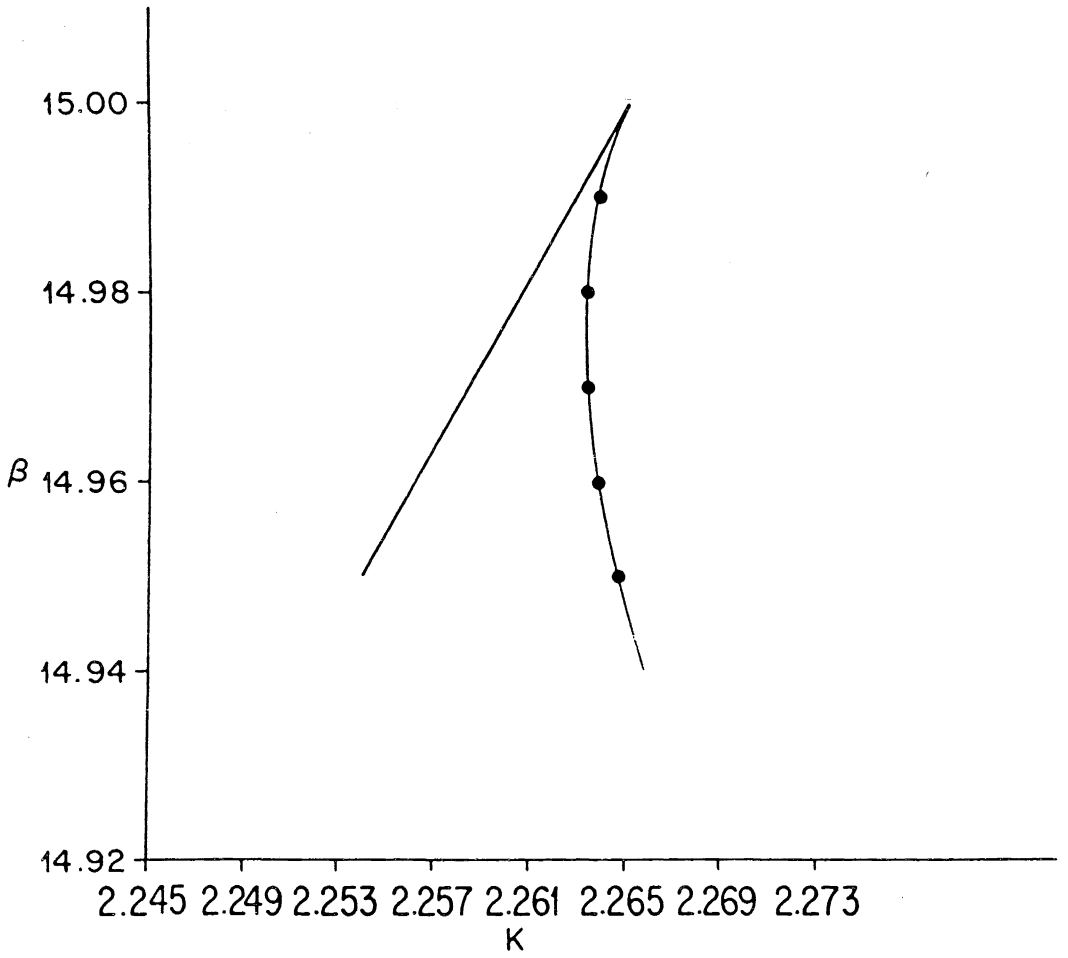

Figure 3.1: The tip of the numerically determined marginal curve plotted in the (k^2, β) plane. Case 1: F = 10.0, U = 1.0, h_2 = 5.0 (β_m = 15.0).

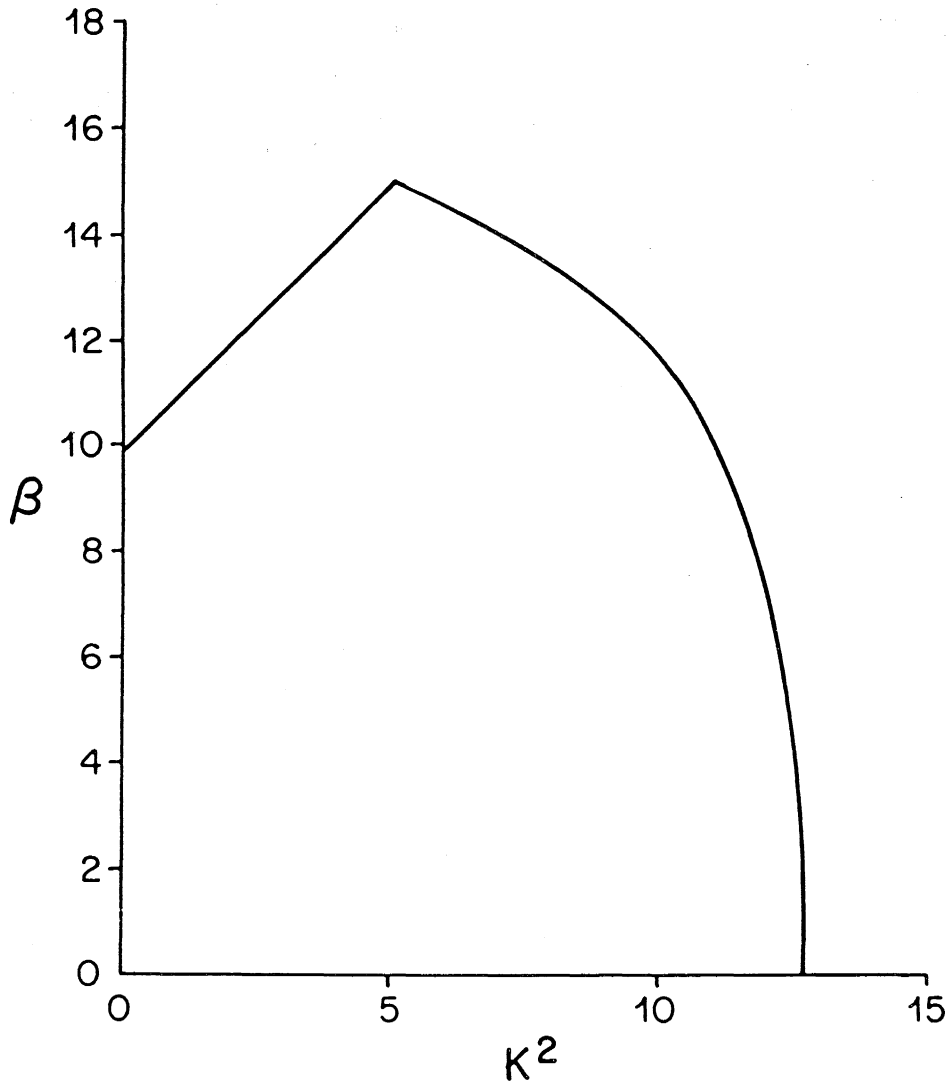

Figure 3.2: The full marginal curve for the gravest unstable mode of Case 1.

exhibits a cusp, the tip being located at $\beta = \beta_m = 15.0$, $k^2 = k_0^2 = 5.13$. The two branches of the marginal curve that leave this point have some distinctive characteristics. The left-hand branch corresponds to the curve $k^2 = (\beta/U - \pi^2)$. In the vicinity of the tip, the right-hand branch is fitted well by the curve

$$k^2 = (\beta/U - \pi^2) + \text{const} \times (\beta - \beta_m)^{3/2} \quad .$$

Near the cusp tip the range of unstable wavenumbers is of $O(\Delta^{3/2})$ in width where, $\Delta = \beta_m - \beta$, the distance below the tip. This interval lies to the left of the critical wavenumber k_0^2. Thus for a range of wavenumbers (approximately $2.2633 < k < 2.265$), if one were to fix k at a value in this interval and increase β from zero, one would observe first instability, then an interval of stability followed by an interval of instability, and finally stability for all $\beta > (k^2 + \pi^2)U$.

For a fixed value of $\Delta > 0$, moving k across the interval of unstable wavenumbers, we find that there are a pair of modes whose phase speeds c are complex conjugates. Considering the variation in $c = c_r + c_i$ for the unstable mode, the numerical results suggest that, as $k \dashrightarrow k_1(\beta)$, the left-hand branch of the marginal curve, $c \dashrightarrow 0$, while as $k \dashrightarrow k_2(\beta)$, the right-hand branch, $c_i \dashrightarrow 0$, $c_r \dashrightarrow$ constant, $c_0(\beta)$, (see Figure 3.3). As Δ is increased, $c_0(\beta)$ increases in proportion to Δ^2 (see Figure 3.4). The maximum value of c_i attained in going between k_1 and k_2 seems commensurate with $c_0(\beta)$.

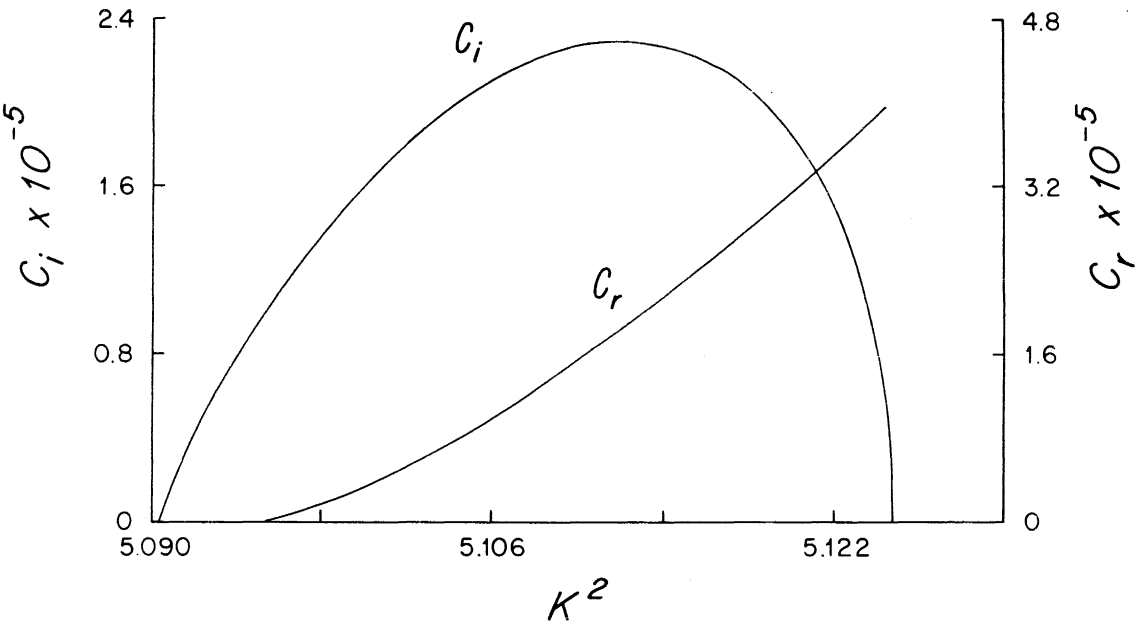

Figure 3.3: The real and imaginary parts of the phase speed, c_r and c_i, plotted against the square of the wavenumber. β = 14.96, Δ = 0.04 (F = 10.0, U = 1.0, h_2 = 5.0).

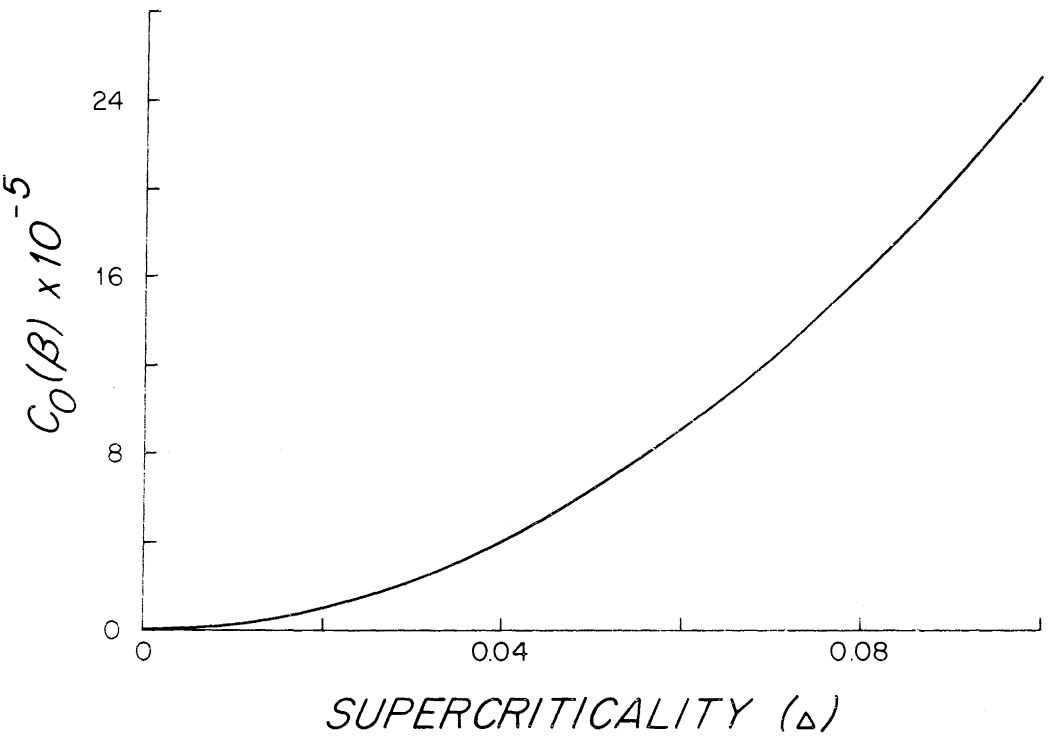

Figure 3.4: The phase speed along the right-hand branch of the marginal curve, $c_0(\beta)$, plotted against the supercriticality Δ. ($F = 10.0$, $U = 1.0$, $h_2 = 5.0$).

Eigenfunction Structure

The structures of eigenfunctions near the cusp point are typified by the example shown in Figures 3.5, which corresponds to $\beta = 14.96$, $k = 2.261$. The upper layer streamfunction differs little from the shape of $\sin \pi y$. The lower layer streamfunction is much weaker than that in the upper layer and is concentrated in a thin region about the mid-line of the channel. As one increases Δ while keeping k near the center of the unstable interval, the lower layer streamfunction increases in amplitude (relative to the upper layer), the width of the central region broadens and the difference in amplitude between the central zone and the region outside this becomes less marked. at the same time the shape of the upper layer streamfunction departs more from that of $\sin \pi y$.

At a fixed value of Δ, as k is moved closer toward the left-hand branch of the marginal curve, the lower layer streamfunction becomes steadily weaker.

Numerical results were also obtained for different settings of the 'fixed' parameters, F, U, and h_2. These results were qualitatively similar to those already discussed. For comparison, Figures 3.6 to 3.7 illustrate some aspects of the case $F = 6.6164$, $U = 1.0$, $h_2 = 9.8836$, for which $\beta_m = 16.5$. Here h_2/FU is larger than the previous example and the relative meridional variation of π_{2y} is correspondingly larger. As a result, the cusp of the marginal curve is more pronounced in Figure 3.6 than in 3.2. The internal layer structure peculiar to the slowly growing normal modes can be seen at larger absolute values of the supercriticality parameter Δ; for example, the structures of the streamfunc-

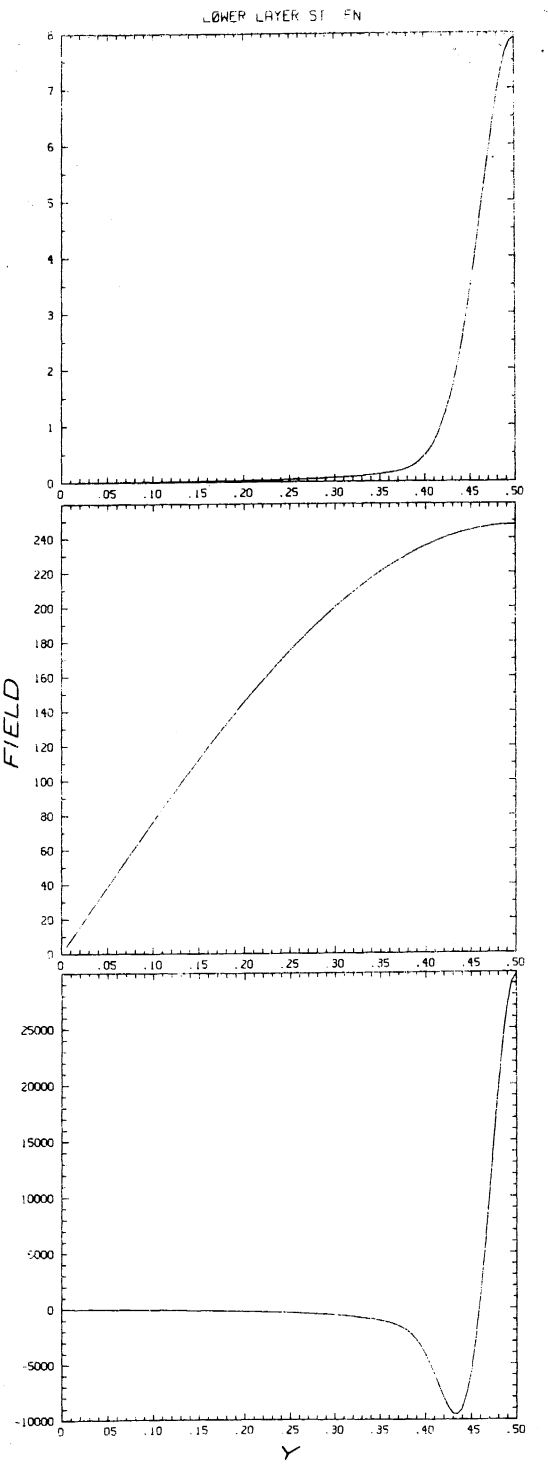

Figure 3.5: a) The magnitude of the lower layer streamfunction for the unstable mode at β = 14.96, k = 2.261 (F = 10.0, U = 1.0, h_2 = 5.0).
b) The magnitude of the upper layer streamfunction.
c) Zonally averaged heat flux (multiplied by F) as a function of y.

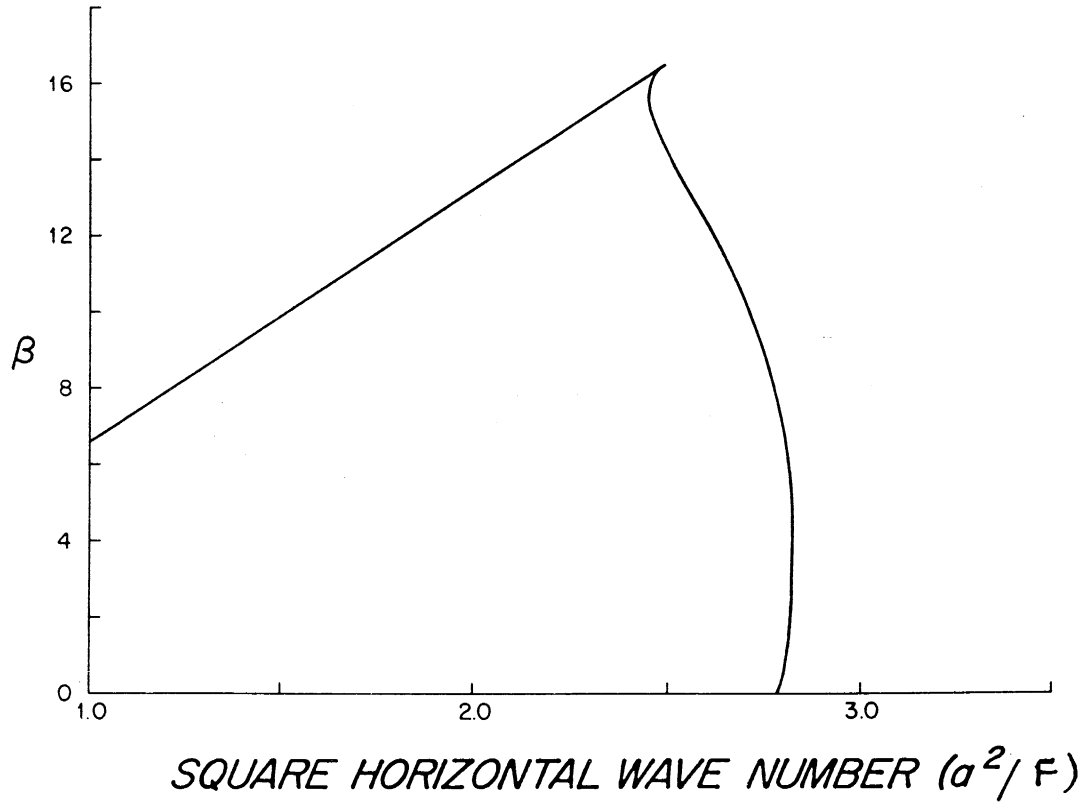

Figure 3.6: The marginal curve for the gravest unstable mode when F = 6.6164, U = 1.0, h_2 = 9.8836 (Case 2).

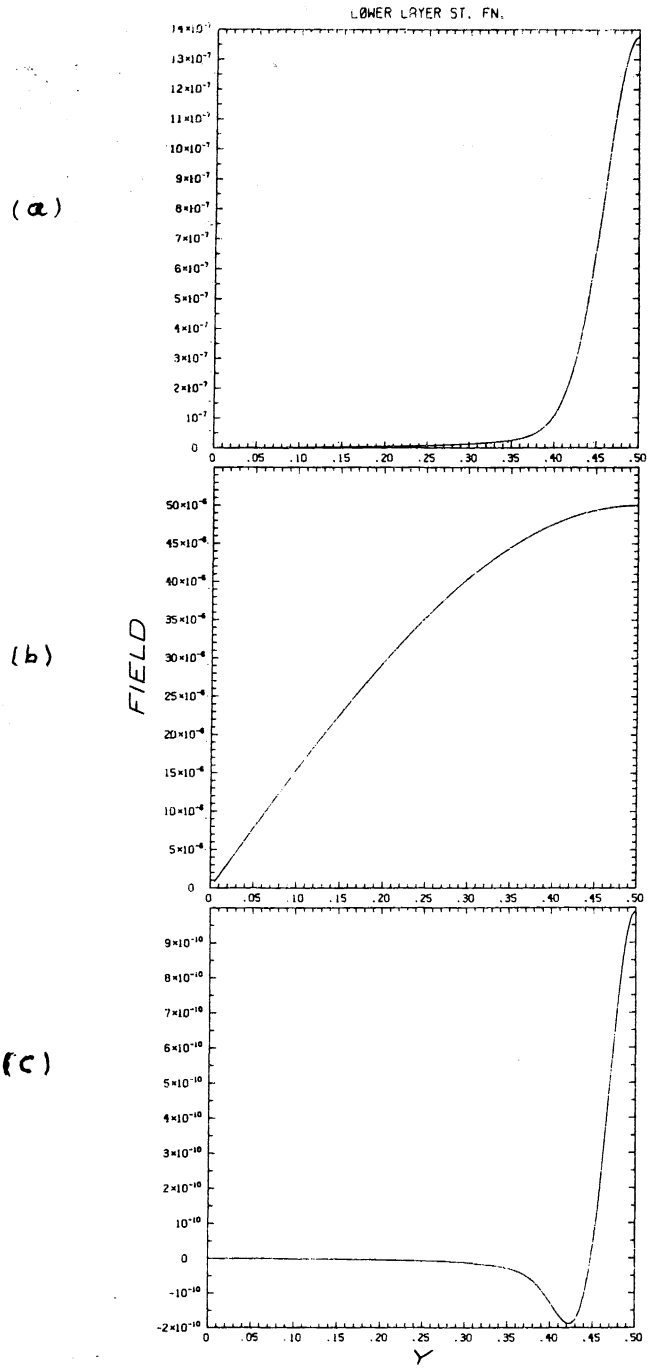

Figure 3.7: a) The magnitude of the lower layer streamfunction for the unstable mode at β = 16.3, k = 2.544 (F = 6.6164, U = 1.0, h_2 = 9.8836).
b) The magnitude of the upper layer streamfunction.
c) Zonally averaged heat flux (multiplied by F) as a function of y.

tions of the unstable normal mode at $\beta = 16.3$ ($\Delta = 0.2$) and $k = 2.544$, which are shown in Figure 3.7, exhibit the same characteristic features as those in Figure 3.5. The larger extent of the weakly supercritical regime is also reflected in the values of the phase speed c which are smaller at a given small value of Δ for the current choice of F, U and h_2 than for the earlier set of parameter values at the same Δ.

For this second choice of parameters we have also calculated several diagnostic fields associated with the unstable linear mode. These are shown in Figure 3.8 and include:

heat flux x F	$F\,\overline{v\theta}$
upper layer momentum flux	$\overline{u_1 v_1}$
lower layer momentum flux	$\overline{u_2 v_2}$
upper layer Reynolds stress divergence	$-\partial_y\,(\overline{u_1 v_1})$
lower layer Reynolds stress divergence	$-\partial_y\,(\overline{u_2 v_2})$
upper mean meridional velocity	$\overline{v}_1$
mean vertical velocity	$\overline{w}$
upper mean zonal momentum tendency	$\overline{u}_{1t}$
lower mean zonal momentum tendency	$\overline{u}_{2t}$
mean temperature tendency	$\overline{\theta}_t$

The overbar denotes a zonal mean.

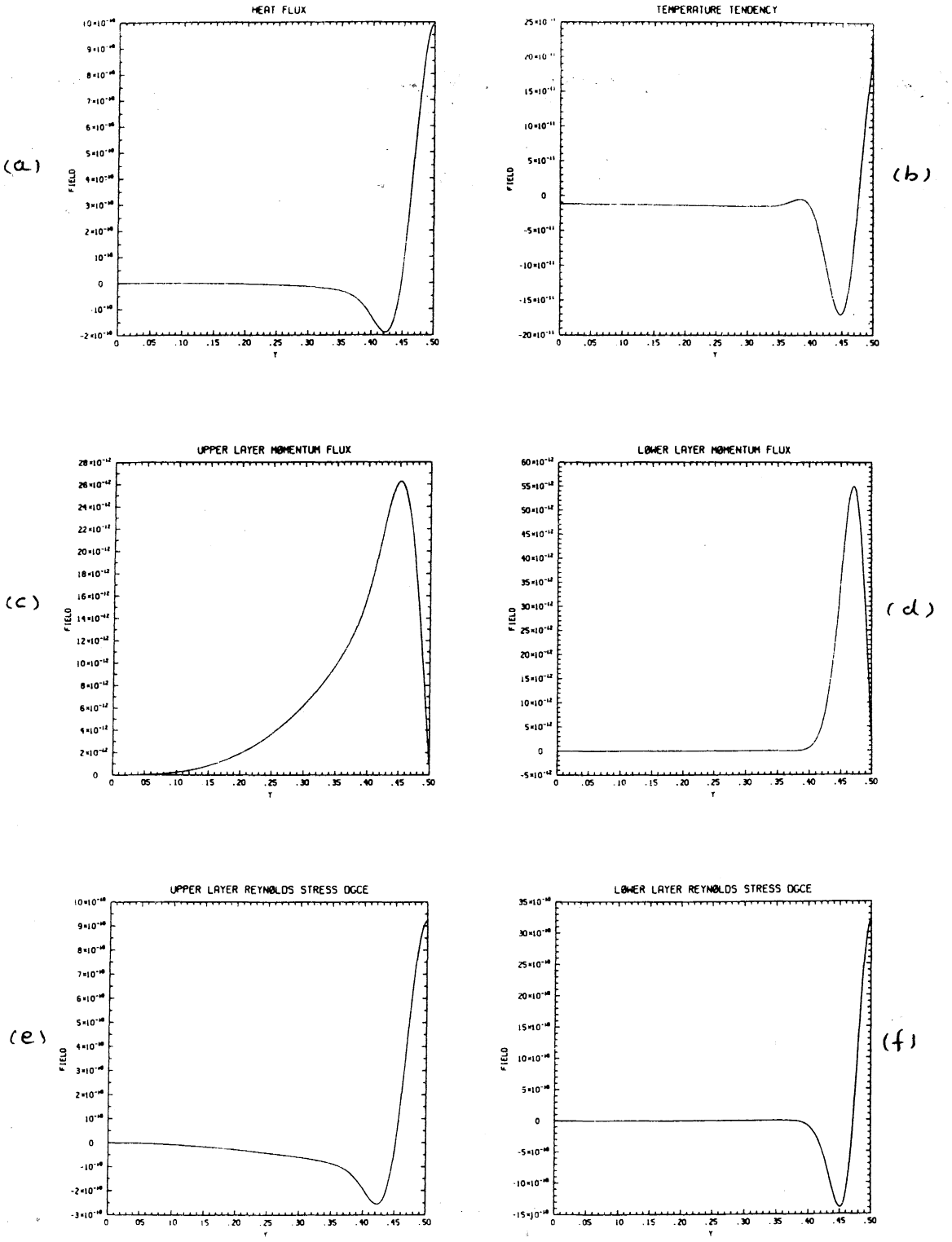

Figure 3.8: Quantities associated with the unstable eigenmode of Fig. 3.7: a) heat flux, b) temperature tendency, c) upper layer momentum flux, d) lower layer momentum flux, e) upper layer Reynolds' stress divergence f) lower layer Reynolds' stress divergence

(g)

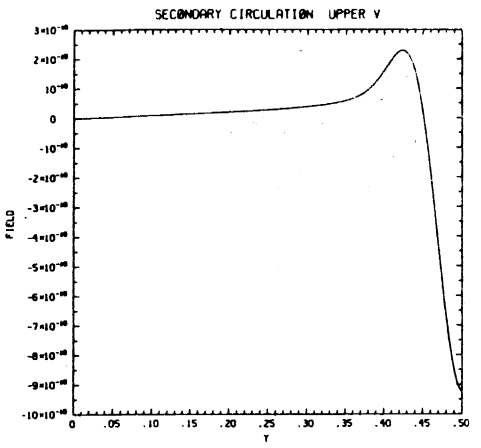

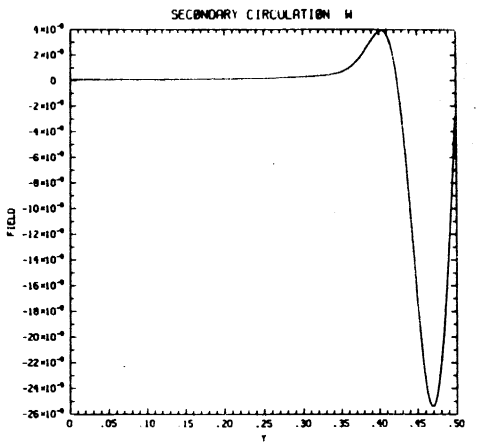

(h)

(i)

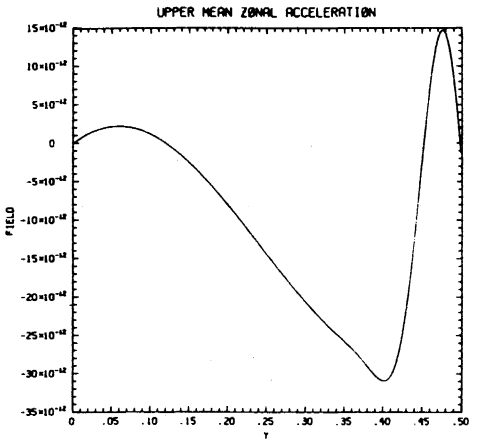

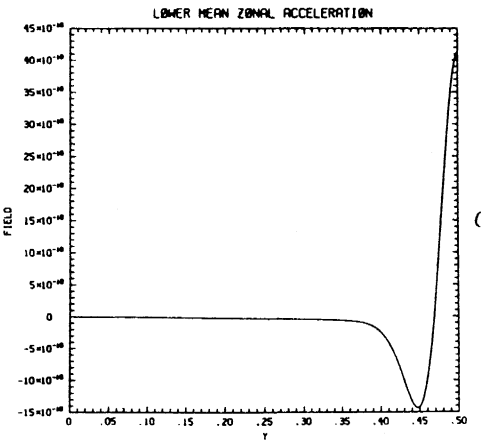

(j)

Figure 3.8 (cont.): g) secondary circulation: upper layer meridional velocity h) secondary circulation: vertical velocity i) upper mean zonal acceleration j) lower mean zonal acceleration.

For reference, the zero-crossings of the basic potential vorticity gradient in the lower layer, π_{2y}, which is parabolic in the neighborhood of $y = 1/2$, occur at $y \simeq 0.47$ and $y \simeq 0.53$.

First, we note that the quadratic fluxes of temperature and momentum induce a three-cell meridional circulation in the sense sketched below.

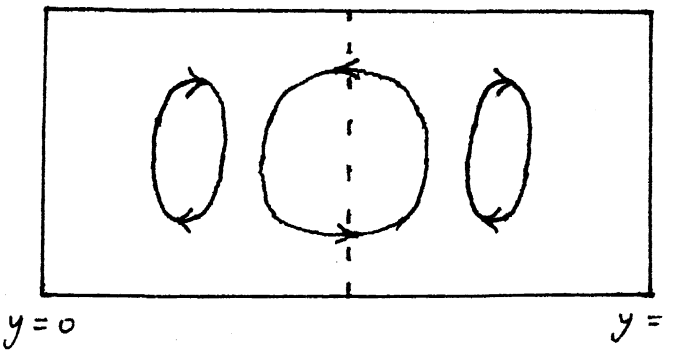

The central cell, which is thermally indirect, is stronger and wider than the two outer, direct cells. Note that in the sketch, the meridional extent of the cells has been exaggerated. The central cell is located within the "inner region" defined by the peak of the lower layer stream function. Note that $\bar{w}$ does not quite return to zero at $y = 0.5$ in 3.8(h). This is a result of error accumulated during an application of Simpson's rule in the algorithm which computes $\bar{v}$.

The meridional eddy heat flux is concentrated in the middle of the channel in a strong poleward peak but there is a significant negative lobe near $y = 0.42$. The heat flux will be discussed in more detail later. The meridional eddy fluxes of zonal momentum are antisymmetric about $y = 1/2$ for this symmetric normal mode. Both show positive peaks within the inner region although the sharper peak is seen in the lower layer.

The tendencies are related to the eddy fluxes and the mean meridional circulation by

$$\partial_t \bar{u}_1 = \bar{v}_1 - \partial_y (\overline{u_1 v_1})$$

$$\partial_t \bar{u}_2 = \bar{v}_2 - \partial_y (\overline{u_2 v_2})$$

$$\bar{\theta}_t = -\frac{1}{F}\bar{w} - \partial_y (\overline{v\theta})$$

and $\bar{v}_2 = -\bar{v}_1$. In 3.8(e) and 3.8(f), we see that the divergence of the Reynold's stress in each layer exhibits a sharp positive central peak and a smaller negative lobe just outside this. The divergence is stronger in the lower layer than in the upper. The senses of the divergences at the center of the channel are such as to accelerate the zonal flow in each layer. However, the Coriolis force on the mean meridional flow in the upper layer is negative at the center of the channel, decelerating the mean flow. In the upper layer, the magnitudes of the effects of the mean circulation and the eddy fluxes are similar so that they cancel. As a result, the mean zonal flow tendency in the upper layer is nearly zero at the center of the channel, although it is weakly positive equatorward and poleward of this. Near the channel center, in the lower layer, the accelerating effects of the mean meridional circulation and the eddy momentum convergence are in the same sense, although that of the momentum convergence is the stronger. The lower zonal flow is accelerated near the channel center.

Equatorward of about y = 0.47, the lower layer zonal flow is decelerated. This deceleration zone still lies within the "inner region" of the problem. South of y = 0.39, the momentum tendency of layer two is very small. The upper layer flow is decelerated south of about y = 0.45 and the deceleration band extends into the outer region. The magnitude of the upper zonal flow tendency is always much smaller [by a factor of O(100)] than the similar lower layer quantity.

The acceleration of the mean vertical shear is dominated by $\bar{u}_{2t}$. The shear is reduced near the center of the channel from about y = 0.47 to y = 0.53 and increased in the regions $0.39 < y < 0.47$ and $0.53 < y < 0.61$. Recall that the mean potential vorticity gradient in the lower layer is

$$\pi_{2y} = \beta - F\,(U + \bar{u}_1 - \bar{u}_2) - \bar{u}_{2yy} + h_2 \cos 2\pi y$$

where we have decomposed the mean zonal velocity in the upper layer into its basic state value U and a modification $\bar{u}_1$. For $y = 1/2 + \eta$, $\eta \ll 1$, this is approximately

$$\pi_{2y} = -\Delta + h_2\, 2\pi^2 \eta^2 - F\,(\bar{u}_1 - \bar{u}_2) - \bar{u}_{2yy}$$

If we consider the $\bar{u}_1$ and $\bar{u}_2$ that would be generated by the eddy fluxes and meridional circulation based on the linear modal structure, then roughly speaking

$$\left| F\,\bar{u}_1 \right| \ll \left| F\,\bar{u}_2 \right| \ll \left| \bar{u}_{2yy} \right|$$

Thus $$\pi_{2y} \simeq -\Delta + h_2\, 2\pi^2 \eta^2 - \bar{u}_{2yy} \quad .$$

In the region where $\eta^2 < \Delta/2\pi^2 h_2$; i.e., where, for the basic state alone, $\pi_{2y} < 0$; $\bar{u}_{2yy}$ is negative. Outside this region, in the domain $\sim 0.6 > 1/2 + \eta > \sim 0.53$, $\bar{u}_{2yy}$ is positive. Schematically, the effect of the corrections is both to reduce the degree of supercriticality in the central region and to flatten π_{2y}, broadening the scale of the inner region in which π_{2y} is small.

In the non-linear discussion we shall refer to both of the choices of parameter settings that have been mentioned. For ease of reference, we shall label the values as follows:

Case 1. $F = 10.0$, $U = 1.0$, $h_2 = 5.0$ $(\beta_m = 15.0)$

Case 2. $F = 6.6164$ $U = 1.0$, $h_2 = 9.8836$ $(\beta_m = 16.5)$

Heuristic Explanation of the Meridional Structure of ϕ_2

There are some striking features in the numerical results. Firstly, as the maximum critical value of β is approached, the phase speed of the unstable mode tends to zero. Secondly, in the same limit, the lower streamfunction of the unstable eigenfunction becomes increasingly concentrated near the center of the channel. Outside this region, $\phi_2 \dashrightarrow 0$ as $\Delta \dashrightarrow 0$. The neighborhood of the center of the channel is distinguished by the fact that π_{2y} is approximately zero there. Elsewhere π_{2y} is O(1). We can explain the qualitative structure of ϕ_2 as follows.

One can obtain a qualitative feeling for why the lower layer streamfunction is concentrated near the center of the channel by considering the potential vorticity dynamics of the lower layer. The potential vorticity balance in the lower layer is given by

$$c\,[(\partial_y^2 - k^2 - F)\ \phi_2 + F\,\phi_1] + \pi_{2y}\,\phi_2 = 0$$

We have seen that ϕ_2 is small so that, as far as an order of magnitude argument is concerned, we have that

$$c\,F\,\phi_1 \sim \pi_{2y}\,\phi_2$$

(In the outer region, $\partial_y^2\,\phi_2 << \phi_1$, and the suggested balance is not only correct in terms of magnitude but is also a good approximation. In the inner region, $\partial_y^2\ \phi_2 \sim \phi_1$ so that the above balance, in general, yields the correct size for ϕ_2 but is no longer a good approximation. Note that the omitted term $\partial_y^2\ \phi_2$ prevents ϕ_2 from becoming singular at the two points in the inner region at which $\pi_{2y} = 0$ as the above balance alone would suggest.)

We can estimate the size of ϕ_2 using

$$\phi_2 \sim c\,F\,\phi_1\ /\ \pi_{2y}(y)$$

In the outer region π_{2y} is O(1) so that

$$\phi_2 \sim O\ (c\,F\,\phi_1)\ ,$$

but in an inner region of width $O(\Delta^{1/2})$ about the channel center, π_{2y} is small, $O(\Delta)$, so that there

$$\phi_2 \sim O\ (\Delta^{-1}\,c\,F\,\phi_1)$$

i.e., larger by a factor Δ^{-1}. If we normalize ϕ_1 to be O(1) and use the fact that c is $O(\Delta^2)$, then we can see that ϕ_2 will be $O(\Delta^2)$, in the outer region and $O(\Delta)$ in the inner region.

In Phillips' model, π_{2y} is independent of y. As $\Delta \to 0$, π_{2y} is then of $O(\Delta)$ over the entire channel while $c \sim O(\Delta^{1/2})$. There is therefore no mechanism similar to that above to force ϕ_2 to be small over some part of the channel.

Analytical Model

Noting the relations between k, c and Δ suggested by the numerical results, one can construct an approximate solution to the equations (3.1) and (3.2) that is asymptotically valid as $\Delta \to 0$. This is not a complete solution in this neighborhood, being restricted to those modes for which $c \to 0$ as $\Delta \to 0$.

Rewriting (3.1) and (3.2) in terms of normal modes yields

$$(U - c)\,[(\nabla^2 - F)\,\phi_1 + F\,\phi_2] + (\beta_m + FU)\,\phi_1 = \Delta\,\phi_1 \qquad (3.7)$$

$$-c\,[(\nabla^2 - F)\,\phi_2 + F\,\phi_1] + h_2\,(1 + \cos 2\pi y)\,\phi_2 = \Delta\,\phi_2 \qquad (3.8)$$

We restrict attention to the case $4\,\pi^2 > \beta_m/U > \pi^2$. The numerical results suggest that the left-hand branch of the marginal curve is the locus of the stationary neutral modes noted earlier, namely

$$k^2 = \beta/U - \pi^2 = (\beta_m/U - \pi^2) - \Delta/U$$

We look at wavenumbers close to this curve and set

$$k^2 = k_0^2 - \Delta\,k_1^2 + \Delta^{3/2}\,k_2^2 \quad \text{where} \quad k_0^2 = \beta_m/U - \pi^2, \quad k_1^2 = 1/U$$

Expand $\quad c = \Delta^2\,c_1 + \ldots$

We divide the y-interval into inner and outer regions, the inner corresponding to

$$\left| y - \frac{1}{2} \right| \sim O(\Delta^{1/2}), \quad \text{and define} \quad \Delta^{1/2}\,\eta = y - \frac{1}{2}$$

The numerical results show that the unstable mode is symmetric about y = 1/2 so we will restrict our attention to symmetric solutions. We expand the streamfunctions:

$$\text{Inner:} \quad \phi_1 = \psi_1^{(0)} + \Delta\psi_1^{(1)} + \Delta^2 \ln(1/\Delta)\psi_1^{(2)} + \Delta^2\psi_1^{(3)} + \ldots$$

$$\phi_2 = \Delta\psi_2^{(1)} + \ldots \tag{3.9}$$

$$\text{Outer:} \quad \phi_1 = \psi_1^{(0)} + \Delta^{3/2}\psi_{1+}^{(2)} + \Delta^2\psi_{1+}^{(3)} + \ldots$$

$$\phi_2 = \Delta^2\psi_2^{(1)} + \ldots \tag{3.10}$$

In the inner expansion of ϕ_1, we have included a term of $O[\Delta^2 \ln(1/\Delta)]$. When we examine the potential vorticity balance in the inner region, we will find no direct forcing for this term. However, when we attempt to match the inner solution to the outer solution, we will discover that the term in question is necessary to allow the two solutions to join smoothly. Note that $\psi_{1\,in}^{(2)}$ will be a homogeneous solution of the relevant inner problem.

The potential vorticity equations become

$$\text{Outer:} \quad (\partial_y^2 + \pi^2)\,\phi_1 = -F\,\phi_2 + \Delta^{3/2}\,k_2^2\,\phi_1 - \Delta^2\,(c_1/U^2)(\beta_m + FU)\,\phi_1 + \ldots$$

$$h_2\,(1 + \cos 2\pi y)\,\phi_2 = \Delta^2\,c_1\,F\,\phi_1 + \ldots \tag{3.11}$$

Inner: $$\partial_\eta^2 \phi_1 = -\Delta \pi^2 \phi_1 - \Delta^2 F \phi_2 + \ldots \tag{3.12}$$

$$\left(\partial_\eta^2 + [1/c_1 - (M/c_1)\,\eta^2]\right)\phi_2 = -\Delta F \phi_1 + \ldots, \quad M = 2\pi^2 h_2$$

Boundary conditions are $\phi_1 = 0 = \phi_2$ at $y = 1$.

From the outer problem we discover that

$$\psi_1^{(0)} = \sin \pi y \tag{3.13}$$

$$\psi_{1+}^{(2)} = -(k_2^2/2\pi)\,(y-1)\,\cos \pi y \tag{3.14}$$

$$\psi_{1+}^{(3)} = \frac{1}{2\pi} c_1 \left[\frac{\beta + FU}{U^2} - \frac{F^2}{h_2}\right](y-1)\cos \pi y + \sin \pi y \left[\frac{c_1 F^2}{4\pi^2 h_2} \ln (1 - \sin^2 \pi y)\right] \tag{3.15}$$

$$\psi_2^{(1)} = \frac{c_1 F \sin \pi y}{h_2 (1+ \cos 2\pi y)} \tag{3.16}$$

In the inner region,

$$\psi_1^{(0)} = 1, \quad \psi_1^{(1)} = -\frac{1}{2}\pi^2 \eta^2, \quad \psi_1^{(2)} = A \tag{3.17}$$

and

$$\psi_1^{(3)} = \frac{1}{24}\pi^4 \eta^4 - F\int_0^\eta d\eta' \int_0^{\eta'} d\eta''\, \psi_2^{(1)}(\eta'') + R^{(3)} \tag{3.18}$$

where A and $R^{(3)}$ are constants.

$\psi_2^{(1)}$ is determined by

$$\left[\partial_\eta^2 + \left(\frac{1}{c_1} - \frac{M}{c_1}\eta^2\right)\right]\psi_2^{(1)} = -F .$$

Rescaling $$\zeta = \left(\frac{4M}{c_1}\right)^{1/4}\eta ,$$

this becomes $$\left[\partial_\zeta^2 + \left(\nu + \frac{1}{2} - \frac{1}{4}\zeta^2\right)\right]\psi_2^{(1)} = -F\left(\frac{c_1}{4M}\right)^{1/2} \qquad (3.19)$$

where $$\nu = \left(\frac{1}{4c_1 M}\right)^{1/2} - \frac{1}{2}$$

Except where $\nu = 0, 2, 4, \ldots$ this has a formal solution

$$\psi_2^{(1)} = -F\left(\frac{c_1}{4M}\right)^{1/2} \sum_{n=0}^{\infty} \frac{1}{\nu-2n}\, 2^{-n}\, \frac{1}{n!}\, D_{2n}(\zeta) \qquad (3.20)$$

which, when $\nu \neq 1, 3, \ldots$, may be re-expressed as

$$\psi_2^{(1)} = F\left(\frac{c_1}{4M}\right)^{1/2} \frac{\Gamma(-\nu)}{(2\pi)^{1/2}}\left[D_\nu(\zeta)\int_{-\infty}^{\zeta} D_\nu(-\zeta') + D_\nu(-\zeta)\int_{\infty}^{\zeta} D_\nu(\zeta')\right] \qquad (3.21)$$

(3.18) may be rewritten

$$\psi_1^{(3)} = \frac{1}{24}\pi^4\eta^4 - F\left(\frac{c_1}{4M}\right)^{1/2}\int_0^{\zeta} d\zeta' \int_0^{\zeta'} d\zeta''\, \psi_2^{(1)}(\zeta'') + R^{(3)}. \qquad (3.22)$$

As $\zeta \to \infty$ $\qquad \psi_2^{(1)}(\zeta) \sim 4F\left(\frac{c_1}{4M}\right)^{1/2} \zeta^{-2} + \ldots$

$$\psi_1^{(3)} \sim \frac{1}{24}\pi^4\eta^4 - F\left(\frac{c_1}{4M}\right)^{1/2}\left[\zeta\int_0^\infty d\zeta\, \psi_2^{(1)}(\zeta) - \left(\frac{4c_1}{M}\right)^{1/2} F \ln\zeta + R^{(3)} + O(\zeta^{-2})\right]$$

The asymptotic form of the inner solution in the upper layer as $\zeta \to \infty$ is then

$$\psi_{1\,in} \sim (1 - \Delta\,\frac{1}{2}\pi^2\eta^2 + \Delta^2\frac{1}{24}\pi^4\eta^4) + \Delta^2 \ln(1/\Delta)\, A \tag{3.23}$$

$$+ \Delta^2\left[-F\left(\frac{c_1}{4M}\right)^{1/2}\zeta\int_0^\infty d\zeta\, \psi_2^{(1)}(\zeta) + \frac{F^2 c_1}{M}\ln\zeta + \tilde{R}^{(3)} + O(\zeta^{-2})\right]$$

For the outer solution, as $\eta \to 0$,

$$\psi_{2\,out} \sim (1 - \Delta\,\frac{1}{2}\pi^2\eta^2 + \Delta^2\frac{1}{24}\pi^4\eta^4) - \frac{c_1F^2}{4\pi^2 h_2}\Delta^2 \ln(1/\Delta) \tag{3.24}$$

$$+ \Delta^2\left[-\frac{1}{4}k_2^2\left(\frac{c_1}{4M}\right)^{1/4}\zeta + \frac{c_1F^2}{2\pi^2h_2}\ln\zeta + \frac{c_1F^2}{2\pi^2h_2}\ln\pi + \ldots\right]$$

Matching the terms proportional to $\Delta^2\zeta$ yields a dispersion relation

$$k_2^2 = 4F\left(\frac{c_1}{4M}\right)^{1/4}\int_0^\infty d\zeta\, \psi_2^{(1)}(\zeta) \tag{3.25}$$

By using an integral transform solution of (3.19), valid for $-1 < \nu < 0$, integrating to find the integral on the right-hand side of (3.25) and then extending the result to $\nu \in \mathbb{C}$, $\nu \neq 0, 2, \ldots$, by analytic continuation, one finds that

$$k_2^2 = \pi F^2 \left(\frac{c_1}{M}\right)^{3/4} \Gamma(-\tfrac{\nu}{2}) \,/\, \Gamma(\tfrac{1}{2} - \tfrac{\nu}{2}) \qquad (3.26)$$

The dispersion relation gives c_1 as an implicit function of k_2^2 for general, real k_2^2. It becomes invalid in the limit $k_2^2 \to \infty$ since then $\nu \to 2n$, where $n = 0, 1, \ldots$, the operator on the left-hand side of equation (3.19) becomes singular and the forcing on the right-hand side does not satisfy the necessary secularity condition. Equation (3.26) is invalid also when $k_2^2 < O(\Delta^{1/2})$ on all branches for which $c_1 \not\to 0$ as $k_2^2 \to 0$ because higher order terms, neglected here, become significant. However, Equation (3.26) remains valid as $k_2^2 \to 0$ on those branches for which $c_1 \to 0$ at the same time. These latter happen to be the branches that correspond to the growing and decaying modes. In both regions of invalidity, the expansion procedure can be reordered to obtain the correct extension of the dispersion relation to these regions.

While it is difficult to plot the two complex branches of Equation (3.26) in order to compare them with the numerical work, we can reproduce some of the features of the numerical results. Regarding k_2^2 as a function of c_1, we find that

$$\frac{dk_2^2}{dc_1} = 0 \quad \text{when} \quad c_1 = \tilde{c}_1 \simeq 0.0255 \quad \text{and} \quad k_2^2 = \tilde{k}_2^2 (c_1) \simeq 4.39 \ .$$

In the neighborhood of this

$$k_2^2 = \tilde{k}_2^2 + \frac{1}{2}(c_1 - \tilde{c}_1)^2 \left.\frac{d^2k_2^2}{dc_1^2}\right|_{\tilde{c}_1}$$

so that

$$c_1 - \tilde{c}_1 = \left[2 \Big/ \left.\frac{d^2k_2^2}{dc_1^2}\right|_{\tilde{c}_1} \left(k_2^2 - \tilde{k}_2^2\right) \right]^{1/2}$$

Thus, provided that $d^2k_2^2/dc_1^2\big|\tilde{c}_1 \neq 0$, $\tilde{k}_2^2 = k_2^2$ should correspond to a bifurcation from a pair of neutral modes to an unstable and a stable mode. Thus $k_2^2 = \tilde{k}_2^2$ is a candidate for the position of the right-hand branch of the marginal curve. Looking at the numerical results in the neighborhood of the cusp tip we can estimate that branch as

$$k^2 - k_0^2 + \Delta / U = \tilde{k}_2^2 \, \Delta^{3/2} \quad \text{where} \quad \tilde{k}_2^2 = 4.34$$

Similarly, we may find numerically that the phase speed of the marginal modes on the right-hand branch of the marginal curve is given by

$$c = \tilde{c}_1 \, \Delta^2 \quad \text{where} \quad \tilde{c}_1 = 0.0258$$

The numerical and theoretical values for $\tilde{k}_2^2$ and $\tilde{c}_1$ are in close agreement.

Energy Balance

From the theoretical results, we know that in the outer region

$$\phi_1 = \sin \pi y + O(\Delta^{3/2})$$

$$\phi_2 = \Delta^2 \, c_1 \frac{F \sin \pi y}{h_2 (1 + \cos 2\pi y)}$$

while in the inner region

$$\phi_1 = 1 + O(\Delta)$$

$$\phi_2 = \Delta \frac{2}{\sqrt{\pi}} F \left(\frac{c_1}{4M}\right)^{1/2} f(\zeta;\nu)$$

where $f(\zeta)$ is a function satisfying $[\partial_\zeta^2 + (\nu + 1/2 - 1/4\,\zeta^2)]\, f = -\sqrt{\pi}/2$. For the unstable mode, the argument of c_1 is generally $O(1)$ and ε $(0, \pi/2)$. The phase shift between the upper and lower layer streamfunctions is $O(1)$ over both the outer and most of the inner region.

The energy equation for the unstable mode may be put in the form

$$\partial_t E = \frac{k}{4} UF \int_0^1 dy \; \mathrm{Im}\,[\phi_1(y)\, \phi_2^*(y)]$$

where E is the sum of the kinetic and potential energies of the two layers averaged over a zonal wavelength and integrated over the channel width. Energy is released by the baroclinic conversion mechanism as the perturbation generates a net rectified heat flux down the meridional temperature gradient of the basic state.

We can decompose the source term into contributions from the inner and outer regions and indicate the scale of the various terms in the energy equation

$$\partial_t E = \frac{k}{4} UF \int_{\text{inner}} \text{Im}\,(\phi_1 \phi_2^*) + \frac{k}{4} UF \int_{\text{outer}} \text{Im}\,(\phi_1 \phi_2^*)$$

$$O(\Delta^2) \quad O(1) \quad O(\Delta^{1/2}) \quad O(1)\ O(\Delta) \quad O(1) \quad O(1)\ O(\Delta^2)$$

$$\text{phase shift} = O(1) \qquad \text{phase shift} = O(1)$$

We see that, locally, the heat flux in the inner region is relatively strong, $O(\Delta)$. The width of the inner region is $O(\Delta^{1/2})$ but most of the heat flux cancels when integrated across the inner region so that the net energy release in the inner region is $O(\Delta^2)$. The energy released in the outer region has a similar order of magnitude, $O(\Delta^2)$, thus both the inner and outer regions are important in the release of available potential energy to the perturbation.

Figure 3.5(c) shows the heat flux, multiplied by F, as a function of y, that is associated with the unstable mode whose streamfunctions were plotted in Figures 3.5(a) and (b). Figure 3.7(c) shows F times the heat flux for the unstable mode of Figures 3.7(a) and (b). In each case, one notes that next to the central positive maximum there lies a negative minimum of the heat flux. These two extrema, which are both associated with the inner region, largely cancel when the heat flux is integrated across the channel.

In addition to the heat fluxes, there are weak, divergent, horizontal Reynolds stresses associated with the unstable mode. In the upper layer, these exist in both the inner and outer regions and are $O(\Delta^2)$. In the lower layer, the horizontal Reynolds stress is $O(\Delta^2)$ in the inner region

but $O(\Delta^4)$ in the outer [see Figure 3.8(b) and (c)]. Because of the absence of horizontal shear, there is no net barotropic energy conversion associated with these divergent stresses. Had the meridional variation been furnished by horizontal shear of the basic velocity field rather than topography, in such a way as to produce similar potential vorticity gradients one would expect to see some barotropic energy exchange with the mean flow occurring alongside the baroclinic conversion. This might either augment or reduce the growth rate of the baroclinic instability depending on the sign of the barotropic exchange. However, provided that the shear is such that the general properties of the potential vorticity gradients are unchanged and the minimum upper layer velocity remains positive, the essential properties of this baroclinic mode of instability should remain unchanged.

Neutral Modes

So far attention has been focussed on the unstable mode of the system. The neutral modes, however, also have some interesting aspects. When k^2 is in the neighborhood of k_0^2, one can divide the neutral modes into two distinct classes. The first class will consist of modes with $c = O(1)$ and streamfunctions that are $O(1)$ in both layers. They will not possess any internal layer structure and formally they will form an infinite set with progressively shorter meridional scales. These are simply analogues of the $\phi = (1,\gamma) \sin n\pi y \exp(ikx)$ normal modes of Phillips' model and will not be considered further.

The second class is an infinite set of neutral modes, all having phase speeds of $O(\Delta^2)$, an upper layer streamfunction of $O(1)$, an internal layer

near the mid-line of the channel, and a lower layer streamfunction that is weak. The dispersion relations, for k^2 near k_0^2, are given by Equation (3.26) and are simply those branches of $c_1(k_2^2)$ that do not correspond to the stable/unstable mode pair discussed above. These branches are shown in Figure 3.9. These modes are nearly stationary (more generally, they propagate at velocities close to the speed of the lower layer). Thinking back to the analytical study, we see that for these modes the zonal structure and fast time dependence ($\omega = 0$ in this case) are determined together in the leading order problem but that the meridional structure problem is degenerate, only the meridional structure of the leading order part of the upper layer streamfunction (i.e., $\sin \pi y$) is determined at this order. The full meridional structure, in particular the internal layer structure of each mode, is not determined until higher order. The neutral modes each have a different internal layer structure which depends on the c_1 appropriate to that mode, i.e., on the slow time scale behavior of the mode.

The existence of this infinite set of neutral modes each having a period comparable to the e-folding time of the unstable mode and differing in their internal layer structures, has a significance for any weakly finite amplitude study. Heuristically, any non-linear interaction that produces a resultant that is "resonant" with the unstable wave will also be "resonant" with these neutral modes. The technical consequence of this is that the determination of the internal layer structure of the finite amplitude solution is coupled to the determination of the slow time scale behavior. This is to be contrasted with the weakly finite amplitude solution for Phillips' model (away from minimum critical shear) where the

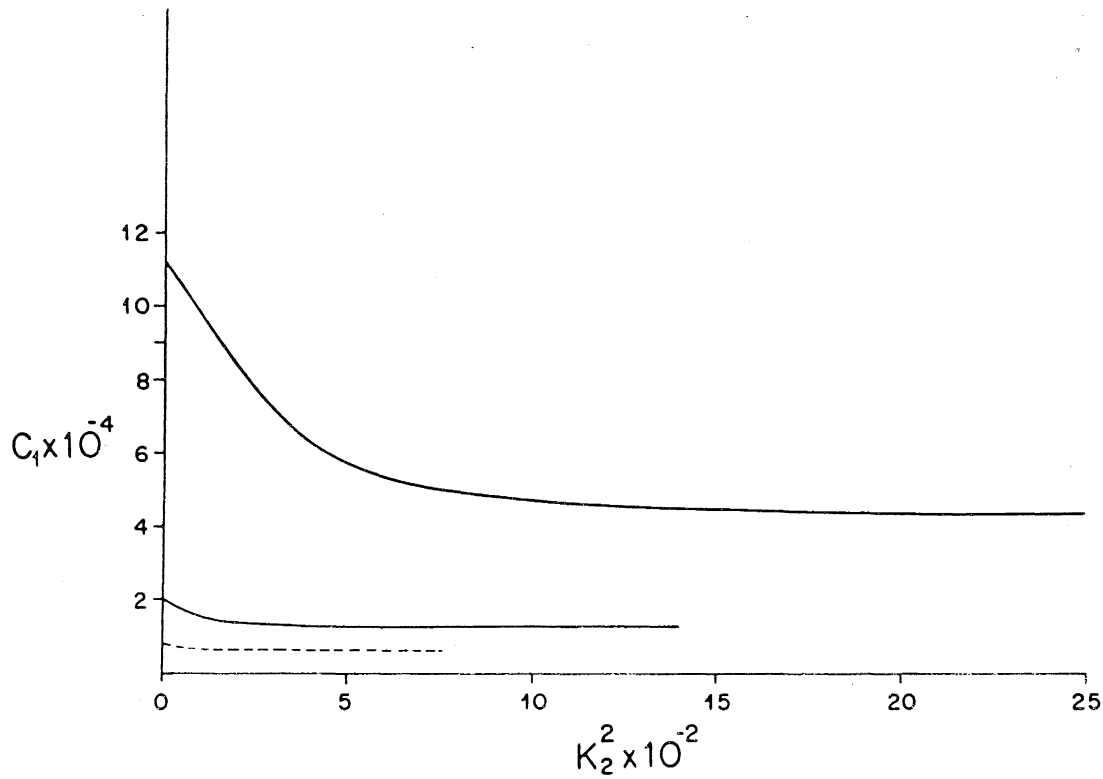

Figure 3.9: Dispersion curves for the first three slow, neutral mode solutions of (3.26).

determination of the spatial structure and the slow evolution are separated.

Concluding Remarks

The results of this chapter have revealed that the introduction of meridional variation into Phillips' model alters the structure of the slowly growing normal modes of the linear problem in a rather novel way. We see a "critical layer" phenomenon in which the lower layer streamfunction is concentrated in a narrow meridional strip in the region in which the potential vorticity gradient of the basic state, in that layer, is small. A similar development is not seen in the meridionally uniform Phillips model because, when the equilibrium flow is slightly supercritical, the region of small lower layer potential vorticity gradient is not localized meridionally. We have observed both a lengthening of the growth rate time scale for the slightly supercritical modes and a tendency for them to move with phase speeds that are almost the same as the velocity of the lower layer.

Although the differences between the meridionally varying model and the uniform model become less pronounced as one moves away from the near-critical region of parameter space, the fact that the slightly unstable modes form the cornerstone of the weakly finite amplitude theory lends significance to the differences between the two linear models. In addition, the appearance of a set of neutral modes having similar zonal structure and fast time dependence as the unstable mode can be expected to influence the finite amplitude dynamics.

In view of the small meridional scale and the reversal of sign of the heat flux associated with a slowly growing mode, a fairly closely spaced set of point measurements of the heat flux associated with any experimental or geophysical realization of such a mode, would be required before the flux could be adequately resolved.

We note the curious feature that, while in this model the presence of topographic relief has a profound effect on the near-critical modes, both the mean flow and the disturbance velocities are weak in the lower layer. One might not, at first, anticipate the role played by topography in the behavior of such modes.

CHAPTER 4

4. Baroclinic instability in a meridionally varying two-layer model: Weakly non-linear theory.

In this chapter we will describe some of the weakly finite amplitude behavior of slowly growing unstable modes in the meridionally varying two-layer model. The results of this should be compared with those of the weakly finite amplitude theory for a meridionally uniform model (Pedlosky, 1970). It will become apparent that there is a considerable difference in the behavior of the two models. This is due to the differences in the structure of the normal mode solution of the two-linear models.

We will not be able to present a complete solution of the weakly finite amplitude problem. Instead, we shall develop a set of amplitude equations that govern the evolution of a slightly supercritical unstable mode in the period immediately following the linear phase of its growth. We shall include interactions between the unstable wave and some of the neutral Rossby waves supported by the system. However, only two neutral waves will be considered and these will be assumed to form a resonant triad with the unstable wave. Here we are selecting only one of the many resonant triads involving the unstable wave that actually exist. In this way, we discover something of the role which wave-wave interaction may play in the evolution of the unstable wave, yet retain some degree of tractability in the problem. In the 'real', physical problem one would have to include all such triads. Instead of solving this complete problem in a consistent way, we are choosing to study a method.

One of the things to come out of the derivation of the amplitude equations will be the result that the contribution to the evolution of the unstable wave that is made by wave/mean flow interaction will be smaller than the terms that arise as a result of interaction with the neutral waves. This is a surprising result. It means that, in the asymptotic limit of small supercriticality, the effects of modification to the mean flow induced by the unstable wave, can be neglected in at least the early stages of the non-linear evolution. In the corresponding theory for the meridionally uniform model, this wave/mean flow interaction was responsible for the vacillation cycle into which the unstable wave was ensnared. If we are forced to neglect that mechanism here, we are left with the question of whether the interaction between the unstable wave and neutral waves can halt the growth of the unstable wave that is being driven by the baroclinic instability mechanism. In fact, we must also pose the question of whether the amplitudes of the sidebands can grow from the very small levels that one might associate with noise-like initial conditions, to levels at which the sidebands can begin to affect the evolution of the unstable wave. In order to do this the sidebands have to be able to extract energy from the unstable wave while it in turn is growing as a result of baroclinic instability. The mechanism of this will be discussed in more detail later.

At the amplitude scales appropriate to a resonant triad interaction on the $O(\Delta^{-2})$ time scale, the harmonics of the three principle waves, including those of the slow, unstable wave, are not important in the determination of the evolution. Provided that the triad mechanism equilibrates the unstable wave, the effects of higher harmonics and of the mean

flow correction will be limited to time scales that are longer than $O(\Delta^{-2})$. If resonant triad interactions are inhibited, say by a quantization of the zonal wavenumbers permitted in the system, then the linear instability mechanism will cause the unstable wave to grow beyond the amplitude level at which triad dynamics would have been important [this level will turn out to be $O(\Delta^2)$]. As the unstable wave grows, the mean flow correction and higher harmonics that accompany it will become larger until they reach an amplitude that enables them to affect the evolution of the unstable wave on the linear growth time scale, $O(\Delta^{-2})$. At this stage, non-linearity has become non-trivial and there arises the possibility of equilibration of the unstable wave by the action of the mean flow and the higher harmonics. It may be shown that the amplitude of the unstable wave at this point is $O(\Delta^{3/2})$. The triad interaction, when present, is a more powerful non-linear mechanism than the wave-mean flow/higher harmonics interaction, in the sense that the former can affect the evolution of the unstable wave on the linear growth time scale at a smaller unstable wave amplitude than can the latter process. We will consider the 'single-wave' problem in which the triad mechanism is excluded, in the latter part of this chapter.

The amplitude equations that we derive for the triad problem are too difficult for us to solve analytically. To answer the two rhetorical questions raised earlier, we turn to numerical simulations of this weakly finite amplitude problem. Some of these are discussed below. They illustrate the fact that some triads exist which do restrain the unstable mode at an amplitude level at which the wave/mean flow interaction can be consistently neglected on the evolution time scale. It may be the case that

the effects of wave/mean flow interaction, though small, are important on a longer time scale.

The remainder of this chapter is arranged in the following way. The section immediately below derives the equations that govern the amplitudes of the unstable wave and the sidebands in the limit of small supercriticality. The first part of this - the material up to Equation (4.1) - explains the choice of temporal and spatial scales, the appropriate amplitude scales for the three waves and the way in which the streamfunction is broken up. The notation used in the rest of the chapter is introduced here. The analysis between Equations (4.1) and (4.26) is the routine application of perturbation methods to obtain the amplitude equations. Some comments on the inner layer structure of the lower layer streamfunction, an important feature of the solution, are made between Equations (4.24) and (4.25). Equation (4.27) summarizes the amplitude equations for the triad interaction which are the main objective of this section, while (4.28) offers an alternative form. The latter part of this section provides a heuristic demonstration that the changes to the mean flow are too small to affect the evolution described by (4.27) on the $O(\Delta^{-2})$ time scale.

The next section, beginning a little above equation (4.31), discusses the formal energy balance for the three wave system. This is followed by an account of some numerical simulations of the evolution of the unstable wave and its sidebands. After this, we turn to the question of the single wave evolution of the unstable mode. A brief prefatory section is succeeded by a section summarizing the derivation of the amplitude equations

for the single wave problem [(4.62), (4.53), (4.54) and (4.55)]. A more detailed account of this derivation is contained in Appendix B. Some aspects of the mean flow corrections and of the higher zonal harmonics are pointed out in a section entitled "Features of the Asymptotic Solution." Finally, the single-wave problem is modelled numerically. Two types of simulation were performed. The first, which is of the full single-wave problem, is related in the section "Numerical Simulations" while the second type, from which the higher harmonics were excluded in an attempt to discover the effects of wave-mean flow interaction alone, is considered in the last section of the chapter.

Asymptotic Evolution Equations

For a weakly supercritical flow with $\beta = \beta_m - \Delta$, $0 < \Delta << 1$, the linear problem suggests that the time scale for the evolution of an unstable mode should be $O(\Delta^2)$. We therefore introduce a slow time scale

$$T = \Delta^2 t , \qquad \partial_t \dashrightarrow \partial_t + \Delta^2 \partial_T$$

The quasigeostrophic potential vorticity equations become

$$\begin{aligned}
&(U\partial_x + \partial_t)\,[(\nabla^2 - F)\,\phi_1 + F\phi_2] + (\beta_m + FU)\,\phi_{1x} + J(\phi_1, (\nabla^2 - F)\,\phi_1 + F\phi_2) \\
&\qquad - \Delta\phi_{1x} + \Delta^2 \partial_T\,[(\nabla^2 - F)\,\phi_1 + F\phi_2] = 0 \\
&\partial_t\,[(\nabla^2 - F)\,\phi_2 + F\phi_1] + (\beta_m - FU + h_y) + J(\phi_2, (\nabla^2 - F)\,\phi_2 + F\phi_1) \\
&\qquad - \Delta\phi_{2x} + \Delta^2 \partial_T\,[(\nabla^2 - F)\,\phi_2 + F\phi_1] = 0
\end{aligned} \tag{4.0}$$

The y-domain is divided into two regions, an inner region of width $O(\Delta^{1/2})$ about the center line of the channel and the outer region made up of the remainder. We will use y as the meridional variable in the outer region but resort to the scaled coordinate, $\eta = \Delta^{-1/2}\ (y - 1/2)$ in the inner region.

We wish to consider a streamfunction dominated by three distinct zonal wavenumbers and we will develop the solution as an asymptotic series in Δ. To keep track of wavenumbers, layers and positions in asymptotic series requires some cumbersome notation which will be explained here.

ϕ will be used to denote a streamfunction when considered as a function of x, y and t. It may also be used to refer to the y-dependent part of a separated modal component of a streamfunction, e.g.,

$$\underset{\sim}{\phi} = \underset{\sim}{\phi}\ (x, y, t)$$

$$\underset{\sim}{\phi} = A(T)\ \underset{\sim}{\phi}\ (y)\ e^{ik(x-ct)}\ .$$

The particular usage should be apparent from the context.

ϕ will carry up to three affixes in the following positions ${}^{(i)}\phi_k^{(j)}$.

Here i is an index denoting a particular zonal wavenumber, either 0, 1 or 2.

j is an index denoting a position in an asymptotic expansion series.

k is a suffix denoting the layer, either 1 or 2.

The abbreviation $\underset{\sim}{\phi}$ denotes (ϕ_1, ϕ_2). E.g.,

$$\underset{\sim}{\phi} = \sum_{n=n_1}^{n_2} ({}^{(n)}\phi_1, {}^{(n)}\phi_2) \; e^{ik_n (x-c_n t)}$$

$${}^{(n)}\phi_1 = {}^{(n)}\phi_1^{(0)} + \Delta^{1/2} \; {}^{(n)}\phi_1^{(1)} + \Delta {}^{(n)}\phi_1^{(2)} + \ldots$$

The notation ${}^{(i)}\psi_k^{(j)}(y)$ will be used for the y-structure of ${}^{(i)}\phi_k^{(j)}$. It will not be necessary to include higher harmonics of the three waves nor corrections to the mean flow as these only become relevant at higher orders in Δ than those to which we need extend our calculations. After the amplitude equations have been obtained, we will indicate the sizes of the mean flow corrections.

In the present problem, zonal wavenumbers are really parameters specified in advance, however, it is convenient to make this specification in the form of a truncated expansion in Δ, thus,

$${}^{(j)}k^2 = {}^{(j)}k_0^2 - \Delta {}^{(j)}k_1^2 + \Delta^{3/2} \, {}^{(j)}k_2^2 + \Delta^2 \, {}^{(j)}k_3^2 \, .$$

Recalling that the natural long time scale for the problem is $O(\Delta^{-2})$, we write the phase speeds of the linear modes found at the above wavenumbers as expansions up to $O(\Delta^{3/2})$: ${}^{(j)}c = {}^{(j)}c_0 + \Delta {}^{(j)}c_1 + \Delta^{3/2} \, {}^{(j)}c_2$. Time-scales up to and including $O(\Delta^{-3/2})$ will be regarded as fast time scales. We require that the three principal waves satisfy the usual conditions for resonant triads on these fast time scales. These conditions are that the sums of the frequencies and wavenumbers vanish to $O(\Delta^{3/2})$. If we assume

that ${}^{(0)}k$ is the wavenumber of the weakly unstable wave while ${}^{(1)}k$ and ${}^{(2)}k$ correspond to the neutral waves, the resonance conditions become

$$ {}^{(0)}k_r + {}^{(1)}k_r + {}^{(2)}k_r = 0 \qquad\qquad r = 0, 1, 2, 3 $$

$$ {}^{(1)}k_0 \, {}^{(1)}c_0 + {}^{(2)}k_0 \, {}^{(2)}c_0 = 0 $$

$$ {}^{(1)}k_0 \, {}^{(1)}c_1 + {}^{(2)}k_0 \, {}^{(2)}c_1 - \tfrac{1}{2}\left({}^{(1)}c_0 \, {}^{(1)}k_1^2/{}^{(1)}k_0 + {}^{(2)}c_0 \, {}^{(2)}k_1^2/{}^{(2)}k_0\right) = 0 $$

$$ {}^{(1)}k_0 \, {}^{(1)}c_2 + {}^{(2)}k_0 \, {}^{(2)}c_2 + \tfrac{1}{2}\left({}^{(1)}c_0 \, {}^{(1)}k_2^2/{}^{(1)}k_0 + {}^{(2)}c_0 \, {}^{(2)}k_2^2/{}^{(2)}k_0\right) = 0 $$

An additional notational device that will sometimes be used but often omitted, is the employment of the suffixes 'out' and 'in' to denote the outer and inner regions of the y-domain.

We re-define the streamfunctions to take into account the natural amplitude scales of the waves. With an obvious abuse of notation,

$$ \left({}^{(1)}\underset{\sim}{\phi}, \, {}^{(2)}\underset{\sim}{\phi}\right) = \Delta^{7/4} \left({}^{(1)}\underset{\sim}{\phi}, \, {}^{(2)}\underset{\sim}{\phi}\right) $$

$$ {}^{(0)}\phi_1 = \Delta^2 \, {}^{(0)}\phi_1 $$

$$ {}^{(0)}\phi_{2 \text{ out}} = \Delta^{7/2} \, {}^{(0)}\phi_{2 \text{ out}} $$

$$ {}^{(0)}\phi_{2 \text{ in}} = \Delta^3 \, {}^{(0)}\phi_{2 \text{ in}} $$

Henceforth we will work with the scaled streamfunctions on the right-hand side of these expressions, unless otherwise indicated.

In comparison to the triad interaction problems considered by Loesch (1974), the amplitude scales for the sidebands are unusual. In this problem, the sideband amplitudes are larger than that of the unstable wave. They are also larger than one would expect from a consideration of more traditional triad interaction problems. In a straightforward resonant triad interaction, the amplitudes of waves interacting on a Δ^{-2} timescale would ordinarily be $O(\Delta^2)$.

The streamfunctions will be expanded

$$\underset{\sim}{\phi}^{(j)} = \underset{\sim}{\phi}^{(j)}(0) + \Delta\, \underset{\sim}{\phi}^{(j)}(1) + \Delta^{3/2}\, \underset{\sim}{\phi}^{(j)}(2) + \Delta^2\, \underset{\sim}{\phi}^{(j)}(3) + \ldots \qquad j = 1,2$$

$$\phi_{1\ \text{out}}^{(0)} = \phi_1^{(0)}(0) + \Delta\, \phi_1^{(0)}(1) + \Delta^{3/2}\, \phi_{1+}^{(0)}(2) + \Delta^2\, \phi_{1+}^{(0)}(3) + \ldots$$

$$\phi_{1\ \text{in}}^{(0)} = \phi_1^{(0)}(0) + \Delta\, \phi_1^{(0)}(1) + \Delta^2 \ln \tfrac{1}{\Delta}\, \phi_1^{(0)}(2) + \Delta^2\, \phi_1^{(0)}(3) + \ldots$$

$$\phi_{2\ \text{out}}^{(0)} = \phi_2^{(0)}(1) + \Delta^{1/2}\, \phi_2^{(0)}(2) + \ldots$$

$$\phi_{2\ \text{in}}^{(0)} = \phi_2^{(0)}(1) + \ldots$$

Because of symmetry considerations we need only solve the problem in $1/2 \leq y \leq 1$. The '+' suffix is used in two of the terms in the expansion of $\phi_{1\ \text{out}}^{(0)}$ to make this explicit since the functional form of these two terms is different in the two halves of the channel.

Some further pieces of nomenclature are: the use of $J_{(j)}(A,B)$ to denote the projection of the Jacobian of A and B onto the $j^{(th)}$ Fourier component, $e^{i(j)kx}$; the use of j' in some equations to denote the second

neutral wave when j denotes the first; and the use of q to symbolize the perturbation potential vorticity associated with ϕ.

Substituting the neutral streamfunctions into the quasigeostrophic potential vorticity equations yields the following equations for the Fourier components corresponding to the neutral waves:

$$(U - {}^{(j)}c_0)\,[(\partial_y^2 - {}^{(j)}k_0^2 - F)\,{}^{(j)}\phi_1 + F\,{}^{(j)}\phi_2] + (\beta_m + FU)\,{}^{(j)}\phi_1 =$$

$$\Delta\left[[1 - (U - {}^{(j)}c_0)\,{}^{(j)}k_1^2]\,{}^{(j)}\phi_1 + {}^{(j)}c_1\,[(\partial_y^2 - {}^{(j)}k_0^2 - F)\,{}^{(j)}\phi_1 + F\,{}^{(j)}\phi_2]\right] +$$

$$+ \Delta^{3/2}\left[(U - {}^{(j)}c_0)\,{}^{(j)}k_2^2\,{}^{(j)}\phi_1 + {}^{(j)}c_2\,[(\partial_y^2 - {}^{(j)}k_0^2 - F)\,{}^{(j)}\phi_1 + F\,{}^{(j)}\phi_2]\right]$$

$$+ \Delta^2\left[(U - {}^{(j)}c_0)\,{}^{(j)}k_3^2\,{}^{(j)}\phi_1 + {}^{(j)}c_1\,{}^{(j)}k_1^2\,{}^{(j)}\phi_1 - \frac{1}{i\,{}^{(j)}k_0}\,\partial_T\,{}^{(j)}q_1\right.$$

$$\left. - \frac{1}{i\,{}^{(j)}k_0}\,[J_{(j)}({}^{(0)}\phi_1, {}^{(j')}q_1) + J_{(j)}({}^{(j')}\phi_1, {}^{(0)}q_1)]\right] \qquad (4.1)$$

$$-{}^{(j)}c_0\,[(\partial_y^2 - {}^{(j)}k_0^2 - F)\,{}^{(j)}\phi_2 + F\,{}^{(j)}\phi_1] + (\beta_m - FU + h_y)\,{}^{(j)}\phi_2 =$$

$$\Delta\left[(1 + {}^{(j)}c_0\,{}^{(j)}k_1^2)\,{}^{(j)}\phi_2 + {}^{(j)}c_1\,[(\partial_y^2 - {}^{(j)}k_0^2 - F)\,{}^{(j)}\phi_2 + F\,{}^{(j)}\phi_1]\right]$$

$$+ \Delta^{3/2}\left[-{}^{(j)}c_0\,{}^{(j)}k_2^2\,{}^{(j)}\phi_2 + {}^{(j)}c_2\,[(\partial_y^2 - {}^{(j)}k_0^2 - F)\,{}^{(j)}\phi_2 + F\,{}^{(j)}\phi_1]\right]$$

$$+ \Delta^2\left[-{}^{(j)}c_0\,{}^{(j)}k_3^2\,{}^{(j)}\phi_2 + {}^{(j)}c_1\,{}^{(j)}k_1^2\,{}^{(j)}\phi_2 - \frac{1}{i\,{}^{(j)}k_0}\,\partial_T\,{}^{(j)}q_2 -\right.$$

$$\left. - \frac{1}{i\,{}^{(j)}k_0}\,J_{(j)}\,({}^{(j')}q_2, {}^{(0)}q_2)\right] \qquad j = 1,2 \qquad (4.2)$$

Here $\beta_m = FU - h_y(1/2)$, as in Chapter 3, so that $\beta = \beta_m - \Delta$.

We use the expansions of the streamfunctions and collect all the terms of similar order to produce a sequence of problems for the successive terms in the expansions. At leading order,

$$(\partial_y^2 - {}^{(j)}k_0^2 - F)\,{}^{(j)}\phi_1^{(0)} + F\,{}^{(j)}\phi_2^{(0)} + \frac{\beta_m + FU}{U - {}^{(j)}c_0}\,{}^{(j)}\phi_1^{(0)} = 0 \qquad (4.2a)$$

$$(\partial_y^2 - {}^{(j)}k_0^2 - F)\,{}^{(j)}\phi_2^{(0)} + F\,{}^{(j)}\phi_1^{(0)} - \frac{\beta_m - FU + h_y}{{}^{(j)}c_0}\,{}^{(j)}\phi_2^{(0)} = 0 \qquad (4.2b)$$

This pair of ODEs with y-dependent coefficients is an eigenvalue problem for the leading order part of the phase speed of the sideband, ${}^{(j)}c_0$. Its solutions can be readily determined numerically. Solving (4.2) yields the dispersion relations for the side bands

$${}^{(j)}c_0 = {}^{(j)}c_0\,({}^{(j)}k_0)$$

and the leading order meridional structure of the streamfunctions. There is, of course, an infinite set of possible meridional modes. We suppose that we have selected a particular meridional mode for each sideband. This fixes ${}^{(j)}c_0$ and the functions ${}^{(j)}\psi_1(y)$, ${}^{(j)}\psi_2(y)$, in the leading order streamfunctions which we write

$$\underset{\sim}{{}^{(j)}\phi^{(0)}} = A_j(T)\begin{pmatrix} {}^{(j)}\psi_1(y) \\ {}^{(j)}\psi_2(y) \end{pmatrix} e^{i\,{}^{(j)}k\,(x - {}^{(j)}ct)}$$

The next two orders $O(\Delta)$ and $O(\Delta^{3/2})$ serve only to determine the corrections to the phase speeds and meridional structures due to the

differences at $O(\Delta)$ and $O(\Delta^{3/2})$ between the true wavenumber ${}^{(j)}k$ and the leading order term ${}^{(j)}k_0$. At $O(\Delta)$, the problem we obtain is

$$L_j \, \underset{\sim}{{}^{(j)}\phi^{(1)}} =$$

$$\left\{ \frac{1}{U_-{}^{(j)}c_0} \left[[{}^{(j)}c_1 \, (\partial_y^2 - {}^{(j)}k_0^2 - F) + 1 - (U_- - {}^{(j)}c_0)\,{}^{(j)}k_1^2] \, {}^{(j)}\phi_1^{(0)} + {}^{(j)}c_1 \, F \, {}^{(j)}\phi_2^{(0)} \right] \right.$$

$$\left. - \frac{1}{{}^{(j)}c_0} \left[{}^{(j)}c_1 \, F \, {}^{(j)}\phi_1^{(0)} + [{}^{(j)}c_1 (\partial_y^2 - {}^{(j)}k_0^2 - F) + (1 + {}^{(j)}c_0 \, {}^{(j)}k_1^2)] \, {}^{(j)}\phi_2^{(0)} \right] \right\} \tag{4.3}$$

where L_j is the matrix differential operator on the left-hand side of 4.2.

Since L_j is a self-adjoint singular operator, the forcing in (4.3) must satisfy a secularity condition,

$$\int dy \; {}^{(j)}\underset{\sim}{\psi} \cdot (\text{r.h.s.}) = 0$$

This yields an auxiliary dispersion relation

$${}^{(j)}c_1 = {}^{(j)}c_1 \, ({}^{(j)}k_1^2) \quad .$$

With this value of ${}^{(j)}c_1$, (4.3) can now be solved for the meridional structure of $\underset{\sim}{{}^{(j)}\phi^{(1)}}$. Because of the singular nature of L_j this will take the form

$$\underset{\sim}{{}^{(j)}\psi^{(1)}} = \underset{\sim}{{}^{(j)}\hat{\psi}^{(1)}} + \alpha_1 \, \underset{\sim}{{}^{(j)}\psi^{(0)}}$$

Here $\underset{\sim}{{}^{(j)}\psi^{(1)}} = (0, \, {}^{(j)}\psi_2^{(1)})$, where ${}^{(j)}\psi_2^{(1)}$ can be determined from the

upper layer equation in (4.3), and an arbitrary multiple of $\underset{\sim}{\psi}^{(j)}(0)$ can be added to the solution. We will choose the constant α_1 so that

$$\int dy \; \underset{\sim}{\phi}^{(j)}(1) \cdot \underset{\sim}{\phi}^{(j)}(0) = 0$$

i.e.,

$$\alpha_1 = - \int dy \; \underset{\sim}{\hat{\psi}}^{(j)}(1) \cdot \underset{\sim}{\psi}^{(j)}(0) \Big/ \int dy \; \underset{\sim}{\psi}^{(j)}(0) \cdot \underset{\sim}{\psi}^{(j)}(0) \quad .$$

The problem at $O(\Delta^{3/2})$ is dealt with in a similar fashion.

The first significant higher order problem occurs at $O(\Delta^2)$ where,

$$L_j \underset{\sim}{\phi}^{(j)}(3) =$$

$$\left(\begin{aligned}
&\frac{1}{U - {}^{(j)}c_0} \left[- \frac{1}{i\,{}^{(j)}k_0} \partial_T \, {}^{(j)}q_1^{(0)} - \frac{1}{i\,{}^{(j)}k_0} J_{(j)} \left({}^{(j')}\phi_1^{(0)}, {}^{(0)}q_1^{(0)} \right) \right. \\
&- \frac{1}{i\,{}^{(j)}k_0} J_{(j)} \left({}^{(0)}\phi_1^{(0)}, {}^{(j')}q_1^{(0)} \right) + \left[{}^{(j)}c_1 \, {}^{(j)}k_1^2 + \left(U - {}^{(j)}c_0 \right) {}^{(j)}k_3^2 \right] {}^{(j)}\phi_1^{(0)} \\
&\left. + \left[{}^{(j)}c_1 \left(\partial_y^2 - {}^{(j)}k_0^2 - F \right) + 1 - \left(U - {}^{(j)}c_0 \right) {}^{(j)}k_1^2 \right] {}^{(j)}\phi_1^{(1)} + {}^{(j)}c_1 \, F \, {}^{(j)}\phi_2^{(1)} \right] \\
&- \frac{1}{{}^{(j)}c_0} \left[- \frac{1}{i\,{}^{(j)}k_0} \partial_T \, {}^{(j)}q_2^{(0)} - \frac{1}{i\,{}^{(j)}k_0} J_{(j)} \left({}^{(j')}\phi_2^{(0)}, {}^{(0)}q_2^{(0)} \right) \right. \\
&+ \left({}^{(j)}c_1 \, {}^{(j)}k_1^2 - {}^{(j)}c_0 \, {}^{(j)}k_3^2 \right) {}^{(j)}\phi_2^{(0)} + \left[{}^{(j)}c_1 \left(\partial_y^2 - {}^{(j)}k_0^2 - F \right) \right. \\
&\left. \left. + \left(1 + {}^{(j)}c_0 \, {}^{(j)}k_1^2 \right) \right] {}^{(j)}\phi_2^{(1)} + {}^{(j)}c_1 \, F \, {}^{(j)}\phi_1^{(1)} \right]
\end{aligned} \right) \qquad (4.4)$$

The secularity condition for this differential problem yields an equation for the evolution of the amplitude A_j on the slow time scale. This equation has the form

$$A_{jT} = i\theta_j A_j + i M_j A_0^* A_j^* , \qquad j = 1,2 \tag{4.5}$$

M_j and θ_j are real constants whose form is rather complicated. They involve integrals of the functions ${}^{(j)}\psi_1^{(0)}(y)$ and ${}^{(j)}\psi_2^{(0)}(y)$ amongst other terms and their evaluation requires a full solution of (4.2) and 4.3). Some values for M_j pertaining to particular choices of triad will be noted later; these were obtained by solving (4.2) and (4.3) numerically, computing the necessary integrals and evaluating the expression for M_j. The formulae for θ_j and M_j are listed in Appendix A. $A_0(T)$ is the amplitude of the dominant part of the upper layer streamfunction associated with the unstable wavenumber and, like A_1 and A_2, varies on the long time scale.

As in the case of a resonant triad of neutral waves, M_j describes the extent of the non-linear interaction between wave (j) and its partners. A non-zero θ_j can be interpreted in terms of the dispersion relation for the linear problem, $\omega = \omega(k)$. We have chosen a wavenumber of the form $(k_0^2 - \Delta k_1^2 + \Delta^{3/2} k_2^2 + \Delta^2 k_3^2)^{1/2}$. In calculating c_0, c_1 and c_2, we have been calculating successive terms in a Taylor series expansion for the phase speed of the true linear mode

$$c\,([k_0^2 - \Delta k_1^2 + \Delta^{3/2} k_2^2 + \Delta^2 k_3^2]) =$$

$$c_0(k_0) + \Delta c_1 (k_0,k_1) + \Delta^{3/2} c_2 (k_0,k_1,k_2) + \ldots$$

In our specification of the wave-like part of the $^{(j)}\phi$, that is, $e^{i(j)k(x-(j)ct)}$, we specified a frequency $\omega = {}^{(j)}k^{(j)}c$ in which we truncated our expansion of the phase speed at $O(\Delta^{3/2})$. If the $O(\Delta^2)$ term in the expansion of the true linear phase speed is zero, then our specified frequency ω, when expanded as a Taylor series, will match the Taylor expansion of the true linear frequency for a mode with wavenumber $(k_0^2 - \Delta k_1^2 + \Delta^{3/2} k_2^2 + \Delta^2 k_3^2)^{1/2}$ up to and including terms of $O(\Delta^2)$. In general, however, our truncated expansion for the phase speed will not be correct to $O(\Delta^2)$ so that our specified frequency ω will differ from the linear eigenfrequency ω by an amount of $O(\Delta^2)$, $\Delta^2\theta$ say. It is this difference in frequency, since it corresponds to a difference in behavior on the long evolutionary time scale that occurs as θ_j in the evolution equation (4.5).

We now address the question of the evolution of the unstable wave. As in the case of the neutral sidebands, we project the vorticity equations onto the Fourier component corresponding to the unstable wavenumber. However, in the linear problem (Chapter 3) we saw that the structure of the unstable wave exhibited two meridional scales, and it is again necessary for us to split the y-domain into an inner region of width $O(\Delta^{1/2})$ about the center of the channel and an outer region comprising the remainder of the channel. In the inner region the meridional variable η will be used. The equations governing $^{(0)}\underset{\sim}{\phi}$ are then, in the outer region,

$$(\partial_y^2 - k_m^2 + \frac{\beta_m}{U})^{(0)}\phi_1 = \Delta(\frac{1}{U} - {}^{(0)}k_1^2)^{(0)}\phi_1 + \Delta^{3/2}\Big[{}^{(0)}k_2^2\ {}^{(0)}\phi_1 - \frac{1}{ik_mU} J_{(0)}({}^{(1)}\phi_1, {}^{(2)}q_1) -$$

$$- \frac{1}{ik_m U} J_{(0)}(^{(2)}\phi_1, {}^{(1)}q_1)\Big] + \Delta^2\Big[-F^{(0)}\phi_2 + {}^{(0)}k_3^2\ {}^{(0)}\phi_1 + \frac{\beta+FU}{ikU_m}\partial_T\ {}^{(0)}\phi_1\Big]$$

$$(\beta_m - FU + h_y)^{(0)}\phi_2 + \frac{1}{ik_m}\Big[J_{(0)}\ (^{(1)}\phi_2, {}^{(2)}q_2) + J_{(0)}\ (^{(2)}\phi_2, {}^{(1)}q_2)\Big]$$

$$+ \Delta^{1/2}\ \frac{F}{ik_m}\partial_T\ {}^{(0)}\phi_1 = 0\ ,$$

(4.6)

in the inner region

$$\partial_\eta^2\ {}^{(0)}\phi_1 = -\Delta\pi^2\ {}^{(0)}\phi_1 - \Delta^2\ F\ {}^{(0)}\phi_2$$

$$2\pi^2 h_2\ \eta^2\ {}^{(0)}\phi_2 - {}^{(0)}\phi_2 + \frac{1}{ik_m}\partial_T\ \partial_\eta^2\ {}^{(0)}\phi_2 + \frac{F}{ik_m}\partial_T\ {}^{(0)}\phi_1\ (\eta) \qquad (4.7)$$

$$+ \frac{\Delta^{-1/2}}{ik_m}\Big[J_{(0)}(^{(1)}\phi_2, {}^{(2)}q_2) + J_{(0)}(^{(2)}\phi_2, {}^{(1)}q_2)\Big] = 0$$

We have used the symbol k_m^2 in place of ${}^{(0)}k_0^2$ to emphasize that the leading order term in the expression for the wavenumber of the unstable wave, is just the wavenumber of the marginal wave at maximum critical β, i.e.,

$${}^{(0)}k_0^2 = k_m^2 = \beta_m/U - \pi^2 \qquad (4.8)$$

The leading order problem for the upper layer streamfunction is then just

$$(\partial_y^2 + \pi^2)\ \phi_1^{(0)} = 0$$

$$\phi_1^{(0)} = 0 \text{ at } y = 0 \text{ and } 1 \qquad (4.9)$$

Thus $$\phi_1^{(0)} = A_0(T) \sin \pi y \quad . \tag{4.10}$$

At $O(\Delta)$:

$$(\partial_y^2 + \pi^2)\, \phi_1^{(1)} = (\frac{1}{U} - {}^{(0)}k_1^2)\, \phi_1^{(0)} = (\frac{1}{U} - {}^{(0)}k_1^2)\, A_0 \sin \pi y$$

$$\phi_1^{(1)} = 0 \quad \text{at} \quad y = 0, 1 \tag{4.11}$$

The solubility condition for (4.11) is that

$${}^{(0)}k_1^2 = 1/U$$

This can be interpreted as a requirement that, to $O(\Delta)$, the wavenumber of the unstable wave must coincide with that of the marginal mode on the left-hand branch of the marginal curve at the true value of β, $\beta = \beta_m - \Delta$. It will turn out that the two wavenumbers mentioned can differ only at a still higher order, $O(\Delta^{3/2})$. The import of this restriction on the $O(\Delta)$ approximation to the unstable wavenumber is that the finite amplitude analysis is more directly an expansion about the marginal mode at $\beta = \beta_m - \Delta$ rather than the marginal mode at β_m. We choose to normalize the solution such that

$$\phi_1^{(1)} \equiv 0 \tag{4.12}$$

The next problem to consider in the upper layer analysis is that at $O(\Delta^{3/2})$, but we will postpone this until after we have examined the lower layer vorticity equation. From (4.6) we have that at leading order

$$(\beta_m - FU+h_y)\ \phi_2^{(1)} = -\frac{1}{ik_m}\left[J_{(0)}\left({}^{(1)}\phi_2^{(0)}, {}^{(2)}q_2^{(0)}\right) + J_{(0)}\left({}^{(2)}\phi_2^{(0)}, {}^{(1)}q_2^{(0)}\right)\right]$$

Replacing the expression enclosed in brackets on the right with $P_2^{(0)}(T,y)$, we find that

$$\phi_2^{(1)} = -\frac{1}{ik_m}\ \frac{P_2^{(0)}(T,y)}{\beta_m - FU+h_y} \tag{4.13}$$

while solving the $O(\Delta^{1/2})$ problem yields

$$\phi_2^{(2)} = -\frac{F}{ik_m}\,\partial_T\,\phi_1^{(0)} \Big/ (\beta_m - FU+h_y) \quad . \tag{4.14}$$

We can now return to the upper layer where the $O(\Delta^{3/2})$ terms in (4.6) imply

$$(\partial_y^2 + \pi^2)\ {}^{(0)}\phi_{1+}^{(2)} = {}^{(0)}k_2^2\ {}^{(0)}\phi_1^{(0)} \tag{4.15}$$

$$-\frac{1}{ik_mU}\left[J_{(0)}\left({}^{(1)}\phi_1^{(0)}, {}^{(2)}q_1^{(0)}\right) + J_{(0)}\left({}^{(2)}\phi_1^{(0)}, {}^{(1)}q_1^{(0)}\right)\right] - F\ {}^{(0)}\phi_2^{(1)}$$

We will again compress the formalism by defining

$$P_1^{(0)}(T,y) = J_{(0)}\left({}^{(1)}\phi_1^{(0)}, {}^{(2)}q_1^{(0)}\right) + J_{(0)}\left({}^{(2)}\phi_1^{(0)}, {}^{(1)}q_1^{(0)}\right)$$

Substitution for ${}^{(0)}\phi_1^{(0)}$ and ${}^{(0)}\phi_2^{(1)}$ in (4.15) yields

$$(\partial_y^2 + \pi^2)\ \phi_{1+}^{(2)} = k_2^2\ A_0 \sin \pi y - \frac{1}{ik_mU}\,P_1^{(0)}(T,y) + \frac{F}{ik_m}\ \frac{P_2^{(0)}(T,y)}{(\beta_m - FU+h_y)} \tag{4.16}$$

At $y = 1$ we have the boundary condition $\phi_{1+}^{(2)} = 0$. As $y \to 1/2$, we

must match this outer solution to a solution in the inner region near $y = 1/2$. This matching will be discussed later.

A particular solution of (4.16) is

$$\phi_{1+}^{(2)} = -\frac{{}^{(0)}k_2^2}{2\pi} A_0 (y-1)\cos \pi y + \frac{1}{\pi}\cos \pi y\, I_c + \frac{1}{\pi}\sin \pi y\, I_s \qquad (4.17)$$

where

$$I_c = \int_y^1 dy' \left[\frac{F}{ik_m (\beta_m - FU+h_y)} P_2^{(0)}(T,y') - \frac{1}{ik_m U} P_1^{(0)}(T,y') \right] \sin \pi y'$$

$$I_s = \int_{1/2}^y dy' \left[\frac{F}{ik_m (\beta_m - FU+h_y)} P_2^{(0)}(T,y') - \frac{1}{ik_m U} P_1^{(0)}(T,y') \right] \cos \pi y'$$

As y approaches 1/2 from above, say $y = 1/2 + \tilde{\eta}$, $\tilde{\eta} \to 0+$, the asymptotic form of $\phi_{1+}^{(2)}$ is

$$\phi_{1+}^{(2)} \sim \left(-\frac{k_2^2}{4} A_0 - K_0 A_1^* A_2^*\right) \tilde{\eta} + 0(\tilde{\eta}^2) \qquad (4.18)$$

where

$$K_0 = \frac{F}{k_m}\left[\frac{1}{{}^{(1)}c_0} - \frac{1}{{}^{(2)}c_0}\right]\int_{1/2}^1 dy \left({}^{(1)}k_0\, {}^{(1)}\psi_2^{(0)}\, {}^{(2)}\psi_{2y}^{(0)} - {}^{(2)}k_0\, {}^{(1)}\psi_{2y}^{(0)}\, {}^{(2)}\psi_2^{(0)}\right)$$

$$- \frac{\beta_m + FU}{Uk_m}\left(\frac{1}{U - {}^{(2)}c_0} - \frac{1}{U - {}^{(1)}c_0}\right)$$

$$\int_{1/2}^1 dy \left({}^{(1)}k_0\, {}^{(1)}\psi_1^{(0)}\, {}^{(2)}\psi_{1y}^{(0)} - {}^{(2)}k_0\, {}^{(1)}\psi_{1y}^{(0)}\, {}^{(2)}\psi_1^{(0)}\right) \qquad (4.19)$$

Continuing to the $O(\Delta^2)$ problem for the upper layer we find from (4.6) that

$$(\partial_y^2 + \pi^2)\,\phi_{1+}^{(3)} = -F\,\phi_2^{(2)} + (0)k_3^2\,\phi_1^{(0)} + \frac{\beta + FU}{ik_m U^2}\,\partial_T\,\phi_1^{(0)}$$

Upon substitution for $\phi_2^{(2)}$ and $\phi_1^{(0)}$ this becomes

$$(\partial_y^2 + \pi^2)\,\phi_{1+}^{(3)} = \sin \pi y \left[(0)k_3^2\,A_0 + \left(\frac{\beta + FU}{ik_m U^2} + \frac{F^2}{ik_m(\beta - FU + h_y)}\right) A_{0T}\right] \tag{4.20}$$

The side conditions on $\phi_{1+}^{(3)}$ are similar to those on $\phi_{1+}^{(2)}$. A particular solution of (4.20) in $1/2 < y \leq 1$ is

$$\phi_{1+}^{(3)} = -\frac{1}{2\pi}(y-1)\cos \pi y \left[(0)k_3^2\,A_0 + \left(\frac{\beta_m + FU}{ik_m U^2} - \frac{F^2}{ik_m h_2}\right) A_{0T}\right] - \frac{F^2 A_{0T}}{2ik_m h_2 \pi^2} \sin \pi y\,[\ln(|\cos \pi y|)] \tag{4.21}$$

We have now developed the outer problem for the unstable wavenumber as far as will be required in the derivation of the amplitude equations. Next we must resolve the spatial structure of the unstable wave in the inner region near $y = 1/2$.

In the inner region, the equations (4.7) apply which may be rewritten as

$$\partial_\eta^2\,\phi_1 = -\Delta\,\pi^2\,\phi_1 - \Delta^2 F\,\phi_1 \tag{4.22}$$

$$2\pi^2 h_2 \eta^2 \phi_2 - \phi_2 + \frac{1}{ik_m}\partial_T \partial_\eta^2\,\phi_2 + \frac{F}{ik_m}\partial_T\,\phi(\eta) + \frac{\Delta^{-1/2}}{ik_m} P_2\left(T, \frac{1}{2} + \Delta^{1/2}\eta\right) = 0$$

We quickly realize that

$$\left.\begin{aligned} \phi_1^{(0)} &= A_0 \\ \text{and} \qquad \phi_1^{(1)} &= -\tfrac{1}{2}\pi^2\eta^2 A_0 \end{aligned}\right\} \tag{4.23}$$

$P_2\ (T,\ 1/2 + \Delta^{1/2}\eta) = O(\Delta)$ so that $\phi_2^{(1)}$ is determined by

$$\partial_T \partial_\eta^2 \phi_2^{(1)} + ik_m\ (2\pi^2 h_2 \eta^2 - 1)\ \phi_2^{(1)} = -F\ \partial_T \phi_1^{(0)} = -F\ A_{0T} \tag{4.24}$$

This latter equation appeared in the linear problem. There the time dependence was simply exponential for a particular normal mode and so we could solve for $\phi_2^{(1)}$. Here the time dependence is more general and we cannot explicitly solve (4.24). Instead we will merely denote the formal solution that is bounded as $|\eta| \to \infty$ by $\phi_2^{(1)}\ (\eta,\ T)$. Note that as $\eta \to \infty$

$$\phi_2^{(1)} \sim -\frac{F\ A_{0T}}{i2k_m \pi^2 h_2}\ \frac{1}{\eta^2}$$

and

$$\int_0^\eta d\eta'\ \phi_2^{(1)}\ (\eta') \sim \int_0^\infty d\eta\ \phi_2^{(1)}\ (\eta) + \frac{F\ A_{0T}}{i2k_m \pi^2 h_2}\ \frac{1}{\eta}$$

A significant feature of (4.24) is that it couples the spatial structure of the lower layer streamfunction in the inner layer to the evolution of the amplitude of the unstable wave. Recall that ${}^{(0)}\phi_{2\ in}^{(1)}$ is the leading order contribution to the lower layer streamfunction of the

unstable wavenumber. Thus, notwithstanding the fact that the lower layer streamfunction is weak when compared to that of the upper layer, the finite amplitude system possesses the feature that part of the leading order spatial structure of the unstable wave evolves on the non-linear interaction time scale. This should be contrasted to the case of the meridionally uniform two-layer model in which the leading order structure of the unstable wave does not vary during the evolution cycle. In that problem, temporal variations in structure are relegated to the higher order correction to the streamfunction that is responsible for the existence of a weak phase shift between the two streamfunctions, and hence for the ability of the unstable wave to exchange energy with the mean flow via the heat flux associated with the wave.

One can heuristically account for the structural variations of the streamfunction in several ways . On the one hand, if we exploit the notion of the finite amplitude disturbance as being built up from a leading order term, that has the structure of an adjacent marginal mode, and higher order corrections associated with finite amplitude effects and with the fact that we are located a small distance away from the marginal curve in parameter space, then we discover that the meridionally varying and uniform cases are not very dissimilar. In each, the temporal variation of spatial structure is associated with the corrections to the marginal mode. The distinction is that the marginal mode in the meridionally varying model does not possess a non-zero lower layer streamfunction so that in the lower layer the "correction" term is the leading order contribution to the structure of the finite amplitude wave.

On the other hand, there is still a profound distinction between the two cases and this is tied to the existence of the slow neutral modes noted in the linear problem (Chapter 3). There we saw that at a slightly supercritical wavenumber $^{(0)}k$ at which we found a slowly growing unstable mode, we also found an infinite set of neutral modes which shared with the unstable mode a lack of any dependence on the fast, O(1), timescale. Instead, their frequencies were of $O(\Delta^2)$. Like the unstable wave, these neutral modes had an upper layer streamfunction that resembled $\sin\pi y$ and a weak lower layer streamfunction, concentrated near the center of the channel. Roughly speaking, the way in which the two sidebands affect the evolution of the unstable wave is by producing, through the advection of one by the other, an interaction resultant that contains a component with the same zonal dependence, $e^{i^{(0)}kx}$, as the unstable wave, and the same absence of fast time scale variation. This component is therefore resonant with the unstable wave and forces a modification to the amplitude of the unstable wave on the longer evolutionary time scale. Because the slow neutral modes have the same dependence on the zonal coordinate and the short time scale as the unstable mode, they, too, are forced resonantly by the product of the interaction between the sidebands. In general the meridional structure of the interaction product will have a projection on all of the slow neutral modes since the meridional structures of the eigenfunctions are non-trigonometric. In general then, the component of the finite amplitude disturbance with the wavenumber $^{(0)}k$ will be a mixture of the unstable wave and the slow neutral modes in the sense of a generalized Fourier sum. The Fourier coefficients

depend on the slow time variable but this dependence is different for each mode. Consequently the mix of modes that make up this sum changes in time which is equivalent to an evolution in the spatial structure of the component with wavenumber ${}^{(0)}k$.

Before completing the derivation of the amplitude equations, we must solve the $O(\Delta^2)$ inner region problem for the upper layer. From (4.22) this is

$$\partial_\eta^2 \phi_1^{(3)} = -\pi^2 \phi_1^{(1)} - F \phi_2^{(1)} \tag{4.25}$$

Part of the forcing for $\phi_1^{(3)}$ is proportional to the function $\phi_2^{(1)}(T,\eta)$ described above so that the spatial structure of $\phi_1^{(3)}$ will also evolve in time. The solution of (4.25) is

$$\phi_1^{(3)} = \frac{1}{24}\pi^4 \eta^4 A_0 - F \int_0^\eta d\eta' \int_0^{\eta'} d\eta'' \phi_2^{(1)}(T, \eta'') + \text{constant}$$

As $\eta \to \infty$ this has the asymptotic form

$$\phi_1^{(3)} \sim \frac{1}{24}\pi^4 \eta^4 A_0 - \eta F \int_0^\infty d\eta \; \phi_2^{(1)}(T, \eta) - \frac{F^2 A_{0T}}{i2k_m \pi^2 h_2} \ln \eta + R$$

where R is an unknown constant.

We have omitted to solve for ${}^{(0)}\phi_{1\,in}^{(2)}$, the term which occurred at $O[\Delta^2 \ln(1/\Delta)]$ in the expansion of ${}^{(0)}\phi_{1\,in}$. There is no direct forcing for this term in (4.22) so that it must satisfy.

$$\partial_\eta^2 \phi_1^{(2)} = 0$$

and hence be a constant, Q. This term is indirectly forced by the condition that the inner and outer solutions match smoothly.

To complete the solution, we must match the inner solution to the outer. To the orders considered, the lower layer matching yields no significant new information. Informally, in the upper layer, expanding the outer solution in the limit $\eta \to 0$ and the inner solution in the limit $\eta \to \infty$ yields asymptotic expressions

$$ {}^{(0)}\phi_{1\ out} \sim A_0 \left(1 - 1/2\ \Delta\ \pi^2\ \eta^2 + \frac{1}{24}\ \Delta^2 \pi^4 \eta^4 + \ldots\right) + \left(\Delta^2 \ln 1/\Delta\right) \frac{F^2\ A_{0T}}{2ik_m\ \pi^2\ h_2} $$

$$ + \Delta^2 \left[\left(- \frac{{}^{(0)}k_2^2}{4} A_0 - K_0\ A_1^*\ A_2^* \right) \eta - \frac{F^2\ A_{0T}}{2ik_m\ \pi^2\ h_2} \ln\ \eta + \text{const.} \right] + \ldots $$

$$ {}^{(0)}\phi_{1\ in} \sim A_0 \left(1 - 1/2\ \Delta\ \pi^2\ \eta^2 + \frac{1}{24}\ \Delta^2 \pi^4 \eta^4 + \ldots\right) + \left(\Delta^2 \ln 1/\Delta\right)\ Q $$

$$ + \Delta^2 \left[- \eta\ F \int_0^\infty d\eta\ \phi_2^{(1)} - \frac{F^2\ A_{0T}}{i2k_m\ \pi^2\ h_2} \ln\ \eta + R \right] + \ldots $$

Matching terms proportional to η at $O(\Delta^2)$ yields the crucial relation

$$ \frac{{}^{(0)}k_2^2}{4} A_0 + K_0\ A_1^*\ A_2^* = F \int_0^\infty d\eta\ {}^{(0)}\phi_{2\ in}^{(1)} \qquad (4.25) $$

This, together with the differential equation for ${}^{(0)}\phi_{2\ in}^{(1)}$, (4.24), and the two equations for the amplitudes of the sidebands, (4.5), form a closed set describing the slow, $O(\Delta^2)$, time scale evolution of the three

zonal Fourier components consisting of the unstable wave and two neutral Rossby waves. For convenience, these evolution equations are collected together here, after dropping some of the affixes to ϕ_2, as (4.27).

$$
\begin{aligned}
A_{1T} &= i\,\theta_1 A_1 + i\,M_1 A_0^* A_2^* \\
A_{2T} &= i\,\theta_2 A_2 + i\,M_2 A_0^* A_1^* \\
\frac{(0)K_2^2}{4} A_0 &+ K_0 A_1^* A_2^* = F \int_0^\infty d\eta\, \phi_2^{(1)} \\
\partial_T\, \partial_\eta^2\, \phi_2^{(1)} &+ ik_m (2\pi^2 h_2 \eta^2 - 1)\, \phi_2^{(1)} = -F\, A_{0T}
\end{aligned}
\qquad (4.27)
$$

The constants θ_1 and θ_2 are significant only to the extent that together they reflect the amount by which the three component waves depart from perfect resonance. To make this explicit, we can transform

$$\hat{A}_j = e^{-i\theta_j T} A_j \; ; \qquad j = 1, 2$$

$$\hat{A}_0 = e^{-i\theta_0 T} A_0 \; ;$$

$$\hat{\phi}_2 = e^{-i\theta_0 T} \phi_2 \; ;$$

using $\theta_0 = -(\theta_1 + \theta_2)$. Whence (4.27) becomes

$$\hat{A}_{1T} = i\, M_1 \hat{A}_0^* \hat{A}_2^*$$

$$\hat{A}_{2T} = i\, M_2 \hat{A}_0^* \hat{A}_1^* \tag{4.28}$$

$$\frac{(0)K_2^2}{4} \hat{A}_0 + K_0 \hat{A}_1^* \hat{A}_2^* = F \int_0^\infty d\eta\, \hat{\phi}_2^{(1)}(\eta, T)$$

$$(\partial_T + i\omega_0)\, \partial_\eta^2 \hat{\phi}_2 + ik_m(2\pi^2 h_2 \eta^2 - 1)\, \hat{\phi}_2 = -F\,(\partial_T + i\omega_0)\, \hat{A}_0$$

It remains for us to verify the initial assertion that the changes made in the mean flow, as a result of the heat fluxes associated with the three evolving waves, have a negligible effect on the evolution process on the $O(\Delta^{-2})$ time scale. A change to the mean flow should be insignificant, if the perturbation to the meridional potential vorticity gradient of the mean flow due to that change is smaller than $O(\Delta)$. Referring to the complete perturbation form of the potential vorticity equations, (4.0), we can see that the changes in the mean flow are generated by the advection of the potential vorticity associated with each of the three main waves by the velocity field associated with that wave, and that the mean field correction ${}^{(j)}\underset{\sim}{\Phi}$ associated with wave ${}^{(j)}\underset{\sim}{\phi}$ satisfies

$$\partial_T\, {}^{(j)}\pi_1 = -\Delta^{-2} J_{(m)}\left({}^{(j)}\phi_1, {}^{(j)}q_1\right)$$

$$j = 0, 1, 2 \tag{4.29}$$

$$\partial_T\, {}^{(j)}\pi_2 = -\Delta^{-2} J_{(m)}\left({}^{(j)}\phi_2, {}^{(j)}q_2\right)$$

Here $^{(j)}\underset{\sim}{\pi}$ is the potential vorticity associated with the mean flow correction $^{(j)}\underset{\sim}{\Phi}$, $^{(j)}\underset{\sim}{q}$ is the potential vorticity of wave j and $J_{(m)}(A,B)$ denotes the x-independent part of J(A,B), A mean flow correction is a higher order effect if

$$^{(j)}\pi_{y} \ll O(\Delta) \quad .$$

In (4.29) we have reverted to the absolute scaling of dimensionless variables. Thus $^{(0)}\phi_1^{(0)}$ is $O(\Delta^2)$, etc. From this point, we will again use the relative scaling, described in this chapter, for the wave variables and try to determine the scales of the mean flow corrections.

We begin with the effects of the sidebands in the outer region. When j = 1 or 2, the first non-zero contribution to the Jacobians of (4.29) come from the interactions between $^{(j)}\underset{\sim}{\phi}^{(0)}$ and $^{(j)}\underset{\sim}{q}^{(3)}$ [and $^{(j)}\underset{\sim}{\phi}^{(3)}$ with $^{(j)}\underset{\sim}{q}^{(0)}$] thus

$$\partial_T \, ^{(j)}\underset{\sim}{\pi} = -\Delta^{7/2}\left[\underset{\sim}{J}_{(m)}\left(^{(j)}\phi^{(0)}, \, ^{(j)}q^{(3)}\right) + \underset{\sim}{J}_{(m)}\left(^{(j)}\phi^{(3)}, \, ^{(j)}q^{(0)}\right)\right]$$

Hence $^{(j)}\underset{\sim}{\pi}$ and $^{(j)}\underset{\sim}{\pi}_y$, in the outer region, are each of $O(\Delta^{7/2})$ and are therefore negligible.

The sideband waves also develop some inner structure as a result of the non-linear interaction. While this is too weak to affect the amplitude evolution, it should be considered when calculating the mean flow correction in the inner region. Because of the symmetry properties of the sidebands, the magnitudes of the inner structure that they develop will differ. Let us use j to refer to the anti-symmetric sideband and j'

to refer to the symmetric one. In the inner region, there will be a correction to the lower layer streamfunction of the anti-symmetric sideband that is of $O(\Delta^{17/4})$. The perturbation to the lower layer potential vorticity that results from this, ${}^{(j)}q_2^{(0)}$ say, will be $O(\Delta^{13/4})$ and its meridional structure is given by

$$ {}^{(j)}q_2^{(c)} = - \frac{{}^{(j')}k_0}{{}^{(j)}k_0 {}^{(j)}c_0} {}^{(j')}\psi_2^{(0)}(1/2)\, {}^{(0)}\phi_{2\,\eta\eta\eta}^{(1)*} A_j^* \qquad (4.30) $$

The corresponding correction to the lower layer streamfunction of the symmetric sideband will be $O(\Delta^{19/4})$ while the associated perturbation to the lower layer potential vorticity, ${}^{(j')}q_2^{(0)}$ will be $O(\Delta^{15/4})$ and given by

$$ {}^{(j')}q_2^{(c)} = $$

$$ - \frac{A_j^*}{{}^{(j')}k_0 {}^{(j')}c_0} {}^{(j')}\psi_{2y}^{(0)}(1/2)\, [\eta\, {}^{(0)}\phi_{2\,\eta\eta\eta}^{(1)*} {}^{(j)}k_0 - {}^{(0)}\phi_{2\,\eta\eta}^{(1)*} {}^{(0)}k_0 - {}^{(0)}k_0\, F\, A_0^*] $$

When these are substituted into the equations for the mean potential vorticity we find that the anti-symmetric mode gives

$$ \partial_T {}^{(j)}\pi_2 = - \Delta^3\, 2 \frac{{}^{(j')}k_0}{{}^{(j)}c_0} {}^{(j)}\psi_{2y}^{(0)}(1/2)\, {}^{(j')}\psi_2^{(0)}(1/2)\, I_m \left[A_j A_{j'} \partial_\eta \left(\eta\, {}^{(0)}\phi_{2\,\eta\eta\eta}^{(1)} \right) \right] $$

while the symmetric mode gives

$$\partial_T {}^{(j')}\pi_2 = -\Delta^3 2 \frac{{}^{(j)}k_0}{{}^{(j')}c_0} {}^{(j)}\psi_{2y}^{(0)}(1/2)\ {}^{(j')}\psi_2^{(0)}(1/2)$$

$$I_m \left[A_j A_{j'} [\partial_\eta ({}^{(0)}\phi_{2\,\eta\eta\eta}^{(1)}) - \frac{{}^{(0)}k_0}{{}^{(j)}k_0} {}^{(0)}\phi_{2\,\eta\eta\eta}^{(1)}] \right]$$

In both cases the correction to π_2 is $O(\Delta^3)$ while the change in π_{2y} is $O(\Delta^{5/2})$. Although larger than that produced in the outer region, the changes in the potential vorticity gradient of the mean flow that are produced by the sidebands are still too small to affect the triad dynamics.

Now we must calculate the size of the potential vorticity gradient correction produced by the heat flux of the unstable wave. As in the case of the sidebands, the largest change in the potential vorticity gradient of the mean flow is produced in the inner region, although in both regions, the changes produced in the velocity of the mean flow are similar, $O(\Delta^{7/2})$. In the inner region, the self-advection of vorticity in both the upper and the lower layer is $O(\Delta^{5/2})$ so that, as a result

$$\partial_T {}^{(0)}\underset{\sim}{\pi} = O(\Delta^{5/2}) \quad .$$

Thus, ${}^{(0)}\underset{\sim}{\pi} \sim O(\Delta^{5/2})$ while ${}^{(0)}\underset{\sim}{\pi}_y \sim O(\Delta^2)$, in this inner region. Again, the change in the mean flow potential vorticity gradient is too small to affect the analysis leading to (4.27).

Although these small changes in the mean flow need not be considered in our calculation of the amplitude equations, they play an important role in the energy balance of the entire system. As the total energy of the three waves fluctuates, energy is being transferred between the waves and the mean flow so that the total energy of the system (waves + mean flow) remains constant. This exchange is effected by the heat fluxes associated with the three waves, and the small perturbations to the mean flow that they produce account for energy lost or gained by the mean flow.

Energy Balance for the Finite Amplitude System

Each wave contributes an $O(\Delta^{7/2})$ change in the velocity and temperature fields of the mean flow over most of the width of the channel which lead to $O(\Delta^{7/2})$ changes in the energy of the mean flow. To produce such changes, each wave must give rise to a heat flux which, when integrated across the channel, has a net magnitude of $O(\Delta^{11/2})$. We can examine these energy exchanges between the waves and the mean flow by studying the energy equation for the disturbance field.

If we multiply the potential vorticity equations by the sum of the three principal Fourier modes of the streamfunctions

$$\underset{\sim}{\phi} = \sum_{j=0}^{2} (j)_{\underset{\sim}{\phi}} \; e^{i(j)_k \, (x_- (j)_{ct})} \; + * \; ,$$

zonally average the resulting equations and then integrate them across the channel we obtain an energy equation for the three principal wavenumbers of the disturbance field. If we take out the leading order scales of each

of the three waves, i.e., make the transformations

$$({}^{(1)}\underset{\sim}{\phi}\ ,\ {}^{(2)}\underset{\sim}{\phi}) = \Delta^{7/4}\ ({}^{(1)}\underset{\sim}{\phi}\ ,\ {}^{(2)}\underset{\sim}{\phi}),$$

$${}^{(0)}\phi_1 = \Delta^2\ {}^{(0)}\phi_1$$

$${}^{(0)}\phi_{2\ \text{out}} = \Delta^{7/2}\ {}^{(0)}\phi_2\ ,\quad {}^{(0)}\phi_{2\ \text{in}} = \Delta^3\ {}^{(0)}\phi_2$$

then this energy equation takes the form

$$\partial_T(\mathcal{E}_1 + \mathcal{E}_2 + \Delta^{1/2}\mathcal{E}_0) =$$

$$\Delta^{-2}\ FU\left[{}^{(1)}k \int dy\ I_m\ (\overline{{}^{(1)}\phi_1\,{}^{(1)}\phi_2^*}) + {}^{(2)}k \int dy\ I_m\ (\overline{{}^{(2)}\phi_1\,{}^{(2)}\phi_2^*})\right] \tag{4.31}$$

$$+\quad FU\ {}^{(0)}k\left[\int_{\text{outer}} dy\ I_m\ (\overline{{}^{(0)}\phi_1\,{}^{(0)}\phi_2^*}) + \int_{\text{inner}} d\eta\ I_m\ (\overline{{}^{(0)}\phi_1\,{}^{(0)}\phi_2^*})\right]$$

$\mathcal{E}_j$ is the energy associated with the j^{th} wave

$$\mathcal{E}_j = \frac{1}{2}\int dy\left(\overline{\left|\nabla\,{}^{(j)}\phi_1\right|^2 + \left|\nabla\,{}^{(j)}\phi_2\right|^2 + F\ ({}^{(j)}\phi_1 - {}^{(j)}\phi_2)^2}\right)$$

The terms on the right-hand side of (4.31) are the baroclinic conversion rates associated with the three waves. Since the phase differences between ${}^{(j)}\phi_1$ and ${}^{(j)}\phi_2$ are $O(\Delta^2)$ when $j = 1$ or 2 but $O(1)$ when $j = 0$, all of the heat flux terms are of potentially similar magnitude. The con-

tribution from wave 0, the wave with the unstable wavenumber, has been split into a contribution from the inner region and a second contribution from the outer region. For convenience we will label the conversion terms so that

$$\partial_T(\mathcal{E}_1 + \mathcal{E}_2 + \Delta^{1/2}\mathcal{E}_0) = {}^{(1)}h + {}^{(2)}h + {}^{(0)}h_{out} + {}^{(0)}h_{in}$$

Using the results of the asymptotic expansion analysis, one can obtain expressions for the leading order parts of the baroclinic conversion rates. These are

$$\begin{aligned} {}^{(j)}h = {} & U\,\frac{\beta_m + FU}{U - {}^{(j)}c_0}\; I_m\,(A_0A_1A_2) \times \left[\frac{M_j}{U - {}^{(j)}c_0}\int_0^1 dy\,({}^{(j)}\psi_1^{(0)})^2\right. \\ & + \left(\frac{1}{U} - \frac{1}{U - {}^{(j)}c_0}\right)\left[{}^{(0)}k_0 \int dy\,{}^{(j)}\psi_1^{(0)}\,{}^{(j')}\psi_{1y}^{(0)}\sin \pi y\right. \\ & \left.\left. - {}^{(j')}k_0\pi \int {}^{(j)}\psi_1^{(0)}\,{}^{(j')}\psi_1^{(0)}\cos \pi y\right]\right] \quad j = 1, 2 \end{aligned} \tag{4.32}$$

In (4.32) we have reverted to the convention that $j' = 3 - j$.

$$\begin{aligned} {}^{(0)}h_{out} = {} & \\ & FU\,I_m\,(A_0A_1A_2) \times \int_0^1 dy\,\sin\pi y \left\{\frac{\left(\frac{{}^{(1)}k_0}{{}^{(2)}c_0} + \frac{{}^{(2)}k_0}{{}^{(1)}c_0}\right)h_{yy}\,{}^{(1)}\psi_2^{(2)}\,{}^{(2)}\psi_1^{(0)}}{\beta_m - FU + h_y}\right. \\ & \left. + \left(\frac{1}{{}^{(1)}c_0} - \frac{1}{{}^{(2)}c_0}\right)\left({}^{(1)}k_0\,{}^{(1)}\psi_2^{(0)}\,{}^{(2)}\psi_{2y}^{(0)} - {}^{(2)}k_0\,{}^{(1)}\psi_{2y}^{(0)}\,{}^{(2)}\psi_2^{(0)}\right)\right\} \end{aligned} \tag{4.33}$$

$$(0)h_{in} = 2\ U\ k_m\ K_0\ I_m\ (A_0A_1A_2) \qquad (4.34)$$

All of the three waves contribute conversion rates that are of $O(\Delta^{11/2})$. Compare this to the rates that would be expected from linear theory for waves of the same amplitude. Wavenumbers 1 and 2 correspond to neutral modes in the linear theory and so have no associated heat fluxes or baroclinic conversion rates. Wavenumber 0 is linearly unstable but the energy conversion rate associated with a wave of amplitude $O(\Delta^2)$ would be $O(\Delta^{12/2})$ i.e., a factor $\Delta^{1/2}$ smaller than the expected conversion rate in the finite amplitude problem. For all three waves the rate of exchange of energy with the mean flow is increased beyond the linear rates. This increase is brought about by the vertical phase shifts produced in each Fourier component as a result of the forcing each wave mode receives from the interaction between the remaining pair of waves. Because it is the non-linear interaction between the waves that is responsible for the necessary heat fluxes, each of the conversion rates is proportional to the triple product $A_0A_1A_2$. It is perhaps a little surprising that the conversion rate associated with the unstable mode should share this dependence. As we saw earlier, the conversion rate associated with the changes in structure of the unstable wave forced by nonlinear interaction dominates the conversion rate that the linear structure of the unstable wave would produce. In this respect, the three wave system here is perhaps more reminiscent of the triad composed of three neutral Rossby waves discussed in Chapter 2 rather than the triad consisting of two neutral waves and a weakly unstable wave in a meridionally uniform two-layer flow that is discussed later in the same chapter.

The way in which the energy conversion rate of the unstable wave is enhanced is perhaps worthy of comment. In the outer region, the interaction between the two neutral waves forces a correction of $O(\Delta^{7/2})$ to the lower layer streamfunction; this is much larger than the $O(\Delta^4)$ streamfunction that the linearized dynamics would dictate. In general, the phase of this correction differs by an O(1) amount from the phase of the upper layer streamfunction and so the net heat flux produced can reach $O(\Delta^{11/2})$. In the inner region, the non-linear interaction between the neutral waves forces a correction to the lower layer streamfunction that is of the same order as the streamfunction dictated by linear theory. However, the correction differs in shape from the latter. The linear, inner region, lower layer streamfunction has a rather special shape which means that the $O(\Delta^{10/2})$ heat flux in the inner region nearly cancels, when integrated across the $O(\Delta^{1/2})$ width of this inner region, to leave only an $O(\Delta^{12/2})$ residual. In general, the part of ${}^{(0)}\phi_{2\ in}$ forced by the interaction between the sidebands does not have a similar property. The local heat flux associated with this correction terms is also $O(\Delta^{10/2})$ but this does not cancel out when integrated across the inner region so that the integrated heat flux is $O(\Delta^{11/2})$. In short, the changes in shape of the inner region ${}^{(0)}\phi_2$ caused by non-linear effects, produce changes of shape in the inner heat flux, unbalancing the delicate cancellation process present in the linear problem.

The presence of heat fluxes that are stronger than those required in the linear theory of an unstable wave is necessary because the energy of the triad is dominated by the energy in the sidebands. The energy fluc-

tuations associated with the vacillation of the sideband amplitudes are larger than those associated with the changes in energy of the unstable wave that occur on the long, e-folding time scale. They require the enhanced energy exchanges noted above to support them.

In this section, we have noted that the baroclinic conversion rates associated with the "neutral" waves have, at least formally, a similar magnitude to that of the unstable wave. It will be observed in the numerical results below that, in the instances examined, the largest of the energy fluxes is associated with the unstable wave.

Numerical Results

The amplitude equations, (4.27), that govern the evolution of the finite amplitude system in the asymptotic limit $\Delta \rightarrow 0$, appear difficult to solve in any closed form. To learn something of the behavior of the solutions, we turn to a numerical study of the finite amplitude system. In view of the many degrees of freedom of (4.27), the detailed behavior of the solutions may be quite complicated. We do not expect to be able to explore much of this detail numerically. Rather, what we seek from the numerical results are answers to the two fairly basic questions outlined in the introductory part of this chapter. The first question asks whether the initial growth of the unstable wave, due to the linear instability mechanism, will trigger the growth of the neutral sidebands of any of the possible resonant triads. Such an effect is necessary if initially small perturbations at the sideband levels are to be able to reach amplitudes at which their interaction can affect the growing unstable mode.

The second question seeks to discover whether any triads exist for which the non-linear interactions between the triad elements suffice to curb the growth of the unstable wave and hold its amplitude at an $O(\Delta^2)$ level at which the theory behind (4.27) remains valid. A secondary purpose of the numerical simulation is to give some sort of general idea of the form that the three wave evolution might take.

The numerical model used integrates the perturbation potential vorticity equations for a two-layer model in an infinitely long, zonal channel on a β-plane. The perturbation is restricted to contain only three zonal Fourier components. These correspond to the three waves of a resonant triad. The basic state corresponds to the one assumed thus far, namely, an upper layer velocity of U and a topographic gradient at the lower boundary proportional to $\cos 2\pi y$. The model includes non-linear interactions between the three zonal spectral components but alterations to the mean flow are neglected, so that the zonally independent flow is always just that of the basic equilibrium state. Similarly, harmonics of the three zonal wavenumbers are not included. These features are in keeping with our theoretical results that indicate that alterations to the mean flow have a negligible effect on the triad evolution when one is in the weakly supercritical regime. What the model is intended to show is what the three-wave evolution might look like in the true asymptotic limit when wave-mean flow interaction is negligible. For practical reasons (computing time required), we will look at cases in which the supercriticality is small but not really in the truly asymptotic regime. To isolate the three-wave dynamics, we are filtering out the wave-mean flow interaction by neglecting it entirely.

Some of the relevant technical details of the model are as follows. The main algorithm uses a spectral implementation of the two-layer, potential vorticity equations. The zonal spectral basis is a set of complex exponentials, e^{ikx}. Only three wavenumbers and the corresponding conjugate exponentials are included in the basis. The meridional spectral basis consists of sine functions, sin $n\pi y$. Because of the meridional symmetry of the problem, the meridional structure associated with a particular zonal Fourier component will be either odd or even and so the number of sine functions required can be halved. The meridional truncation used was varied. For most of the results presented here the truncation is at either sin $38\pi y$/sin $39\pi y$ or sin $58\pi y$/sin $59\pi y$ for the odd/even modes. The non-linear interaction terms were calculated using a combination of pseudo-spectral and direct evaluation techniques. Each zonal component of each variable involved in a non-linear product was transformed into the physical y-domain, while retaining a purely spectral representation of the zonal dependence. The interaction terms were computed using these half-transformed variables and the results were then transformed back into the full spectral domain. An alias-free technique was used for this step. A fourth-order temporal integration scheme was used to preserve the phases of the individual Fourier components accurately over periods of time equal to many sideband periods. The code was executed on a CRAY-1A processor.

Several tests of the model were made. These included reproducing some of the vacillations of a neutral Rossby wave triad of small amplitude in a meridionally uniform version of the model and reproducing some of the results of the linear theory for the meridionally varying conditions.

There are really four time scales of interest in the model runs. The shortest is that of the time step used. The second is that of the period of the neutral waves that the model system can support. These span a certain range, but the period of the two sideband waves involved in the main resonant triad interaction is fairly typical. The third scale is the e-folding period of the unstable wave according to linear theory, while the fourth is the length of the model run. We are interested in the weakly supercritical regime in which there is a large separation between the two dynamical time scales, the neutral wave periods and the e-folding period. In order to approach the asymptotic theory as closely as possible, we would like to make this separation as large as possible. Since the ratios of the longer to the shorter period scales as $O(\Delta^{-2})$, even a fairly large ratio amounts to only a moderately small value of Δ. For the results to be presented this ratio will be of O(100). The asymptotic theory suggests that the slow e-folding time will be the natural time scale for the variations in amplitude of the three waves in our triad. For this reason we would like the total length of our modelling runs to be several times longer than the e-folding scale, T_e. We have used runs of $O(10\ T_e)$. As a result of the relations between the latter three time scales, the modelling runs represent integration over $O(10^3)$ Rossby wave periods. Because we want to model weak non-linear interactions between the three components of the triad, we must represent the phases of the three waves rather accurately over the entire length of the run, tolerating only errors that are a small fraction of 2π. The parameter that determines the accuracy of our time integration scheme is the

ratio of the individual time step to the Rossby wave period scale. To achieve the necessary accuracy we have used a fourth order time scheme and a rather short time step, $O(10^{-2} \times$ Rossby wave period). The number of time steps in a full run is therefore of $O(10^5)$.

Four numerical runs will be discussed below. These will be labelled A1, B1, A2, and B2. Two sets of model parameters (β, F, U) and wavenumbers will be used; A1 and A2 will correspond to one set, while B1 and B2 will refer to runs made with the second set. The difference between A1 and A2 will be in the initial conditions used. The same will be true of B1 and B2. A1 and B1 will correspond to comparatively strong initial amplitudes. In these the three waves show significant non-linear interaction from the beginning of the run. They serve to demonstrate that there exist triads that lead to containment of the growth of the unstable wave. A2 and B2 will begin with very weak wave amplitudes and verify that for these triads the growth of the unstable wave, caused by the linear instability mechanism, is sufficient to trigger the growth of the sidebands.

The sets of parameters used are as follows:

A: $F = 10.0$, $U = 1.0$, $h_2 = 5.0$ $(\beta_m = 15.0)$

$\beta = 14.92$, $\Delta = .08$

$k_0 = 2.261$, $k_1 = -1.29806251$, $k_2 = -0.96293749$

B: $F = 6.6164376$, $U = 1.0$, $h_2 = 9.8835624$ $(\beta_m = 16.5)$

$\beta = 16.3$, $\Delta = .2$

$k_0 = 2.544$, $k_1 = -1.46881526$, $k_2 = -1.07518474$

The values of F, U and h_2 in (A) correspond to those of Case 1 in the linear study of Chapter 3. Those in (B) match the values used in Case 2 of the linear study. The topography is relatively stronger in Case B, so that the slow growth rates and peaked ϕ_2 structure characteristic of the weakly supercritical regime can be found at slightly larger values of Δ in this case than for the values of F, U and h_2 used in (A).

The time scales of the linear modes associated with the wavenumbers listed above are as follows:

A: The unstable wave ($^{(0)}k$) has an e-folding time, T_e, of 4889.44. The sidebands ($^{(1)}k$ and $^{(2)}k$) have periods, T_R, of 9.74.

B: The unstable wave has an e-folding time of 1619.38. The sidebands have periods of length 8.25.

In both A and B the separation of time scales is quite marked: T_e/T_R is O(500) for A and O(200) for B. The spatial structure of the unstable wave that is given by linear theory is shown in Figure 3.5 for Case A and Figure 3.7 for Case B. In both 3.5(a) and 3.7(a), the sharp central peak of the lower layer streamfunction is well defined.

In order to find the amplitudes at which the interaction between the unstable wave and the two neutral waves is sufficiently strong as to be comparable with the tendency of the unstable wave to grow as a result of the linear instability mechanism, some preliminary runs were made with different initial conditions. The first set of initial conditions used were very weak so that the waves were effectively independent linear modes. The intensity of the initial conditions was repeatedly increased until significant non-linear interaction was observed. Once this

"tnreshold" had been found, a longer run was made using this latter set of initial conditions. It is this run that we will identify as run A1 for Case A. A similar run using the parameters of Case B will be identified as B1. Because we are beginning with non-linear initial conditions, the interaction between the two sidebands generates some of the higher meridional modes associated with wavenumber $^{(0)}k$. These are not close to marginal and have both the smoother structures and shorter time scales of neutral Rossby waves. Their presence will be observed later as a high frequency noise in some of the heat fluxes. Because the amplitude of these "ringing" modes is small and their period much shorter than the evolutionary time scale, their averaged effects are negligible.

Figure 4.1 shows the evolution of the kinetic energy of the upper layer streamfunction for the unstable wave during run A1. This is the larger part of the total energy associated with the unstable wave and is proportional to $|A_0|^2$. If the unstable wave was behaving according to linear theory, the energy would increase by a factor of e in a time of roughly 2450, and hence by a factor of about 7.5×10^8 over the length of the run. Figure 4.1 clearly demonstrates that the interaction of the unstable wave with this particular pair of sidebands is sufficient to curb the growth that the linear instability mechanism alone would produce. The behavior of the energy is rather irregular which seems consistent with the large number of degrees of freedom that we know the asymptotic system (Equation 4.27) to possess. There seems to be no reason to think that the period of small energy near the end of the run is anything other than temporary. The time scale of the major fluctuations in amplitude remains

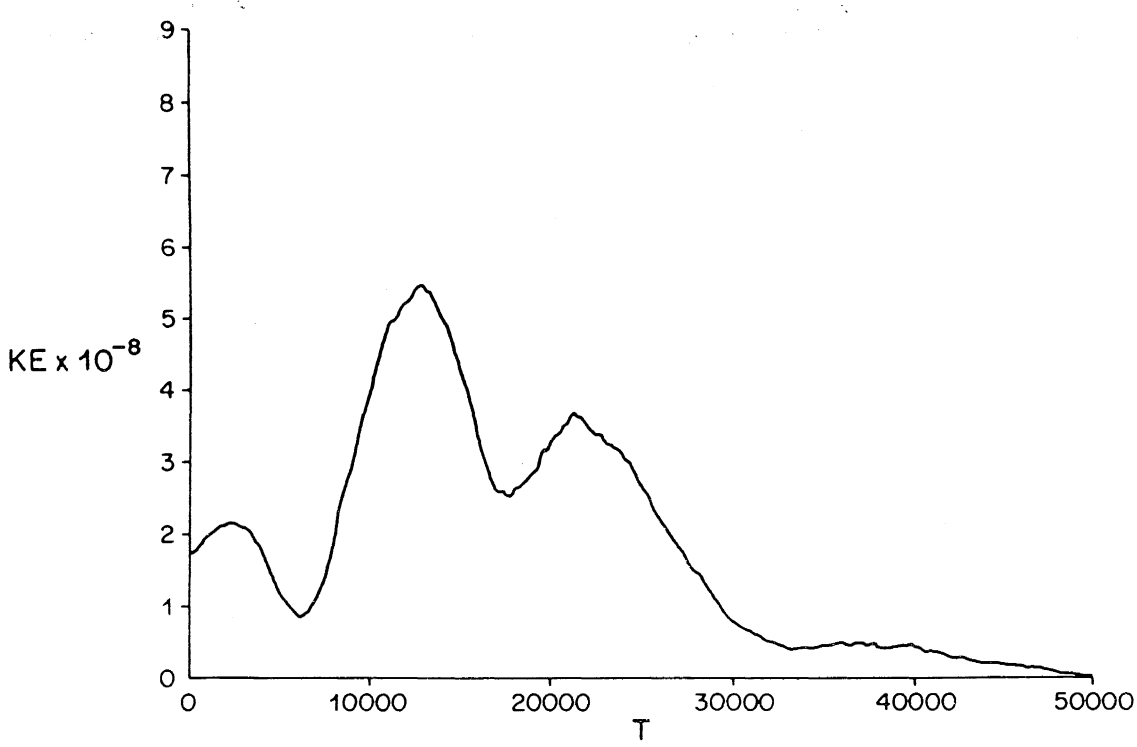

Figure 4.1: Kinetic energy of the $^{(0)}k$ Fourier component (wave 0) of the upper layer perturbation during run A1.

of $O(T_e)$. (That it should initially be so is really a consequence of the way we selected the initial conditions.)

Figure 4.2 shows the evolution of the upper layer kinetic energies of all three waves. Since, at leading order, the spatial structures of the sidebands do not change during the evolution, the upper layer kinetic energies of the sidebands are proportional to $|A_1|^2$ and $|A_2|^2$. We see that the energies of the sidebands are larger than that of the unstable wave as the asymptotic theory suggested. The sideband energies fluctuate on the same time scale as the energy of the unstable wave: the tendency is for the sideband energies to vary in anti-phase with the energy of the unstable wave. The energy of the triad as a whole varies by amounts comparable with the energies of the sidebands. This variation is achieved by exchanges of energy between the three waves and the mean flow. Since the fluctuations in total triad energy are larger than the energy associated with the unstable wave, the rate of exchange of energy between the triad and the mean flow exceeds that which would be observed between a mean flow and an unstable wave of similar amplitude to that of the unstable wave here, but which was evolving (growing) as linear theory alone would dictate. We have already seen, in our theoretical discussion of the energy balance of the triad, how non-linear effects can both increase the rate at which the unstable wave exchanges energy with the mean flow and modify the structure of the neutral waves sufficiently that they, too, can exchange energy with the mean flow at similar rates. However, computations of the heat flux from the numerical results indicate that the energy exchange associated with the unstable wave is the largest

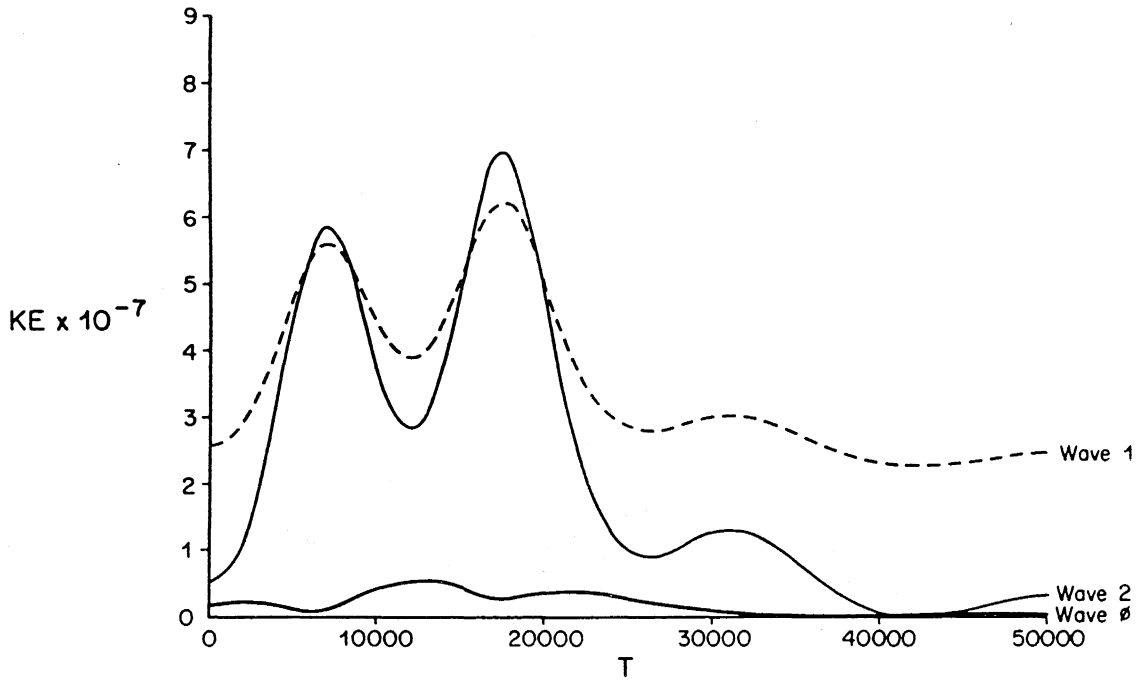

Figure 4.2: As Fig. 4.1 but showing all three principal Fourier components (waves 0-2).

contribution to the energy fluctuations of the triad. This will be taken up more below.

Figure 4.3 is similar to Figure 4.1 but shows the results of run B1. The curve plotted is again the kinetic energy of the upper layer streamfunction of the unstable wave. Again we see that the non-linear interactions between the unstable wave and the sidebands curtail the growth of the unstable wave. For this run, linear theory would give an e-folding period for the energy of about 810. Over the length of time shown in Figure 4.3, this would imply an increase by a factor of about 2.5×10^{13}. Again, the behavior of the energy is that of an irregular vacillation on a time scale comparable to the linear e-folding period of the amplitude of the unstable wave.

Figure 4.4 presents the evolution of the upper layer kinetic energies of all three waves for B1. Again, on average, the energies of the sidebands are larger than those of the unstable wave, but the difference is not as pronounced as that in A1.

The rates of baroclinic conversion of energy between each wave and the mean flow for run B1 are shown in Figure 4.5. The strongest is that associated with the unstable wave. This indicates the following picture of energy balances within the system. The largest fluctuations in energy are associated with the sideband energies. These dominate the fluctuation in the combined energies of the three waves. These fluctuations are balanced by transfers of energy between the triad and the mean flow. The major part of these transfers occurs between the unstable wave and the mean flow and takes place at a rate more rapid than the rate associated

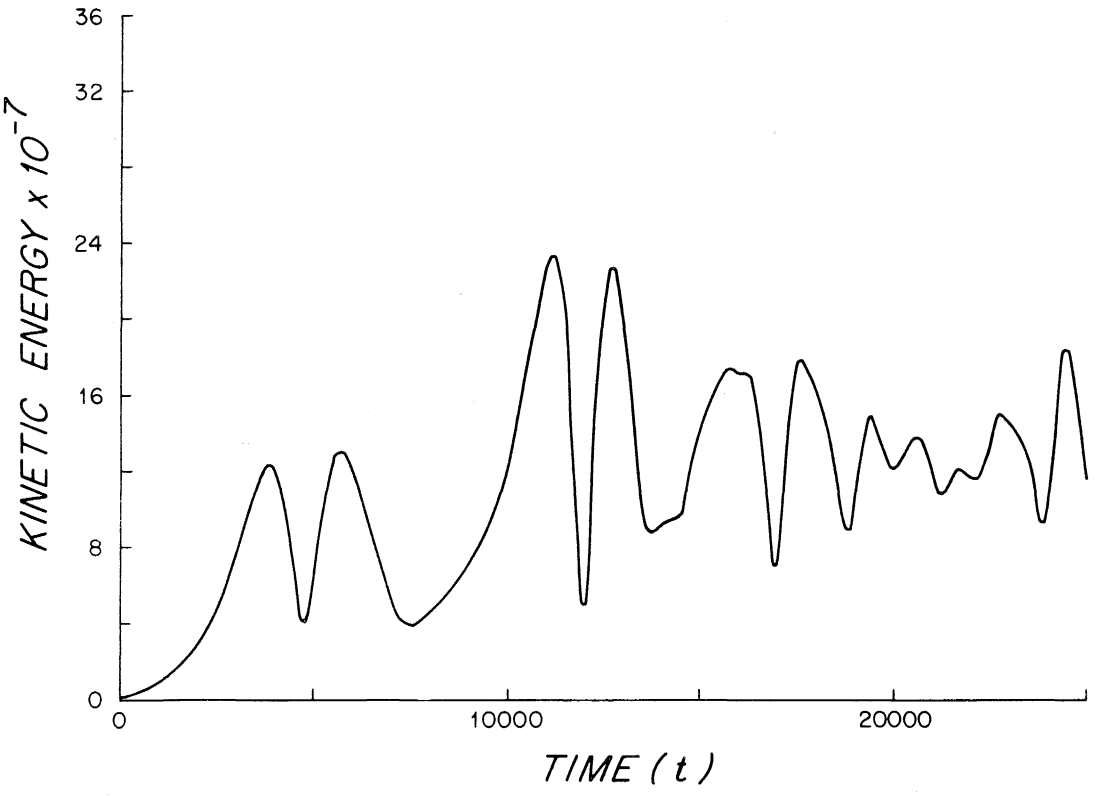

Figure 4.3: As Fig. 4.1 but during run B1.

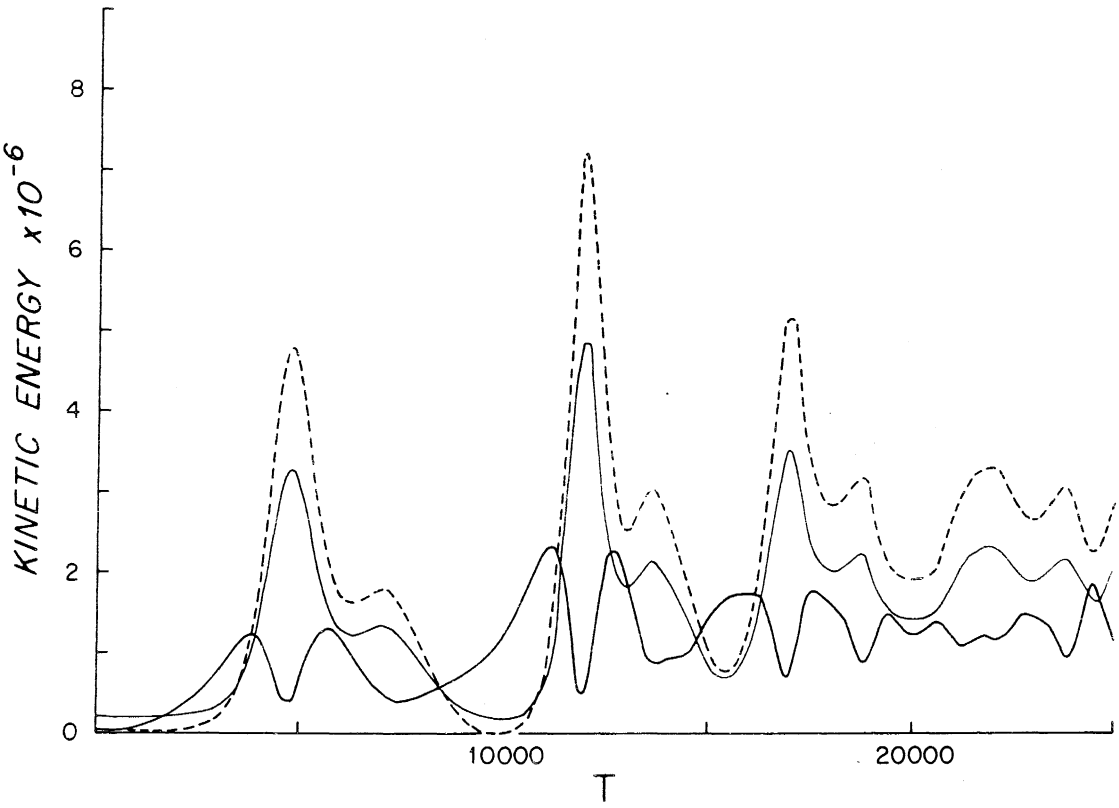

Figure 4.4: As Fig. (4.2) but during run B1.

wave 0, ——— wave 1, - - - - wave 2.

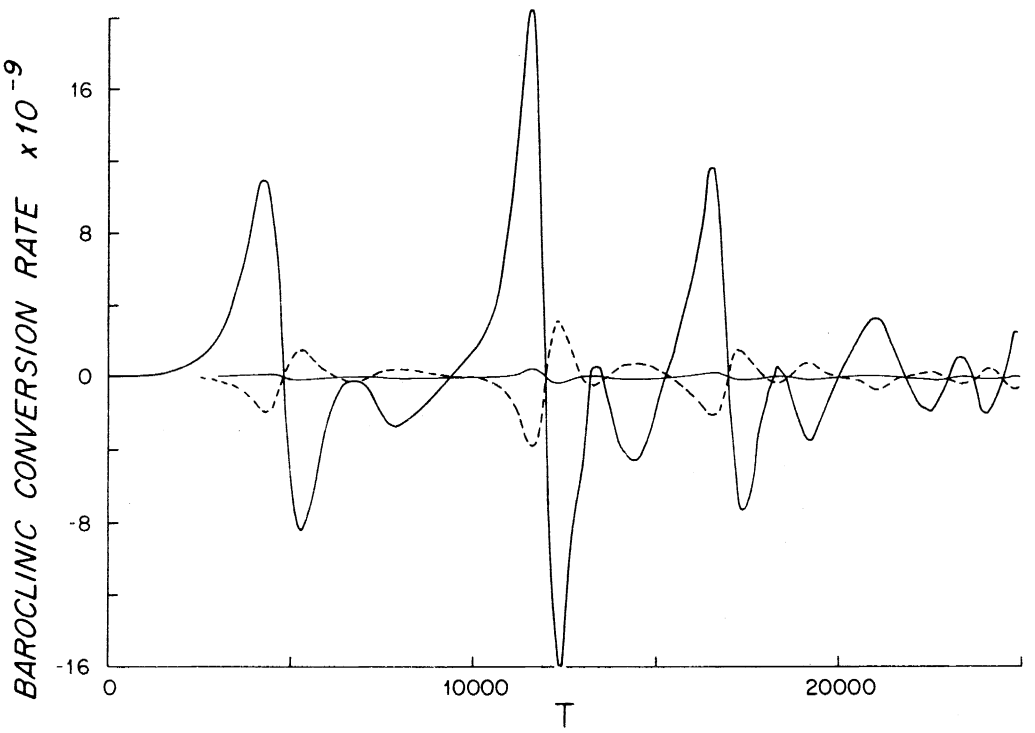

Figure 4.5: Rates of baroclinic conversion of energy between an individual wave and the mean flow during B1.

——— wave 0, ——— wave 1, - - - - - wave 2.

with the linear instability of the unstable wave. This is achieved by modifying the shape of the heat flux associated with the unstable wave (see below). At the same time that energy is being shifted between the unstable wave and the mean flow, wave-wave interactions are transferring energy between the unstable wave and the sidebands at a similar rate. The result of this is that the energy of the unstable wave changes only by amounts that are comparable with the relatively small energy of that wave while the main effect of the triad/mean flow energy exchanges is passed on to the sidebands.

We noted that the energies of the side bands were generally decreasing while that of the unstable wave increases and vice versa. Because most of the triad/mean flow energy exchange occurs through the action of the heat flux associated with the unstable wave, this means that usually the sense of this heat flux opposes the rate of increase of the energy of the unstable wave. When the energy of the unstable wave is decreasing, it is often extracting energy from the mean flow.

The larger magnitude of the integrated heat flux associated with the unstable wave, in comparison to the integrated heat flux of a growing wave governed by linear theory, is brought about by changes in shape of the heat flux. In the linear case, Figures 3.10 and 3.11, the zonally averaged heat flux was concentrated near the center of the channel and exhibited both positive and negative lobes which almost cancel each other when the meridional integral is computed. Figure 4.6 shows the meridional profile of the zonally averaged heat flux at various times during the non-linear run, B1. One can see that there are no longer nearly equal

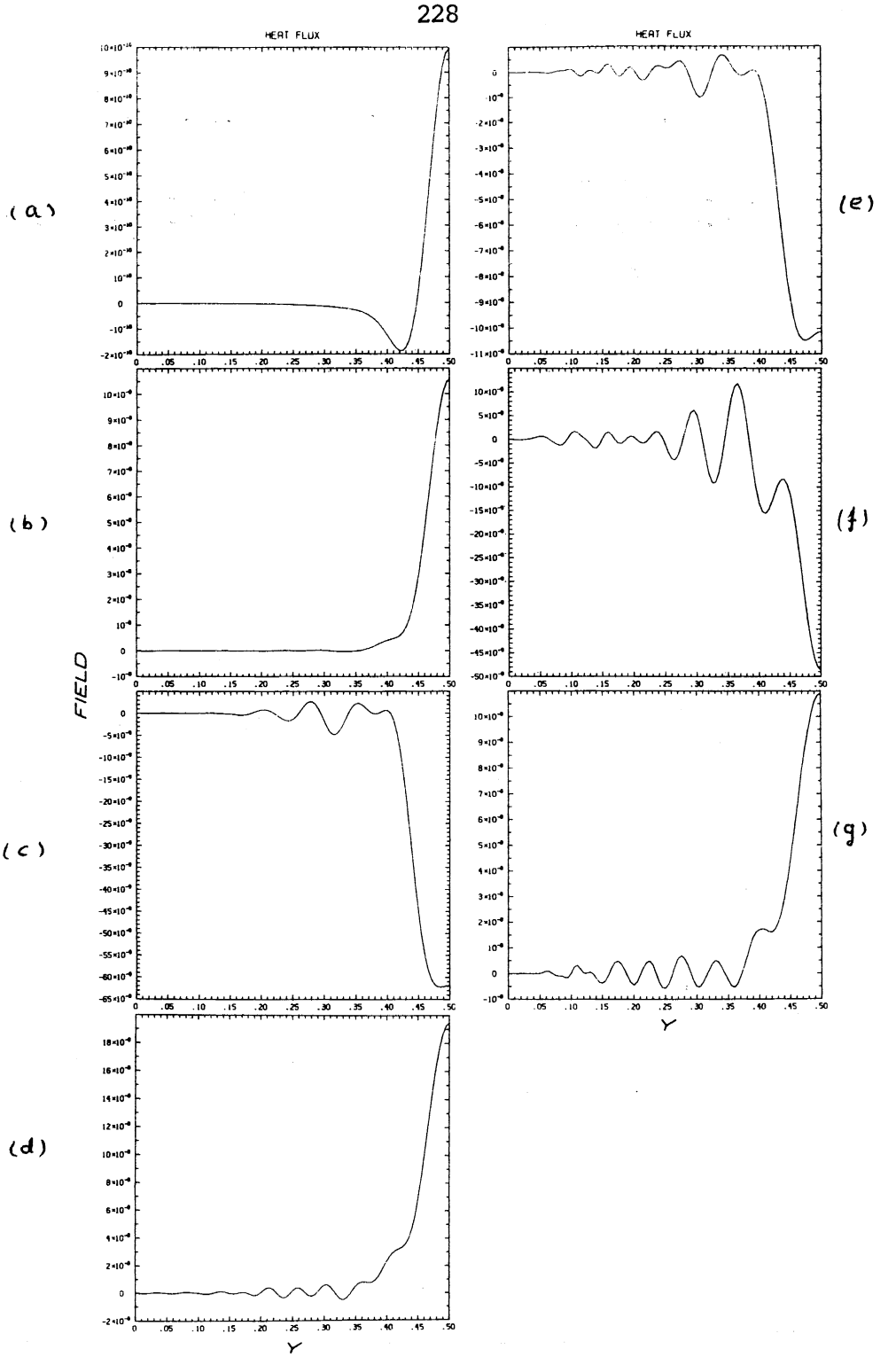

Figure 4.6: Meridional profiles of the heat flux associated with the unstable wave, wave 0, at several times during run B1. Profiles are plotted only for $0 < y < 0.5$, they are symmetric about $y = 0.5$. a) $t = 0.0$, b) $t = 4000.0$, c) $t = 5500.0$, d) $t = 11500.0$, e) $t = 12500.0$, f) $t = 14500.0$, g) $t = 16500.0$

areas of positive and negative heat transport. The changes in shape of ${}^{(0)}\phi_2^{(1)}{}_{in}$ that were produced by the action of the non-linear interaction of the two sidebands have altered the shape of the heat flux and destroyed this balance. In doing so they permit the unstable wave to exchange more energy with the mean flow than was previously possible.

So far, we have only looked at one set of initial conditions for each of two different sets of model parameters. To demonstrate that there is a certain degree of robustness to the ability of a triad to prevent the exponential growth of an unstable wave, we include Figure 4.7 which shows the evolution of the upper kinetic energy of the unstable wave for several runs made with the parameters similar to those used in Run A1. The values of F, β, U and h_2 remain as they were in A1. Two of the runs shown in Figure 4.7 use the same three waves as A1 but feature different initial conditions. For one, the amplitudes of the sidebands were twice as large as in A1 while for the other, the initial sideband amplitudes were twice as small as in A1. Also included are two runs made using similar initial amplitudes to A1 but in which the wavenumbers of the triads have been changed slightly. In particular, this alters ${}^{(0)}k_2^2$.

In the runs shown in Figure 4.7, the important property, that the growth of the unstable wave is curtailed by the wave-wave interactions remains. The time scale of the evolution continues to be of $O(T_e)$, with the timescale of the higher energy run (the run with larger initial amplitudes for the sidebands) being slightly shorter than that of A1. The amplitude of the "equilibrated" unstable wave is of a similar magnitude for the experiments of Figure 4.7 and for A1, although those of Figure 4.7 are a little larger than that of A1.

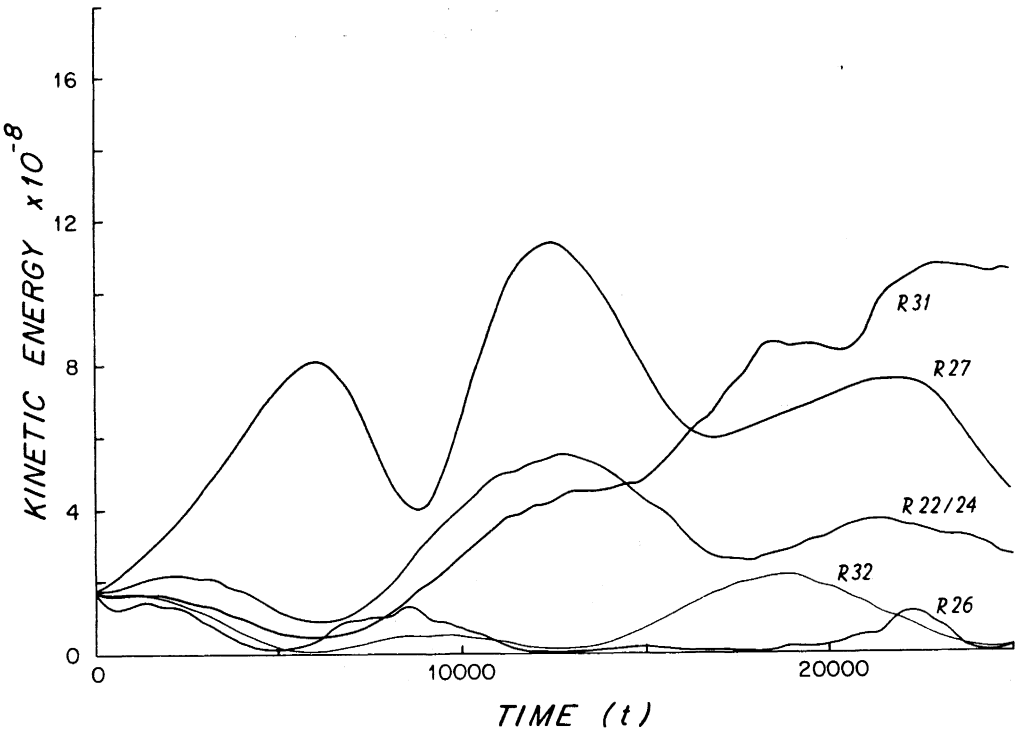

Figure 4.7: The kinetic energy of the upper layer perturbation associated with wave 0 during several different runs. The initial amplitude of wave 0 was the same for each run. The values of F, U, β and h_2 are the same as those used in run A1. The wavenumbers and/or the initial sideband amplitudes differ between runs.

R22/24 is the first part of run B1.

R26 As R22/24 but with initial sideband amplitudes increased by a factor of 2.

R27 As R22/24 but with initial sideband amplitudes decreased by a factor of 2.

R31 Similar initial amplitudes as R22/24 but with $^{(0)}k = 2.253$, $^{(1)}k = -1.2944$, $^{(2)}k = -0.95858$. This corresponds to a triad in which wave 0 has a smaller value of k_2^2 than in R22/24.

R32 Similar initial amplitudes as R22/24 but with $^{(0)}k = 2.267$, $^{(1)}k = -1.3008$, $^{(2)}k = -0.96622$. Here k_2^2 is larger than in R22/24.

Experiments A1 and B1 have shown that it is possible to find a triad which will prevent the continued growth of a weakly unstable wave that linear theory would call for. We have therefore answered one of the questions we posed at the outset of the numerical investigation. Note that not all possible triads involving the unstable wave possess this property. There are other choices of sideband pairs which allow the unstable wave to grow more or less unchecked.

We now turn to the second question; if we start with very weak (quasi-linear) initial conditions, will the at first exponential growth of the unstable wave be accompanied by the growth of the sidebands to such a level that they become strong enough to curb the growth of the unstable wave To show that, in the instances of the parameter values used in Cases A and B, the answer to this is yes, we conducted experiments A2 and B2. These differ from A1 and B1 only in that the initial conditions are very much weaker. The initial upper layer kinetic energies for A2 were

$$\text{Wave } \phi: \quad 4.3147 \times 10^{-11}$$
$$\text{Wave } 1: \quad 6.4132 \times 10^{-10}$$
$$\text{Wave } 2: \quad 1.2841 \times 10^{-10}$$

while those for B2 were

$$\text{Wave } \phi: \quad 8.1708 \times 10^{-12}$$
$$\text{Wave } 1: \quad 8.3272 \times 10^{-11}$$
$$\text{Wave } 2: \quad 2.2055 \times 10^{-11}$$

The subsequent evolution of these energies is shown in Figures 4.8 (A2) and 4.9 (B2). In each case, much the same thing happens. At first the

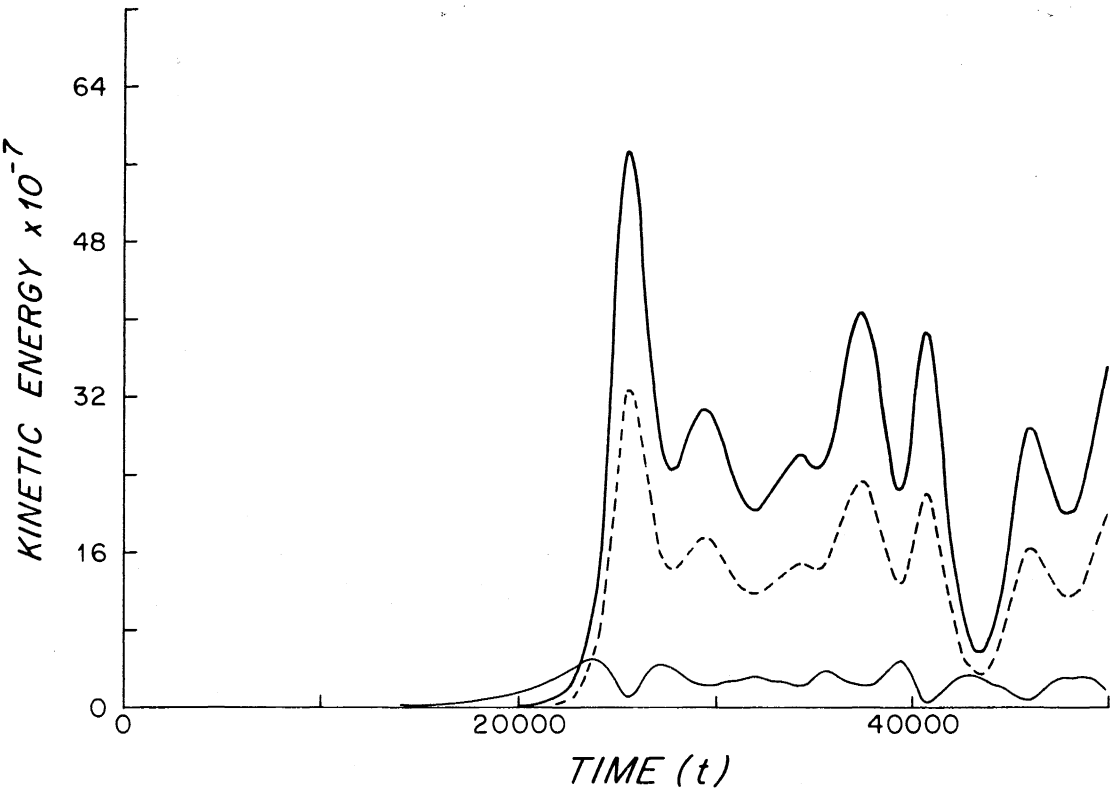

Figure 4.8: As Fig. (4.2) but during run A2.

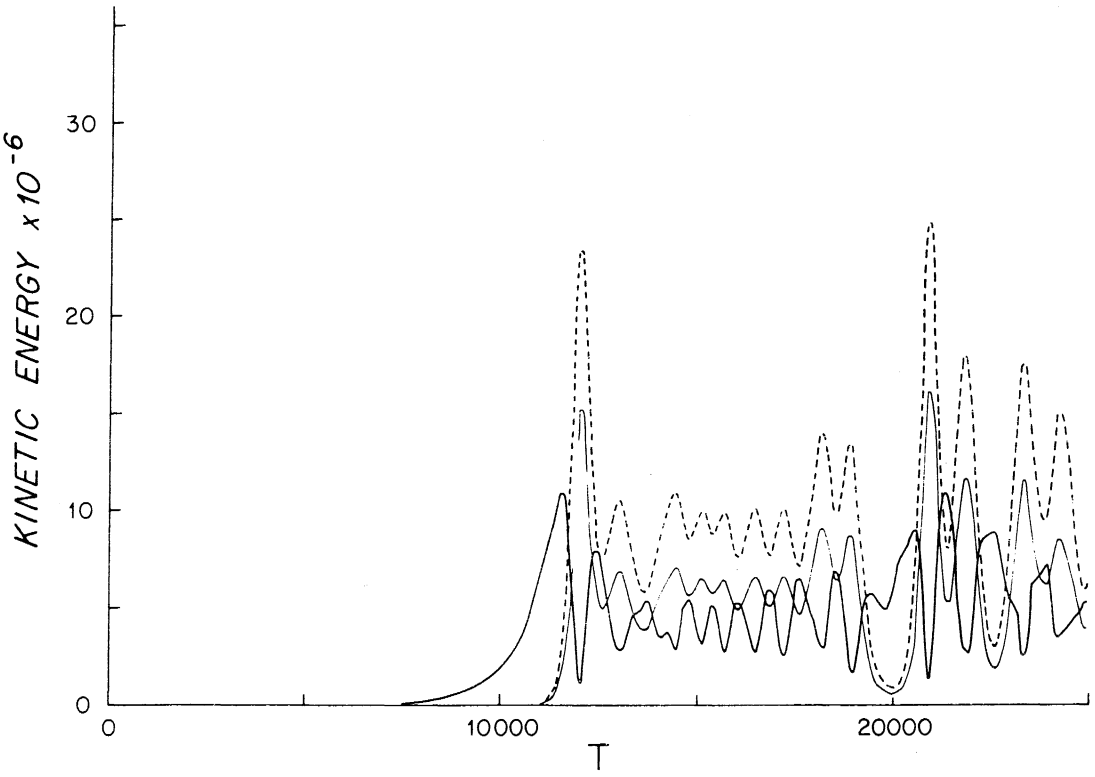

Figure 4.9: As Figure (4.2) but during run B2.

unstable wave grows exponentially with the linear growth rate, while the amplitudes of the sidebands remain constant. Eventually the amplitude of the unstable wave reaches the level at which the asymptotic theory is applicable. At this level the time scale of changes in the sideband amplitudes, that are forced by interactions between the unstable wave and the sidebands becomes comparable to the growth rate of the unstable wave. In other words, the unstable wave has reached a level at which its upper layer streamfunction is $O(\Delta^2)$ so that resonant interactions between the unstable wave and the much weaker sidebands forces changes in the amplitudes of the sidebands on a time scale of $O(\Delta^{-2})$. The equations governing the evolution of the sideband amplitudes are the first two equations in (4.28). Because the coefficients M_1 and M_2 in these equations have the same sign (for A2, $M_1 = 4.074$, $M_2 = 1.852$ while for B2, $M_1 = 4.915$, $M_2 = 1.725$) the "large amplitude" unstable wave is unstable to the two sidebands and these grow on the $O(\Delta^{-2})$ time scale. This process is analogous to the instability of a Rossby wave discussed by Gill (1974) in the weak interaction limit.

As long as the sidebands are sufficiently weak that their influence on the unstable wave can be neglected, the amplitude of the unstable wave has the form

$$A_0 = \alpha_0 e^{\sigma T}$$

The first two equations of (4.28) become

$$\hat{A}_{jT} = iM_j \alpha_0^* e^{\sigma T} \hat{A}_{j'}^* \qquad (j, j') = (1, 2) \text{ or } (2, 1)$$

From these

$$\hat{A}_1(T) = \frac{1}{2}\left[A_1(0) + \left(\frac{M_1}{M_2}\right)^{1/2} e^{i[\pi/2-\arg(\alpha_0)]}\,\hat{A}_2^*(0)\right] \exp\left[(M_1M_2)^{1/2}\,\frac{|\alpha_0|}{\sigma}\,e^{\sigma T}\right]$$

$$+ \frac{1}{2}\left[A_1(0) - \left(\frac{M_1}{M_2}\right)^{1/2} e^{i[\pi/2-\arg(\alpha_0)]}\,\hat{A}_2^*(0)\right] \exp\left[-(M_1M_2)^{1/2}\,\frac{|\alpha_0|}{\sigma}\,e^{\sigma T}\right]$$

while $\hat{A}_2(T)$ is given by a similar expression. For most initial conditions, the coefficients of exp $[(M_1M_2)^{1/2}\ (|\alpha_0|/\sigma)\ e^{\sigma T}]$ will be non-zero. The sideband amplitudes will therefore grow very rapidly, like an exponential of an exponential. This analysis becomes invalid once the amplitude of the sidebands approaches $O(\Delta^{7/4})$ because they then begin to affect the evolution of the unstable wave whose amplitude ceases to be given by $A_0 = \alpha_0\, e^{\sigma T}$. However, we see two things here. First, in the presence of an unstable wave whose growth is being fed by linear instability, the sidebands will also begin to grow whenever the triad chosen is such that the product of the two interactions coefficients M_1 and M_2 is positive. Second, this growth is faster than exponential so that the sidebands can catch up to the unstable wave.

Figures 4.8 and 4.9 show the growth of the sidebands once the amplitude of the unstable wave becomes sufficiently large, $O(\Delta^2)$, that the growth of the sidebands occurs on the same time scale as that of the exponential growth of the unstable wave. The energy of the sidebands increases beyond that of the unstable wave since it is not until the sideband amplitudes reach $O(\Delta^{7/4})$ that they strongly influence the unstable wave. The presence of the strong sidebands then inhibits the further growth of the unstable wave and the evolution progresses in a similar way to those of A_1 and B_1.

In growing from very weak initial conditions, the average energies of each wave, once the triad has settled down into an "equilibrated" regime, are several times larger than the average energies in runs A1 and B1 where we started with initial conditions close to the threshold at which an "equilibrated" state is possible. As a consequence of the higher energies, the time scales of the energy fluctuations are a little shorter, being of O(2000) in run A2.

Runs A2 and B2 demonstrate that there are indeed triads which, starting from very weak initial conditions, nevertheless result in a bounded energy state in which the growth of the unstable wave has been halted purely by the effects of wave-wave interactions between the elements of the resonant triad. Our numerical study has shown that the dynamics of wave-wave interaction, which the earlier theoretical discussion suggested should become important before wave/mean flow interactions for weakly supercritical waves and be described by (4.27), is sufficient to produce a bounded energy state for some choices of triad. It was remarked earlier that not all triads will halt the growth of the unstable wave. In any physical realization of our theoretical model, the unstable wave will be simultaneously a member of many resonant triads whose other elements are neutral waves. Some of these triads will be ones which, at least by themselves, will halt the growth of the unstable wave. We have confined this study to a case in which only one triad is considered. It is not clear what will happen when more than one triad is at work, modifying the evolution of the unstable wave. While it is, in principle, straightforward to obtain the extension of equations (4.27) to the case in which a

finite number of triads, each involving the unstable wave and two neutral waves, are present, a more sophisticated (and slower) numerical model will be required to follow the evolution of this system.

The Single-Wave Problem for the Meridionally Varying Model

In the limit of small supercriticality, the effects of interactions between the unstable wave and modifications to the mean flow are of secondary importance when three-wave interactions of the sort discussed above are occurring. Similarly, interactions between the unstable wave and its zonal harmonics may be neglected in the three wave problem. Nevertheless, the single-wave problem, in which the evolution of a slightly supercritical unstable wave is modified through its interaction with the mean flow and with higher harmonics of the unstable wave, retains some theoretical significance. It has practical relevance in instances when a quantization condition imposed on the zonal wavenumbers does not admit any stabilizing resonant triads. Such a condition could occur in the case of a spherical or annular domain. (In practice, such a condition might also fail to admit wavenumbers corresponding to weak instability at minimum critical shear). It also has some pedagogic relevance: in regimes in which the supercriticality is small but not very small, both three-wave and wave-mean flow interactions can be expected to be present; a rather complicated situation, yet one that is still short of the fully non-linear case. By considering the three-wave and single-wave problems in isolation, we hopefully provide some basis for understanding this coupled regime.

One of the aims of the single-wave theory is to determine whether the combined effects of wave-mean flow and wave-harmonic interactions can

equilibrate the slightly supercritical wave at small amplitude. We will discover later, as a result of some numerical simulations, that the finite-amplitude processes can indeed equilibrate the weakly unstable linear mode.

We saw that the amplitude scales used in the three-wave problem were too small to produce a wave-mean flow or a wave-harmonic interaction that could affect the amplitude of the unstable wave on the e-folding time-scale $O(\Delta^{-2})$. In the single-wave case, it turns out that we must rescale the amplitude of the unstable wave to be $O(\Delta^{3/2})$ in the upper layer. Because of this amplitude scale, one of the differences between the single-wave case and the three-wave theory is that the energy density of the wave-field, in the "equilibrated state", is larger than was the case in the three-wave problem; $O(\Delta^{3})$ rather than $O(\Delta^{7/2})$. A second feature that we will discover is that the wave-mean flow interaction is accompanied by the generation of, and the interaction of the unstable wave with, the zonal harmonics of the unstable wave. This process seems analogous to the critical layer effect noted by Pedlosky (1982) in the meridionally uniform two-layer model at minimum critical shear. There are, however, some differences in the details of the manner in which the harmonics are created when one compares the two models. In the meridionally uniform situation, if one starts from initial conditions in which only the unstable linear mode is present, then one finds that the zonal harmonics are generated indirectly. The self-interaction of the unstable wave cannot generate a second harmonic, only a correction to the mean flow. However, the latter has a non-trigonometric structure. The inter-

action between the unstable mode and the mean flow correction then generates a series of meridional harmonics of the unstable wave. Lastly, these meridional harmonics interact with the unstable wave to produce higher zonal harmonics of the latter. We will see later that the introduction of meridional variation changes this. Since the eigenfunction structure of the unstable wave is no longer trigonometric, the self-interaction of the unstable wave directly generates a second zonal harmonic. The interaction between the unstable wave and its second harmonic creates a third harmonic and so on.

There are also differences in the way in which the harmonics affect the evolution of the unstable wave. In Phillips' model the sin $3\pi y$ meridional harmonic, with the same zonal structure as the fundamental, alters the mean flow through its interaction with the unstable wave. None of the higher meridional harmonics of the fundamental directly affect the mean flow, nor do any of the zonal harmonics. No harmonics appear explicitly in the evolution equation for the amplitude of the unstable wave. Zonal harmonics are important but their influence is due to the changes they force in the third meridional harmonic at the fundamental zonal wavenumber. In the amplitude equations that we derive below, it will be seen that, in the meridionally varying case, the higher zonal harmonics enter both the equation for the mean flow and that determining the amplitude of the unstable wave.

In Pedlosky's model, the meridional extent of the higher zonal harmonics involved in the dynamics of the unstable wave, was the entire channel width. For such a meridionally uniform model, the meridional

extent of the region of the small lower-layer potential vorticity gradient is also the width of the channel. In our meridionally varying model, we will find that the higher harmonics are strongest in the inner layer region about the center of the channel that corresponds to small values of the potential vorticity gradient of the lower layer.

In what follows, we shall show how the asymptotic governing equations for the weakly supercritical case may be obtained and indicate the generation of higher harmonics. Again, these equations are rather complicated. We include a couple of numerical simulations to show that the unstable wave is equilibrated. These also show the production of the overtone spectrum.

Amplitude Equations

Most of the symbols used in this discussion and their definitions will be similar to those used in the earlier parts of this chapter. We will discard the leading superfixes used earlier to distinguish between the three principal waves of the triad problem. As in the three-wave case, we take

$$\beta = \beta_m - \Delta \qquad \Delta << 1$$

and

$$T = \Delta^2 t$$

We expand the streamfunctions,

$$\phi_{1\ out} = \Delta^{3/2}\Big[A(T)\sin \pi y\, e^{ikx} + * + \Delta\,\phi_1^{(2)}(x,y,T)$$

$$+ \Delta^{3/2}\,[\phi_1^{(3)}(x,y,T) + \bar{\Phi}_1^{(3)}(y,T)] + \Delta^2 \ln(1/\Delta)\,\textcircled{H}_1^{(4)}(y,T)$$

$$+ \Delta^2\,[\phi_1^{(4)}(x,y,T) + \bar{\Phi}_1^{(4)}(y,T)] + \Delta^{5/2}\ln(1/\Delta)\,\textcircled{H}_1^{(5)}(y,T)$$

$$+ \Delta^{5/2}\,[\phi_1^{(5)}(x,y,T) + \bar{\Phi}_1^{(5)}(y,T)] + \ldots.\Big] \qquad (4.35)$$

$$\phi_{2\ out} = \Delta^{7/2}\Big[\Delta^{-1/2}\bar{\Phi}_2^{(-1)}(y,T) + \ln(1/\Delta)\,\textcircled{H}_2^{(0)}(y,T) +$$

$$+ [\phi_2^{(0)}(x,y,T) + \bar{\Phi}_2^{(0)}(y,T)]$$

$$+ \Delta^{1/2}\ln(1/\Delta)\,\textcircled{H}_2^{(1)}(y,T) + \Delta^{1/2}\bar{\Phi}_2^{(1)}(y,T) +$$

$$+ \Delta\ln(1/\Delta)\,\textcircled{H}_2^{(2)}(y,T)$$

$$+ \Delta\,[\phi_2^{(2)}(x,y,T) + \bar{\Phi}_2^{(2)}(y,T)]$$

$$+ \Delta^{3/2}\ln(1/\Delta)\,[\theta_2^{(3)}(x,y,T) + \textcircled{H}_2^{(3)}(y,T)]$$

$$+ \Delta^{3/2}\,[\phi_2^{(3)}(x,y,T) + \bar{\Phi}_2^{(3)}(y,T)] + \ldots \qquad (4.36)$$

$$\phi_{1\ in} = \Delta^{3/2}\,A\,(1-\Delta\,\tfrac{1}{2}\pi^2\eta^2 + \Delta^2\,\tfrac{1}{24}\pi^4\eta^4 - \Delta^3\,\tfrac{1}{720}\pi^6\eta^6 + \ldots)\,e^{ikx} + *$$

$$+ \Delta^{3/2}\,[\phi_1^{(3)}(x,\eta,T) + \bar{\Phi}_1^{(3)}(\eta,T)]$$

$$+ \Delta^2\ln(1/\Delta)\,[\zeta_1^{(4)}(\eta,T) + \tilde{\mathcal{H}}^{(4)}(x,\eta,T)] + \Delta^2\,[\phi_1^{(4)}(x,\eta,T) + \bar{\Phi}_1^{(4)}(\eta,T)] +$$

$$+ \Delta^{5/2} \ln(1/\Delta)[\zeta_1^{(5)}(\eta,T) + \mathcal{F}^{(5)}(x,\eta,T)] + \Delta^{5/2}[\phi_1^{(5)}(x,\eta,T) + \Phi_1^{(5)}(\eta,T)]$$

$$+ \Delta^3 \ln(1/\Delta)[\zeta_1^{(6)}(\eta,T) + \mathcal{F}^{(6)}(x,\eta,T)] + \Delta^3[\phi_1^{(6)}(x,\eta,T) + \Phi_1^{(6)}(\eta,T)] + \ldots$$

$$+ \Delta^4 [\ln(1/\Delta)]^2 [I_0^{(8,2)}(\eta,T) + I_1^{(8,2)}(x,\eta,T)] + \ldots$$

$$+ \Delta^5 [\ln(1/\Delta)]^3 [I_0^{(10,3)}(\eta,T) + I_1^{(10,3)}(x,\eta,T)] + \ldots \qquad (4.37)$$

$$\phi_{2\,in} = \Delta^{5/2} [\phi_2^{(0)}(x,\eta,T) + \Phi_2^{(0)}(\eta,T)] + \Delta^{1/2} [\phi_2^{(1)}(x,\eta,T) + \Phi_2^{(1)}(\eta,T)]$$

$$+ \Delta \ln(1/\Delta) [P^{(2)}(\eta,T) + R^{(2)}(x,\eta,T)]$$

$$+ \Delta [\phi_2^{(2)}(x,\eta,T) + \Phi_2^{(2)}(\eta,T)] + \Delta^{3/2} \ln(1/\Delta)[P^{(3)}(\eta,T) + R^{(3)}(x,\eta,T)]$$

$$+ \Delta^{3/2}[\phi_2^{(3)}(x,\eta,T) + \Phi_2^{(3)}(\eta,T)] + \Delta^2[\ln(1/\Delta)]^2[L_0^{(4,2)}(\eta,T) + L_1^{(4,2)}(x,\eta,T)]$$

$$+ \Delta^2 \ln(1/\Delta)[P^{(4)}(\eta,T) + R^{(4)}(x,\eta,T)] + \Delta^2[\phi_2^{(4)}(x,\eta,T) + \Phi_2^{(4)}(\eta,T)] + \ldots$$

$$(4.38)$$

In the above, symbols such as $\phi_1^{(2)}$ may refer to two distinct functions, one defined in the outer region and one in the inner. For clarity, we will not bother with additional notation to distinguish these two. Instead, it should be obvious from the context which function is implied.

Some of the x-dependent terms contain not only a component proportional to e^{ikx}, but also higher Fourier components; e^{inkx}, $n = 2, 3, \ldots$. The full resolution of the form of these harmonics of the primary wave and of the mean flow perturbation in all of the sub-domains of the problem is quite a lengthy process. Here we shall sketch the main steps necessary to determine the evolution of the amplitude of the primary, A.

These have much in common with the steps used in the three-wave problem. We will also list, but not derive, some of the terms in the expansion of the harmonics and the mean flow. A more detailed outline of the solution is postponed to Appendix B.

We define k by

$$k^2 = k_m^2 - \Delta\, k_1^2 + \Delta^{3/2}\, k_2^2$$

$$k_m^2 = \beta_m/U - \pi^2$$

The inner meridional variable is

$$\eta = \Delta^{-1/2}\,(y - 1/2)$$

Rescaling the streamfunctions so that their leading terms are O(1) and substituting them in the potential vorticity equations, we can obtain modified potential vorticity equations that show the relative importance of the several terms in them. In the outer part of the domain, the upper and lower layer equations become respectively,

$$(U\nabla^2 + \beta_m)\,\phi_{1x} = \Delta\phi_{1x} - \Delta^{3/2}\,J(\phi_1, \nabla^2\phi_1) - \Delta^2\,(\partial_T\,[\nabla^2 - F]\,\phi_1 + FU\,\phi_{2x})$$

$$- \Delta^3\,[J\,(\Phi_1, q_1) + J\,(\phi_1, Q_1)] \qquad (4.39)$$

$$- \Delta^{7/2}\left[J\,(\phi_1, F\phi_2) + \partial_T\,[(\partial_y^2 - F)\Phi_1 + F\Phi_2]\right] - \Delta^4\,F\phi_{2T}$$

$$(\beta_m - FU + hy)\,\phi_{2x} = -F\,\phi_{1T} + \Delta\,[\phi_{2x} - J(\Phi_2, F\phi_1)]$$

$$- \Delta^{3/2}\left[J(\phi_2, F\phi_1) + \partial_T[(\partial_y^2 - F)\Phi_2 + F\,\Phi_1]\right] \qquad (4.40)$$

$$- \Delta^2\partial_T\,(\nabla^2 - F)\,\phi_2 - \Delta^3\,[J(\phi_2, Q_2) + J\,(\Phi_2, (\nabla^2 - F)\,\phi_2)]$$

In these equations q_j is the potential vorticity in the j^{th} layer that is associated with the x-dependent part of the disturbance field while Q_j is a similar quantity associated with the x-independent part of the disturbance.

Substituting the ϕ expansions into these equations and considering each order in Δ separately, we obtain a series of differential problems for the various terms that compose the streamfunction. Taking the upper layer first:

At O(1) $$[U(\partial_y^2 - k_m^2) + \beta_m]\;\phi_{1x}^{(0)} = 0$$

which is satisfied by $\phi_1^{(0)} = A \sin \pi y\; e^{ikx} + *$ except for terms of $O(\Delta)$.

At $O(\Delta)$ $$[U(\partial_y^2 - k_m^2) + \beta_m]\,\phi_{1x}^{(2)} = (1 - U\,k_1^2)\,\phi_{1x}^{(0)}$$

which yields $k_1^2 = 1/U$ as a solvability condition. We normalize the solution so that $\phi_1^{(1)}$ 0.

At $O(\Delta^{3/2})$ $$[U(\partial_y^2 - k_m^2) + \beta_m]\,\phi_{1x}^{(3)} = U\,k_2^2\;\phi_{1x}^{(0)}\;.$$

It is at this order that higher harmonics first appear in the outer solution. They are not directly forced at this order, but we will see later that they are generated during the matching process. In general, we will make the Fourier decomposition:

$$\phi_1^{(m)} = \sum_{n=1}^{\infty} \left(W_n^{(m)} e^{inkx} + *\right)$$

Then

$$W_1^{(3)} = \frac{-k^2}{2\pi} (y-1) \cos \pi y \, A$$

and

$$W_n^{(3)} = B_n^{(3)} \sin h \, \lambda_n (y-1) \qquad (4.41)$$

where $\lambda_n^2 = k^2 n^2 - \beta_m/U$

$B_n^{(3)}$ is as yet unknown.

Switching now to the lower layer, we find that at O(1)

$$(\beta_m - FU + h_y) \phi_{2x}^{(0)} = - F \phi_{1T}^{(0)} = - F \sin \pi y \, (A_T e^{ikx} + *)$$

thus

$$\phi_2^{(0)} = \frac{F}{k} \frac{\sin \pi y}{\beta_m - FU + h_y} (i A_T e^{ikx} + *) \qquad (4.42)$$

From here we return to the upper layer where, at $O(\Delta^2)$, we find

$$U (\nabla^2 + \beta_m/U) \phi_{1x}^{(4)} = - FU \phi_{2x}^{(0)} - (\nabla^2 - F) \phi_{1T}^{(0)}$$

After making a Fourier decomposition of $\phi_1^{(4)}$ this becomes

$$(\partial_y^2 + \pi^2)\, W_1^{(4)} = -\frac{F}{2k\, h_2}\frac{\sin \pi y}{\cos^2 \pi y}\, iA_T - (k^2 + \pi^2 + F)\frac{iA_T}{Uk}\sin \pi y$$

$$(\partial_y^2 - \lambda_n^2)\, W_n^{(4)} = 0 , \qquad n \geq 2$$

Therefore

$$W_1^{(4)} = iA_T\left[\frac{1}{2\pi}(y-1)\cos \pi y\left[\frac{\beta_m + FU}{k\, U^2} - \frac{F^2}{k\, h_2}\right] + \frac{F^2}{2k h_2 \pi^2}\sin \pi y \ln(|\cos \pi y|)\right]$$

(4.43)

$$W^{(4)} = B_n^{(4)} \sinh \lambda_n (y-1) , \qquad n \geq 2$$

By now we have taken the potential vorticity equations in the outer region to the same order that we did when developing the linear solution. We have not yet seen any trace of non-linearity. The latter will finally make itself felt a couple of orders hence, but it does not significantly affect the evolution of A(T) on the Δ^{-2} time scale. It is the action of non-linearity in the inner region that is important in determining A(T) so we will leave the outer problem at this stage.

Inner Region

After scaling $\phi_{1\ in}$ with $\Delta^{3/2}$ and $\phi_{2\ in}$ with $\Delta^{5/2}$, the potential vorticity equations in the inner region become

$$U\,\partial_\eta^2 \phi_{1x} + \Delta(U\partial_x^2 + \beta_m)\,\phi_{1x} = \Delta^2(\phi_{1x} - FU\,\phi_{2x}) - \Delta J(\phi_1, q_1) - \Delta^2\,\partial_T q_1$$

(4.44)

and

$$(2\pi^2 h_2 \eta^2 - \Delta \frac{2}{3} h_2 \pi^4 \eta^4 + \ldots) \phi_{2x} + \partial_T \partial_\eta^2 \phi_2 - \phi_{2x} + F \phi_{1T}$$

$$+ J(\phi_2, \partial_\eta^2 \phi_2 + F \phi_1) + \Delta (\partial_x^2 - F) \phi_{2T} + \Delta J(\phi_2, \partial_x^2 \phi_2) = 0 \tag{4.45}$$

In the above equations $J(a,b) \equiv a_x b_\eta - a_\eta b_x$ and

$$q = \partial_\eta^2 \phi_1 + \Delta (\partial_x^2 - F) \phi_1 + \Delta^2 F \phi_2 \quad . \tag{4.46}$$

We turn first to the upper layer. Referring to the streamfunction expansions given in (4.37) and (4.38), we see that the first few terms in ϕ_1 are just the asymptotic form of $A \sin \pi y \, e^{ikx} + *$, the leading part of the outer solution, as $y \to 1/2$. The $O(1)$ and $O(\Delta)$ parts of (4.44) are automatically satisfied. There is no direct forcing for the $O(\Delta^{3/2})$ and $O[\Delta^2 \ln(1/\Delta)]$ terms in the expansion of ϕ_1 in. Rather these satisfy homogeneous equations,

$$U \partial_\eta^2 \partial_x \phi_1^{(3)} = 0 \, , \qquad U \partial_\eta^2 \partial_x \mathcal{F}^{(4)} = 0$$

and so are linear in η,

$$\phi_1^{(3)} = H_1^{(3)}(x,T) \, \eta + H_0^{(3)}(x,T) \tag{4.47}$$

$$\mathcal{F}^{(4)} = \mathcal{F}_1^{(4)}(x,T) \, \eta + \mathcal{F}_0^{(4)}(x,T) \tag{4.48}$$

These functions can contain several zonal harmonics, so we set

$$H_m^{(3)} = \sum_{n=1} (H_{n,m}^{(3)} \; e^{inkx} + *)$$

$$\overset{(4)}{m} = \sum_{n=1} (\overset{(4)}{n,m} \; e^{inkx} + *)$$

At $O(\Delta^2)$ $\qquad U \, \partial_y^2 \, \phi_{1x}^{(4)} = - FU \, \phi_{2x}^{(0)} \, ,$

The contribution from the non-linear term being identically zero. As in the linear problem, $\phi_1^{(4)}$ is given in terms of the lower layer streamfunction by

$$\phi_1^{(4)} = - F \int_0^{\eta} d\,\eta' \int_0^{\eta'} d\,\eta' \; \phi_2^{(0)} + G_1^{(4)}(x,T)\,\eta + G_0^{(4)}(x,T) \qquad (4.49)$$

After making the decomposition

$$[\phi_1^{(m)}, \phi_2^{(m)}, G_1^{(m)}, G_0^{(m)}] = \sum_{n=1} [Z_n^{(m)}, Y_n^{(m)}, G_1^{(m,n)}, G_0^{(m,n)}] \, e^{inkx} + * \qquad (4.50)$$

and noting the symmetry of the problem, this becomes

$$Z_{2n}^{(4)} = - F \int_0^{\eta} d\,\eta' \int_0^{\eta'} d\,\eta'' \; Y_{2n}^{(0)} + G_1^{(4,2n)}\,\eta$$

$$n \geq 1 \qquad (4.51)$$

$$Z_{2n-1}^{(4)} = - F \int_0^{\eta} d\,\eta' \int_0^{\eta'} d\,\eta'' \; Y_{2n-1}^{(0)} + G_1^{(4,2n-1)}$$

In contrast to the upper layer, everything we wish to determine from the lower layer potential vorticity balance will come out of the leading order equation. This is

$$2\pi^2 h_2 \eta^2 \phi_{2x}^{(0)} - \phi_{2x}^{(0)} + \partial_T \partial_\eta^2 \phi_2^{(0)} + F \phi_{1T}^{(0)} + J(\phi_2^{(0)}, \partial_\eta^2 \phi_2^{(0)}) + J(\phi_2^{(0)}, \partial_\eta^2 \phi_2^{(0)} + F \phi_1^{(0)}) + \partial_T \partial_\eta^2 \phi_2^{(0)} + J(\phi_2^{(0)}, \partial_\eta^2 \phi_2^{(0)} + F \phi_1^{(0)}) = 0 \tag{4.52}$$

The last term on the left side of (4.63) contains a component which is x-independent and components that are proportional to the zonal harmonics of the fundamental wave. We note two consequences of this. The first is that the mean flow in the lower layer has the same amplitude (in terms of Δ) as that Fourier component of ϕ_2 which has the wavenumber of the unstable wave. The structure of this mean flow correction is determined at the same order as $\phi_2^{(0)}$. The second consequence is that the leading order x-dependent part of the lower streamfunction, $\phi_2^{(0)}(x,\eta,T)$, is not simply proportional to e^{ikx}, but contains all of the zonal harmonics e^{inkx}, $n \geq 1$.

To clarify the way in which the zonal harmonics are forced, we will use the Fourier decomposition of $\phi_2^{(0)}$ indicated in (4.50). Substituting this into (4.52) produces a rather complicated equation. If we look at the part of this equation that is proportional to e^{ipkx}, $p = 0, 1, 2, \ldots$, taking each p in turn, we obtain

$\underline{e^{io\,kx}}$:

$$\partial_T \partial_\eta^2 \phi_2^{(0)} = ikF (A Y_{1\eta}^{(0)*} - A^* Y_{1\eta}^{(0)}) + ik \sum_{n=1} n \partial_\eta^2 [Y_{n\eta}^{(0)} Y_n^{(0)*} - *] \tag{4.53}$$

e^{ikx}:

$$2\pi^2 h_{2\eta}{}^2\, ik\, Y_1^{(0)} + Y_{1\eta\eta T}^{(0)} - ik\, Y_1^{(0)} + FA_T + ik\, Y_1^{(0)} \Phi_{2\eta\eta\eta}^{(0)}$$

$$- ik\,(Y_{1\eta\eta}^{(0)} + FA)\,\Phi_{2\eta}^{(0)} + ik\, FA^*\, Y_{2\eta}^{(0)}$$

$$+ ik \sum_{n=1}^{\infty} [(n+1)\; Y_{n+1}^{(0)}\, Y_{n\eta\eta\eta}^{(0)*} - n\, Y_n^{(0)*}\, Y_{(n+1)\eta\eta\eta}^{(0)}$$

$$+ n\, Y_{n\eta\eta}^{(0)*}\, Y_{(n+1)\eta}^{(0)} - (n+1)\, Y_{(n+1)\eta\eta}^{(0)}\, Y_{n\eta}^{(0)*}] = 0 \qquad (4.54)$$

e^{ipkx}, $p \geq 2$:

$$2\pi^2 h_{2\eta}{}^2\, ikp\, Y_p^{(0)} + Y_{p\eta\eta T}^{(0)} - ipk\, Y_p^{(0)} + ipk\,(Y_p^{(0)}\Phi_{2\eta\eta\eta}^{(0)} - Y_{p\eta\eta}^{(0)}\Phi_{2\eta}^{(0)})$$

$$- ikF\,(AY_{(p-1),\eta}^{(0)} - A^*Y_{(p+1),\eta}^{(0)}) + ik\left(\sum_{n=1}^{p-1} n\,(Y_n^{(0)}Y_{(p-n)\eta\eta\eta}^{(0)} - Y_{n\eta\eta}^{(0)}Y_{(p-n)\eta}^{(0)})\right.$$

$$+ \sum_{n=1}^{\infty} \Big[(n+p)(Y_{n+p}^{(0)}\, Y_{n\eta\eta\eta}^{(0)*} - Y_{(n+p)\eta\eta}^{(0)}\, Y_{n\eta}^{(0)*})$$

$$\left. + n(Y_{n\eta\eta}^{(0)*}\, Y_{(n+p)\eta}^{(0)} - Y_n^{(0)*}\, Y_{(n+p)\eta\eta\eta}^{(0)})\Big]\right) = 0 \qquad (4.55)$$

In each of the above equations, there is only one T derivative. (4.53) is an evolution equation for $\Phi_2^{(0)}$, (4.54) is an evolution equation for $Y_1^{(0)}$ and (4.55) determines the evolution of $Y_p^{(0)}$, $p \geq 2$. These equations are partial differential equations with η-derivatives. They determine

the meridional structure of $\Phi_2^{(0)}$ and $Y_p^{(0)}$. These meridional structures are intimately coupled to the evolution of $\Phi_2^{(0)}$ and $Y_p^{(0)}$. The evolution of the mean flow and each harmonic, including the first, cannot be described by a T-dependent amplitude coefficient multiplying a stationary meridional structure. Instead, the meridional shape of each harmonic changes with time as well as its norm. Another feature of (4.53)-(4.55) is that they are coupled non-linear equations. The development of each $Y_p^{(0)}$ and $\Phi_2^{(0)}$ is inextricably linked to all of the others.

We should verify that all of the spectral components are directly forced. We will consider an initial condition containing only the linear unstable mode. Thus A and $Y_1^{(0)}$ (and $Y_{1\eta}^{(0)}$) are non-zero while $\Phi_2^{(0)}$ and $Y_p^{(0)}$, $p \geq 2$ are all initially zero. The $AY_{1\eta}^{(0)*}$ - $A^*Y_{1\eta}^{(0)}$ term in (4.53) will force the mean flow, $\Phi_2^{(0)}$. In (4.55), let us consider the $AY_{(p-1)\eta}^{(0)}$ term. The presence of the $(p-1)^{th}$ Fourier component will force the next highest component $Y_p^{(0)}$. We know that $Y_1^{(0)}$ is initially non-zero, hence $Y_2^{(0)}$, $Y_3^{(0)}$, ... will be successively forced. Moreover, we might expect that at a time not too far removed from zero, the energy associated with the p^{th} Fourier component will progressively decrease with increasing p.

Equations (4.53)-(4.55) possess some symmetry properties. As a result, all odd-numbered harmonics are even functions of η and vice versa.

The central problem at hand is the determination of the evolution of A(T), at least in principle. We have not yet closed the system. To do so, we must link the inner solution to the outer. The necessary step is the same as the one used to complete the linear solution in Chapter 3.

We match $\phi_{1\ in}$ to $\phi_{1\ out}$ to relative order Δ^2. We need only consider the e^{ikx} dependent part of ϕ_1. From (4.51), for $\phi_{1\ in}^{(0)}$ this is

$$Z_1^{(4)} = - F\int_0^{\eta} d\eta' \int_0^{\eta'} d\eta''\ Y_1^{(0)}\ (\eta'',\ T) + G_0^{(4,1)} \tag{4.56}$$

where $G_0^{(4,1)}$ is an as yet undetermined function of T.

From (4.53), as $\eta \to \infty$

$$Y_1^{(0)} \sim \frac{iF}{2\pi^2 h_2 k}\ A_T\ \eta^{-2} \tag{4.57}$$

Thus $$Z_1^{(4)} \sim - \eta\ F\int_0^{\infty} d\eta\ Y_1^{(0)}\ (\eta,\ T) + \frac{F^2 i A_T}{2k\pi^2 h_2} \ln\ \eta + R \tag{4.58}$$

where R is a free constant.

We will perform the matching somewhat informally by comparing the asymptotic form of the outer solution in the limit $y-1/2 \sim O(\Delta)$, $\Delta \to 0$ with the form of the inner solution in the limit $\eta \to \infty$. Using (4.35), (4.41) and (4.43), we find that the part of the outer solution that is proportional to e^{ikx} is asymptotically

$$\Delta^{-3/2}\ \phi_{1\ out} \sim A(1- \frac{1}{2}\ \Delta\ k^2\eta^2 + \frac{1}{24}\ \Delta^2\pi^4\eta^4 +\ldots) - \Delta^2 \ln\ (\frac{1}{\Delta})\ \frac{iF^2A_T}{4k\pi^2h_2}$$

$$+\ \Delta^2\ [-\ \frac{k_2^2}{4}\ A\ \eta + \frac{iF^2A_T}{2k\pi^2h_2} \ln\ \eta + \text{const}] + \ldots \tag{4.59}$$

while (4.37), (4.47) and (4.58) imply that the same part of the inner solution is given by

$$\Delta^{-3/2}\,\phi_{1\ in} \sim A\left(1 - \frac{1}{2}\Delta\,\pi^2\eta^2 + \frac{1}{24}\Delta^2\pi^4\eta^4 + \ldots\right) + \Delta^{3/2}\,H_{1,0}^{(3)} \tag{4.60}$$

$$+ \Delta^2 \ln(1/\Delta)\,\mathcal{F}_0^{(4,1)} + \Delta^2\left[-\eta\,F\int_0^\infty d\eta\; Y_1 + \frac{iF^2A_T}{2k\pi^2h_2}\ln\eta + R\right] + \ldots$$

Matching these two forms tells us two things. Firstly, it shows that the term $\Delta^2 \ln(1/\Delta)\,\mathcal{F}_0^{(4,1)}$ in the expansion of $\phi_{1\ in}$, which was not directly forced in the expansion of the vorticity equation, must be included in order to correctly fit the incoming outer solution. Thus

$$\mathcal{F}_0^{(4,1)} = -\frac{iF^2A_T}{4k\pi^2h_2} \tag{4.61}$$

The term $H_{1,0}^{(3)}$ is not forced by the matching conditions and so is zero.

The second and more important matching condition comes from the $\Delta^2\eta$ terms in (4.54) and (4.60). It is

$$\frac{k_2^2}{4}A = F\int_0^\infty d\eta\; Y_1^{(0)} \tag{4.62}$$

The infinite set of equations (4.62), (4.53), (4.54) and (4.55) completely determine $A(T)$, $Y_n^{(0)}(T,\eta)$ and $\Phi_2^{(0)}(T,\eta)$. Finding their solution will

enable us to discover how the single-wave model evolves on the Δ^{-2} time scale. Unfortunately, obtaining such a solution analytically is very difficult. We will instead resort to a numerical procedure.

Features of the Asymptotic Solution

If one pursues the asymptotic analysis further, one can obtain details of the mean flow and harmonics in each of the sub-domains of the problem. The mean flow correction is most prominent in the inner region of the lower layer where the associated streamfunction is $O(\Delta^{5/2})$. The attendant zonal velocity is $O(\Delta^2)$ while the corresponding alteration in the mean meridional potential vorticity gradient for layer two is $O(\Delta)$. The changes in π_{2y} are therefore of a similar scale to the supercriticality in the inner region, as one might expect. In the inner part of the upper layer, the changes in the zonally independent streamfunction and mean velocity are $O[\Delta^{7/2} \ln (1/\Delta)]$ and $O[\Delta^3 \ln (1/\Delta)]$, respectively.

The alterations to the zonally independent part of the streamfunction in the outer region are similar in each layer, being of $O(\Delta^3)$. The concomitant changes in mean velocity are also of $O(\Delta^3)$. The leading contributions to the streamfunctions are $\Phi_1^{(3)}$ and $\Phi_2^{(-1)}$. If we form barotropic and baroclinic streamfunctions,

$$\Phi^{(T)} = \frac{1}{2}(\Phi_1^{(3)} + \Phi_2^{(-1)}) \qquad \Phi^{(c)} = \frac{1}{2}(\Phi_1^{(3)} - \Phi_2^{(-1)})$$

then these take the form

$$\Phi^{(T)} = \left[\frac{1}{4U^2}(\beta_m + FU)\left(\frac{\sin 2\pi y}{2\pi} - y + \frac{1}{2}\right) + \frac{F^2}{4h_2}\left(\frac{\tan \pi y}{\pi} - y + \frac{1}{2}\right) + c^{(T)}\right](|A|^2 - |A(0)|^2)$$

$$\underline{\Phi}^{(c)} = \left[\frac{\pi^2}{(4\pi^2+2F)U^2} (\beta_m + FU) \left(\frac{\sin 2\pi y}{2\pi} - \frac{\sinh [\sqrt{2F}(y-1/2)]}{\sqrt{2F} \cosh \sqrt{F/2}} \right) \right.$$

$$- \frac{F^2}{4h_2} \left(\frac{\tan \pi y}{\pi} - y + \frac{1}{2} \right) - \frac{F^2 \sqrt{F/2}}{4h_2} e^{\sqrt{2F}y} \int_1^y \left(\frac{\tan \pi y}{\pi} - y + \frac{1}{2} \right) e^{-\sqrt{2F}y}$$

$$\left. - e^{-\sqrt{2F}y} \int_1^y \left(\frac{\tan \pi y}{\pi} - y + \frac{1}{2} \right) e^{\sqrt{2F}y} \right] \left(|A|^2 - |A(0)|^2 \right)$$

In the inner region, the amplitudes of the zonal harmonics of the primary wave, in the lower layer, are all similar and match that of the mean flow correction. The meridional structures and evolutionary behavior of these harmonics are determined by the coupled system formed by (4.53), (4.54), (4.55) and (4.62). The corrections to $\phi_{2\ in}$ are $O(\Delta^{5/2})$ while those to $\phi_{1\ in}$ are $O(\Delta^{7/2})$ for even harmonics and $O(\Delta^3)$ for the odd harmonics. The leading contributions to the harmonic components in $\phi_{1\ in}$ are

$$\Delta^{7/2} \quad F \int_0^{\eta} d\eta' \int_{\eta'}^{\infty} d\eta'' \; Y_n^{(0)} \qquad \text{(even harmonics)}$$

and

$$\Delta^3 \quad \frac{F}{\lambda_n} \tanh \frac{\lambda_n}{2} \int_0^{\infty} d\eta \; Y_n^{(0)} \qquad \text{(odd harmonics)}$$

In the lower layer, the zonal velocities associated with the harmonics dominate the meridional velocities. The former are $O(\Delta^2)$ while the

latter are $O(\Delta^{5/2})$. In the upper layer, the situation is a little different. The zonal velocities are $O(\Delta^3)$ for both even and odd harmonics while the meridional velocities are $O(\Delta^3)$ for the odd harmonics, but $O(\Delta^{7/2})$ for the even harmonics.

Let us move now to the outer domain. Here, too, the amplitudes of the leading order terms are different for the two sets of harmonics. This time, however, the second harmonic differs from the remaining even harmonics. For the odd harmonics, the leading order contributions to the upper and lower layer streamfunctions are

$$\text{(upper)} \qquad -\Delta^3 \frac{F}{\lambda_n} \operatorname{sech} \frac{\lambda_n}{2} \sinh \lambda_n (y-1) \int_0^\infty d\eta \, Y_n^{(0)}(\eta) \tag{4.63}$$

and

$$-\Delta^5 \frac{iF^2}{2h_2 nk\lambda_n} \sec^2 \pi y \operatorname{sech} \frac{\lambda_n}{2} \sinh \lambda_n (y-1) \int_0^\infty d\eta \, Y_{nT}^{(0)}(\eta) \tag{4.64}$$

respectively. Associated perturbation velocities in the upper and lower layers are also $O(\Delta^3)$ and $O(\Delta^5)$, respectively. For each of the even harmonics except the second, the largest contributions to the streamfunctions are smaller than those above by a factor $\Delta^{1/2}$. They are

$$\text{(upper)} \qquad -\Delta^{7/2} F \operatorname{cosech} \frac{\lambda_n}{2} \sinh \lambda_n (y-1) \int_0^\infty d\eta \int_\eta^\infty d\eta' \, Y_n^{(0)} \tag{4.65}$$

$$-\Delta^{11/2} \frac{iF^2}{2h_2 nk} \sec^2 \pi y \operatorname{cosech} \frac{\lambda_n}{2} \sinh \lambda_n (y-1) \int_0^\infty d\eta \int_\eta^\infty d\eta' \, Y_{nT}^{(0)}(\eta) \tag{4.66}$$

and produce upper and lower layer velocity components of $O(\Delta^{7/2})$ and $O(\Delta^{11/2})$. In the second harmonic component, the highest order part of the upper layer streamfunction is given by (4.65) with n = 2 but that of the lower layer streamfunction is given by

$$\Delta^5 \quad \frac{i\pi F^2}{8h_2^2 k} \sec^2 \pi y \tan^3 \pi y \quad (A^2)_T \tag{4.67}$$

which is $\Delta^{-1/2}$ larger than (4.66).

The difference between the second harmonics and the higher overtones is a reflection of how non-linear processes are working in this system. In the outer region, we see the sort of phenomenon we might expect in a weak amplitude system containing quadratic interactions. With some over-simplification: a single (zonal) Fourier component e^{ikx}, is "forced" with some small amplitude $O(\varepsilon)$ say, $\varepsilon << 1$. In our model e^{ikx} is "forced" by the linear baroclinic instability mechanism. The meridional and vertical structure of this mode are determined by the leading order linear parts of the governing equations. The non-linear interaction of this mode with itself produces an e^{i2kx} component of $O(\varepsilon^2)$ and successive quadratic interactions produce the higher harmonics with a hierarchical sequence of amplitudes; $\varepsilon^n e^{inkx}$. Because of the difference in amplitudes between the upper and lower layer streamfunctions, the form of the coupling between the upper and lower layer potential vorticity equations and the nature of the meridional structures of the streamfunctions, the relative strengths of the non-linearly generated harmonics is a little different for the two streamfunctions.

The inner region presents a different picture. Although the streamfunction amplitudes are still formally small, we have to take into account the critical layer effect. The linear balance in the lower layer is anomalously small because of the small size of the coefficient that corresponds to the lower potential vorticity gradient of the equilibrium flow. The non-linear perturbation terms are the same size as this weakened linear balance. Despite the small streamfunction amplitudes, this is a fully non-linear sort of dynamics. The absence of any difference in size between the non-linear and linear terms of the lower layer prevents the system from being able to rank the harmonics. Instead, all the harmonics in $\phi_{2\ in}$ have the same amplitude as the fundamental. Their dynamics are intimately interwoven [see (4.53)-(4.55)]. The presence of ϕ_2 in the upper layer potential vorticity equation forces the harmonic components of ϕ_1.

As we make the transition from the inner region to the outer region, π_{2y} becomes O(1) once more, the linear balance in layer two again becomes dominant. However, the harmonics in $\phi_{1\ in}$ are related to the non-linear forcing (which ultimately resides in the lower layer potential vorticity equation) not by a simple algebraic relation but as the solution of a forced, linear differential problem. The harmonics of $\phi_{1\ in}$ do not decay as one moves to the outer region even though the non-linear terms do become relatively less important. Harmonics in the outer region are therefore forced indirectly by the matching condition as a result of non-linear effects occurring within the inner region. This is the reason for the integrals of $Y_n^{(0)}$ that appear in (4.63)-(4.66). Direct non-

linear forcing in the outer region is only strong enough to surpass the effects of the indirect forcing in the case of the second harmonic in the lower layer, (4.67).

Numerical Simulations

The analysis above indicates that, once the amplitude of the unstable wave has grown to $O(\Delta^{3/2})$, non-linear effects modify the hitherto exponential growth of the former. For as long as the unstable wave amplitude remains at this order, the $O(\Delta^{-2})$ time scale behavior of A will be described by (4.53)-(4.55) and (4.62) which include the effects of interactions with the mean flow perturbation and higher harmonics. Since we have not solved these equations we do not know whether these interactions are stabilizing or destabilizing. We have therefore resorted to some numerical simulations of the single wave problem. While their results do not eliminate the possibility of there being some parameter choices for which equilibration does not occur, the cases examined seem to indicate stabilization.

The numerical model used is a spectral model with aliasing removed. The equations solved are the non-linear quasigeostrophic potential vorticity equation for the two-layer model that we have been considering theoretically. Perturbations to the zonally independent flow, generated by non-linear effects are included, unlike the three-wave model considered earlier. The x-dependent parts are spectrally decomposed both meridionally and zonally as

$$\underset{\sim}{\phi} = \sum_{n,m=1}^{n=N,m=M} [(A^{(1)}_{n,m}, A^{(2)}_{n,m})\, e^{imkx} \sin n\pi y + *]$$

where k is the wavenumber of the fundamental unstable wave. Parameters such as U, β, F and h_2 were chosen so that the equilibrium flow was only weakly supercritical. The meridional structure of the mean flow perturbations was also resolved spectrally.

We shall show results obtained for two different set of parameters, these are the single-wave counterparts of the three-wave runs shown earlier. We will therefore label these numerical experiments A3 and B3.

For A3:

$$F = 10.0,\quad U = 1.0,\quad \beta = 14.92,\quad h_2 = 5.0\quad (\Delta = 0.08)\quad k = 2.261$$

The spectral series were truncated zonally at m = 5 and meridionally at sin 38 πy or sin 39 πy (according as the harmonic is even or odd).

For B3:

$$F = 6.6164,\quad U = 1.0,\quad \beta = 16.3,\quad h_2 = 9.8836\quad (\Delta = 0.2)\quad k = 2.254$$

The spectral series were truncated zonally at m = 5 and meridionally at sin 38 πy or sin 39 πy.

In A3, the initial conditions used consisted of setting the meridional spectrum of the e^{ikx} component equal to that of an unstable linear mode and choosing an amplitude equal to that used in the three-wave problem, A1. The initial amplitudes of the remaining zonal harmonics and the mean flow perturbation were chosen to be zero. The initial conditions for B3 bore a similar relation to B1.

In both A3 and B3, we start with the weakly unstable linear mode present at a small but finite amplitude. During the early stages of the com-

puter runs the unstable wave should grow through the action of the linear instability mechanism, while non-linear interactions begin to generate higher harmonics and perturbations to the mean flow. Eventually the latter should begin to modify the evolution of the former.

We present, in Figures 4.10 and 4.11, the kinetic energy of the upper layer flow associated with the fundamental as it evolves during the computer run, for cases A3 and B3, respectively. Both of these show similar behavior. The unstable wave initially grows at a rate given by the linear growth rate. This is eventually overpowered by non-linear effects and the growth of the unstable wave halts. This suggests that the combined effects of the mean flow corrections and the higher harmonics are indeed stabilizing.

It would be interesting to follow the evolution numerically for a longer period of time. This has not been done for two reasons. The first is that the model requires a substantial amount of computer resources. The second is more fundamental. We have shown that the dynamics of the non-linear evolution of the weakly supercritical system rapidly generate a large number of higher harmonics. Each of these harmonics is sufficiently strong, in the inner region, to affect the evolution of the fundamental, in particular, and of the system as a whole. Our numerical model uses a fairly small zonal truncation limit. This spectral domain starts to fill fairly rapidly and so before long the finite truncation of the model begins to influence the evolution of the system. The subsequent development of the system should be sensitive to the truncation level used. Continuing the computational runs further will furnish details not of the

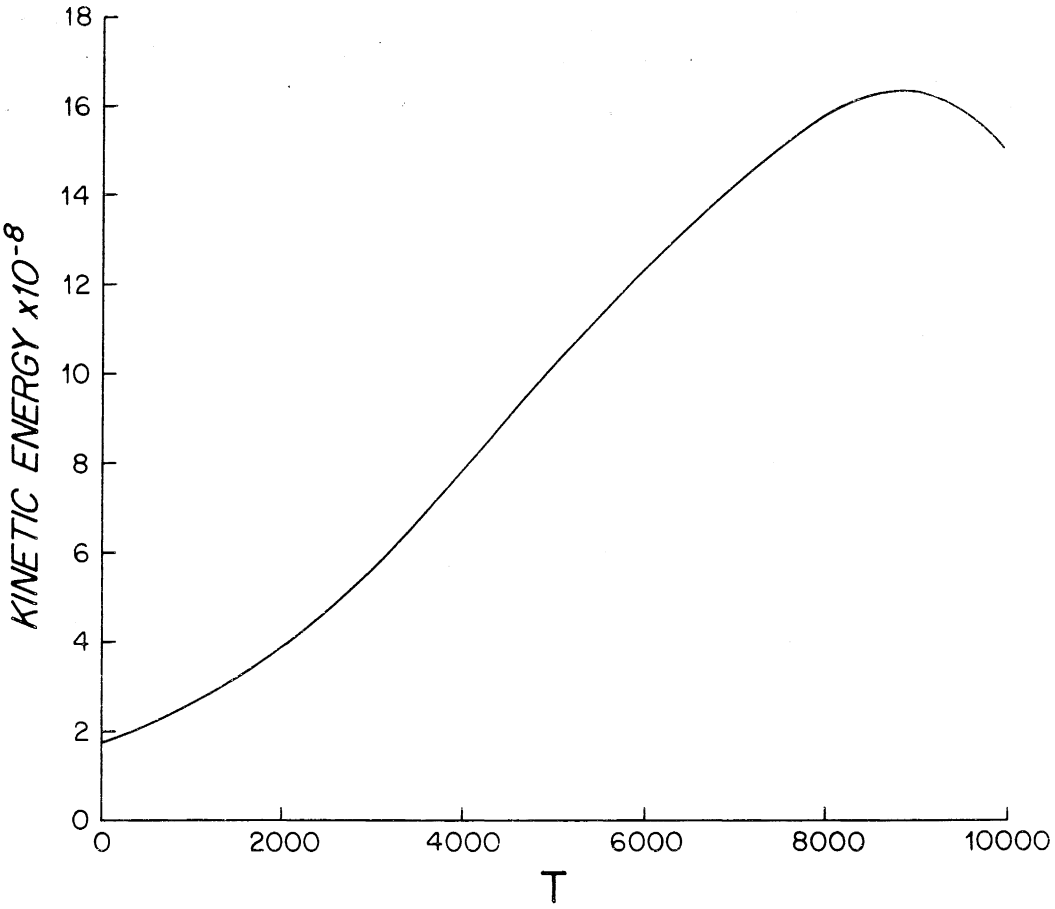

Figure 4.10: As Fig. 4.1 but during run A3.

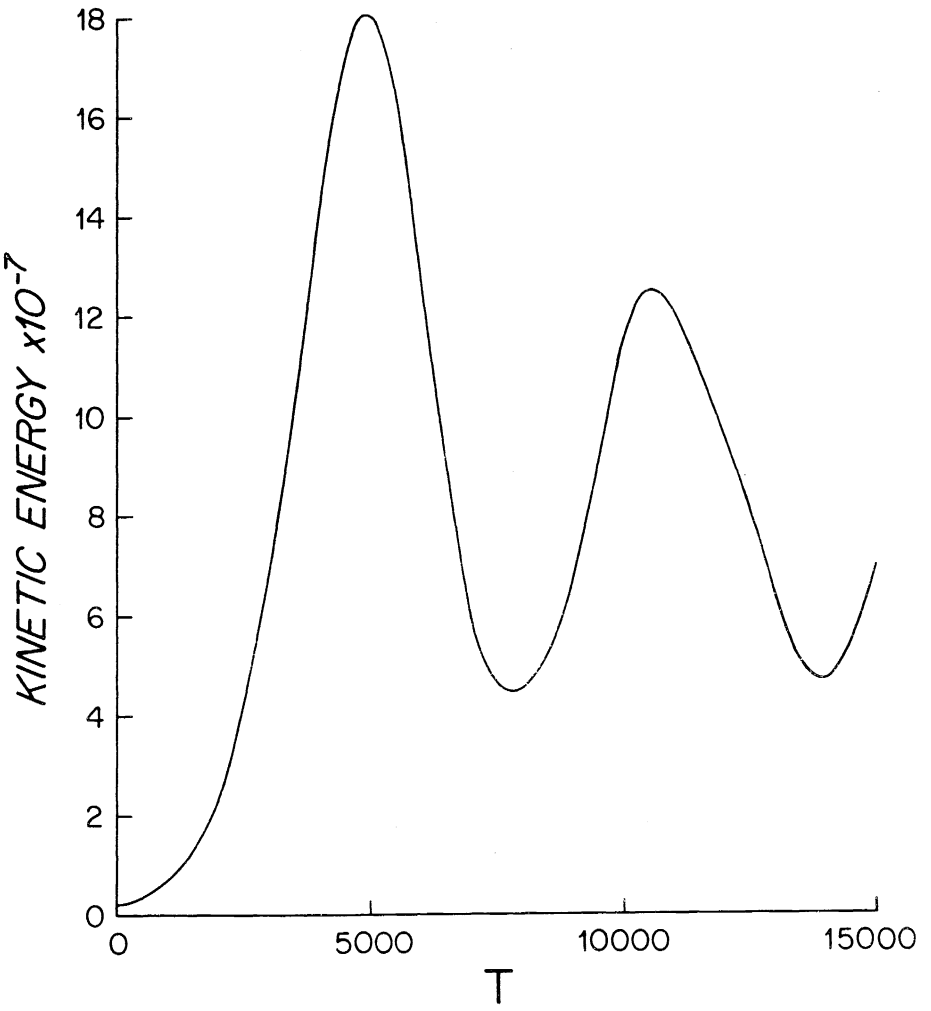

Figure 4.11: As Fig. 4.1 but during run B3.

physical system we wish to model but of a numerical system that departs more and more from the physical system because of its failure to allow the appropriate cascade of energy through wavenumber space.

In Table 4.1, we list the energies associated with the various harmonics at the end of run A3. These show both how, in the inner region of the lower layer, the harmonics are approaching levels comparable with the unstable wave and the differences in energies between the even and odd harmonics. We have listed the formal amplitude scales for the energies of each zonal mode that the asymptotic theory suggests in Table 4.2. The patterns of the two tables are similar.

Table 4.1: Energies of the Fourier Component e^{inkx} at the End of A3

n	KE1[+]	KE2	PE
1	1.5×10^{-7}	2.8×10^{-10}	9.8×10^{-8}
2	1.8×10^{-15}	1.0×10^{-11}	6.8×10^{-14}
3	4.1×10^{-14}	3.4×10^{-11}	3.6×10^{-13}
4	2.9×10^{-16}	1.7×10^{-11}	3.8×10^{-14}
5	2.1×10^{-14}	3.6×10^{-11}	4.9×10^{-13}

[+]KE1 is the kinetic energy per unit channel length of the sin (nkx) component of the velocity fluctuations in the upper layer. KE2 is the similar quantity in the lower layer. KE1, KE2 and PE contain contributions from both the inner and outer regions of the flow.

Table 4.2:

Scales for the Energies of Each Fourier Component
Suggested by the Asymptotic Theory

n	KE1$^+$	KE2	PE
1	Δ^3	$\Delta^{9/2}$	Δ^3
2	$\Delta^{13/2}$	$\Delta^{9/2}$	$\Delta^{11/2}$
3	$\Delta^{12/2}$	$\Delta^{9/2}$	$\Delta^{11/2}$
4	$\Delta^{13/2}$	$\Delta^{9/2}$	$\Delta^{11/2}$
5	$\Delta^{12/2}$	$\Delta^{9/2}$	$\Delta^{11/2}$

The Single-Wave Problem With the Higher Harmonics Excluded

The single-wave problem here contains the phenomenon of zonal harmonic production that is characteristic of non-linear critical layers (e.g., Pedlosky, 1982). The evolution of the unstable wave is modified by the influence of both the harmonics and of interactions with the mean flow. It would be interesting to obtain some feel for the way in which these two non-linear processes contribute to the evolutionary dynamics. Analytically, this is rather difficult because of the complexity of the problem. Numerically, we can very easily remove the higher zonal harmonics of the fundamental from the computational model and examine how the unstable wave evolves when it is only influenced by the mean flow. One should introduce a note of caution at this point. The way in which higher harmonics influence the fundamental is rather complicated. Interactions between higher harmonics can influence the fundamental directly by appearing as a forcing term in (4.54) or indirectly by first of all modifying the mean flow. The dynamics of fundamental/harmonics are thus rather intricately linked to the fundamental/mean flow interactions. The modifications to the mean flow that will appear in the proposed numerical experiment will not bear a direct relation to those in the full experiments A3 and B3.

Figure 4.12 shows the evolution of the upper layer kinetic energy associated with the fundamental in a numerical run lacking any higher zonal harmonics but including the mean flow. This run, which we will label B4, uses the same basic state, unstable wavenumber and initial conditions as B3, with which it should be compared. We see that the

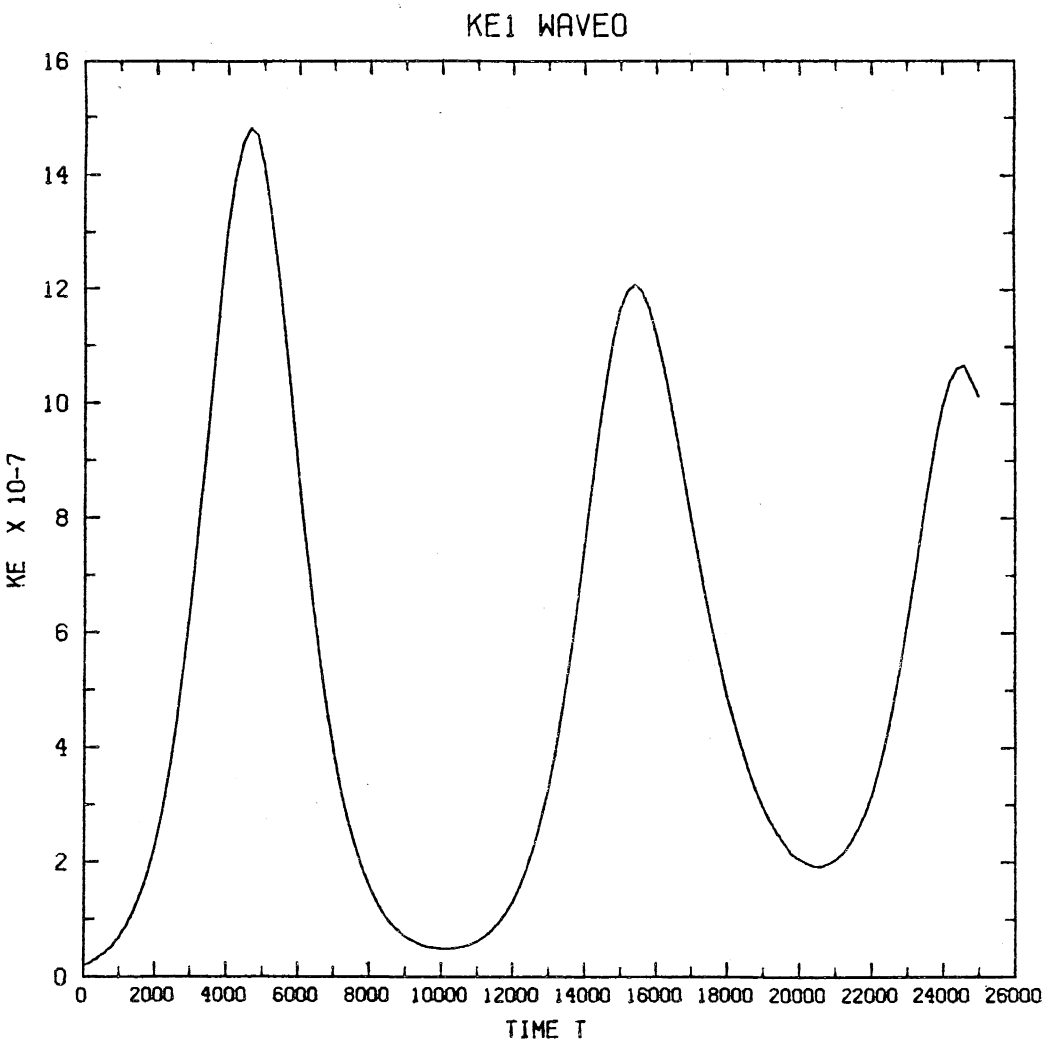

Figure 4.12: As Fig. 4.1 but during B4.

maximum energy attained is less in B4 than in B3, the differences in energy between successive extrema are larger, and the time scale of the energy vacillation is longer.

One could claim that the mean flow alone is more effective in countering the linear instability mechanism than the combined action of the mean flow and the higher harmonics. However, the difference in peak perturbation energy between the two runs B3 and B4 is only about 20 percent.

CHAPTER 5

5. Concluding Remarks

Examples of turbulent flows are often strongly non-linear, exhibiting large amplitude eddy motions. However, a small amplitude eddy field may also exhibit some of the aspects of turbulence, in particular, a broad content of spatial scales continuously exchanging energy in a temporally intricate fashion. From considerations similar to those involved in the non-interaction theorem of Charney and Drazin (1962), one can see that weak wave-like disturbances in a smooth background flow may evolve into a spectrally rich weak wave-field, if there are two or more linear modes initially present, or if the amplitude of the wave-mode initially present is time dependent due to external forcing or some intrinsic instability of the background flow. The time scale for the generation of additional spatial scales would, in general, vary as the inverse of the amplitude of the wavefield. The subsequent evolution of this spatially complex field will occur on a similar time scale, a scale that is longer than the characteristic time scale of the wave periods. In possessing this separation of time scales, a complicated but weak eddy field differs noticeably from strongly non-linear turbulence.

The weak wave-like disturbances generated by baroclinic instability in an unstable flow that lies close to minimum critical shear follows this pattern, at least in the instance of Phillips model in an infinite zonal channel. We will pause here to consider how the production of a multi-scale flow occurs. In the case of the meridionally uniform model, the production of energy at scales other than that which is directly

unstable occurs predominantly through resonant interactions between the unstable wave and neutral waves. Although harmonics of the unstable wave are generated by the critical layer dynamics, they are weaker in amplitude than the unstable wave [$O(\Delta)$ cf. $O(\Delta^{1/2})$]. The neutral waves that interact resonantly with the unstable wave have an amplitude similar to that of the unstable wave. What is more, this amplitude is sufficient for secondary transfers of energy to occur from the sidebands to other neutral waves on the same time scale as that of the linear instability. In general, each of the sidebands in the primary triad involving the unstable wave will also be an element in other resonant triads composed of the sideband and an additional pair of neutral waves. Let us call such a triad a secondary triad and the additional neutral waves, secondary neutral waves. Some of the possible secondary triads will satisfy the configurational condition necessary for the secondary neutral waves to be able to grow from very small amplitudes to amplitudes comparable to the sideband. Because the amplitudes of the sidebands are $O(\Delta^{1/2})$, energy transfers between a sideband and secondary neutral waves will occur on a time scale of $O(\Delta^{-1/2})$, i.e., the same time scale as that of the evolution of the primary triad. In a similar fashion the secondary neutral waves can transfer energy to more neutral waves through more triad interactions. In this way we see that energy released from the mean flow at a particular scale by baroclinic instability can be transferred to a broad range of scales producing a spatially complex eddy field.

Loesch (1974) has indicated that there is a threshold value of F below which this energy cascade is quenched. For $F < 2\sqrt{2}\,\pi^2$, there is only

one resonant triad possible that includes the unstable wave. For F below 10.5, the unstable wave is not unstable to the sidebands because of the signs of the interaction coefficients. If we imagine initial conditions in which wave amplitudes are much less than $O(\Delta^{1/2})$, then the growth of the unstable wave to an $O(\Delta^{1/2})$ level will not be accompanied by any growth of the sidebands. An energy cascade [on the $O(\Delta^{-1/2})$ time scale cannot begin and the unstable wave (equilibrated by interaction with the mean flow) dominates the eddy field.

Our work on the meridionally varying problem has demonstrated that significant energy transfer from the unstable wavelength to other zonal scales can occur in that too. Again, the generation of harmonics of the unstable wave is not a major process in the production of energy at other scales. Instead, it is resonant interaction with neutral waves that is responsible for transferring energy from the unstable wave. Because, unlike the meridionally uniform case, the meridional structure of the linear normal modes were not trigonometric, more than one pair of neutral waves can form a resonant triad with the unstable wave. The sidebands of the primary triads will once again be able to take part in the dynamics of secondary triads.

In the meridionally varying model we expect baroclinic instability to generate a cascade of energy to other (neutral) length scales. However, it is not clear how to describe this process. The model discussed in chapter four was artificially limited to an unstable wave and only two neutral waves. The predicted amplitudes for the sidebands, $O(\Delta^{+7/4})$, were larger than that of the unstable wave, $O(\Delta^2)$. This suggests that

the propensity for energy transfer to other lengtn scales is stronger in the meridionally varying model. However, a sideband of amplitude $O(\Delta^{7/4})$ that is taking part in a secondary triad interaction will tend to experience amplitude fluctuations on an $O(\Delta^{-7/4})$ time scale, i.e., more rapidly than the evolution of the primary triad. It is not clear how this will affect the evolution of the primary triad nor how to consistently formulate a description of energy transfers between the primary triad and the secondary neutral waves.

If we prevent triad resonance, e.g., by introducing a suitable quantization condition, then as in the meridionally uniform model, we observe energy generation at other scales in the form of harmonics of the fundamental wave. Introducing meridional variation into the problem has not removed the critical layer effect observed in Phillips' model. It has, however, changed the latter somewhat. The nigher harmonics, instead of being of uniform magnitude over the width of the channel and within each layer, are now strongest in the inner region of the lower layer flow, where their amplitude is similar to that of the unstable wave in that region. The harmonics are still, however, small compared to the amplitude of the unstable wave in the outer part of the upper layer.

One point to be borne in mind is that the linear and non-linear results indicate that the neighborhood of minimum critical shear in which one can clearly differentiate between the single-wave and three-wave mechanisms is rather small. For Equations (4.27) to describe the evolution of the system requires a very small value of Δ. For values of Δ that are larger but still small, one would expect the evolution of the

unstable wave to exhibit aspects of both three-wave and single-wave processes.

Our entire analysis has been inviscid. It is likely that when the mechanisms that we have discussed are present in a physical system, they will be modified by the action of dissipation. On the one hand, the structure of the unstable mode exhibits an interior region of small meridional scale which may be vulnerable to dissipation. However, it should be noted that the meridional gradient of the background potential vorticity, which is responsible for the presence of the inner layer, does not itself contain small meridional scales. On the other hand, transfer of energy through the wavenumber spectrum that should arise as a result of the three-wave interaction mechanism will be influenced by the rate at which energy is dissipated at smaller scales.

Appendix A

The constants θ_j and M_j appearing in (4.5) are giving by the following expressions

$$\theta_j = -{}^{(j)}k_0 \left[\frac{\beta_m + FU}{(U - {}^{(j)}c_0)^2} \int ({}^{(j)}\psi_1(0))^2 + \frac{h_2}{{}^{(j)}c_0{}^2} \int ({}^{(j)}\psi_2(0))^2 (1+\cos 2\pi y) \right]^{-1} \times$$

$$\left\{ \left[{}^{(j)}k_3^2 + \frac{{}^{(j)}c_1}{(U - {}^{(j)}c_0)^2} - \frac{{}^{(j)}c_1^2 (\beta_m + FU)}{(U - {}^{(j)}c_0)^3} \right] \int ({}^{(j)}\psi_1(0))^2 \right.$$

$$+ \left({}^{(j)}k_3^2 + \frac{{}^{(j)}c_1}{{}^{(j)}c_0^2} \right) \int ({}^{(j)}\psi_2(0))^2 + \left[\frac{{}^{(j)}c_1^2 h_2}{{}^{(j)}c_0^3} \right] \int ({}^{(j)}\psi_2(0))^2 (1+\cos 2\pi y)$$

$$+ \left[-{}^{(j)}k_1^2 + \frac{1}{U - {}^{(j)}c_0} - \frac{{}^{(j)}c_1 (\beta_m + FU)}{(U - {}^{(j)}c_0)^2} \right] \int {}^{(j)}\psi_1(0)\, {}^{(j)}\psi_1(1)$$

$$\left. - \left({}^{(j)}k_1^2 + \frac{1}{{}^{(j)}c_0} \right) \int {}^{(j)}\psi_2(0) {}^{(j)}\psi_2(1) - \frac{{}^{(j)}c_1 h_2}{{}^{(j)}c_0^2} \int (1+\cos 2\pi y) {}^{(j)}\psi_2(0) {}^{(j)}\psi_2(1) \right\}$$

$$M_j = -\left[\frac{\beta_m + FU}{(U - {}^{(j)}c_0)^2} \int ({}^{(j)}\psi_1(0))^2 + \frac{h_2}{{}^{(j)}c_0{}^2} \int ({}^{(j)}\psi_2(0))^2 (1+\cos 2\pi y) \right]^{-1} \times$$

$$\left[\frac{\beta_m + FU}{U - {}^{(j)}c_0} \left(\frac{1}{U - {}^{(j)}c_0} - \frac{1}{U} \right) \left[\pi {}^{(j')}k_0 \int {}^{(j)}\psi_1(0) {}^{(j')}\psi_1(0) \cos \pi y - \right. \right.$$

$$\left. - {}^{(0)}k_0 \int {}^{(j)}\psi_1(0) {}^{(j')}\psi_{1y}(2) \sin \pi y \right]$$

$$\left. + \frac{F}{{}^{(j)}c_0} \left[{}^{(0)}k_0 \int {}^{(j)}\psi_2(0) {}^{(j')}\psi_{2y}(0) \sin \pi y - \pi {}^{(j')}k_0 \int {}^{(j)}\psi_2(0) {}^{(j')}\psi_2(0) \cos \pi y \right] \right]$$

In these, $j = 1, 2$; $j' = 3 - j$; $\int = \int_0^1 dy$

APPENDIX B

The following is a summary of the calculations which describe the weakly finite amplitude evolution of the single-wave; meridionally varying problem discussed in Chapter 4. The goal of this is to predict the spatial structure and the evolution of the leading terms in the Fourier components which correspond to higher zonal harmonics of the unstable wave. Some of the results of the analysis here were presented in Chapter 4, e.g., the evolution equations (4.62), (4.53), (4.54) and (4.55). The analysis is presented without comment for the most part. Perturbation expansion techniques are used to obtain an approximate solution to the non-linear, quasi-geostrophic potential vorticity equations under the assumption that the equilibrium state is only weakly unstable and that the disturbance amplitude is small. The expansion parameter is the supercriticality Δ or equivalently the disturbance amplitude and the notation follows that used in Chapter 4. A multiple (two) time scale technique is used and the meridional domain is divided into an inner and outer domain as before. Asymptotic matching is used to link the solutions in these two domains. We will present this latter part informally, i.e., matching series that we obtain by allowing the inner variable to tend to infinity and the outer variable, to zero.

Because of the interlocking nature of the method of solution, the reader who is intrepid enough to read on should be prepared for a calculation which weaves backwards and forwards between the inner and outer regions and the upper and lower layers.

$$\Delta = \beta_m - \beta \quad , \qquad \beta_m = FU + h_2$$

$$T = \Delta^2 t \qquad , \qquad y = \frac{1}{2} + \Delta^{1/2}\eta$$

Expansions

$$\phi_{1\ out} = \Delta^{3/2}\Big[A(T)\sin \pi y\, e^{ikx} + * + \Delta\,\phi_1^{(2)}(x,y,T)$$

$$+ \Delta^{3/2}\,[\phi_1^{(3)}(x,y,T) + \Phi_1^{(3)}(y,T)] + \Delta^2 \ln(1/\Delta)\,\textcircled{H}_1^{(4)}(y,T)$$

$$+ \Delta^2\,[\phi_1^{(4)}(x,y,T) + \Phi_1^{(4)}(y,T)] + \Delta^{5/2}\ln(1/\Delta)\,\textcircled{H}_1^{(5)}(y,T)$$

$$+ \Delta^{5/2}\,[\phi_1^{(5)}(x,y,T) + \Phi_1^{(5)}(y,T)] + \ldots.\Big]$$

$$\phi_{2\ out} = \Delta^{7/2}\Big[\Delta^{-1/2}\Phi_2^{(-1)}(y,T) + \ln(1/\Delta)\,\textcircled{H}_2^{(0)}(y,T) +$$

$$+ [\phi_2^{(0)}(x,y,T) + \Phi_2^{(0)}(y,T)]$$

$$+ \Delta^{1/2}\ln(1/\Delta)\,\textcircled{H}_2^{(1)}(y,T) + \Delta^{1/2}\Phi_2^{(1)}(y,T) +$$

$$+ \Delta\ln(1/\Delta)\,\textcircled{H}_2^{(2)}(y,T)$$

$$+ \Delta\,[\phi_2^{(2)}(x,y,T) + \Phi_2^{(2)}(y,T)]$$

$$+ \Delta^{3/2}\ln(1/\Delta)\,[\theta_2^{(3)}(x,y,T) + \textcircled{H}_2^{(3)}(y,T)]$$

$$+ \Delta^{3/2}\,[\phi_2^{(3)}(x,y,T) + \Phi_2^{(3)}(y,T)] + \ldots\Big]$$

$$\phi_{1\ in} = \Delta^{3/2}\Big[A\,(1-\Delta\,\tfrac{1}{2}\pi^2\eta^2 + \Delta^2\,\tfrac{1}{24}\pi^4\eta^4 - \Delta^3\,\tfrac{1}{720}\pi^6\eta^6 + \ldots)\,e^{ikx} + *$$

$$+ \Delta^{3/2}\,[\phi_1^{(3)}(x,\eta,T) + \Phi_1^{(3)}(\eta,T)]$$

$$+ \Delta^2 \ln(1/\Delta)\,[\mathcal{G}^{(4)}(\eta,T) + \mathcal{F}^{(4)}(x,\eta,T)] + \Delta^2\,[\phi_1^{(4)}(x,\eta,T) + \Phi_1^{(4)}(\eta,T)]$$

$$+ \Delta^{5/2} \ln(1/\Delta)[\mathcal{G}^{(5)}(\eta,T) + \mathcal{F}^{(5)}(x,\eta,T)] + \Delta^{5/2}[\phi_1^{(5)}(x,\eta,T) + \Phi_1^{(5)}(\eta,T)]$$

$$+ \Delta^3 \ln(1/\Delta)[\mathcal{G}^{(6)}(\eta,T) + \mathcal{F}^{(6)}(x,\eta,T)] + \Delta^3[\phi_1^{(6)}(x,\eta,T) + \Phi_1^{(6)}(\eta,T)] + \ldots$$

$$+ \Delta^4\,[\ln(1/\Delta)]^2\,[I_0^{(8,2)}(\eta,T) + I_1^{(8,2)}(x,\eta,T)] + \ldots$$

$$+ \Delta^5\,[\ln(1/\Delta)]^3\,[I_0^{(10,3)}(\eta,T) + I_1^{(10,3)}(x,\eta,T)] + \ldots \Big]$$

$$\phi_{2\ in} = \Delta^{5/2}\Big[[\phi_2^{(0)}(x,\eta,T) + \Phi_2^{(0)}(\eta,T)] + \Delta^{1/2}\,[\phi_2^{(1)}(x,\eta,T) + \Phi_2^{(1)}(\eta,T)]$$

$$+ \Delta \ln(1/\Delta)\,[P^{(2)}(\eta,T) + R^{(2)}(x,\eta,T)]$$

$$+ \Delta\,[\phi_2^{(2)}(x,\eta,T) + \Phi_2^{(2)}(\eta,T)] + \Delta^{3/2} \ln(1/\Delta)[P^{(3)}(\eta,T) + R^{(3)}(x,\eta,T)]$$

$$+ \Delta^{3/2}[\phi_2^{(3)}(x,\eta,T) + \Phi_2^{(3)}(\eta,T)] + \Delta^2[\ln(1/\Delta)]^2[L_0^{(4,2)}(\eta,T) + L_1^{(4,2)}(x,\eta,T)]$$

$$+ \Delta^2 \ln(1/\Delta)[P^{(4)}(\eta,T) + R^{(4)}(x,\eta,T)] + \Delta^2[\phi_2^{(4)}(x,\eta,T) + \Phi_2^{(4)}(\eta,T)] + \ldots \Big]$$

Rescaling the streamfunctions to remove the outer scalings shown above, the potential vorticity equations become

Exterior Region

$$(U\nabla^2 + \beta_m)\,\phi_{1x} = \Delta\phi_{1x} - \Delta^{3/2}\,J(\phi_1, \nabla^2\phi_1) - \Delta^2\,[\partial_T(\nabla^2 - F)\,\phi_1 + FU\,\phi_{2x}]$$

$$- \Delta^3\,[J(\Delta^{-3/2}\Phi_1, q_1) + J(\phi_1, \Delta^{-3/2}\,Q_1)] -$$

$$- \Delta^{7/2}\Big[J(\phi_1, F\phi_2) + \partial_T\,[\Delta^{-3/2}\,(\partial_y^2 - F)\Phi_1 + F\,\Delta^{1/2}\Phi_2]\Big] - \Delta^4\,F\,\phi_{2T}$$

$$(\beta_m - FU + h_y)\,\phi_{2x} = -F\,\phi_{1T} + \Delta\,[\phi_{2x} - J\,(\Delta^{1/2}\Phi_2,\, F\,\phi_1)]$$

$$- \Delta^{3/2}\left[\, J(\phi_2,\, F\phi_1) + \partial_T\,[\,\Delta^{1/2}\,(\partial_y^2 - F)\Phi_2 + F\Delta^{-3/2}\,\Phi_1]\,\right]$$

$$- \Delta^2\,\partial_T\,(\nabla^2 - F)\,\phi_2$$

$$- \Delta^3\left[\, J(\phi_2,\, \Delta^{1/2}Q_2) + J(\phi_2,\, \nabla^2\,\phi_2)\,\right]$$

where

$$Q_1 = (\partial_y^2 - F)\,\Phi_1 + F\,\Delta^2\,\Phi_2 \quad ; \quad Q_2 = (\partial_y^2 - F)\,\Phi_2 + F\Delta^{-2}\,\Phi_1$$

Inner Region

$$U\partial_\eta^2\,\phi_{1x} + \Delta(U\partial_x^2 + \beta_m)\phi_{1x} = \Delta^2\,(\phi_{1x} - FU\phi_{2x}) - \Delta J(\phi_1,\, q_1) - \Delta^2\,\partial_T q_1$$

$$q_1 = \partial_\eta^2\,\phi_1 + \Delta(\partial_x^2 - F)\phi_1 + \Delta^2\,F\phi_2$$

$$(2\pi^2 h_2 \eta^2 - \Delta\tfrac{2}{3}h_2\pi^4\eta^4 + \ldots)\,\phi_{2x} + \partial_T\partial_\eta^2\,\phi_2 - \phi_{2x} + F\phi_{1T}$$

$$+ J(\phi_2,\, \partial_\eta^2\,\phi_2 + F\phi_1) + \Delta\,(\partial_x^2 - F)\phi_{2T} + \Delta J(\phi_2,\, \partial_x^2\,\phi_2) = 0$$

The wavenumber of the fundamental zonal Fourier component is given by

$$k^2 = k_m^2 - \Delta k_1^2 + \Delta^{3/2}\,k_2^2 \quad , \quad k_m^2 = \beta_m/U - \pi^2$$

We proceed by substituting the streamfunction expansions into the potential vorticity equations and considering the balance of terms at each successive order.

Inner

Lower, O(1)

$$2\pi^2 h_2\eta^2 \phi_{2x}^{(0)} - \phi_{2x}^{(0)} + \partial_T \partial_\eta^2 \phi_1^{(0)} + F\,\phi_{1T}^{(0)} + J(\phi_2^{(0)}, \partial_\eta^2 \Phi_2^{(0)})$$

$$+ J(\Phi_2^{(0)}, \partial_\eta^2 \phi_2^{(0)} + F\phi_1^{(0)}) + \partial_T \partial_\eta^2 \Phi_2^{(0)} + J(\phi_2^{(0)}, \partial_\eta^2 \phi_2^{(0)} + F\phi_1^{(0)}) = 0$$

Set $$\phi_2^{(0)} = \sum_{n=1}^{\infty} [Y_n^{(0)}(\eta,T)\, e^{ink x} + * \,]$$

Project: $e^{i0.kx}$

$$\partial_T \partial_\eta^2 \Phi_2^{(0)} = ikF\,(AY_{1\eta}^{(0)*} - A^*\, Y_{1\eta}^{(0)}) + ik \sum_{n=1}^{\infty} n\partial_\eta^2\, [Y_{n\eta\eta}^{(0)} Y_n^{(0)*} - *\,]$$

e^{ikx}

$$2\pi^2 h_2\eta^2 ikY_1^{(0)} + Y_{1\eta\eta T}^{(0)} - ikY_1^{(0)} + FA_T + ikY_1^{(0)} \Phi_{2\eta\eta\eta}^{(0)} - (Y_{1\eta\eta}^{(0)} + FA)\, \Phi_{2\eta}^{(0)}$$

$$+ ikFA^* Y_{2\eta}^{(0)} + ik \sum_{n=1}^{\infty} [(n+1) Y_{n+1}^{(0)} Y_{n\eta\eta\eta}^{(0)*} - nY_n^{(0)*} Y_{(n+1)\eta\eta\eta}^{(0)} + nY_{n\eta\eta}^{(0)*} Y_{(n+1)\eta}^{(0)}$$

$$- (n+1)\, Y_{(n+1)\eta\eta}^{(0)}\, Y_{n\eta}^{(0)*}\,] = 0$$

e^{ipkx}, $p > 1$

$$2\pi^2 h_2\eta^2 ikpY_p^{(0)} + Y_{p\eta\eta T}^{(0)} - ipkY_p^{(0)} + ipk(Y_p^{(0)} \Phi_{2\eta\eta\eta}^{(0)} - Y_{p\eta\eta}^{(0)} \Phi_{2\eta}^{(0)})$$

$$- ikF(AY_{(p-1),\eta}^{(0)} - A^* Y_{(p+1),\eta}^{(0)}) + ik \left\{ \sum_{n=1}^{p-1} n(Y_n^{(0)} Y_{(p-n)\eta\eta\eta}^{(0)} - Y_{n\eta\eta}^{(0)} Y_{(p-n)\eta}^{(0)}) \right.$$

$$\left. + \sum_{n=1}^{\infty} [(n+p)(Y_{n+p}^{(0)} Y_{n\eta\eta\eta}^{(0)} - Y_{(n+p)\eta\eta}^{(0)} Y_{n\eta}^{(0)*}) + n(Y_{n\eta\eta}^{(0)*} Y_{(n+p)\eta}^{(0)} - Y_n^{(0)*} Y_{(n+p)\eta\eta\eta}^{(0)})] \right\} = 0$$

Asymptotic forms. As $\eta \to \infty$,

$$Y_1^{(0)} \sim \frac{iFA_T}{2\pi^2 h_2 k}\,\eta^{-2}$$

$$Y_p^{(0)} \sim O(\eta^{-(3p-1)})$$

$$\Phi_2^{(0)} \sim -\frac{F^2}{2\pi^2 h_2}\,(|A|^2 - |A(0)|^2)\,(\eta^{-1} + \frac{1}{6\pi^2 h_2}\,\eta^{-3})$$

The dominant balance in the equation for the exp(ikx) component is

$$2\pi^2 h_2 \eta^2 ikY_1^{(0)} - ikY_1^{(0)} + FA_T - ikFA\,\Phi_{2\eta}^{(0)} \simeq 0$$

$$\therefore\ Y_1^{(0)} \sim \frac{iFA_T}{2\pi^2 h_2 k}\,\eta^{-2} + \left[\frac{iF}{4\pi^4 h_2^2 k}\,A_T + \frac{F^3}{4\pi^4 h_2^2}\,A\,(|A|^2 - |A(0)|^2)\right]\eta^{-4}$$

Lower, $O(\Delta^{1/2})$

$$2\pi^2 h_2 \eta^2 \phi_{2x}^{(1)} + \partial_T \partial_\eta^2 \phi_2^{(1)} - \phi_{2x}^{(1)} + J(\phi_2^{(1)}, \partial_\eta^2 \phi_2^{(0)}) + J(\phi_2^{(0)}, \partial_\eta^2 \phi_2^{(1)})$$

$$+ \partial_T \partial_\eta^2 \Phi_2^{(1)} + J(\Phi_2^{(1)}, \partial_\eta^2 \phi_2^{(0)}) + J(\phi_2^{(0)}, \partial_\eta^2 \Phi_2^{(1)}) + J(\Phi_2^{(0)}, \partial_\eta^2 \phi_2^{(1)})$$

$$+ J(\phi_2^{(1)}, F\phi_1^{(0)}) + J(\Phi_2^{(1)}, F\phi_1^{(0)}) + J(\phi_2^{(1)}, \partial_\eta^2 \Phi_2^{(0)}) = 0$$

The zonally independent part of this is

$$\partial_T \partial_\eta^2 \Phi_2^{(1)} = -J_{(0)}(\phi_2^{(1)}, \partial_\eta^2 \phi_2^{(0)}) - J_{(0)}(\phi_2^{(0)}, \partial_\eta^2 \phi_2^{(1)})$$

$$- J_{(0)}(\phi_2^{(1)}, F\phi_1^{(0)})$$

so that

$$\Phi_2^{(1)} = -\int_0^T dT \int_0^\eta d\eta' \int_0^{\eta'} d\eta'' \left[J_{(0)}(\phi_2^{(1)}, \partial_\eta^2 \phi_2^{(0)}) + J_{(0)}(\phi_2^{(0)}, \partial_\eta^2 \phi_2^{(1)}) \right.$$

$$\left. + J_{(0)}(\phi_2^{(1)}, F\phi_1^{(0)}) \right] + M^{(1)}{}_\eta$$

Hence, as $\eta \to$

$$\Phi_2^{(1)} \sim \tilde{M}^{(1)}{}_\eta + \int_0^T dT \int_0^\infty d\eta' \int_{\eta'}^\infty d\eta'' \left[J_{(0)}(\phi_2^{(1)}, \partial_\eta^2 \phi_2^{(0)}) \right.$$

$$\left. + J_{(0)}(\phi_2^{(1)}, \partial_\eta^2 \phi_2^{(1)}) + J_{(0)}(\phi_2^{(1)}, F\phi_1^{(0)}) \right] + \text{h.o.t.}$$

The x - dependent part of the potential vorticity balance yields

$$2\pi^2 h_2 \eta^2 \phi_{2x}^{(1)} + \partial_T \partial_\eta^2 \phi_2^{(1)} - \phi_{2x}^{(1)} + J_{(x)}(\phi_2^{(1)}, \partial_\eta^2 \phi_2^{(0)})$$

$$+ J_{(x)}(\phi_2^{(0)}, \partial_\eta^2 \phi_2^{(1)}) - F\phi_{1x}^{(0)} \phi_{2\eta}^{(1)} - F\phi_{1x}^{(0)} \Phi_{2\eta}^{(1)} - \partial_\eta^2 \phi_{2x}^{(0)} \Phi_{2\eta}^{(1)}$$

$$+ \phi_{2x}^{(0)} \Phi_{2\eta\eta\eta}^{(1)} - (\partial_\eta^2 \phi_{2x}^{(1)}) \Phi_{2\eta}^{(0)} + \phi_{2x}^{(1)} \partial_\eta^3 \Phi_2^{(0)} = 0$$

Setting $\phi_2^{(1)} = \sum_{n=1}^{\infty} (Y_n^{(1)} e^{inkx} + *)$ we find that

$$Y_1^{(1)} \sim \frac{F}{2\pi^2 h_2} \tilde{M}^{(1)}{}_\eta - 2 A$$

Lower, $O(\Delta)$

$$2\pi^2 h_2 \eta^2 \phi_{2x}^{(2)} + \partial_T \partial_\eta^2 \phi_2^{(2)} - \phi_{2x}^{(2)} + F(-\tfrac{1}{2} \pi^2 \eta^2)(A_T e^{ikx} + *)$$

$$- \frac{2}{3} h_2 \pi^4 \eta^4 \phi_{2x}^{(0)} + J(\phi_2^{(2)}, \partial_\eta^2 \phi_2^{(0)} + F\phi_1^{(0)}) + J(\phi_2^{(1)}, \partial_\eta^2 \phi_2^{(1)})$$

$$+ J(\phi_2^{(0)}, \partial_\eta^2 \phi_2^{(2)}) + J(\phi_2^{(0)}, - \frac{F}{2} \pi^2 \eta^2 (Ae^{ikx} + *)) + \partial_T \partial_\eta^2 \Phi_2^{(2)}$$

$$+ J(\Phi_2^{(2)}, \partial_\eta^2 \phi_2^{(0)} + F\phi_1^{(0)}) + J(\Phi_2^{(1)}, \partial_\eta^2 \phi_2^{(1)}) + J(\phi_2^{(0)}, \partial_\eta^2 \Phi_2^{(2)})$$

$$+ J(\phi_2^{(1)}, \partial_\eta^2 \Phi_2^{(1)}) + J(\phi_2^{(2)}, \partial_\eta^2 \Phi_2^{(0)}) + J(\Phi_2^{(0)}, - F \frac{\pi^2}{2} \eta^2 (Ae^{ikx} + *))$$

$$+ J(\Phi_2^{(0)}, \partial_\eta^2 \phi_2^{(2)}) + (\partial_x^2 - F)\phi_{2T}^{(0)} - F\Phi_{2T}^{(0)} + J(\phi_2^{(0)}, \partial_x^2 \phi_2^{(0)})$$

$$+ J(\Phi_2^{(0)}, \partial_x^2 \phi_2^{(0)}) = 0$$

Set $$\phi_2^{(2)} = \sum_{n=1}^{\infty} (Y_n^{(2)}(\eta, T)\, e^{inkx} + *)$$

$$\phi_2^{(2)} \sim \frac{-iF}{4h_2 k} (A_T e^{ikx} - *) + \frac{1}{3} \pi^2 \eta^2 \phi_2^{(0)} \quad \text{as} \quad \eta \to \infty$$

$$\therefore \quad Y_1^{(2)} \sim - \frac{1}{12} \frac{iFA_T}{h_2 k}$$

$$Y_n^{(2)} \sim \frac{1}{3} \pi^2 \eta^2 Y_n^{(0)}$$

The mean flow is governed by

$$\partial_T \partial_\eta^2 \Phi_2^{(2)} = - J_{(0)}(\phi_2^{(2)}, \partial_\eta^2 \phi_2^{(0)} + F\phi_1^{(0)}) - J_{(0)}(\phi_2^{(0)}, \partial_\eta^2 \phi_2^{(2)})$$

$$- J_{(0)}(\phi_2^{(1)}, \partial_\eta^2 \phi_2^{(1)}) - J_{(0)}[\phi_2^{(0)}, - \frac{F}{2} \pi^2 \eta^2 (Ae^{ikx} + *)] + F\Phi_{2T}^{(0)}$$

$$+ J_{(0)}(\phi_2^{(0)}, \partial_x^2 \phi_2^{(0)})$$

$$\partial_T \bar{\Phi}_2^{(2)} = ikF(A \int_0^\eta Y_1^{(2)*} - *) + ikF \frac{\pi^2}{2} [A^* \int_0^\eta \eta^2 Y_1^{(0)} - *]$$

$$+ F\partial_T \int_0^\eta \int_0^{\eta'} \bar{\Phi}_2^{(0)} + \int_\sigma (\phi_{2x}^{(2)}\phi_{2\eta}^{(0)} + \phi_{2x}^{(0)}\phi_{2\eta}^{(2)} + \phi_{2x}^{(1)}\phi_{2\eta}^{(1)}) + M^{(2)}{}_\eta$$

where $M^{(2)}(T)$ is a free constant and $\int_\sigma$ denotes the zonally uniform part.

$$\therefore \quad \bar{\Phi}_2^{(2)} \sim \frac{-F^3}{2\pi^2 h_2} (|A|^2 - |A(0)|^2)\, \eta \ln\eta + \tilde{M}^{(2)}{}_\eta + \text{const.} + \text{h.o.t.}$$

$\tilde{M}^{(2)}(T)$ is a free constant.

As $\eta \to \infty$, the dominant balance for the exp(ikx) component is

$$2\pi^2 h_2 \eta^2 Y_1^{(2)} - Y_1^{(2)} + \frac{i\pi^2 F}{2k} \eta^2 A_T - \frac{2}{3} h_2 \pi^4 \eta^4 Y_1^{(0)} - FA\bar{\Phi}_{2\eta}^{(2)} + F\frac{\pi^2}{2}\eta^2 A \bar{\Phi}_{2\eta}^{(0)} \simeq 0$$

whence $$Y_1^{(2)} \sim \frac{-iF}{12h_2 k} A_T - (\eta^{-2}\ln\eta) \frac{F^4}{4\pi^4 h_2^2} A (|A|^2 - |A(0)|^2)$$

$$+ \eta^{-2} \left\{ \frac{iF}{24h_2^2\pi^2 k} A_T + \frac{F\tilde{M}^{(2)}}{2\pi^2 h_2} A - \left(\frac{F^3}{24\pi^2 h_2^2} + \frac{F^4}{4\pi^4 h_2^2}\right) A (|A|^2 - |A(0)|^2) \right\}$$

Upper

The O(1) and $O(\Delta)$ balances are trivial

$O(\Delta^{3/2})$ $$U\partial_\eta^2 \partial_x \phi_1^{(3)} = 0$$

$$\therefore \quad \phi_1^{(3)} = H_1^{(3)}(x,T)\eta + H_0^{(3)}(x,T)$$

$O(\Delta^2 \ln 1/\Delta)$ $$U\partial_\eta^2 \partial_x \mathcal{F}^{(4)}(x,\eta,T) = 0$$

$$\therefore \qquad \mathcal{F}^{(4)} = \eta\, \mathcal{F}_1^{(4)}(x,T) + \mathcal{F}_0^{(4)}(x,T)$$

$O(\Delta^2)$

$$U\partial_\eta^2\, \phi_{1x}^{(4)} = -\, FU\phi_{2x}^{(0)} + J(\phi_1^{(0)},\ \pi^2(Ae^{ikx} + *\,)) + J(\phi_1^{(0)},\ (k^2 + F)\phi_1^{(0)})$$

$$\therefore \qquad \phi_1^{(4)} = -\, F \int_0^\eta \int_0^{\eta'} \phi_2^{(0)} + G_1^{(4)}(x,T)\eta + G_0^{(4)}(x,T)$$

Set $$\phi_1^{(4)} = \sum_{n=1}^{\infty} (Z_n^{(4)} e^{ink x} + *\,)$$

$$Z_{2n}^{(4)} = -\, F \int_0^\eta \int_0^{\eta'} Y_{2n}^{(0)} + G_1^{(4,2n)}\eta$$

$$Z_{2n+1}^{(4)} = -\, F \int_0^\eta \int_0^{\eta'} Y_{2n+1}^{(0)} + G_0^{(4,2n+1)}$$

$O(\Delta^{5/2})$ $$U\partial_\eta^2\, \phi_{1x}^{(5)} = k_2^2\, U\phi_{1x}^{(0)} - (U\partial_x^2 + \beta_m)\phi_{1x}^{(3)} - FU\phi_{2x}^{(1)}$$

$$\phi_1^{(5)} = \tfrac{1}{2}\, k_2^2\, \eta^2(Ae^{ikx} + *\,) - \tfrac{1}{6}\, \eta^3(\partial_x^2 + \tfrac{\beta}{U}m)H_1^{(3)} - \tfrac{1}{2}\, \eta^2(\partial_x^2 + \tfrac{\beta}{U}m)H_0^{(3)}$$

$$+ \eta\, H_1^{(5)} + H_0^{(5)} - F \int_0^\eta \int_0^{\eta'} \phi_2^{(1)}$$

$O(\Delta^3)$

$$U\partial_\eta^2 \phi_{1x}^{(6)} = -\, (U\partial_x^2 + \beta_m)\phi_{1x}^{(4)} - FU\phi_{2x}^{(2)} - J(\phi_1^{(0)},\ \tfrac{1}{2}\pi^4\eta^2(Ae^{ikx} + *) + \Phi_{1\eta\eta}^{(4)} + \phi_{1\eta\eta}^{(4)})$$

$$- J(\phi_1^{(0)},\ (k^2 + F)\tfrac{1}{2}\, \pi^2\eta^2(Ae^{ikx} + *\,)) - J(\phi_1^{(0)},\ F\phi_2^{(0)})$$

$$- J(\tfrac{1}{2}\pi^2\eta^2[Ae^{ikx} + *],\ [\pi^2 + k^2 + F]\phi_1^{(0)}) + (\pi^2+k^2+F)\partial_T(Ae^{ikx} + *)$$

$$\therefore\ \partial_\eta^2\,\phi_1^{(6)} = -(\partial_x^2 + \tfrac{\beta_m}{U})\phi_1^{(4)} - F\phi_2^{(2)} - \frac{1}{U}\,\Phi_{1\eta\eta\eta}^{(4)}(Ae^{ikx} + *)$$

$$- \frac{i(\pi^2 + k^2 + F)}{kU}(A_T e^{ikx} - *)$$

Set $$\phi_1^{(6)} = \sum_{n=1}^{\infty}(Z_n^{(6)} e^{inkx} + *)$$

Define $$\lambda_n^2 = n^2k^2 - \beta_m / U$$

$$Z_1^{(6)} = -(\beta_m / U - k^2)\int_0^\eta\int_0^{\eta'} Z_1^{(4)} - F\int_0^\eta\int_0^{\eta'} Y_1^{(2)} + G_0^{(4,1)}(T)$$

$$- \frac{i(\pi^2 + k^2 + F)}{2kU}\,\eta^2 A_T - \frac{1}{U}\,\Phi_{1\eta}^{(4)}\,A$$

$$Z_{2n}^{(6)} = \lambda_{2n}^2\int_0^\eta\int_0^{\eta'} Z_{2n}^{(4)} - F\int_0^\eta\int_0^{\eta'} Y_{2n}^{(2)} + \eta G_1^{(4,2n)}(T)$$

$$Z_{2n+1}^{(6)} = \lambda_{2n+1}^2\int_0^\eta\int_0^{\eta'} Z_{2n+1}^{(4)} - F\int_0^\eta\int_0^{\eta'} Y_{2n+1}^{(2)} + G_0^{(4,2n+1)}(T)$$

$O(\Delta^3 \ln 1/\Delta)$ $$U\partial_\eta^2\,\mathcal{F}_x^{(6)} = -(u\partial_x^2 + \beta_m)\,\mathcal{F}_x^{(4)}$$

$$\therefore\ \mathcal{F}^{(6)} = -\frac{1}{6}\eta^3(\partial_x^2 + \tfrac{\beta}{U}m)\,\mathcal{F}_1^{(4)} - \frac{1}{2}\eta^2(\partial_x^2 + \tfrac{\beta}{U}m)\,\mathcal{F}_0^{(4)} + \eta\,\mathcal{F}_1^{(6)} + \mathcal{F}_0^{(6)}$$

Lower, $O(\Delta^{3/2})$

$$2\pi^2 h_2\eta^2\phi_{2x}^{(3)} + \partial_T\partial_\eta^2\,\phi_2^{(3)} - \phi_{2x}^{(3)} + F\phi_{1T}^{(3)} + J(\phi_2^{(3)},\ \partial_\eta^2\,\phi_2^{(0)} + F\phi_1^{(0)})$$

$$+ J(\phi_2^{(0)}, \partial_\eta^2 \phi_2^{(3)} + F\phi_1^{(3)}) + J[\phi_2^{(1)}, \partial_\eta^2 \phi_2^{(2)} - \tfrac{1}{2}\pi^2\eta^2 F(Ae^{ikx} + *)]$$

$$+ J(\phi_2^{(2)}, \partial_\eta^2 \phi_2^{(1)}) = 0$$

$$\therefore \quad 2\pi^2 h_2 \eta^2 \phi_{2x}^{(3)} + \partial_T \partial_\eta^2 \phi_2^{(3)} - \phi_{2x}^{(3)} + F\phi_{1T}^{(3)} - F\phi_{2\eta}^{(3)}(Ae^{ikx} + *)_x$$

$$+ \phi_{2x}^{(3)}\phi_{2\eta\eta\eta}^{(0)} - \phi_{2\eta}^{(3)}\phi_{2\eta\eta x}^{(0)} + \phi_{2x}^{(0)}\phi_{2\eta\eta\eta}^{(3)} - \phi_{2\eta}^{(0)}\phi_{2\eta\eta x}^{(3)} + F\phi_{2x}^{(0)}H_1^{(3)}$$

$$- F\phi_{2\eta}^{(0)}(H_{1x}^{(3)}\eta + H_{0x}^{(3)}) + \phi_{2x}^{(1)}\phi_{2\eta\eta\eta}^{(2)} - \phi_{2\eta}^{(1)}\phi_{2\eta\eta x}^{(2)} + ik\frac{\pi^2}{2}\eta^2 F\phi_{2\eta}^{(1)}(Ae^{ikx} - *)$$

$$- \pi^2 \eta F\phi_{2x}^{(1)}(Ae^{ikx} + *) + \phi_{2x}^{(2)}\phi_{2\eta\eta\eta}^{(1)} - \phi_{2\eta}^{(2)}\phi_{2\eta\eta x}^{(1)} = 0$$

We will later see that $H_1^{(3)} = 0$ so we will assume this here. Also

$$H_0^{(3)}(x,T) = \sum_{n=1}^{\infty}[H_{(2n+1),0}^{(3)} e^{i(2n+1)kx} + *] \quad ,$$

Project onto $e^{i0.kx}$, e^{ikx}, $e^{i2\tilde{n}kx}$, $e^{i(2\tilde{n}+1)kx}$

$\underline{e^{i0.kx}}$: $\partial_T \partial_\eta^2 \Phi_2^{(3)} - F\Phi_{1T}^{(3)} + iFk(A^* Y_{1\eta}^{(3)} - AY_{1\eta}^{(3)*})$

$$+ ik\sum_{n=1}^{\infty} n(Y_n^{(3)}Y_{n\eta\eta\eta}^{(0)*} - Y_{n\eta\eta}^{(0)}Y_{n\eta}^{(3)*} + Y_n^{(0)}Y_{n\eta\eta\eta}^{(3)*} - Y_{n\eta\eta}^{(3)}Y_{n\eta}^{(0)*} - FH_{n,0}^{(1)}Y_{n\eta}^{(0)*}$$

$$+ Y_n^{(2)}Y_{n\eta\eta\eta}^{(1)*} - Y_{n\eta\eta}^{(1)}Y_{n\eta}^{(2)*} + Y_n^{(1)}Y_{n\eta\eta\eta}^{(2)*} - Y_{n\eta\eta}^{(2)}Y_{n\eta}^{(1)*} - *)$$

$$- ikF\pi^2(\tfrac{1}{2}\eta^2 A^* Y_{1\eta}^{(1)} + \eta AY_1^{(1)} - *)$$

e^{ikx}:

$$2\pi^2 h_{2\eta}{}^2 Y_1^{(3)} - \frac{i}{k}\partial_T \partial_\eta^2 Y_1^{(3)} - Y_1^{(3)} + FA^* Y_{2\eta}^{(3)} - FA\,\Phi_{2\eta}^{(3)}$$

$$+ \sum_{n=1}^{\infty} [(n+1)Y_{n+1}^{(3)} Y_{n\eta\eta\eta}^{(0)*} - nY_n^{(3)*} Y_{(n+1)\eta\eta\eta}^{(0)}] - [(n+1)Y_{(n+1)}^{(0)} Y_{n\eta}^{(3)*}$$

$$- nY_{n\eta\eta}^{(0)*} Y_{(n+1)\eta}^{(3)}] + [(n+1)Y_{n+1}^{(0)} Y_{n\eta\eta\eta}^{(3)*} - nY_n^{(0)*} Y_{(n+1)\eta\eta\eta}^{(3)}]$$

$$- [(n+1)Y_{(n+1)\eta\eta}^{(3)} Y_{n\eta}^{(0)*} - nY_{n\eta\eta}^{(3)*} Y_{(n+1)\eta}^{(0)}] + [(n+1)Y_{n+1}^{(2)} Y_{n\eta\eta\eta}^{(1)*}$$

$$- nY_n^{(2)*} Y_{(n+1)\eta\eta\eta}^{(1)}] - [(n+1)Y_{(n+1)\eta\eta}^{(1)} Y_{n\eta}^{(2)*} - nY_{n\eta\eta}^{(1)*} Y_{(n+1)\eta}^{(2)}]$$

$$+ [(n+1)Y_{n+1}^{(1)} Y_{n\eta\eta\eta}^{(2)*} - nY_n^{(1)*} Y_{(n+1)\eta\eta\eta}^{(2)}] - [(n+1)Y_{(n+1)\eta\eta}^{(2)} Y_{n\eta}^{(1)*}$$

$$-nY_{n\eta\eta}^{(2)*} Y_{(n+1)\eta}^{(1)}] - F[(n+1)H_{(n+1),0}^{(3)} Y_{n\eta}^{(0)*} - nH_{n,0}^{(3)*} Y_{(n+1)\eta}^{(0)}]$$

$$- \frac{1}{2}\pi^2 \eta^2 F(A^* Y_{2\eta}^{(1)} - A\,\Phi_{2\eta}^{(1)}) - 2\pi^2 \eta F A^* Y_2^{(1)} + Y_1^{(3)} \Phi_{2\eta\eta\eta}^{(0)} + Y_1^{(0)} \Phi_{2\eta\eta\eta}^{(3)}$$

$$- Y_{1\eta\eta}^{(0)} \Phi_{2\eta}^{(3)} - Y_{1\eta\eta}^{(3)} \Phi_{2\eta}^{(0)} - FH_{1,0}^{(3)} \Phi_{2\eta}^{(0)} + Y_1^{(2)} \Phi_{2\eta\eta\eta}^{(1)} + Y_1^{(1)} \Phi_{2\eta\eta\eta}^{(2)}$$

$$- Y_{1\eta\eta}^{(1)} \Phi_{2\eta}^{(2)} - Y_{1\eta\eta}^{(2)} \Phi_{2\eta}^{(1)} = 0$$

$e^{i2\tilde{n}kx}$: $(p = 2\tilde{n})$

$$2p\pi^2 h_{2\eta}{}^2 Y_p^{(3)} - \frac{i}{k}\partial_T \partial_\eta^2 Y_p - pY_p^{(3)} - F(AY_{(p-1)\eta}^{(3)} - A^* Y_{(p+1)\eta}^{(3)})$$

$$+ \frac{1}{2}\pi^2 \eta^2 F(AY_{(p-1)\eta}^{(1)} - A^* Y_{(p+1)\eta}^{(1)}) - \pi^2 \eta F[(p-1)AY_{(p-1)}^{(1)} + (p+1)A^* Y_{(p+1)}^{(1)}]$$

$$+\sum_{n+1}^{\infty}\Big\{[(n+p)Y^{(3)}_{n+p}Y^{(0)*}_{n\eta\eta\eta}-nY^{(3)*}_{n}Y^{(0)}_{(p+n)\eta\eta\eta}]-[(n+p)Y^{(0)}_{(n+p)\eta\eta}Y^{(3)*}_{n\eta}$$

$$-nY^{(0)*}_{n\eta\eta}Y^{(3)}_{(p+n)\eta}]+[(n+p)Y^{(0)}_{n+p}Y^{(3)*}_{n\eta\eta\eta}-nY^{(0)*}_{n}Y^{(3)}_{(p+n)\eta\eta\eta}]$$

$$-[(n+p)Y^{(3)}_{(n+p)\eta\eta}Y^{(0)*}_{n\eta}-nY^{(3)*}_{n\eta\eta}Y^{(0)}_{(p+n)\eta}]+[(n+p)Y^{(2)}_{n+p}Y^{(1)*}_{n\eta\eta\eta}$$

$$-nY^{(2)*}_{n}Y^{(1)}_{(p+n)\eta\eta\eta}]-[(n+p)Y^{(1)}_{(n+p)\eta\eta}Y^{(2)*}_{n\eta}-nY^{(1)*}_{n\eta\eta}Y^{(2)}_{(p+n)\eta}]$$

$$+[(n+p)Y^{(1)}_{n+p}Y^{(2)*}_{n\eta\eta\eta}-nY^{(1)*}_{n}Y^{(2)}_{(p+n)\eta\eta\eta}]-[(n+p)Y^{(2)}_{(n+p)\eta\eta}Y^{(1)*}_{n\eta}$$

$$-nY^{(2)*}_{n\eta\eta}Y^{(1)}_{(p+n)\eta}]-F[(n+p)H^{(3)}_{(n+p),0}Y^{(0)*}_{n\eta}-nH^{(3)*}_{n,0}Y^{(0)}_{(p+n)\eta}]\Big\}$$

$$+\sum_{n=1}^{p-1}n\Big\{Y^{(3)}_{n}Y^{(0)}_{(p-n)\eta\eta\eta}-Y^{(0)}_{n\eta\eta}Y^{(3)}_{(p-n)\eta}+Y^{(0)}_{n}Y^{(3)}_{(p-n)\eta\eta\eta}-Y^{(3)}_{n\eta\eta}Y^{(0)}_{(p-n)\eta}$$

$$-FH^{(3)}_{n,0}Y^{(0)}_{(p-n)\eta}+Y^{(2)}_{n}Y^{(1)}_{(p-n)\eta\eta\eta}-Y^{(1)}_{n\eta\eta}Y^{(2)}_{(p-n)\eta}+Y^{(1)}_{n}Y^{(2)}_{(p-n)\eta\eta\eta}$$

$$-Y^{(2)}_{n\eta\eta}Y^{(1)}_{(p-n)\eta}\Big\}$$

$$+p\Big\{Y^{(3)}_{p}\bar{\Phi}^{(0)}_{2\eta\eta\eta}-Y^{(0)}_{p\eta\eta}\bar{\Phi}^{(3)}_{2\eta}+Y^{(0)}_{p}\bar{\Phi}^{(3)}_{2\eta\eta\eta}-Y^{(3)}_{p\eta\eta}\bar{\Phi}^{(0)}_{2\eta}+Y^{(2)}_{p}\bar{\Phi}^{(1)}_{2\eta\eta\eta}$$

$$-Y^{(1)}_{p\eta\eta}\bar{\Phi}^{(2)}_{2\eta}+Y^{(1)}_{p}\bar{\Phi}^{(2)}_{2\eta\eta\eta}-Y^{(2)}_{p\eta\eta}\bar{\Phi}^{(1)}_{2\eta}\Big\}=0$$

$e^{i(2\tilde{n}+1)kx}$: $(p=2\tilde{n}+1)$

$$2p_{\pi}{}^{2}h_{2\eta}{}^{2}Y^{(3)}_{p}-\frac{i}{k}\partial_{T}\partial^{2}_{\eta}Y^{(3)}_{p}-pY^{(3)}_{p}-\frac{iF}{k}\partial_{T}H^{(3)}_{p,0}-F(AY^{(3)}_{(p-1)\eta}-A^{*}Y_{(p+1)\eta})$$

$$+\sum_{n=1}^{\infty}\Big\{[(n+p)Y^{(3)}_{(n+p)}Y^{(0)*}_{n\eta\eta\eta}-nY^{(3)*}_{n}Y^{(0)}_{(p+n)\eta\eta\eta}]-[(n+p)Y^{(0)}_{(n+p)\eta\eta}Y^{(3)*}_{n\eta}$$

$$- n\gamma^{(0)*}_{n\eta\eta}\gamma^{(3)}_{(p+n)\eta}] + [(n+p)\gamma^{(0)}_{n+p}\gamma^{(3)*}_{n\eta\eta\eta} - n\gamma^{(0)*}_{n}\gamma^{(3)}_{(p+n)\eta\eta\eta}]$$

$$- [(n+p)\gamma^{(3)}_{(n+p)\eta\eta}\gamma^{(0)*}_{n\eta} - n\gamma^{(3)*}_{n\eta\eta}\gamma^{(0)}_{(p+n)\eta}] - F[(n+p)H^{(3)}_{(n+p),0}\gamma^{(0)*}_{n\eta}$$

$$-nH^{(3)*}_{n,0}\gamma^{(0)}_{(p+n)\eta}] + [(n+p)\gamma^{(2)}_{n+p}\gamma^{(1)*}_{n\eta\eta\eta} - n\gamma^{(2)*}_{n}\gamma^{(1)}_{(p+n)\eta\eta\eta}] + [n\gamma^{(1)*}_{n\eta\eta}\gamma^{(2)}_{(p+n)\eta}$$

$$- (n+p)\gamma^{(1)}_{(n+p)\eta\eta}\gamma^{(2)*}_{n\eta}] + [(n+p)\gamma^{(1)}_{n+p}\gamma^{(2)*}_{n\eta\eta\eta} - n\gamma^{(1)*}_{n}\gamma^{(2)}_{(p+n)\eta\eta\eta}]$$

$$- [(n+p)\gamma^{(2)}_{(n+p)\eta\eta}\gamma^{(1)*}_{n\eta} - n\gamma^{(2)*}_{n\eta\eta}\gamma^{(1)}_{(p+n)\eta}] + \sum_{n=1}^{p-1} n\left\{\gamma^{(3)}_{n}\gamma^{(0)}_{(p-n)\eta\eta\eta}\right.$$

$$- \gamma^{(0)}_{n\eta\eta}\gamma^{(3)}_{(p-n)\eta} + \gamma^{(0)}_{n}\gamma^{(3)}_{(p-n)\eta\eta\eta} - \gamma^{(3)}_{n\eta\eta}\gamma^{(0)}_{(p-n)\eta} - FH^{(3)}_{n,0}\gamma^{(0)}_{(p-n)\eta}$$

$$+ \gamma^{(2)}_{n}\gamma^{(1)}_{(p-n)\eta\eta\eta} - \gamma^{(1)}_{n\eta\eta}\gamma^{(2)}_{(p-n)\eta} + \gamma^{(1)}_{n}\gamma^{(2)}_{(p-n)\eta\eta\eta} - \gamma^{(2)}_{n\eta\eta}\gamma^{(1)}_{(p-n)\eta}$$

$$+ p\left\{\gamma^{(3)}_{p}\bar{\Phi}^{(0)}_{2\eta\eta\eta} - \gamma^{(0)}_{p\eta\eta}\bar{\Phi}^{(3)}_{2\eta} + \gamma^{(0)}_{p}\bar{\Phi}^{(3)}_{2\eta\eta\eta} - \gamma^{(3)}_{p\eta\eta}\bar{\Phi}^{(0)}_{2\eta} - FH^{(3)}_{p,0}\bar{\Phi}^{(0)}_{2\eta}\right.$$

$$\left.\left. + \gamma^{(2)}_{p}\bar{\Phi}^{(1)}_{2\eta\eta\eta} - \gamma^{(1)}_{p\eta\eta}\bar{\Phi}^{(2)}_{2\eta} + \gamma^{(1)}_{p}\bar{\Phi}^{(2)}_{2\eta\eta\eta} - \gamma^{(2)}_{p\eta\eta}\bar{\Phi}^{(1)}_{2\eta}\right\}\right] = 0$$

Thus, for p odd, $p \neq 1$, $\gamma^{(3)}_{p} \sim \frac{iF}{2pk\pi^2 h_2}\eta^{-2}\partial_T H^{(3)}_{p,0}$, $\eta \to \infty$

For p even,

$$\gamma^{(3)}_{p} \sim \frac{iF^2}{2pk\pi^4 h_2^2}\eta^{-5}\left(\frac{1}{p+1}A^*\partial_T H^{(3)}_{(p+1),0} - \frac{1}{p-1}A\,\partial_T H^{(3)}_{(p-1),0}\right)$$

Lower, $O(\Delta^2)$

$$2\pi^2 h_2\eta^2\phi^{(4)}_{2x} + \partial_T\partial^2_\eta\,\phi^{(4)}_{2} - \phi^{(4)}_{2x} + F\phi^{(4)}_{1T} + F\left(\frac{1}{24}\pi^4\eta^4\right)(A_T e^{ikx} + *)$$

$$- \frac{2}{3} h_2 \pi^4 \eta^4 \phi_{2x}^{(2)} + \frac{4}{45} h_2 \pi^6 \eta^6 \phi_{2x}^{(0)} + J(\phi_2^{(4)}, \partial_\eta^2 \phi_2^{(0)} + F\phi_1^{(0)})$$

$$+ J(\phi_2^{(4)}, \partial_\eta^2 \Phi_2^{(0)}) + J(\phi_2^{(2)}, \partial_\eta^2 \phi_2^{(2)} - \frac{1}{2} F\eta^2 \pi^2 \phi_1^{(0)}) + J(\phi_2^{(2)}, \partial_\eta^2 \Phi_2^{(2)})$$

$$+ J(\phi_2^{(3)}, \partial_\eta^2 \phi_2^{(1)}) + J(\phi_2^{(1)}, \partial_\eta^2 \phi_2^{(3)} + F\phi_1^{(3)}) + J(\phi_2^{(3)}, \partial_\eta^2 \Phi_2^{(1)})$$

$$+ J(\phi_2^{(1)}, \partial_\eta^2 \Phi_2^{(3)}) + J(\phi_2^{(0)}, \partial_\eta^2 \phi_2^{(4)} + \frac{1}{24} \pi^4 \eta^4 F\phi_1^{(0)} + F\phi_1^{(4)})$$

$$+ J(\phi_2^{(0)}, \partial_\eta^2 \Phi_2^{(4)} + F\Phi_1^{(4)}) + J(\Phi_2^{(4)}, \partial_\eta^2 \phi_2^{(0)} + F\phi_1^{(0)})$$

$$+ J(\Phi_2^{(2)}, \partial_\eta^2 \phi_2^{(2)} - \frac{1}{2} F\eta^2 \pi^2 \phi_1^{(0)}) + J(\Phi_2^{(1)}, \partial_\eta^2 \phi_2^{(3)} + F\phi_1^{(3)})$$

$$+ J(\Phi_2^{(3)}, \partial_\eta^2 \phi_2^{(1)}) + J(\Phi_2^{(0)}, \partial_\eta^2 \phi_2^{(4)} + \frac{1}{24} \pi^4 \eta^4 F\phi_1^{(0)} + F\phi_1^{(4)})$$

$$+ (\partial_x^2 - F)\phi_{2T}^{(2)} + \partial_T \partial_\eta^2 \Phi_2^{(4)} - F\Phi_{2T}^{(2)} + F\Phi_{1T}^{(4)} + J(\phi_2^{(2)} + \Phi_2^{(2)}, \partial_x^2 \phi_2^{(0)})$$

$$+ J(\phi_2^{(0)} + \Phi_2^{(0)}, \partial_x^2 \phi_2^{(2)}) + J(\phi_2^{(1)} + \Phi_2^{(1)}, \partial_x^2 \phi_2^{(1)}) = 0$$

To obtain the leading behavior of $Y_n^{(4)}$ as $\eta \to \infty$, we note the dominant balance

$$2\pi^2 h_2 \eta^2 \phi_{2x}^{(4)} \simeq - \frac{1}{24} F\pi^4 \eta^4 (A_T e^{ikx} + *) + \frac{2}{3} h_2 \pi^4 \eta^4 \phi_{2x}^{(2)} - \frac{4}{45} h_2 \pi^6 \eta^6 \phi_{2x}^{(0)}$$

$$- F\phi_{1T}^{(4)}$$

Thus $Y_1^{(4)} \sim - \frac{i\pi^2 F}{h_2 k} \frac{7}{240} A_T \eta^2$

$$Y_n^{(4)} \sim \frac{1}{3} \pi^2 \eta^2 Y_n^{(2)} - \frac{2}{45} \pi^4 \eta^4 Y_n^{(0)} + \frac{iF}{2\pi^2 h_2 nk} Z_{nT}^{(4)} \eta^{-2}, \qquad n > 1$$

The mean flow component of the above potential vorticity balance is

$$\partial_T \partial_\eta^2 \bar{\Phi}_2^{(4)} + J_{(0)}(\phi_2^{(4)}, \partial_\eta^2 \phi_2^{(0)} + F\phi_1^{(0)}) + J_{(0)}(\phi_2^{(3)}, \partial_\eta^2 \phi_2^{(1)})$$

$$+ J_{(0)}(\phi_2^{(2)}, \partial_\eta^2 \phi_2^{(2)} - \tfrac{1}{2} F\eta^2\pi^2\phi_1^{(0)}) + J_{(0)}(\phi_2^{(1)}, \partial_\eta^2 \phi_2^{(3)} + F\phi_1^{(3)})$$

$$+ J_{(0)}(\phi_2^{(0)}, \partial_\eta^2\phi_2^{(4)} + \tfrac{1}{24}\pi^4\eta^4 F\phi_1^{(0)} + F\phi_1^{(4)}) + F(\bar{\Phi}_{1T}^{(4)} - \bar{\Phi}_{2T}^{(2)})$$

$$+ J_{(0)}(\phi_2^{(2)}, \partial_x^2 \phi_2^{(0)}) + J_{(0)}(\phi_2^{(0)}, \partial_x^2 \phi_2^{(2)}) + J_{(0)}(\phi_2^{(1)}, \partial_x^2 \phi_2^{(1)}) = 0$$

whence

$$\bar{\Phi}_{2T}^{(4)} = ikF(A\int^\eta Y_1^{(4)*} - *) + ikF\tfrac{\pi^2}{2}[A^*\int^\eta \eta^2 Y_1^{(2)} - *]$$

$$+ ikF\tfrac{\pi^4}{24}[A\int^\eta \eta^4 Y_1^{(0)*} - *] + F\int^\eta\int^{\eta'}(\bar{\Phi}_{1T}^{(4)} - \bar{\Phi}_{2T}^{(2)})$$

$$+ O(\eta \ln^2\eta)$$

Before proceeding further with this, we need to calculate $\bar{\phi}_1^{(3)}$ and $\bar{\phi}_1^{(4)}$. We return to the upper layer balance for the inner region and skip consideration of $O(\Delta^{7/2} \ln 1/\Delta)$, $O[\Delta^4(\ln 1/\Delta)^2]$ and $O[\Delta^4(\ln 1/\Delta)]$.

$O(\Delta^{7/2})$

$$U\partial_\eta^2 \phi_{1x}^{(7)} = -(U\partial_x^2 + \beta_m)\phi_{1x}^{(5)} + \phi_{1x}^{(3)} - FU\phi_{2x}^{(3)}$$

$$- J(\phi_1^{(0)}, \phi_{1\eta\eta}^{(5)} + \bar{\Phi}_{1\eta\eta}^{(5)} + (\partial_x^2 - F)\phi_1^{(3)} - F\bar{\phi}_1^{(3)} + F\phi_2^{(1)} + F\bar{\phi}_2^{(1)})$$

$$+ J(\tfrac{1}{2}\eta^2\pi^2[Ae^{ikx} + *], \phi_{1\eta\eta}^{(3)} + \bar{\phi}_{1\eta\eta}^{(3)})$$

$$- J(\phi_1^{(3)}, (\partial_x^2 - \pi^2 - F)\phi_1^{(0)}) - J(\bar{\phi}_1^{(3)}, (\partial_x^2 - \pi^2 - F)\phi_1^{(0)})$$

$$- \partial_T \phi^{(3)}_{1\eta\eta} - \partial_T \Phi^{(3)}_{1\eta\eta}$$

Taking the zonally independent component

$$\partial_T \Phi^{(3)}_{1\eta\eta} = - J_{(0)}(\phi^{(0)}_1, \phi^{(5)}_{1\eta\eta} + (\partial^2_x - F)\phi^{(3)}_1 + F\phi^{(1)}_2)$$

$$+ J_{(0)}(\tfrac{1}{2}\eta^2\pi^2[\, Ae^{ikx} + * \,], \phi^{(3)}_{1\eta\eta}) - J_{(0)}(\phi^{(3)}_1, (\partial^2_x - \pi^2 - F)\phi^{(0)}_1) = 0$$

$$\Longrightarrow \quad \Phi^{(3)}_1 = N^{(3)}{}_\eta$$

$\underline{O(\Delta^4)}$

$$U\partial^2_\eta \phi^{(8)}_{1x} = - (U\partial^2_x + \beta_m)\phi^{(6)}_{1x} + (\phi^{(4)}_{1x} - \tfrac{1}{24}\pi^2\eta^4[Ae^{ikx} + * \,]_x) - FU\phi^{(4)}_{2x}$$

$$- J(\phi^{(0)}_1, \phi^{(6)}_{1\eta\eta} + \Phi^{(6)}_{1\eta\eta} + (\partial^2_x - F)\phi^{(4)}_1 - F\Phi^{(4)}_1 + F\phi^{(2)}_2 + F\Phi^{(2)}_2)$$

$$+ J(\tfrac{1}{2}\eta^2\pi^2[\, Ae^{ikx} + * \,], \phi^{(4)}_{1\eta\eta} + \Phi^{(4)}_{1\eta\eta} + F\phi^{(0)}_2 + F\Phi^{(0)}_2)$$

$$- J(\phi^{(4)}_1, (\partial^2_x - \pi^2 - F)\phi^{(0)}_1) - J(\Phi^{(4)}_1, (\partial^2_x - \pi^2 - F)\phi^{(0)}_1)$$

$$- \partial_T [\phi^{(4)}_{1\eta\eta} + F\phi^{(0)}_2] - \partial_T [\Phi^{(4)}_{1\eta\eta} + F\Phi^{(0)}_2]$$

Taking the zonally independent component

$$\partial_T [\Phi^{(4)}_{1\eta\eta} + F\Phi^{(0)}_2] = - J_{(0)}(\phi^{(0)}_1, \phi^{(6)}_{1\eta\eta} + (\partial^2_x + \tfrac{\beta_m}{U})\phi^{(4)}_1 + F\phi^{(2)}_2)$$

$$+ J_{(0)}(\tfrac{1}{2}\eta^2\pi^2[\, Ae^{ikx} + * \,], \phi^{(4)}_{1\eta\eta} + F\phi^{(0)}_2) = 0$$

$$\Longrightarrow \qquad \Phi^{(4)}_{1\eta\eta T} = - F\Phi^{(0)}_{2T}$$

Hence

$$\Phi_{1T}^{(4)} = - ikF^2\Big(A \int_0^\eta \int_0^{\eta'} \int_0^{\eta''} Y_1^{(0)*} - * \Big) - ikF \sum_{n=1}^{\infty} n \Big(\int_0^\eta \int_0^{\eta'} Y_{n\eta}^{(0)} Y_n^{(0)*} - * \Big)$$

$$- \frac{F}{6} M_T^{(0)} \eta^3 + N_T^{(4)} \eta$$

$N_T^{(4)}(T)$ is a free constant.

As $\eta \to \infty$

$$\Phi_1^{(4)} \sim - \frac{F}{6} M^{(0)} \eta^3 + \frac{F^3}{2\pi^2 h_2} \left(|A|^2 - |A(0)|^2 \right) \eta \ln \eta + \mu\eta + \ldots$$

where μ is a disposable constant. Thus,

$$\Phi_{1T}^{(4)} - \Phi_{2T}^{(2)} \sim - \frac{F}{6} M_T^{(0)} \eta^3 + \frac{F^3}{\pi^2 h_2} \left(|A|^2 \right)_T \eta \ln \eta + \left(\mu - \tilde{M}^{(2)} \right)_T \eta$$

We can now substitute for $\Phi_{1T}^{(4)} - \Phi_{2T}^{(2)}$ in our expression for $\Phi_{2T}^{(4)}$ to obtain

$$\Phi_2^{(4)} \sim \frac{F^4}{6\pi^2 h_2} \left(|A|^2 - |A(0)|^2 \right) \eta^3 \ln \eta + F \left(\mu - \tilde{M}^{(2)} \right) \frac{1}{6} \eta^3$$

$$+ \left[\frac{F^2 \pi^2}{h_2} \left(\frac{1}{48} - \frac{7}{720} \right) - \frac{11F^4}{36\pi^2 h_2} \right] \left(|A|^2 - |A(0)|^2 \right) \eta^3$$

To improve our estimate of $Y_1^{(4)}$ as $\eta \to \infty$ we use the fact that the most prominent terms in the potential vorticity balance give

$$2\pi^2 h_2 \eta^2 Y_1^{(4)} - Y_1^{(4)} - i \frac{F\pi^4}{24k} \eta^4 A_T - \frac{2}{3} h_2 \pi^4 \eta^4 Y_1^{(2)} + \frac{4}{45} h_2 \pi^6 \eta^6 Y_1^{(0)}$$

$$- FA \Phi_{2\eta}^{(4)} + \frac{1}{2} \pi^2 F \eta^2 A \Phi_{2\eta}^{(2)} - \frac{1}{24} F \pi^4 \eta^4 A \Phi_{2\eta}^{(0)} \simeq 0$$

From this, as $\eta \to \infty$

$$Y_1^{(4)} \sim - i\frac{\pi^2 F}{h_2 k}\frac{7}{240} A_T \eta^2 + \frac{F}{\pi^2 h_2^2} A \left(|A|^2 - |A(0)|^2 \right)\left(\frac{1}{24} + \frac{F}{4\pi^2}\right) \ln \eta$$

$$+ \left[- \frac{17}{1440}\frac{iF}{k h_2^2} A_T - \frac{\mu F^2}{4 h_2 \pi^2} A - \frac{F\tilde{M}^{(2)}}{4 h_2} A \left(1 + \frac{F}{\pi^2}\right) \right.$$

$$\left. + \frac{F^3}{h_2^2} A \left(|A|^2 - |A(0)|^2 \right)\left(- \frac{1}{32} + \frac{1}{24}\frac{F}{\pi^2} + \frac{5}{24}\frac{F^2}{\pi^4}\right) \right]$$

Outer Solution

$$\phi_{1\ out}^{(0)} = A \sin \pi \quad e^{ikx} + *$$

$$\phi_{1\ out}^{(2)} = 0$$

$$\phi_{2\ out}^{(0)} = \frac{i F A_T}{2 k h_2 \cos^2 \pi y} \sin \pi y\, e^{ikx} + *$$

Upper, $O(\Delta^{3/2})$

Set $$\phi_1^{(p)} = \sum_{n=1}^{\infty} \left(W_n^{(p)} e^{inkx} + * \right) , \qquad p \geq 3$$

$$U \left(\partial_y^2 + \pi^2\right) W_1^{(3)} = U k_2^2 \; A \; \sin \pi y$$

$$\Longrightarrow \quad W_1^{(3)} = - \frac{k_2^2}{2\pi} (y-1) \cos \pi y \; A$$

Define $$\lambda_n^2 = k^2 n^2 - \beta_m / U$$

$$U(\partial_y^2 - \lambda_n^2)\, W_n^{(3)} = 0$$

$$\Longrightarrow \quad W_n^{(3)} = B_n^{(3)} \operatorname{sh} \lambda_n (y-1)$$

$O(\Delta^2)$

$$U(\nabla^2 + \beta_m/U)\, \phi_{1x}^{(4)} = - FU\, \phi_{2x}^{(0)} - (\nabla^2 - F)\, \phi_{1T}^{(0)}$$

$$\therefore\ (\partial_y^2 + \pi^2)\, W_1^{(4)} = - \frac{F^2}{2kh_2} \frac{\sin \pi y}{\cos^2 \pi y}\, iA_T - \frac{1}{Uk} (k^2 + \pi^2 + F)\, iA_T \sin \pi y$$

$$\Longrightarrow \quad W_1^{(4)} = iA_T \left[\frac{1}{2\pi} (y-1) \cos \pi y \left[\frac{\beta_m + FU}{kU^2} - \frac{F^2}{kh_2} \right] + \frac{F}{2kh_2 \pi^2} \sin \pi y \ln (|\cos \pi y|) \right]$$

$$(\partial_y^2 - \lambda_n^2)\ W_n^{(4)} = 0$$

$$\Longrightarrow \quad W_n^{(4)} = B_n^{(4)} \operatorname{sh} \lambda_n (y-1)$$

Lower, $O(\Delta)$

$$(\beta_m - FU + h_y)\, \phi_{2x}^{(2)} = \phi_{2x}^{(0)} + F\, \phi_{1x}^{(0)}\, \Phi_{2y}^{(-1)}$$

$$\Longrightarrow \phi_2^{(2)} = \frac{F}{4kh_2^2} \frac{\sin \pi y}{\cos^4 \pi y} (iA_T\, e^{ikx} + *) + \frac{F\, \Phi_{2y}^{(-1)} \sin \pi y}{2h_2 \cos^2 \pi y} (A\, e^{ikx} + *)$$

We will determine $\Phi_{2y}^{(-1)}$ later.

$O(\Delta^{3/2})$

$$(\beta_m - FU + h_y)\, \phi_{2x}^{(3)} = - F\phi_{1T}^{(3)} - J(\phi_2^{(0)}, F\phi_1^{(0)}) - \partial_T [(\nabla^2 - F)\, \Phi_2^{(-1)} + F\, \Phi_1^{(3)}]$$

$$- J\,(\Phi_2^{(0)},\ F\,\phi_1^{(0)})$$

Set $$\phi_2^{(3)} = \sum_{n=1}^{\infty} (V_n^{(3)}\, e^{inkx} + *)$$

$$V_1^{(3)} = \frac{-Fk_2^2}{4\pi k h_2}\ \frac{(y-1)}{\cos \pi y}\ iA_T + \frac{F\Phi_{2y}^{(0)} \sin \pi y}{2h_2 \cos^2 \pi y}\ A$$

$$V_2^{(3)} = \frac{F^2\pi}{8h_2^2 k}\ \frac{\tan^3 \pi y}{\cos^2 \pi y}\ i(A^2)_T + \frac{iF}{4kh_2}\ \frac{sh\lambda_2(y-1)}{\cos^2 \pi y}\ B_{2T}^{(3)}$$

$$V_n^{(3)} = \frac{iF}{2h_2 nk}\ \frac{sh\lambda_n(y-1)}{\cos^2 \pi y}\ B_{nT}^{(3)} \qquad n \geq 3$$

and from the mean flow component of the potential vorticity balance

$$(\partial_y^2 - F)\,\Phi_2^{(-1)} + F\,\Phi_1^{(3)} = \frac{F\pi}{h_2} \sec^2 \pi y \tan \pi y\ (|A|^2 - |A(0)|^2)$$

$O[\Delta^{3/2} \ln(1/\Delta)]$

$$(\beta_m - FU + h_y)\ \theta_{2x}^{(3)} = - J\,(\textcircled{H}_2^{(0)},\ F\,\phi_1^{(0)})$$

Upper, $O(\Delta^{5/2})$

$$U\,(\nabla^2 + \beta_m/U)\ \phi_{1x}^{"(5)"} = \phi_{1x}^{(3)}$$

The inverted commas denote the inclusion of terms like $k_1^2\,\phi_1^{(n-2)}$ and $-k_2^2\,\phi_1^{(n-3)}$ in $\nabla^2\,\phi_{1x}^{"(n)"}$ for the e^{ikx} Fourier component.

$$\therefore\ U\,(\partial_y^2 + \pi^2)\ W_1^{(5)} = 0$$

We normalize the solution by choosing $W_1^{(5)} = 0$

$$U\,(\partial_y^2 - \lambda_n^2)\,W_n^{(5)} = W_n^{(3)} = B_n^{(3)}\ \mathrm{sh}\ \lambda_n\,(y-1) \qquad n \geq 2$$

$$W_n^{(5)} = \frac{B_n^{(3)}}{2\lambda_n U}\,(y-1)\ \mathrm{ch}\ \lambda_n\,(y-1) + B_n^{(5)}\ \mathrm{sh}\ \lambda_n\,(y-1)$$

$O(\Delta^3)$

$$U\,(\nabla^2 + \beta_m/U)\,\phi_{1x}^{"(6)"} = \phi_{1x}^{(4)} - J\,(\phi_1^{(0)}, \nabla^2\,\phi_1^{(3)})$$

$$- J\,(\phi_1^{(3)}, \nabla^2\,\phi_1^{(0)}) - FU\,\phi_{2x}^{(2)} - J\,(\Phi_1^{(3)}, q_1^{(0)}) - J\,(\phi_1^{(0)}, Q_1^{(3)})$$

Projecting onto e^{ikx} yields

$$(\partial_y^2 + \pi^2)\,W_1^{(6)} = k_2^2\,W_1^{(3)} - F\,V_1^{(2)} - \frac{1}{U}\,[\Phi_{1y}^{(3)}\,(k^2 + \pi^2 + F) + Q_{1y}^{(3)}]\,A$$

while the projection onto e^{inkx} gives

$$(\partial_y^2 - \lambda_n^2)\,W_n^{(6)} = \frac{1}{U}\,W_n^{(6)} \qquad n \geq 2$$

i.e., $$W_n^{(6)} = \frac{B_n^{(4)}}{2\lambda_n U}\,(y-1)\ \mathrm{ch}\ \lambda_n\,(y-1) + B_n^{(6)}\ \mathrm{sh}\ \lambda_n\,(y-1)$$

In pursuit of the mean flow we carry on to yet higher orders.

$O(\Delta^{7/2})$

$$U\,(\nabla^2 + \beta_m/U)\,\phi_{1x}^{"(7)"} = \phi_{1x}^{(5)} - J\,(\phi_1^{(0)}, \nabla^2\,\phi_1^{(4)}) - J\,(\phi_1^{(4)}, \nabla^2\,\phi_1^{(0)})$$

$$- \partial_T (\nabla^2 - F) \phi_1^{(3)} - FU \phi_{2x}^{(3)} - J (\Phi_1^{(4)}, q_1^{(0)}) - J (\phi_1^{(0)}, Q_1^{(4)})$$

$$- J (\phi_1^{(0)}, F \phi_2^{(0)}) - \partial_T [(\partial_y^2 - F) \Phi_1^{(3)} + F \Phi_2^{(-1)}]$$

The zonally independent part of this yields

$$(\partial_y^2 - F) \Phi_1^{(3)} + F \Phi_2^{(-1)} = - \frac{\pi^2 + k^2 + F}{U} \pi \sin 2\pi y \, (|A|^2 - |A(0)|^2)$$

while the e^{ikx} component gives

$$(\partial_y^2 + \pi^2) W_1^{(7)} = k_2^2 W_1^{(4)} + \frac{i}{Uk} (\partial_y^2 - k^2 - F) W_{1T}^{(3)} - F V_1^{(3)}$$

$$- \frac{1}{U} [\Phi_{1y}^{(4)} (k^2 + \pi^2 + F) + Q_{1y}^{(4)}] A$$

and the e^{inkx} furnishes the relation

$$(\partial_y^2 - \lambda_n^2) W_n^{(7)} = \frac{1}{U} W_n^{(5)} + \frac{i}{nkU} (\partial_y^2 - n^2 k^2 - F) W_{nT}^{(3)} - F V_n^{(3)}$$

$O[\Delta^{7/2} \ln (1/\Delta)]$

$$U (\nabla^2 + \beta_m/U) \theta_{1x}^{(7)} = - fU \theta_{2x}^{(3)} - J (\textcircled{H}_1^{(4)}, q_1^{(0)}) - J (\phi_1^{(0)}, \ddot{Q}_1^{(4)})$$

where $$\ddot{Q}_1^{(4)} = (\partial_y^2 - F) \textcircled{H}_1^{(4)} + F \textcircled{H}_2^{(0)}$$

Lower, $O(\Delta^2)$

$$(\beta_m - FU + h_y) \phi_{2x}^{(4)} = - F \phi_{1T}^{(4)} + \phi_{2x}^{(2)} - J (\Phi_2^{(1)}, F \phi_1^{(0)})$$

$$- \partial_T [(\partial_y^2 - F)\Phi_2^{(0)} + F\Phi_1^{(4)}] - \partial_T (\nabla^2 - F)\phi_2^{(0)}$$

Projecting onto $e^{io.kx}$, e^{ikx} and e^{inkx}; $n \geq 2$ in turn yields

$$(\partial_y^2 - F)\Phi_2^{(0)} + F\Phi_1^{(4)} = 0$$

$$V_1^{(4)} = \frac{-F}{2h_2 k} A_{TT}\left[\frac{1}{2\pi}\frac{(y-1)}{\cos\pi y}\left(\frac{\beta_m + FU}{kU^2} - \frac{F^2}{kh_2}\right) + \frac{F^2}{2kh_2\pi^2}\frac{\sin\pi y}{\cos^2\pi y}\ln(|\cos\pi y|)\right]$$

$$+ \frac{F}{8kh_2^3}\frac{\sin\pi y}{\cos^6\pi y} iA_T + \frac{F\Phi_{2y}(-1)}{4h_2^2}\frac{\sin\pi y}{\cos^4\pi y} A$$

$$+ \frac{F}{2h_2}\Phi_{2y}^{(1)}\frac{\sin\pi y}{\cos^2\pi y} A - \frac{F}{4k^2h_2^2} A_{TT}\frac{1}{\cos^2\pi y}(\partial_y^2 - k^2 - F)\left(\frac{\sin\pi y}{\cos^2\pi y}\right)$$

$$V_n^{(4)} = \frac{iF}{2nkh_2} B_{nT}^{(4)}\frac{-h\lambda_n(y-1)}{\cos^2\pi y}$$

$O[\Delta^4 \ln(1/\Delta)]$

$$(\beta_m - FU + h_y)\theta_{2x}^{(4)} = -J(\Theta_2^{(1)}, F\phi_1^{(0)}) - \partial_T[(\partial_y^2 - F)\Theta_2^{(0)} + F\Theta_1^{(4)}]$$

Projecting onto $e^{io.kx}$ gives

$$(\partial_y^2 - F)\Theta_2^{(0)} + F\Theta_1^{(4)} = 0$$

$O(\Delta^{5/2})$

$$2h_2\cos^2\pi y\ \phi_{2x}^{(5)} = -F\phi_{1T}^{(5)} + \phi_{2x}^{(3)} + F\phi_{1x}^{(0)}\Phi_{2y}^{(2)} + F\phi_{1x}^{(3)}\Phi_{2y}^{(-1)} - J(\phi_2^{(2)}, F\phi_1^{(0)})$$

$$-\partial_T[(\partial_y^2 - F)\Phi_2^{(1)} + F\Phi_1^{(5)}]$$

Projecting this onto individual zonal components yields

$$(\partial_y^2 - F)\,\Phi_2^{(1)} + F\Phi_1^{(5)} = \frac{F^2\pi}{4h_2^2}\left(\frac{4\sin^3\pi y}{\cos^5\pi y} + \frac{2\sin\pi y}{\cos^3\pi y}\right)(|A|^2 - |A(0)|^2)$$

$$V_1^{(5)} = \frac{-Fk_2^2}{8\pi k h_2^2}\frac{(y-1)}{\cos^3\pi y}\,iA_T + \left[\frac{F}{2h_2}\Phi_{2y}^{(2)}\frac{\sin\pi y}{\cos^2\pi y} + \frac{F}{4h_2^2}\Phi_{2y}^{(0)}\frac{\sin\pi y}{\cos^2\pi y}\right.$$

$$\left. - \frac{k_2^2 F}{4\pi h_2}\Phi_{1y}^{(-1)}\frac{(y-1)}{\cos^3\pi y}\right] A$$

$$^{(5)}V_2 = \frac{F}{8h_2\lambda_n Uk}\,iB_{2T}^{(3)}\frac{(y-1)\mathrm{ch}\,\lambda_n(y-1)}{\cos^2\pi y} + \frac{F}{4h_2 k}\,iB_{2T}^{(5)}\frac{\mathrm{sh}\,\lambda_n(y-1)}{\cos^2\pi y}$$

$$+ \frac{F^2\pi}{16kh_2^3}\frac{\tan^3\pi y}{\cos^4\pi y}\,i(A^2)_T + \frac{F}{8h_2^2 k}\frac{\mathrm{sh}\,\lambda_n(y-1)}{\cos^4\pi y}\,iB_{2T}^{(3)}$$

$$+ \frac{F}{2h_2}\frac{\Phi_{1y}^{(-1)}\mathrm{sh}\,\lambda_n(y-1)}{\cos^2\pi y}\,B_2^{(3)}$$

$$+ \left[\frac{F^2\pi}{8h_2^3}\frac{2\sin^3\pi y}{\cos^7\pi y}\,(A^2)_T - \frac{F^2\pi k}{2h_2^2}\Phi_{2y}^{(-1)}\frac{\tan^3\pi y}{\cos^2\pi y}\,iA^2\right]$$

$n \geq 3$:

$$V_n^{(5)} = \frac{F}{4nk\,\lambda_n\,Uk}\,iB_{nT}^{(3)}\frac{(y-1)\mathrm{ch}\,\lambda_n(y-1)}{\cos^2\pi y} + \frac{F}{2nh_2 k}\,iB_{nT}^{(5)}\frac{\mathrm{sh}\,\lambda_n(y-1)}{\cos^2\pi y}$$

$$+ \frac{F}{4kh_2^2 Uk}\frac{\mathrm{sh}\,\lambda_n(y-1)}{\cos^4\pi y}\,iB_{nT}^{(3)} + \frac{F}{2h_2}\Phi_{1y}^{(-1)}\frac{\mathrm{sh}\,\lambda_n(y-1)}{\cos^2\pi y}\,B_n^{(3)}$$

Upper, $O(\Delta^4)$

$$U(\nabla^2 + \frac{\beta_m}{U})\phi_{1x}^{"(8)"} = \phi_{1x}^{(6)} - J(\phi_1^{(5)}, \nabla^2\phi_1^{(0)}) - J(\phi_1^{(0)}, \nabla^2\phi_1^{(5)})$$

$$-\partial_T(\nabla^2 - F)\phi_1^{(4)} - FU\phi_{2x}^{(4)} - J(\bar{\Phi}_1^{(5)}, q_1^{(0)}) - J(\phi_1^{(0)}, Q_1^{(5)})$$

$$-\partial_T[(\partial_y^2 - F)\bar{\Phi}_1^{(4)} + F\bar{\Phi}_2^{(0)}] + k_1^2 J(\phi_1^{(0)}, [\sum_{n=2}^{\infty} W_n^{(3)} e^{inkx} + *]) - \partial_T F\phi_2^{(0)}$$

The zonally independent part of this yields

$$\partial_T[(\partial_y^2 - F)\bar{\Phi}_1^{(4)} + F\bar{\Phi}_2^{(0)}] = 0$$

We previously obtained the result,

$$\partial_T[(\partial_y^2 - F)\bar{\Phi}_2^{(0)} + F\bar{\Phi}_1^{(4)}] = 0$$

Hence $\bar{\Phi}_1^{(4)} = \beta^{(4)} \operatorname{ch}\sqrt{2F}\,(y-1) + \gamma^{(4)}$, $\bar{\Phi}_2^{(0)} = -\beta^{(4)} \operatorname{ch}\sqrt{2F}\,(y-1) + \gamma^{(4)}$

The x-dependent components of the $O(\Delta^4)$ equation yield:

e^{ikx}:

$$(\partial_y^2 + \pi^2)W_1^{(8)} = k_2^2 W_1^{(5)} - FV_1^{(4)} - \frac{i}{kU}(k^2+\pi^2+F)W_{1T}^{(4)} - \frac{1}{U}[\bar{\Phi}_{1y}^{(5)}(k^2+\pi^2+F) + Q_{1y}^{(5)}]\ A$$

e^{inkx}: (after integration)

$$W_n^{(8)} = \frac{B_n^{(4)}}{8\lambda_n^3 U^2}[\lambda_n(y-1)^2 \operatorname{sh}\lambda_n(y-1) - (y-1)\operatorname{ch}\lambda_n(y-1)]$$

$$+\left[\frac{B_n^{(6)}}{2\lambda_n U} - \frac{\pi^2 + k^2 + F}{2\lambda_n nkU}\, iB_{nT}^{(4)}\right](y-1)\operatorname{ch}\lambda_n(y-1)$$

$$- \frac{iF^2 B_{nT}^{(4)}}{2h_2 nk} (\partial_y^2 - \lambda_n^2)^{-1} \frac{\text{sh } \lambda_n(y-1)}{\cos^2 \pi y}$$

$O(\Delta^4 \ln(1/\Delta))$

$$U(\nabla^2 + \frac{\beta_m}{U})\theta_{1x}^{(8)} = - FU\theta_{2x}^{(4)} - J(\Theta_1^{(5)}, q_1^{(0)}) - J(\phi_1^{(0)}, \ddot{Q}_1^{(5)})$$

$$- \partial_T[(\partial_y^2 - F)\Theta_1^{(4)} + F\Theta_2^{(0)}]$$

The x-independent part of this is

$$\partial_T[(\partial_y^2 - F)\Theta_1^{(4)} + F\Theta_2^{(0)}] = 0$$

With $\partial_T[(\partial_y^2 - F)\Theta_2^{(0)} + F\Theta_1^{(4)}] = 0$ this implies

$$\Theta_1^{(4)} = \rho^{(4)} \text{ ch } \sqrt{2F}(y-1) + \tau^{(4)} \quad , \Theta_2^{(0)} = - \rho^{(4)} \text{ ch } \sqrt{2F}(y-1) + \tau^{(4)}$$

Upper, $O(\Delta^{9/2})$

$$U(\nabla^2 + \frac{\beta_m}{U})\phi_{1x}^{"(9)"} = \phi_{1x}^{(7)} - J(\phi_1^{(6)}, \nabla^2\phi_1^{(0)}) - J(\phi_1^{(0)}, \nabla^2\phi_1^{(6)}) - J(\phi_1^{(3)}, \nabla^2\phi_1^{(3)})$$

$$-(\partial_T[\nabla^2 - F]\phi_1^{(5)} + FU\phi_{2x}^{(5)}) + q_{1x}^{(0)}\bar{\Phi}_{1\eta}^{(6)} + q_{1x}^{(3)}\bar{\Phi}_{1\eta}^{(3)} - \phi_{1x}^{(0)}Q_{1\eta}^{(6)} - \phi_{1x}^{(3)}Q_{1\eta}^{(3)}$$

$$-J(\phi_1^{(0)}, F\phi_2^{(2)}) - k_2^2 J(\phi_1^{(0)}, \sum_{n=2}^{\infty}[W_n^{(3)} e^{ikx} + *]) - \partial_T[(\partial_y^2 - F)\bar{\Phi}_1^{(5)} + F\bar{\Phi}_2^{(1)}]$$

$$+ k_1^2 J(\phi_1^{(0)}, \phi_1^{(4)})$$

Taking the zonally independent portion of this we find that

$$[(\partial_y^2 - F)\bar{\Phi}_1^{(5)} + F\bar{\Phi}_2^{(1)}] = k_1^2 k(|A|^2 - |A(0)|^2)$$

$$\times\, \partial_y \left\{ \frac{1}{4\pi}(y-1)\, \sin 2\pi y \left[\frac{\beta_m + FU}{kU^2} - \frac{F^2}{kh_2} \right] + \frac{F^2}{2kh_2\pi^2} \sin^2 \pi y \, \ln\left(|\cos \pi y|\right) \right\}$$

We now have expressions for the $O(\Delta^3)$ and $O(\Delta^4)$ corrections to the mean potential vorticity for both layers. We will invert these to find the changes to the zonally independent streamfunctions.

From above

$$(\partial_y^2 - F)\Phi_2^{(-1)} + F\Phi_1^{(3)} = \frac{\pi F^2}{h_2} \sec^2 \pi y \tan \pi y (|A|^2 - |A(0)|^2)$$

$$(\partial_y^2 - F)\Phi_1^{(3)} + F\Phi_2^{(-1)} = -\frac{\pi^2 + k^2 + F}{U} \pi \sin 2\pi y (|A|^2 - |A(0)|^2)$$

In normal form,

$$\partial_y^2 \Phi^{(T)} = -\left[\frac{\pi}{2U}(\pi^2 + k^2 + F) \sin 2\pi y - \frac{F^2 \pi}{2h_2} \sec^2 \pi y \tan \pi y \right] (|A|^2 - |A(0)|^2)$$

$$(\partial_y^2 - 2F)\Phi^{(c)} = -\left[\frac{\pi}{2U}(\pi^2 + k^2 + F) \sin 2\pi y + \frac{F^2 \pi}{2h_2} \sec^2 \pi y \tan \pi y \right] (|A|^2 - |A(0)|^2)$$

where $$\Phi^{(T)} = \frac{1}{2}(\Phi_1^{(3)} + \Phi_2^{(-1)}) \,, \quad \Phi^{(c)} = \frac{1}{2}(\Phi_1^{(3)} - \Phi_2^{(-1)})$$

Thus,

$$\Phi^{(T)} = \left[\frac{\pi^2 + k^2 + F}{4U}\left(\frac{\sin 2\pi y}{2\pi} - y + \frac{1}{2} \right) + \frac{F^2}{4h_2}\left(\frac{\tan \pi y}{\pi} - y + \frac{1}{2} \right) + C^{(T)} \right] (|A|^2 - |A(0)|^2)$$

$$\Phi^{(C)} = \left[\frac{\pi^2(\pi^2 + k^2 + F)}{(4\pi^2 + 2F)U} \left(\frac{\sin 2\pi y}{2\pi} - \frac{\sinh[\sqrt{2F}(y - \frac{1}{2})]}{\sqrt{2F} \cosh \sqrt{F/2}} \right) - \frac{F^2}{4h_2}\left(\frac{\tan \pi y}{\pi} - y + \frac{1}{2} \right) \right.$$

$$- \frac{F^2\sqrt{\frac{F}{2}}}{4h_2}\left[e^{\sqrt{2F}\,y} \int_1^y \left(\frac{\tan\pi y}{\pi} - y + \frac{1}{2}\right)e^{-\sqrt{2F}\,y}\right.$$

$$\left. -e^{\sqrt{2F}\,y} \int_1^y \left(\frac{\tan\pi y}{\pi} - y + \frac{1}{2}\right) e^{\sqrt{2F}\,y}\right]\Bigg] (|A|^2 - |A(0)|^2)$$

Hence

$$\Phi_1^{(3)} = \left[\frac{(\pi^2+k^2+F)}{(4\pi^2+2F)2U}\left[(4\pi^2+F)\,\frac{\sin 2\pi y}{2\pi} - (2\pi^2+F)\left(y - \frac{1}{2}\right) - \frac{2\pi^2 \sinh\left[\sqrt{2F}\left(y - \frac{1}{2}\right)\right]}{\sqrt{2F}\cosh\sqrt{F/2}}\right]\right.$$

$$\left. - \frac{F^2\sqrt{F/2}}{4h_2}\left[e^{\sqrt{2F}\,y}\, I_- - e^{-\sqrt{2F}\,y}\, I_+\right] + C^{(T)}\right] (|A|^2 - |A(0)|^2)$$

$$I_\pm = \int_1^y \left(\frac{\tan\pi y}{\pi} - y + \frac{1}{2}\right) e^{\pm\sqrt{2F}\,y}$$

$$\Phi_2^{(-1)} = \left[\frac{(\pi^2+k^2+F)}{(2\pi^2+F)4U}\left[F\,\frac{\sin\pi y}{2\pi} - (2\pi^2+F)\left(y - \frac{1}{2}\right) + \frac{2\pi^2\sinh\left[\sqrt{2F}\left(y - \frac{1}{2}\right)\right]}{\sqrt{2F}\cosh\sqrt{F/2}}\right]\right.$$

$$+ \frac{F^2\sqrt{F/2}}{4h_2}\left[e^{\sqrt{2F}y}\, I_- - e^{-\sqrt{2F}y}\, I_+\right]$$

$$\left. + \frac{F^2}{2h_2}\left(\frac{\tan\pi y}{\pi} - y + \frac{1}{2}\right) + C^{(T)}\right] (|A|^2 - |A(0)|^2)$$

The next significant parts of the mean flow are governed by

$$[(\partial_y^2 - F)\Phi_1^{(5)} + F\Phi_2^{(1)}] = k_1^2 k(|A|^2 - |A(0)|^2)$$

$$\times\, \partial_y\left\{\frac{1}{4\pi}(y-1)\,\sin 2\pi y\left[\frac{\beta_m + FU}{kU^2} - \frac{F^2}{kh_2}\right] + \frac{F^2}{2kh_2\pi^2}\sin^2\pi y\,\ln(|\cos\pi y|)\right\}$$

$$\left[(\partial_y^2 - F)\Phi_2^{(1)} + F\Phi_1^{(5)}\right] = \frac{\pi F^2}{4h_2^2}\left(\frac{4\sin^3\pi y}{\cos^5\pi y} + \frac{2\sin\pi y}{\cos^3\pi y}\right)(|A|^2 - |A(0)|^2)$$

Setting $\hat{\Phi}^{(T)} = \frac{1}{2}(\Phi_1^{(5)} + \Phi_2^{(1)})$, $\hat{\Phi}^{(c)} = \frac{1}{2}(\Phi_1^{(5)} - \Phi_2^{(1)})$ we obtain

$$\partial_y^2\hat{\Phi}^{(T)} = \left[\frac{F^2\pi}{4h_2^2}\left(\frac{2\sin^3\pi y}{\cos^5\pi y} + \frac{\sin\pi y}{\cos^3\pi y}\right)\right.$$

$$+ k_1^2 k\left[\left(\frac{1}{4}(y-1)\cos 2\pi y + \frac{1}{8\pi}\sin 2\pi y\right)\left(\frac{\beta_m + FU}{kU^2} - \frac{F^2}{kh_2}\right)\right.$$

$$\left.\left. + \frac{F^2}{2kh_2\pi^2}\left[\sin\pi y\cos\pi y\,\ln(\cos\pi y) + \frac{\pi}{2}\frac{\sin^3\pi y}{\cos\pi y}\right]\right]\right.$$

$$\times\,(|A|^2 - |A(0)|^2)$$

$$(\partial_y^2 - 2F)\hat{\Phi}^{(c)} = \left[-\frac{\pi F^2}{4h_2^2}\left(\frac{2\sin^3\pi y}{\cos^5\pi y} + \frac{\sin\pi y}{\cos^3\pi y}\right) + \right.$$

$$+ k_1^2 k\left[\left(\frac{1}{4}(y-1)\cos 2\pi y + \frac{1}{8\pi}\sin 2\pi y\right)\left(\frac{\beta_m + FU}{kU^2} - \frac{F^2}{kh_2}\right)\right.$$

$$\left.\left. + \frac{F^2}{2kh_2\pi^2}\left[\sin\pi y\cos\pi y\,\ln(|\cos\pi y|) + \frac{\pi}{2}\frac{\sin^3\pi y}{\cos\pi y}\right]\right]\right.$$

$$\times(|A|^2 - |A(0)|^2)$$

$$\therefore \quad \hat{\Phi}^{(T)} = \left\{ \frac{F^2}{24h_2{}^2\pi} \left(\frac{\sin\pi y}{\cos^3\pi y} - \tan\pi y \right) + \text{h.o.t.} \right\} \left(|A|^2 - |A(0)|^2 \right)$$

$$\hat{\Phi}^{(c)} = \left\{ \frac{F^2}{24h_2{}^2\pi} \left(- \frac{\sin\pi y}{\cos^3\pi y} + \left(- \frac{F}{\pi^2} + 1 \right) \tan\pi y \right) + \text{h.o.t.} \right\} \left(|A|^2 - |A(0)|^2 \right)$$

Thus

$$\Phi_2^{(1)} = \left\{ \frac{F^2}{24h_2{}^2\pi} \left(\frac{\sin\pi y}{\cos^3\pi y} + \left(\frac{F}{\pi^2} - 2 \right) \tan\pi y \right) + \text{h.o.t.} \right\} \left(|A|^2 - |A(0)|^2 \right)$$

$$\Phi_1^{(5)} = \left\{ - \frac{F^3}{24h_2{}^2\pi^3} \tan\pi y + \text{h.o.t.} \right\} \left(|A|^2 - |A(0)|^2 \right)$$

We do not intend to calculate any terms of the form $\Delta^{n/2}[\ln(1/\Delta)]^m$, $m \geq 2$, in the innter expansions of ϕ_1 and ϕ_2. However, we will have to try and obtain some information about the $O(\Delta^{n/2}\ln(1/\Delta))$ terms in ϕ_2 which we have not yet dealt with.

Inner, lower, $O[\Delta\ln(1/\Delta)]$

$$2\pi^2 h_2 \eta^2 R_X^{(2)} + \partial_y \partial_\eta{}^2 R^{(2)} - R_X^{(2)} + J(R^{(2)}, \partial_\eta{}^2 \phi_2^{(0)}) + J(\phi_2^{(0)}, \partial_\eta{}^2 R^{(2)})$$

$$+ \partial_T \partial_\eta{}^2 P^{(2)} + J(P^{(2)}, \partial_\eta{}^2 \phi_2^{(0)}) + J(\phi_2^{(0)}, \partial_\eta{}^2 P^{(2)}) + J(\Phi_2^{(0)}, \partial_\eta{}^2 R^{(2)})$$

$$+ J(R^{(2)}, F\phi_1^{(0)}) + J(P^{(2)}, F\phi_1^{(0)}) + J(R^{(2)}, \partial_\eta{}^2 \Phi_2^{(0)}) = 0$$

Note that there is no direct forcing term in this equation; the $O(\Delta\ln 1/\Delta)$ part of ϕ_2 is forced by the matching conditions which join it to the

outer solution. The zonally uniform part of the above equation is

$$\partial_T \partial_y {}^2 P^{(2)} = - J_{(0)}(R^{(2)}, \partial_\eta {}^2 \phi_2^{(0)}) - J_{(0)}(\phi_2^{(0)}, \partial_\eta {}^2 R^{(2)}) - J_{(0)}(R^{(2)}, F\phi_1^{(0)})$$

$$P^{(2)} = - \int_0^T dT \int_0^\eta d\eta' \int_0^{\eta'} d\eta'' \, [J_{(0)}(R^{(2)}, \partial_\eta {}^2 \phi_2^{(0)}) + J_{(0)}(\phi_2^{(0)}, \partial_\eta^2 R^{(2)})$$

$$+ J_{(0)}(R^{(2)}, F\phi_1^{(0)})] + S^{(2)}{}_\eta$$

As $\eta \to \infty$, $P^{(2)} \sim \tilde{S}^{(2)}{}_\eta$ + const. + h.o.t. where $\tilde{S}^{(2)}(T)$ is a disposable constant. Looking now at the x-dependent part of the potential vorticity balance gives

$$2\pi^2 h_{2\eta} {}^2 R_x^{(2)} + \partial_T \partial_\eta^2 R^{(2)} - R_x^{(2)} + J_{(x)}(R^{(2)}, \partial_\eta^2 \phi_2^{(0)}) + J_{(x)}(\phi_2^{(0)}, \partial_\eta^2 R^{(2)})$$

$$-F\phi_{1x}^{(0)} R_\eta^{(2)} - F\phi_{1x}^{(0)} P_\eta^{(2)} - \partial_\eta {}^2 \phi_{2x}^{(0)} P_\eta^{(2)} + \phi_{2x}^{(0)} P_{\eta\eta\eta}^{(2)} - \partial_\eta {}^2 R_x^{(2)} \Phi_{2\eta}^{(0)}$$

$$+ R_x^{(2)} \partial_\eta {}^3 \Phi_2^{(0)} = 0$$

Set $$R^{(2)} = \sum_{n=1}^{\infty} (R^{(2,n)} e^{inkx} + *)$$

$$R^{(2,1)} \sim \frac{F}{2\pi^2 h_2} \tilde{S}^{(2)}{}_\eta {}^{-2} A$$

To calculate the mean part of the $O[\Delta^4 \ln (1/\Delta)]$ term in $\phi_{1\ in}$, we must look at

Upper, $O[\Delta^4 \ln (1/\Delta)]$

$$U\,\partial_y^2 \mathcal{F}_x^{(8)} = -(U\,\partial_x^2 + \beta_m)\mathcal{F}_x^{(6)} + \mathcal{F}_x^{(4)} - FU\,R_x^{(4)}$$

$$- J(\phi_1^{(0)}, \mathcal{F}_{\eta\eta}^{(6)} + \mathcal{G}_{\eta\eta}^{(6)} + (\partial_x^2 - F)\mathcal{F}^{(4)} - F\mathcal{G}^{(4)} + F\,R^{(2)} + F\,P^{(2)})$$

$$+ J\left(\tfrac{1}{2}\eta^2\pi^2[Ae^{ikx}+*], \mathcal{F}_{\eta\eta}^{(4)} + \mathcal{G}_{\eta\eta}^{(4)}\right) - J\,[\mathcal{F}^{(4)}, (\partial_x^2 - \pi^2 - F)\,\phi_1^{(0)}]$$

$$- J\,[\mathcal{G}^{(4)}, (\partial_x^2 - \pi^2 - F)\,\phi_1^{(0)}] - \partial_T \mathcal{F}_{\eta\eta}^{(4)} - \partial_x \mathcal{G}_{\eta\eta}^{(4)}$$

Mean component is

$$\partial_T \mathcal{G}_{\eta\eta}^{(4)} = -F\,J_{(0)}(\phi_1^{(0)}, R^{(2)}) = -ikF\,(A\,R_\eta^{(2,1)*} - A^*\,R_\eta^{(2,1)})$$

$$\Longrightarrow \quad \mathcal{G}^{(4)} = -ikF \int_0^T dT\,\left(A\int_0^\eta R^{(2,1)*} - A^*\int_0^\eta R^{(2,1)}\right) + G_1^{(4)}(T)\,\eta$$

The next task is to try to match the inner and the outer solutions.

MATCHING

We will first try to match the x-independent parts of the inner and outer solutions

$$\phi_{1\ out} = \Delta^3 \Phi_1^{(3)} + \Delta^{7/2} \ln(1/\Delta)\,\textcircled{H}_1^{(4)} + \Delta^{7/2}\Phi_1^{(4)} + \Delta^4 \ln(1/\Delta)\,\textcircled{H}_1^{(5)} + \Delta^4 \Phi_1^{(5)} + \ldots.$$

$$\phi_{2\ out} = \Delta^3 \Phi_1^{(-1)} + \Delta^{7/2} \ln(1/\Delta)\,\textcircled{H}_2^{(0)} + \Delta^{7/2}\Phi_2^{(0)} + \Delta^4 \ln(1/\Delta)\,\textcircled{H}_2^{(1)} + \Delta^4 \Phi_2^{(1)} + \ldots.$$

We will not try to go so far as including the $\Delta^4 \ln(1/\Delta)$ terms in the matching process. These terms are omitted henceforth

$$\phi_{1\ in} = \Delta^3 \Phi_1^{(3)} + \Delta^{7/2} \ln(1/\Delta)\, G_1^{(4)} + \Delta^{7/2} \Phi_1^{(4)} + \ldots.$$

$$\phi_{2\ in} = \Delta^{5/2} \Phi_2^{(0)} + \Delta^3 \Phi_2^{(1)} + \Delta^{7/2} \ln(1/\Delta)\, P^{(2)} + \Delta^{7/2} \Phi_2^{(2)} + \ldots.$$

$$\phi_{1\ out} \sim (|A|^2 - |A(0)|^2)\left(\left[\Delta^3[C^{(T)} - \frac{F^2\sqrt{F/2}}{4h_2}(D_+ - D_-)] - \Delta^{7/2} \ln(1/\Delta) \frac{F^3}{4h_2\pi^2}\eta\right.\right.$$

$$+ \Delta^{7/2}\, \eta \ln \eta \frac{F^3}{2h_2\pi^2}$$

$$\left.\left. + \Delta^{7/2}\eta\left(-\frac{(\pi^2+k^2+F)}{2U}\left(1+\frac{\pi^2(1+\operatorname{sech}\sqrt{F/2})}{2\pi^2+F}\right) - \frac{F^3}{2\pi^2 h_2}\left[1 - \ln 2 + \frac{\pi^2}{2}(D_+ + D_-)\right]\right)\right]$$

$$+ \Delta^{7/2} \ln(1/\Delta)\left[\rho^{(4)} \cosh\sqrt{F/2} + \tau^{(4)}\right] + \Delta^{7/2}\left[\beta^{(4)} \cosh\sqrt{F/2} + \gamma^{(4)}\right]$$

$$\left. + \Delta^{7/2}\left[\frac{F^3}{24h_2^2\pi^4}\eta^{-1}\right]\right)$$

$$D_\pm = \int_0^{1/2}\left[\left(\frac{\cot\pi y}{\pi} + y\right) e^{-\sqrt{2Fy}} - \frac{1}{\pi^2 y}\right]$$

$$\phi_{1\ in} \sim \Delta^3 N^{(3)}\eta + \Delta^{7/2} \ln(1/\Delta)\, G_1^{(4)}\, \eta$$

$$+ \Delta^{7/2}\left[-\frac{F}{6} M^{(0)}\eta^3 + \frac{F^3}{2\pi^2 h_2}(|A|^2 - |A(0)|^2)\,\eta \ln \eta + \mu\eta\right.$$

$$+ \text{const} + \eta^{-1} \frac{F^3}{24\pi^4 h_2^2} \left(|A|^2 - |A(0)|^2\right)]$$

μ is a free constant and "const" is a determined constant of a complicated form

Matching yields

$$N^{(3)} = 0 \quad (\text{and hence } \Phi_{1\ in}^{(3)} \equiv 0)$$

$$c^{(T)} = \frac{F^2 \sqrt{F/2}}{4 h_2} (D_+ - D_-)$$

$$G_1^{(4)} = - \frac{F^3}{4 h_2 \pi^2}$$

$$M^{(0)} = 0$$

$$\mu = (|A|^2 - |A(0)|^2)\left[- \frac{1}{2U} (\pi^2 + k^2 + F)\left(1 + \frac{\pi^2 (1 + \operatorname{sech} \sqrt{F/2})}{2\pi^2 + F}\right)\right.$$

$$\left. - \frac{F^3}{2\pi^2 h_2} \left[1 - \ln 2 + \frac{\pi^2}{2} (D_+ + D_-)\right]\right]$$

$$(\beta^{(4)} \operatorname{ch} \sqrt{F/2} + \gamma^{(4)}) (|A|^2 - |A(0)|^2) = \text{"const"}, \quad \text{known.}$$

$$(\rho^{(4)} \operatorname{ch} \sqrt{F/2} + \tau^{(4)}) = 0$$

In the lower layer

$$\phi_{2\ out} \sim (|A|^2 - |A(0)|^2)\left(\left[\Delta^{5/2}\left[- \frac{F^3}{2 h_2 \pi^2} \eta^{-1}\right] + \Delta^3 \left[c^{(T)} + \frac{F^2 \sqrt{F/2}}{4 h_2} (D_+ - D_-)\right]\right.\right.$$

$$+ \Delta^{7/2} \ln (1/\Delta) \frac{F^3}{4h_2\pi^2} \eta - \Delta^{7/2} \eta \ln \eta \frac{F^3}{2h_2\pi^2}$$

$$+ \Delta^{7/2} \eta \left[- \frac{\pi^2+k^2+F}{(2\pi^2+F)2U} (\pi^2 + F - \pi^2 \operatorname{sech} \sqrt{F/2}) + \frac{F^3}{2\pi^2 h_2} [1 - \ln 2 + \frac{\pi^2}{2} (D_+ + D_-)] \right.$$

$$\left. - \frac{F}{3h_2} \right]$$

$$+ \Delta^{7/2} [- \beta^{(4)} \operatorname{ch} \sqrt{F/2} + \gamma^{(4)}] + \Delta^{7/2} \ln (1/\Delta) [- \rho^{(4)} \operatorname{ch} \sqrt{F/2} + \tau^{(4)}]$$

$$\left. + \left[\Delta^{5/2} [- \frac{F^2}{12h_2^2\pi^4} \eta^{-3}] + \Delta^{7/2} [\frac{F^2}{24h_2^2\pi^2} (2 - \frac{F}{\pi^2}) \eta^{-1}] \right] \right)$$

$$\phi_2 \text{ in } \sim \Delta^{5/2} \left[- \frac{F^2}{2\pi^2 h_2} \eta^{-1} (|A|^2 - |A(0)|^2) - \frac{F^2}{12\pi^4 h_2^2} \eta^{-3} (|A|^2 - |A(0)|^2) \right]$$

$$+ \Delta^3 \left[\tilde{M}^{(1)} \eta + \int_0^T dT \int_0^\infty d\eta' \int_{\eta'}^\infty d\eta'' [J_{(0)}(\phi_2^{(1)}, \partial_\eta^2 \phi_2^{(0)}) + J_{(0)}(\phi_2^{(0)}, \partial_\eta^2 \Phi_2^{(1)}) \right.$$

$$\left. + J_{(0)}(\Phi_2^{(1)}, F \phi_1^{(0)})] \right]$$

$$+ \Delta^{7/2} \ln (1/\Delta) [\tilde{S}^{(2)} \eta + \text{const}]$$

$$+ \Delta^{7/2} \left\{ - \frac{F^3}{2\pi^2 h_2} (|A|^2 - |A(0)|^2) \eta \ln \eta + \tilde{M}^{(2)} \eta \right.$$

$$\left. + kF \int_0^\infty d\eta [i \int_0^T (A Y_1^{(2)*} - *) + \frac{F}{12h_2 k} (|A|^2 - |A(0)|^2)] \right.$$

$$+ \frac{\pi^2}{2} kF \int_0^\infty d\eta \left[i \int_0^T (\eta^2 Y_1^{(0)} A^* - *) + \frac{F}{2\pi^2 h_2 k} (|A|^2 - |A(0)|^2) \right]$$

$$- F \int_0^\infty \int_\eta^\infty [\Phi_2^{(0)} + \eta^{-1} \frac{F^2}{2\pi^2 h_2} (|A|^2 - |A(0)|^2)]$$

$$+ \eta^{-1} \left[\frac{F^2}{24 h_2^2 \pi^2} \left(2 - \frac{F}{\pi^2} \right) (|A|^2 - |A(0)|^2) + \frac{F^2 k}{4\pi^2 h_2} |A|^2 \, \mathrm{Im}(\tilde{M}^{(2)}) \right]$$

Matching yields:

$$(|A|^2 - |A(0)|^2)[c^{(T)} + \frac{F^2 \sqrt{F/2}}{4h_2} (D_+ - D_-)] = \int_0^T dT \int_0^\infty d\eta' \int_{\eta'}^\infty d\eta''$$

$$[J_{(0)}(\phi_2^{(1)}, \partial_\eta^2 \phi_2^{(0)}) + J_{(0)}(\phi_2^{(0)}, \partial_\eta^2 \Phi_2^{(1)}) + J_{(0)}(\Phi_2^{(1)}, F \phi_1^{(0)})]$$

$$\tilde{S}^{(2)} = \frac{F^3}{4h_2 \pi^2} (|A|^2 - |A(0)|^2)$$

$$- \rho^{(4)} \operatorname{ch} \sqrt{F/2} + \tau^{(4)} = \text{a known constant}$$

$$\tilde{M}^{(2)} = (|A|^2 - |A(0)|^2) \left[- \frac{\pi^2 + k^2 + F}{(2\pi^2 + F) 2U} (\pi^2 + F - \pi^2 \operatorname{sech} \sqrt{F/2}) \right.$$

$$\left. + \frac{F^3}{2\pi^2 h_2} [1 - \ln 2 + \frac{\pi^2}{2} (D_+ + D_-)] - \frac{F^2}{3h_2} \right] \qquad \text{and is real.}$$

$$- \beta^{(4)} \operatorname{ch} \sqrt{F/2} + \gamma^{(4)} = kF \int_0^\infty d\eta \left[i \int_0^T dT \, (A Y_1^{(2)*} - *) + \frac{F}{12 h_2 k} (|A|^2 - |A(0)|^2) \right]$$

$$+ \frac{\pi^2}{2} kF \int_0^\infty d\eta \left[i \int_0^T dT \, (\eta^2 Y_1^{(0)} A^* - *) + \frac{F^2}{2\pi^2 h_2 k} (|A|^2 - |A(0)|^2) \right]$$

$$- F \int_0^\infty d\eta \int_\eta^\infty d\eta' \left[\Phi_2^{(0)} + \eta'^{-1} \frac{F^2}{2\pi^2 h_2} (|A|^2 - |A(0)|^2) \right]$$

$$\tilde{M}^{(1)} = 0$$

We will now match some of the e^{ikx} terms. For convenience we expand

$$\mathcal{F}^{(p)}(x, \eta, T) = \sum_{n=1}^{\infty} (E_n^{(p)} e^{inkx} + *)$$

Upper

$$\phi_{1 \text{ out}} = \Delta^{3/2} A \sin \pi y \, e^{ikx} + \Delta^3 \phi_1^{(3)} + \Delta^{7/2} \phi_1^{(4)} + \Delta^4 \phi_1^{(5)}$$

$$\sim \Delta^{3/2} A \left(1 - \frac{1}{2} \pi^2 \eta^2 \Delta + \frac{1}{24} \pi^4 \eta^4 \Delta^2 - \ldots \right)$$

$$+ \left[- \Delta^{7/2} A \frac{k_2^2}{4} \eta + \Delta^4 A \frac{k_2^2}{2} \eta^2 \right]$$

$$+ iA_T \left[- \Delta^{7/2} \ln (1/\Delta) \frac{F^2}{4kh_2\pi^2} + \Delta^{7/2} \left[\frac{F^2}{2kh_2\pi^2} \ln \eta + \frac{F^2}{2kh_2\pi^2} \ln \pi \right] \right.$$

$$\left. + \Delta^4 \frac{1}{4} \eta \left[\frac{k^2 + \pi^2 + F}{kU} - \frac{F^2}{kh_2} \right] \right]$$

$\phi_{1 \text{ in}} =$

$$\Delta^{3/2} A \left(1 - \frac{1}{2} \pi^2 \eta^2 \Delta + \frac{1}{24} \pi^4 \eta^4 \Delta^2 - \ldots\right) + \Delta^{7/2} \ln (1/\Delta) E_1^{(4)} + \Delta^{7/2} Z_1^{(4)} + \Delta^4 Z_1^{(5)}$$

$$\phi_{1\ in} \sim \Delta^{3/2} A \left(1 - \frac{1}{2}\pi^2\eta^2\Delta + \frac{1}{6}\pi^4\eta^4\Delta^2 - \ldots\right) + \Delta^{7/2} \ln(1/\Delta)\, E_1^{(4)}$$

$$+ \Delta^{7/2} \left[-\eta F \int_0^\infty Y_1^{(0)} + \frac{iA_T F^2}{2k\pi^2 h_2} \ln\eta + \tilde{G}_0^{(4,1)}\right]$$

$$+ \Delta^4 \left[\left[\frac{1}{2}k_2^2 A - \frac{1}{2}\left(\frac{\beta m}{U} - k^2\right) H_0^{(3,1)}\right]\eta^2 - \eta F \int_0^\infty Y_1^{(1)} + F \int_0^\infty \int_{\eta'}^\infty Y_1^{(1)} + H_0^{(5,1)}\right]$$

Matching gives

$$E_1^{(4)} = -iA_T \frac{F^2}{4kh_2\pi^2}$$

$$\frac{k_2^2}{4} A = F \int_0^\infty Y_1^{(0)} \quad \text{as stated earlier}$$

$$\tilde{G}_0^{(4,1)} = iA_T \frac{F^2}{2kh_2\pi} \ln\pi$$

$$H_0^{(3,1)} = 0$$

$$F \int_0^\infty Y_1^{(1)} = \frac{1}{4}\left[\frac{k^2+\pi^2+F}{kU} - \frac{F^2}{kh_2}\right] iA_T$$

$$H_0^{(5,1)} = -F \int_0^\infty \int_{\eta'}^\infty Y_1^{(1)}$$

Lower layer

$$\phi_{2\ out} = \Delta^{7/2}\,\phi_2^{(0)} + \Delta^{9/2}\,\phi_2^{(2)} + \Delta^{5}\,\phi_2^{(3)} + \Delta^{11/2}\,\phi_2^{(4)} + \ldots$$

$$\phi_{2\ out} \sim \Delta^{5/2}\left[\frac{iFA_T}{2kh_2\pi^2}\,\eta^{-2} + \eta^{-4}\,\frac{F}{4h_2^2\pi^2}\,[F^2A(|A|^2 - |A(0)|^2) + \frac{i}{k}\,A_T]\right]$$

$$+ \Delta^{7/2}\,\ln\,(1/\Delta)\,\frac{F^4}{16h_2^3\pi^6}\,A(|A|^2 - |A(0)|^2)[\eta^{-4} + 2h_2\,\pi^2\,\eta^{-2}]$$

$$+ \Delta^{7/2}\left[-\frac{iFA_T}{12kh_2} + \eta^{-2}\left[\frac{FA(|A|^2 - |A(0)|^2)}{2h_2\pi^2}\left(\frac{\pi^2 + k^2 + F}{(2\pi^2+F)2U}\right.\right.\right.$$

$$\left.\left.\left.\times\,[-(F^2 + \pi^2) + \pi^2\,\mathrm{sech}\,\sqrt{F/2}] + \frac{F^3}{4h_2}\,[(D_+ + D_-) - \frac{2}{\pi^2}\,\ln\,2] - \frac{5F^2}{12h_2}\right)\right]\right.$$

$$- \eta^{-2}\,\ln\,\eta\,\frac{F\,A(|A|^2 - |A(0)|^2)}{4h_2^2\pi^4}$$

$$\phi_{2\ in} \sim \Delta^{5/2}\,Y_1^{(0)} + \Delta^{3}\,Y_1^{(1)} + \Delta^{7/2}\,\ln\,(1/\Delta)\,R^{(2,1)} + \Delta^{7/2}\,Y_1^{(2)}$$

$$\sim \Delta^{5/2}\left\{\eta^{-2}\left[\frac{iFA_T}{2\pi^2h_2k}\right] + \eta^{-4}\left[\frac{F^3}{4\pi^4h_2^2}\,A(|A|^2 - |A(0)|^2) + \frac{iFA_T}{4kh_2^2\pi^4}\right] + \ldots\right\}$$

$$+ \Delta^{3}\left[\frac{F}{2\pi^2h_2}\,\tilde{M}^{(1)}\,\eta^{-2}\,A + \ldots\right] + \Delta^{7/2}\,\ln\,(1/\Delta)\left[\eta^{-2}\,\frac{FA}{2\pi^2h_2}\,\tilde{S}^{(2)} + \ldots\right]$$

$$+ \Delta^{7/2}\left\{\frac{-iF}{12h_2k}\,A_T - (\eta^{-2}\,\ln\,\eta)\,\frac{F^4}{4\pi^4h_2^2}\,A(|A|^2 - |A(0)|^2)\right.$$

$$\left.+ \eta^{-2}\left[\frac{iFA_T}{24h_2^2\pi^2k} + \frac{F\tilde{M}^{(2)}}{2\pi^2h_2}\,A - \left(\frac{F^3}{24\pi^2h_2^2} + \frac{F^4}{4\pi^4h_2^2}\right)A\,(|A|^2 - |A(0)|^2)\right] + \ldots\right\}$$

Using the forms that we have already derived for $\tilde{M}^{(1)}$, $\tilde{M}^{(2)}$ and $\tilde{S}^{(2)}$ it may be seen that all of the terms match correctly.

We will now try to match the exp(i2kx) components in the upper layer

$$\phi_{1out}^{(.,2)} = \Delta^3 W_2^{(3)} + \Delta^{7/2} W_2^{(4)} + \Delta^4 W_2^{(5)} + \Delta^{9/2} W_2^{(6)}$$

$$\sim \Delta^3 [-B_2^{(3)} \operatorname{sh}\lambda_2/2] + \Delta^{7/2} [-B_2^{(4)} \operatorname{sh} \lambda_2/2 + \eta\lambda_2 B_2^{(3)} \operatorname{ch} \lambda_2/2]$$

$$\Delta^4 [(-B_2^{(5)} \operatorname{sh} \lambda_2/2 - \frac{B_2^{(3)}}{4\lambda_2 U} \operatorname{ch} \lambda_2/2) + \eta\lambda_2 B_2^{(4)} \operatorname{ch} \lambda_2/2$$

$$- \eta^2 \frac{1}{2} \lambda_2^2 B_2^{(3)} \operatorname{sh} \lambda_2/2] + \Delta^{9/2} [(-B_2^{(6)} \operatorname{sh} \lambda_2/2 - \frac{B_2^{(4)}}{4\lambda_2 U} \operatorname{ch} \lambda_2/2)$$

$$+ \eta(\lambda_2 B_2^{(3)} \operatorname{ch} \lambda_2/2 + \frac{B_2^{(3)}}{4\lambda_2 U} [2 \operatorname{ch} \lambda_2/2 - \lambda_2 \operatorname{sh} \lambda_2/2])$$

$$- \eta^2 \frac{1}{2} \lambda_2^2 B_2^{(4)} \operatorname{sh} \lambda_2/2 + \eta^3 \frac{1}{6} \lambda_2^3 B_2^{(3)} \operatorname{ch} \lambda_2/2]$$

$$\phi_{1in}^{(.,2)} = \Delta^3 Z_2^{(3)} + \Delta^{7/2} \ln(1/\Delta) E_2^{(4)} + \Delta^{7/2} Z_2^{(4)} + \Delta^4 Z_2^{(5)} + \Delta^{9/2} \ln(1/\Delta) E_2^{(6)}$$

$$+ \Delta^{9/2} Z_2^{(6)} + \ldots$$

$$\phi_{1in}^{(.,2)} \sim \Delta^3 [\eta H_{2,1}^{(3)}] + \Delta^{7/2} \ln(1/\Delta) [\eta E_{2,1}^{(4)}] + \Delta^{7/2} [\eta (G_1^{(4,2)} - F \int_0^\infty Y_2^{(0)})$$

$$+ F \int_0^\infty \int_{\eta'}^\infty Y_2^{(0)}] + \Delta^4 [\frac{1}{6} \eta^3 \lambda_2^2 H_{2,1}^{(3)} + \eta (H_{2,1}^{(5)} - F \int_0^\infty Y_2^{(1)})$$

$$+ F \int_0^\infty \int_{\eta'}^\infty Y_2^{(1)}] + \Delta^{9/2} \ln(1/\Delta) [\frac{1}{6} \eta^3 \lambda_2^2 E_{2,1}^{(4)} + \eta E_{2,1}^{(6)}]$$

$$+ \Delta^{9/2}\left[\lambda_2^2\eta^3\left(\frac{1}{6}G_1^{(4,2)} - \frac{1}{6}F\int_0^\infty Y_2^{(0)}\right) + \lambda_2^2 F\frac{1}{2}\eta^2\int_0^\infty\int_{\eta'}^\infty Y_2^{(0)}\right.$$

$$+ \eta\left(G_1^{(6,2)} - F\int_0^\infty Y_2^{(2)} - \lambda_2^2 F\int_0^\infty\int_{\eta'}^\infty\int_{\eta''}^\infty Y_2^{(0)}\right)$$

$$\left.+ \left(F\lambda_2^2\int_0^\infty\int_{\eta'}^\infty\int_{\eta''}^\infty\int_{\eta'''}^\infty Y_2^{(0)} + F\int_0^\infty\int_{\eta'}^\infty Y_2^{(2)}\right)\right]$$

Matching we find that

$$H_{2,1}^{(3)} = 0 \quad , \qquad B_2^{(3)} = 0$$

$$E_{2,1}^{(4)} = 0$$

$$G_1^{(4,2)} = F\int_0^\infty Y_2^{(0)}$$

$$B_2^{(4)} = -\text{cosech}\left(\lambda_2/2\right) F\int_0^\infty\int_{\eta'}^\infty Y_2^{(0)}$$

$$H_{2,1}^{(5)} = F\int_0^\infty Y_2^{(1)} + \lambda_2 B_2^{(4)}\text{ch}\left(\lambda_2/2\right)$$

$$= F\int_0^\infty Y_2^{(1)} - F\lambda_2\coth\left(\lambda_2/2\right)\int_0^\infty\int_{\eta'}^\infty Y_2^{(0)}$$

$$B_2^{(5)} = -\text{cosech}\left(\lambda_2/2\right) F\int_0^\infty\int_{\eta'}^\infty Y_2^{(1)}$$

$$E_{2,1}^{(6)} = 0$$

$$G_1^{(6,2)} = F \int_0^\infty Y_{(2)}^{(2)} + \lambda_2^2 F \int_0^\infty \int_{\eta'}^\infty \int_{\eta''}^\infty Y_2^{(0)}$$

$$B_2^{(6)} \text{sh}(\lambda_2/2) = -\frac{B_2^{(4)}}{4\lambda_2 U} \text{ch}(\lambda_2/2) - [F\lambda_2^2 \int_0^\infty \int_{\eta'}^\infty \int_{\eta''}^\infty \int_{\eta'''}^\infty Y_2^{(0)} + F \int_0^\infty \int_{\eta'}^\infty Y_2^{(2)}]$$

$$B_2^{(6)} = \frac{F}{4\lambda_2 U} \coth(\lambda_2/2) \,\text{cosech}(\lambda_2/2) \int_0^\infty \int_{\eta'}^\infty Y_2^{(0)}$$

$$- F \,\text{cosech}(\lambda_2/2) \int_0^\infty \int_{\eta'}^\infty Y_2^{(2)} - F\lambda_2^2 \,\text{cosech}(\lambda_2/2) \int_0^\infty \int_{\eta'}^\infty \int_{\eta''}^\infty \int_{\eta'''}^\infty Y_2^{(0)}$$

In the lower layer,

$$\phi_{2out}^{(\cdot,2)} \sim \Delta^5 \ln(1/\Delta)\, \theta_2^{(3)} + \Delta^5 [\frac{F^2\pi}{8h_2^2 k} \frac{\tan^3 \pi y}{\cos^2 \pi y} i(A^2)_T] + \Delta^{11/2} \ln(1/\Delta) \theta_2^{(4)}$$

$$+ \Delta^{11/2} \left[\frac{iF}{4kh_2} B_{2T}^{(4)} \frac{\text{sh}[(\lambda_2)(y-1)]}{\cos^2 \pi y} \right]$$

$$\phi_{2in}^{(\cdot,2)} \sim \Delta^{5/2} Y_2^{(0)} + \Delta^3 Y_2^{(1)} + \Delta^{7/2} \ln(1/\Delta) R^{(2,2)} + \Delta^{7/2} Y_2^{(2)}$$

$$+ \Delta^4 \ln(1/\Delta) R^{(3,2)} + \Delta^4 Y_2^{(3)} + \Delta^{9/2} \ln(1/\Delta) R^{(4,2)} + \Delta^{9/2} Y_2^{(4)}$$

We have not calculated $\theta_2^{(3)}$, $\theta_2^{(4)}$, $R^{(2,2)}$, $R^{(3,2)}$ and $R^{(4,2)}$ so no attempt will be made to match those terms that include a factor of $\ln(1/\Delta)$. These will be omitted hereafter.

$$\phi_{2out}^{(\cdot,2)} \sim \Delta^{5/2} \left[-\frac{F^2 \pi i (A^2)_T}{8h_2^2 \pi^5 k} \eta^{-5} \right] + \Delta^{7/2} \left[\frac{F^2 \pi i (A^2)_T}{12 h_2^2 \pi^3 k} \eta^{-3} \right]$$

$$+ \Delta^{9/2}\left[- \frac{iFB_{2T}^{(4)}}{4kh_2\pi^2} \sh(\lambda_2/2)\ \eta^{-2}\ \right]$$

$$\phi_{2in}^{(.,2)} \sim \Delta^{5/2}\left[- \frac{iF^2(A^2)_T}{8h_2^2\pi^4k}\ \eta^{-5}\ \right] + \Delta^3\ O(\eta^{-6}) + \Delta^{7/2}\left[\ \frac{iF^2(A^2)_T}{12h_2^2\pi^2k}\ \eta^{-3}\right]$$

$$+ \Delta^4\ O(\eta^{-5}) + \Delta^{9/2}\ \ \frac{iF^2\partial_T \int_0^\infty \int_\eta^\infty Y_2^{(0)}}{4k\pi^2h_2}\ \ \eta^{-2}$$

All of the calculated terms match correctly

<u>exp[i(2p+1)kx], upper, n = 2p + 1</u>

$$\phi_{1\ out}^{(odd)} = \Delta^3\ W_n^{(3)} + \Delta^{7/2}\ W_n^{(4)} + \Delta^4\ W_n^{(5)} + \Delta^{9/2}\ W_n^{(6)} + \ldots$$

$$\sim \Delta^3\left[- B_n^{(3)}\sh(\lambda_n/2)\ \right] + \Delta^{7/2}\left[- B_n^{(4)}\sh(\lambda_n/2) + \eta\lambda_nB_n^{(3)}\ch(\lambda_n/2)\ \right]$$

$$+ \Delta^4\left[(- B_n^{(5)}\sh(\lambda_n/2) - \frac{B_n^{(3)}}{4\lambda_nU}\ch(\lambda_n/2)) + \eta\lambda_nB_n^{(4)}\ch(\lambda_n/2)\right.$$

$$\left. - \eta^2\ \frac{1}{2}\ \lambda_n^2\ B_n^{(3)}\ \sh\ \lambda_n/2\right]$$

$$+ \Delta^{9/2}\left[(- B_n^{(6)}\ \sh\ \lambda_n/2 - \frac{B_n^{(4)}}{4\lambda_nU}\ \ch\ \lambda_n/2\ )\right.$$

$$+ \eta(\ \lambda_nB_n^{(5)}\ch(\lambda_n/2) + \frac{B_n}{4\lambda_nU}\left[2\ch(\lambda_n/2) - \lambda_n\sh(\lambda_n/2)\right])$$

$$\left. - \eta^2\ \frac{1}{2}\ \lambda_n^2\ B_n^{(4)}\sh(\lambda_n/2) + \eta^3\ \frac{1}{6}\ \lambda_n^3\ B_n^{(3)}\ch(\lambda_n/2)\ \right]$$

$$\phi_{1in}^{(odd)} = \Delta^3 Z_n^{(3)} + \Delta^{7/2} \ln(1/\Delta)\, E_n^{(4)} + \Delta^{7/2} Z_n^{(4)} + \Delta^4 Z_n^{(5)} + \Delta^{9/2} \ln(1/\Delta)\, E_n^{(6)}$$

$$+ \Delta^{9/2} Z_n^{(6)} + \ldots$$

$$\sim \Delta^3 [\, H_{n,0}^{(3)} \,] + \Delta^{7/2} \ln(1/\Delta)\, E_{n,0}^{(4)}$$

$$+ \Delta^{7/2} [- \eta F \int_0^\infty Y_n^{(0)} + (G_0^{(4,n)} + F \int_0^\infty \int_{\eta'}^\infty Y_n^{(0)})]$$

$$+ \Delta^4 [\tfrac{1}{2} \eta^2 \lambda_n^2 H_{n,0}^{(3)} + H_{n,0}^{(5)}] + \Delta^{9/2} \ln(1/\Delta) [\tfrac{1}{2} \eta^2 \lambda_n^2 E_{n,0}^{(4)} + E_{n,0}^{(6)}]$$

$$+ \Delta^{9/2} [- \eta^3 \tfrac{1}{6} \lambda_n^2 F \int_0^\infty Y_n^{(0)} + \tfrac{1}{2} \eta^2 \lambda_n^2 (G_0^{(4,n)} + F \int_0^\infty \int_{\eta'}^\infty Y_n^{(0)})$$

$$+ \eta(-F \int_0^\infty Y_n^{(2)} - \lambda_n^2 F \int_0^\infty \int_{\eta'}^\infty \int_{\eta''}^\infty Y_n^{(0)})$$

$$+ (F\lambda_n^2 \int_0^\infty \int_{\eta'}^\infty \int_{\eta''}^\infty \int_{\eta'''}^\infty Y_n^{(0)} + F \int_0^\infty \int_{\eta'}^\infty Y_n^{(2)} + G_0^{(6,n)})]$$

On matching we obtain,

$$B_n^{(3)} = -\frac{F}{\lambda_n} \operatorname{sech}(\lambda_n/2) \int_0^\infty Y_n^{(0)}$$

$$H_{n,0}^{(3)} = \frac{F}{\lambda_n} \operatorname{th}(\lambda_n/2) \int_0^\infty Y_n^{(0)}$$

$$E_{n,0}^{(4)} = 0$$

$$B_n^{(4)} = 0$$

$$G_0^{(4,n)} = -F \int_0^\infty \int_{\eta'}^\infty Y_n^{(0)}$$

$$E_{n,0}^{(6)} = 0$$

$$B_n^{(5)} = -\frac{F}{\lambda_n}\,\mathrm{sech}(\lambda_n/2) \int_0^\infty Y_n^{(2)} - \lambda_n F \mathrm{sech}(\lambda_n/2) \int_0^\infty \int_{\eta'}^\infty \int_{\eta''}^\infty Y_n^{(0)}$$

$$+ \frac{F}{4\lambda_n^3 U}\left[2\mathrm{sech}(\lambda_n/2) - \lambda_n \mathrm{sech}(\lambda_n/2)\,\mathrm{th}(\lambda_n/2)\right] \int_0^\infty Y_n^{(0)}$$

$$H_{n,0}^{(5)} = \frac{F}{\lambda_n}\,\mathrm{th}(\lambda_n/2) \int_0^\infty Y_n^{(2)} + \lambda_n F\,\mathrm{th}(\lambda_n/2) \int_0^\infty \int_{\eta'}^\infty \int_{\eta''}^\infty Y_n^{(0)}$$

$$+ \frac{F}{4\lambda_n^3 U}\left(\lambda_n[1 + \mathrm{th}^2\lambda_n/2] - 2\,\mathrm{th}(\lambda_n/2)\right) \int_0^\infty Y_n^{(0)}$$

$$G_0^{(6,n)} + F\lambda_n^2 \int_0^\infty \int_{\eta'}^\infty \int_{\eta''}^\infty \int_{\eta'''}^\infty Y_n^{(0)} + F \int_0^\infty \int_{\eta'}^\infty Y_n^{(2)} = -B_n^{(6)}\,\mathrm{sh}(\lambda_n/2)$$

Lower Layer

$$\phi_{2out}^{(odd)} \sim \Delta^5 \ln(1/\Delta)\,\theta_2^{(3)} + \Delta^5\left[\frac{iF}{2h_2 nk}\,\frac{\mathrm{sh}\,[\lambda_n(y-1)]}{\cos^2\pi y}\,B_{nT}^{(3)}\right]$$

$$+ \Delta^{11/2}\ln(1/\Delta)\,\theta_2^{(4)} + \Delta^6 \ln(1/\Delta)\,\theta_2^{(5)}$$

$$+ \Delta^6\left[\frac{F}{4h_2^2 nk}\,\frac{\mathrm{sh}\,\lambda_n(y-1)}{\cos^4\pi y}\,iB_{nT}^{(3)} + \frac{F}{2h_2}\,\Phi_{1y}^{(-1)}\,\frac{\mathrm{sh}\,\lambda_n(y-1)}{\cos^2\pi y}\,B_n^{(3)}\right.$$

$$\left. + \frac{F}{4nk\lambda_n U h_2}\,iB_{nT}^{(3)}\,\frac{(y-1)\mathrm{ch}\,\lambda_n(y-1)}{\cos^2\pi y} + \frac{F}{2nkh_2}\,iB_{nT}^{(5)}\,\frac{\mathrm{sh}\,\lambda_n(y-1)}{\cos^2\pi y}\right]$$

$$\phi_{2in}^{(odd)} \sim \Delta^{5/2}\, Y_n^{(0)} + \Delta^{7/2}\ln(1/\Delta)\, R^{(2,n)} + \Delta^{7/2} Y_n^{(2)} + \Delta^4 \ln(1/\Delta)\, R^{(3,n)}$$

$$+ \Delta^4\, Y_n^{(3)} + \Delta^{9/2}\ln(1/\Delta)\, R^{(4,n)} + \Delta^{9/2}\, Y_n^{(4)} + \ldots$$

Again, since we have not calculated $\theta_2^{(3)}$, $\theta_2^{(4)}$, $R^{(2,n)}$, $R^{(3,n)}$ etc., we cannot attempt to match those terms which include a factor of $\ln(1/\Delta)$. Once more we shall omit these in what follows.

$$\phi_{2\ out}^{(odd)} \sim \Delta^4 \left[\eta^{-2}\left(-\sh\lambda_n/2\ \frac{iFB_{nT}^{(3)}}{2h_2 nk\pi^2}\right)\right.$$

$$\left. + \eta^{-4}\left(-\frac{iFB_{nT}^{(3)}\sh(\lambda_n/2)}{4nkh_2^2\pi^4} - \frac{F^3B_n^{(3)}(|A|^2 - |A(0)|^2)\sh(\lambda_n/2)}{4h_2^2\pi^4}\right)\right]$$

$$+ \Delta^{9/2}\left[\eta^{-1}\lambda_n \ch(\lambda_n/2)\frac{iFB_{nT}^{(3)}}{2h_2 nk\pi^2}\right.$$

$$\left. + \eta^{-3}\left(\frac{iFB_{nT}^{(3)}\lambda_n \ch(\lambda_n/2)}{4nkh_2^2\pi^4} + \frac{F^3B_n^{(3)}(|A|^2 - |A(0)|^2)\lambda_n \ch(\lambda_n/2)}{4h_2^2\pi^4}\right)\right]$$

$$\phi_{2in}^{(odd)} \sim \Delta^{5/2}\left[O(\eta^{-(3n-1)})\right] + \Delta^{7/2}\left[O(\eta^{-(3n-3)})\right]$$

$$+ \Delta^4\left[\frac{iF}{2nk\pi^2 h_2}\partial_T H_{n,0}^{(3)}\eta^{-2}\right] + \Delta^{9/2}\left[\eta^{-1}\left(\frac{-iF^2}{2nk\pi^2 h_2}\int_0^\infty Y_{nT}^{(0)}\right) + O(\eta^{-3})\right]$$

The leading order terms at $O(\Delta^4)$ and $O(\Delta^{9/2})$ do indeed match correctly.

The form that the matching procedure takes in the case of the Fourier components exp(i2nkx), $n > 1$, may be inferred from the case $n = 1$

At this point the asymptotic solution has been developed sufficiently for the purposes of chapter four.

References

Boville, B. A. (1981) Amplitude vacillation on a β-plane. J. Atmos. Sci., 38: 609-618.

Brown, J. A. (1969) A numerical investigation of hydrodynamic instability and energy conversions in the quasi-geostrophic atmosphere: Part I. J. Atmos. Sci., 26: 352-365.

Bryden, H. L. (1979) Poleward heat flux and conversion of available potential energy in Drake Passage. J. Mar. Res., 37: 1-22.

Bryden, H. L. (1982) Sources of eddy energy in the Gulf Stream recirculation. J. Mar. Res., 40: 1047-1068.

Charney, J. G. (1947) The dynamics of long waves in a baroclinic westerly current. J. Meteorol., 4: 135-162.

Charney, J. G. (1948) On the scale of atmospheric motions. Geof. Publ., 17(2).

Charney, J. G. (1959) On the theory of the general circulation of the atmosphere. In: The Atmosphere and the Sea in Motion, pp. 178-193.

Charney, J. G. and M. E. Stern (1962) On the stability of internal baroclinic jets in a rotating atmosphere. J. Atmos. Sci., 19: 159-172.

Dantzler, H. L. (1977) Potential energy maxima in the tropical and subtropical North Atlantic. J. Phys. Oceanogr., 7: 512-519.

Domaracki, A. and A. Z. Loesch (1977) Non-linear interactions among equatorial waves. J. Atmos. Sci., 34: 486-498.

Drazin, P. G. (1970) Non-linear baroclinic instability of a continuous zonal flow. Quart. J. Roy. Meteorol. Soc., 96: 667-676.

Eady, E. T. (1949) Long waves and cyclone waves. Tellus, 1(3): 33-52.

Farrell, B. (1984) Modal and non-modal baroclinic waves. J. Atmos. Sci., 41: 668-673.

Flierl, G. R. (1978) Models of vertical structure and the calibration of two-layer models. Dyn. Atmos. Oceans, 2: 341-382.

Gill, A. E. (1974) The stability of planetary waves on an infinite beta-plane. Geophys. Fluid Dyn., 6: 29-47.

Holland, W. R. (1978) The role of mesoscale eddies in the general circulation of the ocean - numerical experiments using a wind-driven quasi-geostrophic model. J. Phys. Oceanogr., 8: 363-392.

Jeffreys, H. (1926) On the dynamics of geostrophic winds. Quart. J. Roy. Meteorol. Soc., 52: 85-101.

Jeffreys, H. (1933) The function of cyclones in the general circulation. In: Proces-Verbaux de l'Association de Meteorologie, UGGI (Lisbon), Part II. 219-230. Reprinted in Theory of Thermal Convection, Ed., B. Saltzman, Dover, 1962.

Jeffreys, H. and B. S. Jeffreys (1956) Methods of Mathematical Physics 3rd Edition, Cambridge University Press, Cambridge, England, 716 pp.

Loesch, A. Z. (1974) Resonant interactions between unstable and neutral baroclinic waves: Part I. J. Atmos. Sci., 31: 1177-1201.

Longuet-Higgins, M. S. and A. E. Gill (1967) Resonant-interactions between planetary waves. Proc. Roy. Soc. London, A299: 120-140.

Lorenz, E. N. (1967) The Nature and Theory of the General Circulation of the Atmosphere. World Meteorological Organization, No. 218, Geneva, Switzerland.

McGoldrick, L. F. (1965) Resonant interactions amongst capillary-gravity waves. J. Fluid Mech., 21: 305-331.

Pedlosky, J. (1964a) An initial value problem in the theory of baroclinic instability. Tellus, 16: 12-17.

Pedlosky, J. (1964b) The stability of currents in the atmosphere and ocean: Part I. J. Atmos. Sci., 21: 201-219.

Pedlosky, J. (1970) Finite amplitude baroclinic waves. J. Atmos. Sci., 27: 15-30.

Pedlosky, J. (1971) Finite amplitude waves with small dissipation. J. Atmos. Sci., 28: 587-597.

Pedlosky, J. (1979a) Finite amplitude baroclinic waves in a continuous model of the atmosphere. J. Atmos. Sci., 36: 1908-1924.

Pedlosky, J. (1979b) Geophysical Fluid Dynamics. Springer-Verlag, New York, 624 pp.

Pedlosky, J. (1982) Finite amplitude baroclinic waves at minimum critical shear. J. Atmos. Sci., 39: 555-562.

Phillips, N. A. (1951) A simple three-dimensional model for the study of large-scale, extra-tropical flow patterns. J. Meteorol., 8: 381-394.

Phillips, N. A. (1954) Energy transformations and meridional circulations associated with simple baroclinic waves in a two-level, quasi-geostrophic model. Tellus, 6: 273-286.

Phillips, N. A. (1956) The general circulation of the atmosphere: a numerical experiment. Quart. J. Roy. Meteorol. Soc., 82: 123-164.

Phillips, O. M. (1960) On the dynamics of unsteady gravity waves of finite amplitude. Part I: The elementary interactions. J. Fluid Mech., 9: 193-217.

Rossby, C.-G. et al. (1939) Relation between variations in the intensity

of the zonal circulation and the displacements of the semi-permanent centers of action. J. Mar. Res., 2: 38-55.

Simmons, A. J. (1974) The meridional scale of baroclinic waves. J. Atmos. Sci., 31: 1515-1525.

Stone, P. H. (1978) Baroclinic adjustment. J. Atmos. Sci., 35: 561-571.